THE UNIVERSITY
of EDINBURGH

The role of 11β-HSD1 in Reference and Working Memory in Ageing: Investigating underlying mechanisms and biomarkers of age-associated cognitive decline

Mei Xuan Lye

Thesis presented at the University of Edinburgh for the

Degree of Doctor of Philosophy

PhD – The University of Edinburgh – 2015

Declaration

I declare that this thesis was written by me and that the data presented within it are a result of my own work, except where outlined specifically in the text.

No part of this work has been submitted for any other degree.

Mei Xuan Lye

January 2015

Edinburgh

Acknowledgements

I would like to thank my supervisors, Professor Megan Holmes and Dr Joyce Yau, for their support and guidance throughout my studies. I would like to thank them especially for their patience and advice throughout my research period and particularly during my write-up.

Special thanks go to the BBSRC; without their support this work would not have been possible.

I would like to extend my thanks to everyone who helped me, particularly June Noble for her invaluable guidance and help through everything from the water maze to immunohistochemistry; Maurits Jansen, Ross Lennen and Ian Marshall for their vital help in ^{1}H-MRS data collection and analysis; the staff in the BRF, particularly Laraine Wells, for their endless help and advice; and to everyone in the lab for helping me more times than I can count and encouraging me when times were tough.

I would also like to thank my friends both in and outside the lab for their unwavering support and friendship - especially for the words of encouragement, prayers, food and accommodation when they were needed.

Finally, special thanks also to my parents for their constant support, love and encouragement and God for His continued faithfulness in my life.

Abstract

Glucocorticoids (GC) have a negative effect on age-associated cognitive decline and the GC metabolising enzyme 11β-hydroxysteroid dehydrogenase Type 1 (11β-HSD1) plays a key role in these effects. Increased glucocorticoids exert detrimental effects on the volume and function of brain regions such as the prefrontal cortex (PFC) and hippocampus that are necessary for cognitive functions such as memory and working memory. Previous research has identified changes in cell populations, metabolite levels and structure within the brain as well as altered levels of inflammation with age, and studies have suggested these biomarkers to be associated with cognitive impairments. Aged mice with a deletion in 11ß-HSD1 (11β-HSD1$^{-/-}$ mice), resulting in lower levels of glucocorticoids within the brain, exhibit attenuated cognitive decline in hippocampal dependent spatial learning and memory with age. However, the mechanisms through which 11β-HSD1 contribute to age-associated cognitive decline remain unknown. However, previous genetic models of 11β-HSD1$^{-/-}$ mice have demonstrated residual 11β-HSD1 activity in the brain which may still exert some effects on cognitive processes. Furthermore, the effect of 11ß-HSD1 on working memory – a more cognitively demanding process essential for everyday decision making - has yet to be determined. This thesis tests the hypothesis that glucocorticoid action mediates age-associated cognitive impairment in spatial learning and memory and spatial working memory through alterations in cell activity, brain metabolite levels and neuroinflammatory processes. Therefore, we aimed to investigate if complete lifelong 11β-HSD1 deficiency would protect against age-associated working memory deficits as well as spatial learning and memory deficits, and its effect on associated neural markers. In particular, we determined

changes in hippocampal metabolite levels, cell activity and inflammation as a function of ageing in a longitudinal manner. At 6, 12, 18 and 22 months, male 11β-HSD1$^{-/-}$ and C57BL/6J control mice were cognitively assessed in the Morris Water Maze (MWM) and Radial Arm Water Maze (RAWM) – tests for spatial reference memory and spatial working memory respectively. Magnetic resonance spectroscopy (^{1}H-MRS) was performed to examine the hippocampal metabolite profile in the same mice at 6, 18 and 22 months. Following their final scan, mice were culled and brains dissected for analysis. Results revealed unaltered spatial learning with age in C57BL/6J and 11β-HSD1$^{-/-}$ mice and pointed to a development of alternative strategies for task completion as a result of repeated testing. Spatial memory was more susceptible to age-associated effects with impairments in wild-type mice but not 11β-HSD1$^{-/-}$ mice, though not completely immune from the effects of repeated testing. These impairments were correlated with glutamate/glutamine levels and glial fibrillary acidic protein (GFAP), whilst GFAP was further correlated with 11β-HSD1 protein expression. Working memory was impaired with age in both 11β-HSD1$^{-/-}$ and wild-type mice, suggesting 11β-HSD1 deletion may be detrimental to cognitive processes in the prefrontal cortex. In conclusion, impaired memory with age may be attributed to increased glial reactivity and altered glutamate/glutamine cycling in the hippocampus, and lifelong removal of 11β-HSD1 may alter these processes. However, lifelong removal of 11β-HSD1 may not be as beneficial to working memory processes suggesting that 11β-HSD1 and glucocorticoid action play a key role in working memory processes.

Lay Abstract

Stress hormones have a negative effect on impairments in learning and memory with age. Changes in processes and structure in the brain have been linked to changes in learning and memory, and increased levels of stress hormones have negative effects on the brain. Aged mice with a genetic mutation resulting in decreased regeneration of stress hormones within the brain do not show the same impairments in learning and memory as normal ageing mice. However, the processes resulting in this protection remain unknown. Furthermore, the effect of lower levels of stress hormones on different types of memory has yet to be determined. This thesis investigates the theory that increased levels of stress hormones with age mediates impairments in learning and various types of memory through changes in cell activity, substances necessary for brain function, and inflammation processes. Therefore, we investigated if mice with a genetic mutation resulting in the termination of stress hormone regeneration would be protected from age-associated impairments in spatial memory (information about one's environment and spatial orientation) and working memory (the storage and manipulation of information). We also examined the effect on cell activity, substances necessary for brain function, and inflammatory processes. Spatial memory was more susceptible to age-associated impairments in normal mice, and related to changes in cell activity and substances playing a key role in cell-to-cell communication. However repeated practice in tasks requiring spatial memory was also able to prevent impairments. Working memory was impaired with age in both normal mice and mice lacking the regeneration of stress hormones, indicating that decreasing stress hormone levels may not be beneficial for all types of memory.

Contents

Chapter 1 : Introduction

1.1 Background

The frequency of age-related health problems is of growing importance as the percentage of older individual's worldwide increases. Projections estimate that by 2050 the number of individuals older than 60 years will account for 22% of the world's population. With dementia being one of the major disabilities in the elderly and a substantial percentage of the elderly population suffering from cognitive decline unrelated to an underlying disease, one increasingly vital healthcare concern is cognitive ageing.

It is estimated that the number of people living with mild cognitive impairment and dementia will almost double every 20 years with approximately 115.4 million people living with mild cognitive impairment or dementia by 2050. Additionally, outside of pathological cognitive dysfunction, preliminary estimates suggest that over 55% of the aged population experience functional cognitive deterioration with normal ageing. Consequently, the health and social burden of cognitive impairment and dementia on societies worldwide is increasing rapidly. Thus, tackling the problem of age-related cognitive impairment is of great importance in not only ensuring a better quality of life for older individuals but also alleviating the growing burden on healthcare communities all over the world.

However, considerable individual differences in cognitive performance are often observed during aging with cognitive abilities ranging from high levels of cognitive

function throughout the lifespan, to pathological aging, with impairment in memory and other cognitive abilities present (Daffner, 2010). Understanding what drives these individual differences in cognitive aging may provide crucial groundwork for developing effective therapeutic interventions to improve the quality of life for the rapidly increasing population of elderly.

It has been proposed that individual differences in both the decline of cognitive function and the differences in cognitive abilities during ageing can be attributed to variations in glucocorticoid levels and glucocorticoid exposure. This hypothesis has resulted in a myriad of studies examining the action of stress and glucocorticoids on cognitive function and ways in which these actions can be modulated. In our laboratory, we utilise a rodent model of intracellular glucocorticoid modulation through the lifelong removal of glucocorticoid metabolising enzyme 11β-HSD1. Indeed, the phenotype of this model is similar to those of low glucocorticoid models, with an attenuation of cognitive impairment with age. The aim of this thesis was to utilise a longitudinal analysis of the 11β-HSD1 knockout model to investigate the effect of lifelong removal of 11β-HSD1 on different types of memory at various time-points throughout ageing, and to further determine the mechanisms through which it may be attenuating age-related cognitive decline.

1.2 Cognitive Ageing

1.2.1 Human Studies of Cognitive Ageing

With the growing ageing population and progressing concerns of age on cognition characterising the effects of age on cognitive function has become increasingly

important, increasing knowledge of the problem at hand and aiding in the development of appropriate therapeutic interventions.

Human studies have identified two major categories of cognitive tests - tests assessing processing ability at the time of assessment and those assessing processing carried out utilising previously acquired knowledge. Tests assessing processing ability at the time of assessment involve the evaluation of memory, efficiency of reasoning, processing speed and executive function and typically comprise of novel problem solving paradigms. These tests assess what is typically referred to as fluid mental abilities, abilities essential for everyday activities and living independently. On the other hand, tests assessing processing utilising previously acquired knowledge examine previously acquired knowledge of general information, verbal ability and numerical ability. These tests assess what is often referred to as crystallized ability.

From examining these aspects of cognitive ability, a vast body of research on cognitive ageing in humans has found three major patterns of age-related patterns of cognitive function: 1) Cognitive function which remains relatively stable across life; 2) Declines that occur late in life; and 3) Declines across the lifespan. These three patterns suggest that, whilst ageing might have global effects on cognitive ability, it affects certain cognitive functions more than others and targeting the mechanisms underlying these cognitive processes may be an effective start to tackling the problem of age-related cognitive dysfunction.

1.2.1.1 Life-Long Stability

Behavioural research examining the effects of age on cognitive function found that not all cognitive abilities decline with age.

Autobiographical memory refers to the memory for an individual's own life events. These memories have been observed to be unaltered in non-pathological cognitive ageing with studies observing unchanged patterns of recall in aged individuals (Fromholt et al., 2003).

Similarly, the ability to attribute mental states to other individuals (emotional processing) has also been noted to remain unaltered with age (Happe et al., 1998) whilst attention to emotions and regulation of emotional states was also found to be unaltered in aged individuals (Carstensen et al., 2003).

Finally, automatic processes – the use of previously learned information for subsequent tasks – also demonstrated limited alterations with age. Studies have found unaltered performance in aged individuals on cognitive tasks requiring the use of automatic processes such as recognition tasks (La Voie and Light, 1994; Spencer and Raz, 1995).

1.2.1.2 Late-life Declines

Crystallised abilities involving numerical and verbal recall and tasks requiring previously acquired knowledge to be drawn on show little decline until very late in life (GrÉGoire and Van Der Linden, 1997). Both longitudinal and cross-sectional studies show declines in vocabulary and semantic knowledge only in late in life with both remaining fairly stable until old age (Park et al., 2002; Schaie et al., 2004).

It has been suggested that a combination of experience and accumulated knowledge in elderly individuals might result in use of preserved knowledge and experience to form more efficient or effective strategies when performing tasks in which younger adults rely on processing ability explaining the relative stability of these cognitive processes throughout ageing (Shimamura et al., 1995; Dixon et al., 2004).

1.2.1.3 Life-Long Declines

Basic mechanisms of cognitive function, such as processing speed, working memory and encoding of information have been noted to decline across the adult lifespan, however, cross-sectional and longitudinal data sets have produced variable results.

In cross-sectional studies by Park et al. (1996, 2002), individuals (matched for education, health and demographic variables) from each age decade from 20 to 80, processing speed, working memory and episodic memory were observed to follow a linear pattern of decline throughout ageing from the age of 20 with no acceleration of decline in later life. These results were also observed in a cross-sectional examination of data from the Seattle Longitudinal Study, linear age-related declines were observed for processing speed, episodic memory, spatial ability and reasoning (Schaie et al., 2004).

However, in a longitudinal analysis of the Seattle Longitudinal Study and other longitudinal studies, cognitive function shows a limited decline from age 20 to 60 with a linear decline similar to the rates observed in cross-sectional studies becoming noticeable only after the age of 60 whilst in other longitudinal studies a sharp decline is observed in late life whilst a curvilinear decline observed prior to this decline (Zelinski and Burnight, 1997; Schaie et al., 2004).

1.2.2 Animal Studies of Cognitive Ageing

As discussed in the section above, human studies have observed variations in cognitive decline with age depending on the type of cognitive function.

Studies utilising animal models to examine the effect of age on cognitive processes stretch far back. In particular, spatial reference and working memory is typically assessed in the Morris water maze and in variations of the radial arm maze respectively.

Early studies by Verzár-Mcdougall (1957) already demonstrated impairments in learning and memory in aged rats with the rate of learning decreasing with age. More studies have further supported non-pathological cognitive deterioration with age showing an age-associated impairment in spatial learning and memory in the Morris water maze with young and middle-aged rats achieving the learning criteria within three trials whilst aged rats required more trials to reach the learning criterion (Gallagher and Burwell, 1989; Jiang et al., 1989). Interestingly, individual differences in cognitive ageing were also observed in these studies with variable learning scores noted within the aged group. Similar studies examining learning and memory in mice and rats utilising the Y-maze (Dean et al., 1981), Morris water maze (Frick et al., n.d.; Wyss et al., 2000; Bizon et al., 2009), radial arm maze (Shukitt-Hale et al., 2004) and passive avoidance (McNamara et al., 1977) have also observed impairments in aged animals compared to their performance when young or a young control group as well as a spread in the performance within the aged groups.

The neuroanatomies behind these behavioural tests assessing spatial reference and working memory are illustrated in Figure 1.1. In particular, the hippocampus plays a

key role in spatial memory, with the hippocampus trisynaptic loop (entohinal-dentate-CA3-CA1) mediating place recall memory (Lee et al., 2005). Furthermore, facilitation of plasticity at the entorhinal-dentate synapse in mice is sufficient to enhance place recall and hippocampal lesions have been found to impair spatial memory (Saab et al., 2016). On the other hand, the prefrontal cortex is a key region in spatial working memory with lesions in the prefrontal cortex resulting impaired radial arm maze performance (Becker et al., 1980). As such, the variability in performance within aged animals has enabled the search for neural alterations which may contribute to age-related cognitive dysfunction. These studies have identified key neural alterations within these brain regions associated with cognitive impairment with age including, though not limited to, alterations in long-term potentiation, blood flow, brain structure and volume, cell morphology, density and expression, and metabolite expression. Below, some of the neural correlates examined in our study are discussed.

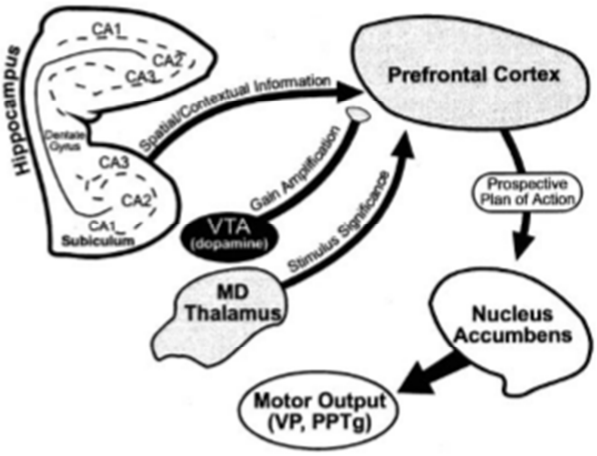

(Floresco et al. 1999; Figure 6)

Figure 1.1 Brain regions and circuits mediating spatial memory and spatial working memory

1.3 Patterns, Neural Correlates and Modifiers of Cognitive Ageing

Understanding the patterns and biological underpinnings of the above changes in cognitive ability is essential in developing appropriate therapeutic interventions. Numerous studies have examined various aspects of changes in the brain with age in the hope of identifying common markers and neural patterns which correlate with cognitive changes with age. In particular, studies have investigated alterations in brain structure, brain metabolite levels and changes in cells expression, morphology and distribution in the brain utilising both cross-sectional and longitudinal approaches.

1.3.1 Structural Markers of Cognitive Ageing

Before the arrival of MRI imaging, investigations into structural changes which may occur in the brain during ageing were limited to post-mortem studies. In a study by Skullerud (1985) to investigate factors which alter brain weight and ventricle volume, age was observed to be a factor resulting in physiological decrease in brain weight and increase in ventricular size. Further combined with studies suggesting a decrease in brain weight and significant increases in ventricle volume in individuals with Alzheimer's disease, the results suggested that the structure of the brain in ageing is a significant marker of cognitive decline and that the supporting structure of the brain is of key importance to cognitive ability.

The recent development of in-vivo imaging techniques has allowed a better insight into structural changes in the brain during healthy ageing and the relationship between these changes and cognitive performance. In a study by Convit et al. (2003),

increasing global atrophy was observed with age whilst Van Petten (2004) found decreased total cerebral volume with age. These results were complemented by Tisserand et al. (2000) who observed a decrease in total brain volume with age and a relationship between total brain volume and memory and executive function whilst MacLullich et al. (2002) who noted that increased general brain size in aged individuals was associated with general cognitive factor as assessed by measures of premorbid intelligence, fluid intelligence, verbal memory, visuospatial memory, verbal fluency, and attention and processing speed, further cementing the relationship between age, brain structure and cognition.

Whilst the results observed have been variable from study to study, cross-sectional studies have also observed associations between age and volume of a number of specific brain structures and have further gone on to establish relationships between the volume of these brain structures and cognition.

In particular, a myriad of studies have examined the hippocampus in ageing – a key structure in cognition. An increase in hippocampal atrophy with age has been well established in these studies with higher levels of global and verbal memory also being associated with increasing hippocampal size. Similarly, Golomb et al. (1993) noted a larger group of individuals exhibiting hippocampal atrophy with age compared to individuals not exhibiting any hippocampal atrophy with better levels of verbal memory and a trend for higher levels of non-verbal memory (attention, working memory and visual memory) in individuals without hippocampal atrophy whilst a further study by O'Brien et al. (1997) noted poorer scores in the Cambridge Cognitive Examination (assessing Global, Abstract Reasoning, Executive Function,

Language, Motor Skills, Verbal & Visual Memory) in aged adults with hippocampal atrophy compared to those not exhibiting hippocampal atrophy. Additional support for alterations in hippocampal structure with age was provided by further studies demonstrating a decrease in hippocampal volume with age and an association between hippocampal volume and verbal memory, visual memory, working memory and executive function (Golomb et al., 1994; Raz et al., 1998, 2000; Tisserand et al., 2000; Hackert et al., 2002; Convit et al., 2003; Dickerson and Eichenbaum, 2009).

In addition to the hippocampus, cross-sectional studies revealed the prefrontal cortex as a second brain structure altered significantly with age and affecting cognitive ability. As was observed with the hippocampus, the prefrontal cortex (PFC) was found to decrease in volume with age and PFC volume was noted to be associated with visuospatial processing, processing speed, working memory and executive function. In particular, Zimmerman et al. (2006) observed that below the age of 40, frontal cortex volume was not associated with executive function, however, in individuals aged above 40, smaller frontal volumes were observed to be related to poorer executive function. Furthermore, Fjell et al. (2006) found that aged adults with high fluid ability had thicker cortex in the PFC as compared to aged adults with average fluid ability.

Finally cross-sectional studies also pointed to a significant relationship between lateral ventricle size, age and cognition. Studies revealed a significant increase in lateral ventricle size with age with ventricle size associated with processing speed (Earnest et al., 1979).

This illustration of how fragile the relationship between cognitive function and supporting structure is further supported by longitudinal studies. In these studies it was noted that increased hippocampal atrophy and decreased hippocampal and prefrontal volume were associated with increasing age with studies further noting an increase in the rate of decrease with increasing age (Cohen et al., 2001; Marquis et al., 2002; Rodrigue and Raz, 2004; Walhovd et al., 2004; Raz et al., 2005). Conversely, lateral ventricle volume was observed to increase with aging (Cook et al., 2004; McArdle et al., 2004). The relationship between these brain structures and cognitive function was also assessed and whilst some studies observed minimal association between volume of each brain region and cognition, a number of studies noted better memory and global cognition levels with larger hippocampal and cortical volumes and higher global cognition levels with smaller lateral ventricle size (Visser et al., 1999; Marquis et al., 2002; McArdle et al., 2004; Walhovd et al., 2004). In particular, McArdle et al. (2004) assessed samples of both young and aged adults and observed that the relationship between lateral ventricle size and memory was strengthened with age.

1.3.2 Metabolite Markers of Cognitive Ageing

Along with the ability to assess the structure of the brain, the development of in-vivo imaging techniques has also allowed the quantification of metabolites within the brain through proton magnetic resonance spectroscopy (^{1}H-MRS). As with MRI techniques, ^{1}H-MRS has been utilised to examine metabolite markers for cognitive ageing although changes in brain metabolite levels throughout ageing is less explored than structural changes.

Previous ^{1}H-MRS studies have examined age-related changes of brain metabolite concentrations with a number of different methods, population size, and variable results. In particular, these studies have largely examined the metabolites Choline (Cho), Creatine (Cr) and N-acetylaspartate (NAA). These metabolites are associated with membrane turnover/breakdown, energy metabolism of neurons and glia, neuronal viability, and glial cells respectively.

No major difference in brain metabolite trends in ageing have been observed, however, results remain debated due to the varying structural properties of white and gray matter and the lack of a common methodological approach leaving results difficult to compare.

Whilst a side-by-side comparison is limited, due to differences in analysis of results and presentation of data, a number of general trends have been observed.

Perhaps the most established trend observed is a reduction in N-acetylaspartate (NAA) with age. Whilst results regarding the rate of decline of NAA in various regions and in gray and white matter remain controversial, several studies have demonstrated reductions in absolute NAA concentration, NAA as a ratio of creatine (NAA/Cr), NAA as a ratio of choline (NAA/Cho) and NAA as a ratio of water (NAA/water) over the course of ageing. In particular, these declines have been noted in the prefrontal cortex (Chang et al., 1996; Brooks et al., 2001; Driscoll et al., 2003; Urrila et al., 2004) and hippocampus (Schuff et al., 1999; Driscoll et al., 2003) of the brain. Further studies have demonstrated an association between NAA and cognitive function.

However, the effect of age on other metabolites remains more controversial. In some studies, Cho-containing compounds, including phosphorylcholine and glycerophosphorylcholine, as precursor and breakdown products of membrane phospholipids, respectively, have also been shown to increase with age in several brain regions (Chang et al., 1996; Soher et al., 1996; Angelie et al., 2001). However, in other contradicting studies, choline has been observed to decrease with age in the brain (Charles et al., 1994) whilst further studies have observed no change in choline levels during ageing (Schuff et al., 1999; Angelie et al., 2001).

A few studies have also looked at the effect of age on levels of myoinositol (Ins), a marker for glial cells, demonstrating an increase in Ins with age. In particular, Chang et al. (1996) noted an increase in Ins in gray matter with ageing.

1.3.3 Cellular Alterations in Cognitive Ageing

In addition to structural and metabolite changes with age, cellular alterations have also been observed with age and are thought to play a key role in affecting the mechanisms of neural plasticity and, in turn, cognitive function.

Early investigations into the ageing brain suggested that ageing was accompanied by a significant loss of neurons in the cortex (Brody, 1955), hippocampus and prefrontal cortex. Further studies continued to suggest that neuronal loss and reductions in dendritic branching were characteristic of normal ageing and age-associated cognitive decline.

However, the recent development of new stereological techniques has allowed a more reliable method of quantification of cells within the brain resulting in new

conclusions regarding changing brain structure and cellular alterations with age. Whilst previous studies concluded that reductions in brain volume were the result of neuronal loss, studies utilising newer techniques have suggested that neuronal loss is in fact not a characteristic of normal ageing (West, 1993; Rapp and Gallagher, 1996; Rasmussen et al., 1996) functions (Wickelgren, 1996; Morrison and Hof, 1997). More recent results support to these conclusions for the cerebral cortex and hippocampus of rodents, primates and humans (Burke and Barnes, 2006) whilst further rodent and human data suggests that brain volume reduction with age may in fact be the result of other cellular alterations (Terry and Katzman, 2001; Hedden and Gabrieli, 2004)n dendritic length and complexity (Cruz-Sánchez et al., 1995; Duan et al., 2003; Markham et al., 2005; Shimada et al., 2006) were observed along with reductions in synaptic density (Itzev et al., 2001, 2003; Adams et al., 2010; Hara et al., 2012) and increased spinal loss (Cruz-Sánchez et al., 1995; Dumitriu et al., 2010). Additionally, some studies have also demonstrated impaired spatial memory with age in mice with decreased synaptic density (Geinisman et al., 1986) and impaired learning and memory as assessed by a DNMS task in mice with reduced synaptic density (Dumitriu et al., 2010; Hara et al., 2012).

Alterations in other cells in the brain have been examined relatively less than age-associated changes in neurons due to the assumption that alterations in glia is secondary to neuronal degeneration. However, recent studies have observed increased glial reaction with age (Kohama et al., 1995). Taken together with the importance of neuronal-glia interactions and cognitive function (Bezzi and Volterra, 2001) this has prompted investigations into the possible role of age-associated glial reactivity and age-associated cognitive impairment. Furthermore, as mentioned

above, studies have suggested that altered synaptic fields with age may play a large role in age-associated cognitive impairment and it is noted that glial cells play a large role in modulation of synaptic fields (Han et al., 2013) further pointing towards a possible role for altered glial cell reactivity in age-associated cognitive impairment.

Glial cells are classified into three main groups – astrocytes, oligodendrocytes and microglia. In aged rats, astrocytic reactivity has been observed in the hippocampus in the form of hypertrophy – an increased number of thickened processes and increased cell volume (Lindsey et al., 1979). With age, expression of glial fibrillary acidic protein (GFAP), a protein found exclusively in astrocytes, and GFAP mRNA was observed to be increased indicating increasing glial reaction with age (Goss et al., 1991; Nichols et al., 1993; Morgan et al., 1997). Additionally, Sugaya et al. (1996) observed that increased GFAP with age was associated with the extent of cognitive impairment with age.

However, it was also noted that there was an increase in microglia reactivity with age with an upregulation of microglial activation markers observed and alterations in microglial morphology and expression. Together this data suggests age-related neuroinflammation which may also play a role in age-associated cognitive impairment and is discussed in further detail below.

1.4 Neuroinflammation

1.4.1 The Inflammatory Response

The immune system is essential in protecting organisms from disease by preventing and responding to the entry of pathogens into an organism. The immune response

can be divided into two main systems – the innate and the adaptive. The innate immune system is the first line of defence, providing an immediate, non-specific response to the detection of pathogens. The adaptive immune system is subsequently activated and responds in a manner more specific to the particular pathogen. This response is stored allowing a faster more efficient response to the pathogen in future.

The immune response is mediated by phagocyticinnate immune cells, macrophages, which detect pathogens via pattern recognition receptors which bind to pathogen-associated molecule patterns. The most widely recognised set of receptors are the toll-like receptors (TLRs) which are activated by a wide variety of pathogens and bacteria. Activation of these receptors has been found to result in the expression of cell surface activation molecules [major histocompatibility complex (MHC) class 1, II, B7.1, B7.2 and CD40] and the secretion of cytokines [tumour necrosis factor (TNF), interleukin (IL)-1, IL-6, IL-12 and IL-18]. The activation of these molecules and cytokines then signals the activation of the adaptive immune system to aid in the defence of the organism.

1.4.2 Microglia

Within the CNS, the immune response is regulated by microglia. Microglial cells comprise 10-15% of the cells in the brain and are concentrated in the hippocampus, hypothalamus, basal ganglia and substantia nigra (Lawson et al., 1990). In the adult brain, microglia exist in a resting state characterised by small soma and ramified processes which continuously scan the environment in the brain (Nimmerjahn et al., 2005; Kettenmann et al., 2011). Minor changes in brain homeostasis activate the microglia resulting in a morphological shift into an amoeboid morphology with

shorter processes and a bigger soma accompanied by the upregulation of cell surface molecules (Davis et al., 1994; Nimmerjahn et al., 2005).

The extent of microglial activation is influenced by the type and duration of the stimulus, however, once activated serve a variety of functions necessary for neuronal survival such as cellular maintenance activities and facilitation of repair. However, prolonged activation of microglia can also have detrimental effects and microglial activation is controlled through interaction with neuronal signalling molecules. Neurons communicate with microglia to maintain their resting state using membrane bound signals such as CD200, CX3CL1 and neurotransmitters (Pocock and Kettenmann, 2007; Biber et al., 2008).

1.4.3 Alternative activation of microglia

As part of the immune response, research has identified two main activation states of microglia - classical (M1) and alternative (M2) – although it must be noted that it has been widely accepted that a number of states inbetween these two states are present.

Classical activation of microglial cells is mediated by the induction of cell surface proteins; in particular receptors involved in the innate immune response are activated by a wide variety of ligands including interferon-y, LPS and other TLR activators and responses to bacterial and viral infections. Although the classical activation of microglia is effective and essential in responding to pathogens, the response can often result in damage to the surrounding tissue and the production of chemokines CCL2 and MCP-1 which mediate the recruitment of more microglia. M1-type activation is typically associated with disease states that are partially driven by low grade inflammation and in particular is associated with Alzheimer's disease.

However, microglia also exhibit a response which inactivates the initial immune response and activates genetic pathways associated with tissue repair. This activity is associated with the production of anti-inflammatory cytokines by glia and neurons. In particular, cytokines IL-4, IL-10, IL-13 and TGFβ are responsible for alternative activation of microglia to M2 state. M2 microglia are characterised by suppression of pro-inflammatory cytokines (For review see Mantovani et al., 2004).

1.4.4 Neuroinflammation in Ageing

Recent evidence has suggested that during ageing the inflammatory status of the brain is altered. In particular, studies have found that the healthy aged brain is characterised by chronic low level inflammation and 'primed' microglia. 'Primed' microglia have a phenotype of heightened reactivity and in response to activation of the immune system demonstrate a more pronounced and prolonged release of pro-inflammatory cytokines compared to microglia in young brains (Sparkman and Johnson, 2008; Frank et al., 2010). They are often characterised by morphological activation (large soma and short processes) but with minimal basal production of pro-inflammatory cytokines. In particular, 'primed' microglia show elevated levels of expression cell surface activation molecules MHCII, CD68, CD80, CD86 and ICAM-1 (Perry et al., 1993; Godbout et al., 2005; Frank et al., 2006, 2010; Bilbo, 2010). Along with these changes in microglial reactivity, elevated levels of pro-inflammatory cytokines IL-1β, IL-6 and TNF-α are observed in the normal aged brains (Godbout et al., 2005; Sierra et al., 2007).

Concurrent with increased microglial reactivity and elevated pro-inflammatory cytokine levels, a decrease in anti-inflammatory cytokine IL-10 and IL-4 is observed

in normal aged brains (Frank et al., 2006). In further support of these findings, studies have found that genes involved in oxidative stress, inflammation and glial activation are increased during ageing whilst genes associated with synaptic function and growth factors decrease (Lee et al., 2000; Blalock et al., 2003; Bishop et al., 2010).

Importantly, age-related microglial priming and the shift of the microenvironment to a pro-inflammatory state not only affects cognitive function and behaviour but also leaves the brain vulnerable to disruptive effects of intrinsic and extrinsic factors such as disease, infection and stress which may in turn exacerbate cognitive dysfunction.

1.4.5 Neuroinflammation and Cognition

The idea that neuroinflammation plays a role in cognitive dysfunction is supported by studies demonstrating an association between inflammatory markers in the brain and a variety of pathological diseases in the brain affecting cognitive function such as Alzheimer's Disease (AD), mild cognitive impairment (MCI) and Parkinson's Disease (PD). Furthermore, studies show that the inflammatory response can affect metabolic and molecular pathways influencing neurotransmitter systems that can ultimately affect neural circuits that regulate behaviour and cognition (Figure 1.2).

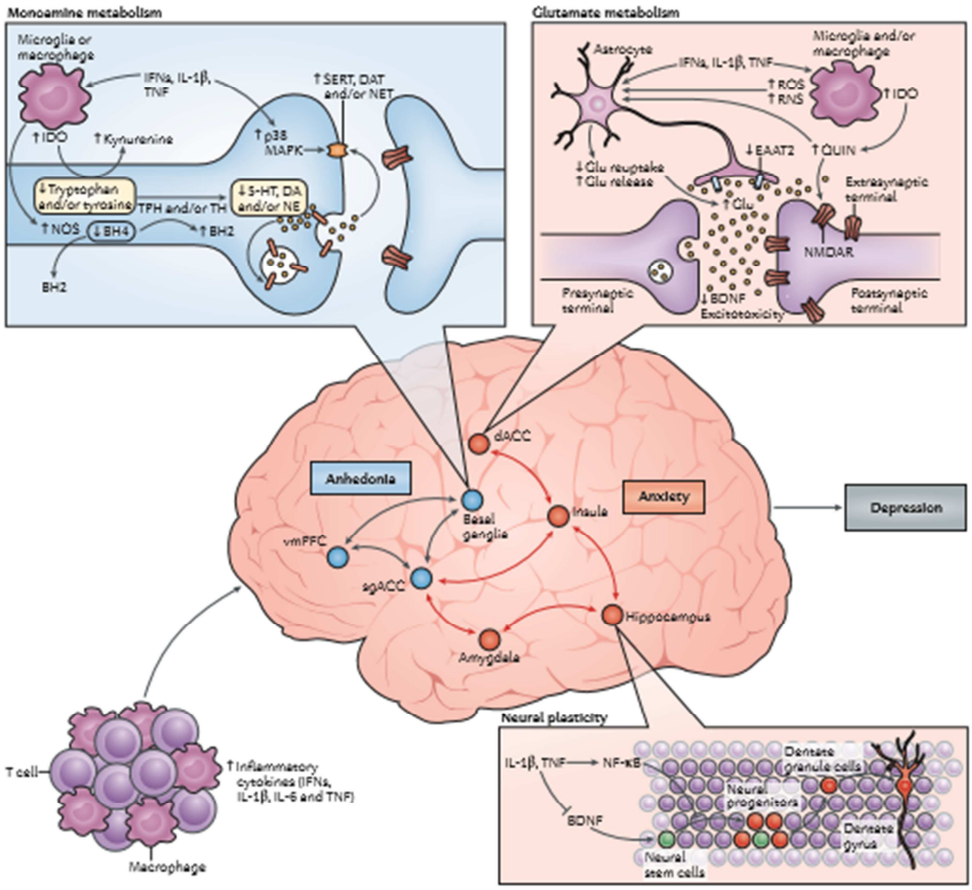

(Miller and Raison, 2016; Figure 3)

Figure 1.2 Effect of inflammation on neural circuits and neurotransmitter systems.

Pro-inflammatory cytokines such as interleukin-1β (IL-1β) and tumour necrosis factor (TNF) reduce the availability of neurotransmitters such as serotonin (5-HT), dopamine (DA) and noradrenaline (NE) through the increased expression and function of the presynaptic reuptake pumps for 5-HT, DA and NE. Pro-inflammatory cytokines also alter glutamate (Glu) reuptake and stimulation of glutamate release, which can in turn lead to decreased expression of genes related to cognition such as brain-derived neurotrophic factor (BDNF) and excitotoxicity. This in turn can alter neuronal integrity including neurogenesis, long-term potentiation and dendritic sprouting and alter learning and memory processes.

In addition to the role of neuroinflammation in neuropathological disease states, evidence has also established a link between neuroinflammation and non-pathological cognitive impairment. Administration of lipopolysaccharide (LPS) or IL-1β to rodents has been found to result in an upregulation of pro-inflammatory cytokines and subsequently impaired spatial working memory in rodents and impaired hippocampal-dependent memory consolidation (Rosi et al., 2006). In support of this, transgenic mice overexpressing the pro-inflammatory cytokine IL-1 demonstrate impaired spatial working memory (Moore et al., 2009) whilst mice deficient in IL-6 show attenuation of LPS-induced spatial memory impairments. Furthermore investigations have established that pro-inflammatory cytokines can act directly on neurons in the hippocampus resulting in impaired synaptic plasticity as well as alter neuronal function, neurogenesis and impair long-term potentiation. More recently, Bonow et al. (2009) revealed during a microarray analysis of cortical tissue from mice injected with LPS that as well as in increase in inflammatory genes, neuroinflammation also leads to a decrease in genes related to learning and memory.

In a complimentary study, it has been found that mice deficient in IL-10, an anti-inflammatory cytokine, show impaired spatial memory following LPS administration accompanied by elevated levels of pro-inflammatory cytokines whilst administration of anti-inflammatory agents reduces age associated increases is MHCII and attenuates impairments in LTP (Griffin et al., 2006).

Also notable is the effect of peripheral inflammation on cognitive function with elevated peripheral cytokine levels associated with lower cognition. Similarly, systemic LPS has been observed to produce deficits in working memory in rodents

and acute infection in humans has alluded to a connection between inflammation and cognitive dysfunction.

However, it has been observed that in situations such as sepsis and chronic stress resulting in the breakdown of the blood brain barrier, peripheral inflammation can result in elevated pro-inflammatory cytokine expression in the brain (Munhoz et al., 2006).

Therefore, the above evidence demonstrates that inflammation plays a large role in neuronal-glial communication and subsequently neuronal function and cognition, whether directly or via peripheral mechanisms, and that both ageing and glucocorticoid exposure play a large role in neuroimmune function. Determining how the processes regulate or contribute to neuroinflammation will provide a greater understanding of age-related cognitive dysfunction.

1.5 Glucocorticoids

Homeostasis is the control of the internal environment and is essential for organisms to survive ensuring maintenance of a dynamic equilibrium with their environment. The control of this internal environment exists at molecular, cellular, physiological and behavioural levels. The condition of stress is a risk to equilibrium and internal environment and successful adaptation to the state of stress confers a survival advantage. Effective adaptation to stress entails not only the ability to react to stress, but also the ability to effectively control the stress response according to the stressor.

The stress system is active even in the absence of stressors, but physical and emotional stressors which surpass a particular threshold result in an increase in

activity of the system. The hypothalamic-pituitary-adrenal (HPA) axis and the sympathetic and adrenomedullary (sympathetic) systems are primary members of the stress system. Increased activity as a result of stress results in central and peripheral changes and consequently behavioural adaptation and redistribution of energy to the central nervous system, muscle, and stressed body sites.

Of particular interest to this study, is activation of the HPA axis in response to stress. HPA axis activation results in glucocorticoid secretion which is thought to modulate the stress response.

1.5.1 Glucocorticoids

Glucocorticoids are steroid hormones and are found as cortisol in humans and corticosterone in rodents. Glucocorticoids have a variety of functions including playing large roles in developmental processes, regulation of inflammatory responses (Sorrells and Sapolsky, 2007), metabolic processes and cognition (Setiawan et al., 2007).

Glucocorticoid action is regulated through two different types of glucocorticoid receptors: 1) Mineralocorticoid receptors (MR); and 2) Glucocorticoid Receptors (GR). Both MR and GR are intracellular ligand-dependent transcription factors which, when activated, mediate the termination of the HPA axis stress response (via negative feedback at intracellular GR and MR) and modulate the responses to stressful experiences (Sapolsky et al., 2000; Oitzl et al., 2001).

The MR has a high affinity for glucocorticoids (Kd, approximately 0.5 nM) and thus facilitates the effect of non-stress basal fluctuations in glucocorticoids. Conversely, the GR has a lower affinity for glucocorticoids and occupied only when

glucocorticoid levels are high. Thus, the GR mediates its effects largely when levels of glucocorticoids are elevated due to stress. Glucocorticoid binding to MR and GR results in the translocation of activated receptors to the cell nucleus. In the nucleus, the ligand-receptor complex binds to the glucocorticoid response element (GRE) resulting in the transcription of activated genes (Fuller and Young, 2005; Kumar and Thompson, 2005). However, the activated GR complex can also repress the transcription of other factors present in the cytoplasm of the cell by preventing their transcription (Buckingham, 2006) (Fig. 1.3).

This complementary action of MR and GR allows varying levels of glucocorticoids to be dealt with appropriately.

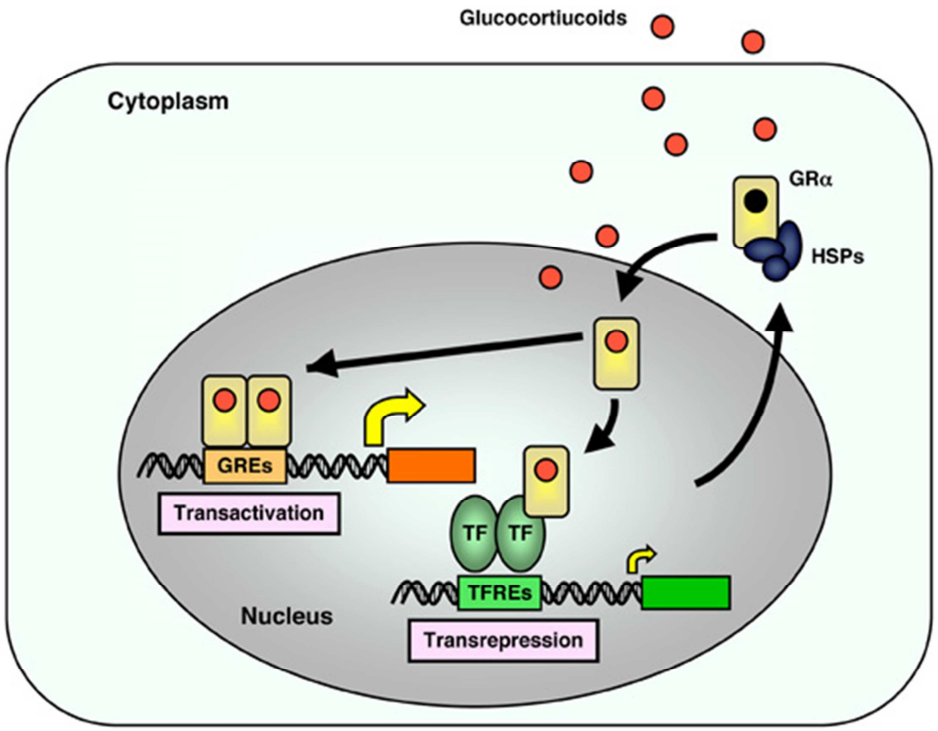

(Kino, 2010; The Glucocorticoid Receptor; www.http://brainimmune.com/the-glucocorticoid-receptor/; Accessed Nov 2014)

Figure 1.3 Mechanisms through which glucocorticoids regulate gene transcription.

Circulating glucocorticoids diffuse through membranes and bind to GR or MR. The activated receptor is then translocated to the nucleus and modulates gene transcription through various mechanisms. The ligand-receptor complex can also repress transcription by occupying binding sites and competing with co-activators.

1.5.2 HPA axis

In response to stress, neurons of the paraventricular nucleus (PVN) of the hypothalamus release corticotrophin-releasing hormone (CRH) into the portal blood vessel. This surge of CRH acts on CRH type 1 receptors resulting in the release of adrenocorticotropic hormone (ACTH) from the anterior pituitary gland into the blood where it is transported to the adrenal cortex of the adrenal gland. ACTH subsequently binds to receptors in the adrenal cortex which stimulates the secretion of glucocorticoids from the adrenal glands (Miller and O'Callaghan, 2005). This results in a surge in circulating glucocorticoid levels, which bind to glucocorticoid and mineralocorticoid receptors, activating mechanisms and processes allowing the body to adapt to and survive both the physical and emotional disturbances. Once the stressor has diminished, negative feedback loops are initiated by binding of glucocorticoids to glucocorticoid receptors (GR) in the PVN and anterior pituitary gland and mineralocorticoid receptors in the PVN (Fig. 1.2). HPA axis activity to stress is in part regulated by the binding of glucocorticoids to the glucocorticoid receptor (GR) and the mineralocorticoid receptor (MR) which alter ACTH and CRH release.

However, despite short-term, immediate benefits of elevated glucocorticoids, long-term exposure to elevated glucocorticoid levels has been found to have deleterious effects both peripherally and within the central nervous system. In particular, chronic exposure to elevated levels of glucocorticoids have been associated with cardiovascular disease, hypertension, type 2 diabetes, obesity as well as a variety of disorders and structural changes within the central nervous system - particularly within the brain (McEwen, 1999; McEwen et al., 1999).

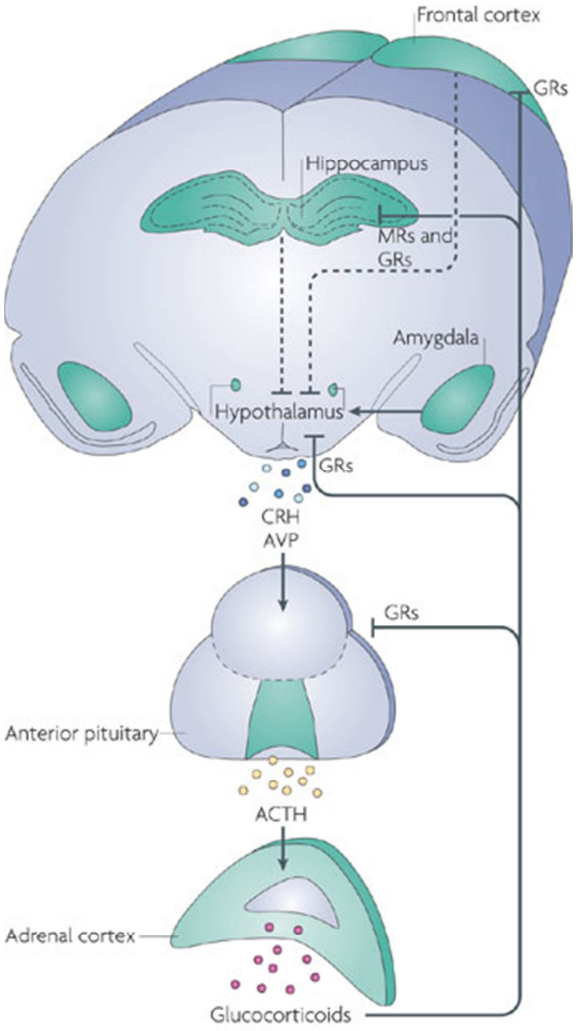

(Lupien et al., 2009; Figure 1)

Figure 1.4. HPA-Axis Activation

The paraventricular nucleus (PVN) in the hypothalamus secretes both CRH and AVP from the paraventricular nucleus which stimulates the production of ACTH in the anterior pituitary. ACTH travels via the blood to the adrenal gland resulting in the secretion of glucocorticoids. A negative feedback mechanism mediated by the action of glucocorticoids on MR and GR in the hypothalamus and GR in the anterior pituitary results in a reduction in CRH, AVP, and ACTH. CRH: corticotrophin releasing hormone; AVP: arginine vasopressin; ACTH: adrenocorticotropic hormone; MR: mineralocorticoid receptor; GR: glucocorticoid receptor.

1.5.3 Glucocorticoids and Cognitive Ageing

The glucocorticoid hypothesis proposes that chronic exposure to elevated circulating glucocorticoids promotes the functional and structural degeneration of the brain, contributing to age-associated cognitive impairments. There are a number of variations to this hypothesis, with different views regarding the mechanisms through which chronic glucocorticoid action, stress related glucocorticoid release and age interact to result in functional decline and neurodegeneration (Landfield et al., 2007). However, they all have the common basis of cooperative interaction of glucocorticoids, ageing and stress in the impairment of cognitive function and hippocampal ageing. Studies consistent with the glucocorticoid hypothesis, have shown that glucocorticoids are elevated in ageing and could adversely affect hippocampal structure and vulnerability (Landfield et al., 2007). Additionally, correlations have been observed between both cognitive decline in aged rats and glucocorticoid levels as well hippocampal degeneration in aged rats and circulating glucocorticoid levels (Issa et al., 1990; Meaney et al., 1995). Other studies have demonstrated accelerated hippocampal ageing in chronic stress studies (Kerr et al., 1991) whilst others have found that excess glucocorticoid exposure results in increased hippocampal vulnerability and CA3 dendritic retraction (Conrad et al., 2007). Most convincingly, studies have shown that maintaining low glucocorticoid levels in rodents from mid-life stops the cognitive decline observed with ageing (Yau et al., 2002).

1.5.4 Glucocorticoids and Neural Correlates of Cognitive Ageing

Recent studies of the brain have suggested that brain plasticity, in particular hippocampal plasticity and function, is highly regulated by hormones. Glucocorticoids in particular have been noted to have a huge impact on neuronal structure and function and consequently brain structure and volume.

Of particular interest to our work, is the effect of glucocorticoids on hippocampal neurons and structure. Hippocampal neurons express MR and GR and the binding of glucocorticoids to these receptors has been observed to play a large role in the regulation of neurogenesis, remodelling of neuronal dendrites and the excitability of hippocampal neurons, processes correlated with age-related cognitive impairment.

Whilst basal levels of glucocorticoids are essential for the above processes to occur, chronic elevated levels glucocorticoids, as observed in ageing, have been found to have adverse effects on brain structure and neuronal expression and morphology. Studies shown that glucocorticoids are elevated in ageing and could adversely affect hippocampal structure and vulnerability (Landfield et al., 2007). Additionally, hippocampal degeneration in aged rats has been observed to be correlated with circulating glucocorticoid levels (Issa et al., 1990) whilst studies have demonstrated accelerated hippocampal ageing in chronic stress studies (Kerr et al., 1991) and increased hippocampal vulnerability and CA3 dendritic retraction in response to excess glucocorticoid exposure (Conrad et al., 2007).

Studies have also shown that chronic elevated glucocorticoid levels have an impact on metabolite levels within the brain. Czéh et al. (2001) observed in-vivo decreases

in NAA, Creatine and Choline in the brain following a 7 day psychosocial stress paradigm to elicit the stress-induced endocrine changes.

1.5.5 Glucocorticoids and Inflammation

Interactions between the nervous system, HPA-axis and elements of the immune system are essential in regulation of the inflammatory response. The release of inflammatory mediators activates peripheral pain receptors and consequently the nociceptive pathway. This is turn results in the activation of the HPA-axis resulting in the release of glucocorticoids. Cytokines act directly on the HPA-axis resulting in the release of glucocorticoids. Glucocorticoids then bind to glucocorticoid receptors inhibiting the synthesis of cytokines and inflammatory mediators and resulting in a negative feedback loop.

1.5.6 Glucocorticoids and Neuroinflammation

Glucocorticoids have generally been considered anti-inflammatory and are used clinically in this aspect. However, this view has recently been challenged with studies demonstrating both a suppressive (neuroprotective with negative feedback on microglial activation) and enhancing (exacerbation of neuroinflammation) role of glucocorticoids in neuroinflammation depending on the magnitude and duration of the stressor in relation to immune activation (Sorrells and Sapolsky, 2007).

Studies have shown that stress increases the expression of TNF-α, IL-1β, IL-6 and IFN-γ in the CNS and peripheral tissues (Johnson et al., 2002; Munhoz et al., 2006) and also induces the release and accumulation of pro-inflammatory mediators such as nitric oxide (NO) and cyclooxygenase-2 (cox-2) (Madrigal et al., 2003). Recent evidence has shown that cytokines and activation of the stress response act together

to potentiate cytokine response resulting in altered cognitive function and behaviour (Munhoz et al., 2010). Acute and chronic stress has been observed to elevate levels of pro-inflammatory cytokines in the hippocampus and frontal cortex of rodents and increase microglial activation, reactivity and proliferation (Johnson et al., 2002; Munhoz et al., 2006). Studies have also found that glucocorticoids suppress neuronal signalling molecules CD200 and CXC3L1 which play a large role in controlling microglia activation (Frank et al., 2007).

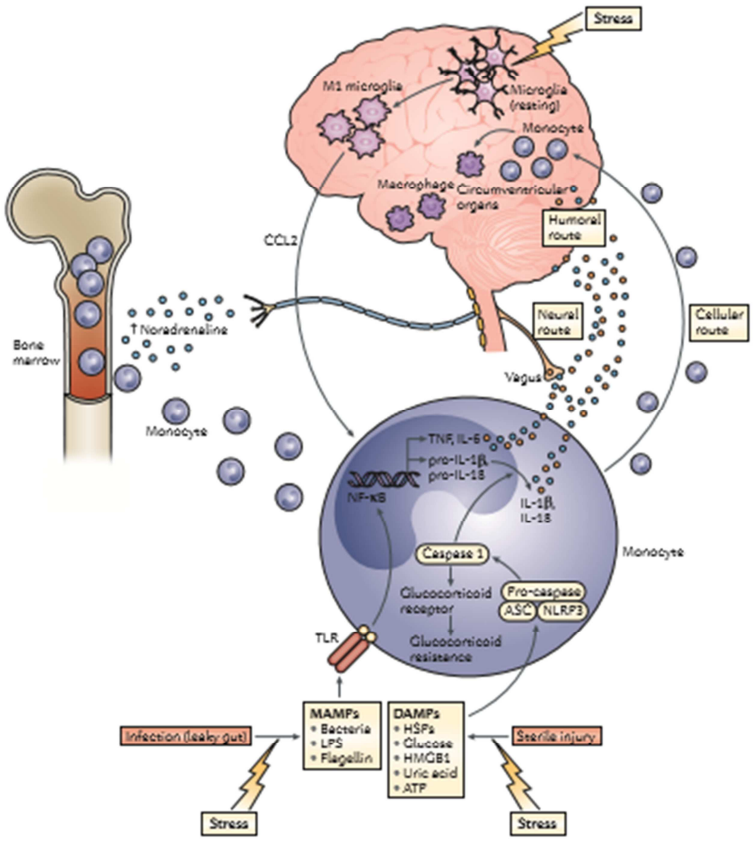

(Miller and Raison, 2016; Figure 2)

Figure 1.5. The role effect of glucocorticoids on inflammatory and neuroinflammatory processes

Glucocorticoids can activate microglia to a M1 pro-inflammatory phenotype perpetuating the central inflammatory responses.

1.6 Intracellular modulation of Glucocorticoid Signalling

As discussed above, excessive and prolonged exposure to glucocorticoids has a detrimental effect on cognitive ageing. However, attempts to attenuate these effects through adrenalectomy or receptor inhibiting drugs prove difficult as glucocorticoids play a large role other processes within the body, such as inflammatory and metabolic processes. Consequently, other components playing a role in the action of glucocorticoids on tissues have been identified.

One such component identified as playing a key role in glucocorticoid action is the enzyme 11β-hydroxysteroid dehydrogenase (11β-HSD) – an enzyme which modulates intracellular signalling of glucocorticoids.

Studies have revealed that intracellular concentrations of glucocorticoids, and consequently glucocorticoid action, are determined not only by circulating blood glucocorticoid levels, but also by glucocorticoid metabolising enzymes which are able to convert active glucocorticoids to 11-keto derivatives and vice versa. The enzymes catalysing these reactions are 11β-hydroxysteroid dehydrogenases.

11β-HSD exists as two isozymes – type 1 (11β-HSD1) and type 2 (11β-HSD2). Whilst the type 1 isozyme catalyses the reduction of 11-keto derivatives to active glucocorticoids - consequently amplifying glucocorticoid action - the type 2 isozyme catalyses the reverse reaction converting glucocorticoids to inactive 11-keto derivatives (White et al., 1997). The benefits of the 11β-HSD2 in their ability to reduce intracellular glucocorticoid activity can be seen in mineralocorticoid target

tissues, where the presence of 11β-HSD2 reduces intracellular glucocorticoid levels allowing mineralocorticoids to bind to the mineralocorticoid receptors which would otherwise bind the more abundant glucocorticoids. Such mechanisms of reducing intracellular glucocorticoid action would be ideal in alleviating the deleterious effects of glucocorticoids in the brain. However, 11β-HSD2 expression in the brain is restricted to the circumventricular regions and is expressed most in mineralocorticoid target tissues such as the kidney (Rashid and Lewis, 2005).

Conversely, 11β-HSD1 has highest expression in glucocorticoid target tissues such as the liver, adipose tissue and brain. In particular and of importance to this study, 11β-HSD1 is expressed abundantly in the hippocampus and frontal cortex of the brain (Moisan et al., 1990) – key structures in cognition and executive function. As stated earlier, 11β-HSD1 catalyses the conversion of 11-keto forms to active glucocorticoids and thus amplifies glucocorticoid actions in the brain. Research has established that this amplification of glucocorticoid action has a significant effect on age-related cognitive function and structural changes in the brain during ageing (MacLullich et al., 2005; Holmes et al., 2010).

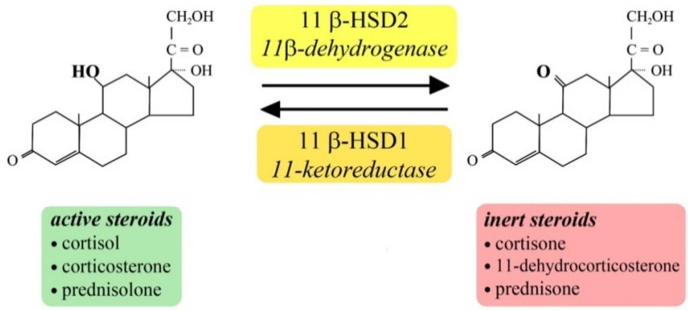

(Atanassova and Koeva, 2012; Figure 5)

Figure 1.6. Interconversion of inert glucocorticoids and active glucocorticoids mediated by 11β-HSD1 and 11β-HSD2

Inactivation of circulating glucocorticoids by 11β-HSD2, then reactivation in peripheral tissues by 11β-HSD1.

1.7 11β-HSD1 and Cognitive Ageing

Investigations have suggested that inhibition of 11β-HSD1 may attenuate the deleterious effects of glucocorticoids on cognitive function and brain integrity in ageing. Importantly, Yau et al. (2001) found that in 11β-HSD1 knockout mice, despite elevated basal corticosterone levels, aged mice showed significantly lower hippocampal corticosterone levels when compared to aged wild-type mice. In addition to this, it was observed that whilst aged wild-type mice experienced learning deficits associated with elevated glucocorticoid levels, no learning deficit was observed in aged knockout mice. Together, these findings suggested that tissue glucocorticoid levels are not completely dependent on plasma glucocorticoid levels and that it is the intracellular tissue levels which affect hippocampal function.

Consistent with suggestions that 11β-HSD1 plays a key role in the impact of glucocorticoid action in ageing, further studies have revealed better spatial memory and enhanced long-term potentiation in 11β-HSD1 knockout mice compared to age matched wild-type controls (Yau et al., 2007). Additionally, the inhibition of 11β-HSDs has been associated with improved memory and cognitive function in healthy elderly humans (Sandeep et al., 2004) and more recent studies have suggested a predictive link between 11β-HSD1 activity, progressive brain atrophy and cognitive decline (MacLullich et al., 2012). Sooy et al. (2010) have also gone on to show that specific inhibition of 11β-HSD1 in C57BL/6J mice results in the prevention of age-related spatial memory impairments.

However, both the animal knockout models and inhibition of 11β-HSD studies have disrupted or inhibited 11β-HSD1 activity on a global scale, affecting not only the brain but peripheral tissues such as the liver and adipose tissue where 11β-HSD1 is

also highly expressed. Along with this, studies have found that peripheral replacement of 11β-HSD1 in the liver, in genetic knockouts of 11β-HSD1, can effectively reverse the altered HPA axis activity observed in knockout mice (Paterson et al., 2007). Together, the data suggest that changes in peripheral 11β-HSD1 may also affect localised central nervous system function, perhaps through metabolic and neuroendocrine mechanisms, thus making the principal role and function of 11β-HSD1 in the brain unclear. Interestingly, Holmes et al. (2010) have found an increase in 11β-HSD1 levels in the hippocampus and parietal cortex with age. Furthermore, they found that this increase in 11β-HSD1 levels correlates with cognitive performance with age as well as showing that fore-brain specific 11β-HSD1 overexpression results in premature age-related cognitive decline. More recently, Yau et al., (2015) demonstrated 11β-HSD1 mediated increased intracellular glucocorticoid levels play a key role in that age and stress related spatial memory impairments and that lifelong removal or inhibition of 11β-HSD1 abolished age and stress related spatial memory impairments. Finally, Wheelen et al. (2014) also noted a reversal of spatial memory impairment in aged wild-type mice upon inhibition of 11β-HSD1 as well as a reduction in fear memory strength and persistence.

Altogether, this data suggests brain 11β-HSD1 can affect cognitive function independent of peripheral 11β-HSD1 effects. However, the 11β-HSD1 knockout mouse models used in these studies demonstrated a small amount of 11β-HSD1 activity in the brain. As such, it has yet to be established if the effects noted will also be seen following complete removal of 11β-HSD1 activity or benefits are only observed when 11β-HSD1 levels are reduced. As such, further work needs to done to fully establish the role of 11β-HSD1 in the brain and age-related cognitive decline.

1.8 Summary and Thesis Aims

To summarise, cognitive impairment in normal ageing has been observed to be associated with changes in brain structure, metabolite levels, cellular alterations and neuroinflammation. At the same time, studies have demonstrated a large role for glucocorticoids in age-associated cognitive decline and in particular have found elevated glucocorticoids to alter brain structure and cellular structure and neuroinflammation. Furthermore, animal models of intracellular glucocorticoid modulation through the removal of glucocorticoid metabolising enzyme 11β-HSD1 have observed attenuated age-associated spatial learning and memory impairments.

However, these animal models were observed to have a small amount of 11β-HSD1 activity in the brain and the effect of complete absence of 11β-HSD1 activity on age-associated spatial memory impairment has yet to be conducted. Furthermore, 11β-HSD1$^{-/-}$ mice have only been examined in cross-sectional studies and with tests looking at only spatial learning and memory preventing the effect of intracellular glucocorticoid modulation on spatial learning and memory and other types of memory to be examined longitudinally. Therefore, this thesis tests the hypothesis that glucocorticoid action mediates age-associated cognitive impairment in spatial learning and memory and spatial working memory through alterations in cell activity, brain metabolite levels and neuroinflammatory processes. This will be achieved by utilising a longitudinal paradigm to examine the effect of complete lifelong 11β-HSD1 removal on spatial memory, working memory and cellular, metabolite and neuroinflammatory processes within the brain over a lifespan in an 11β-HSD1 knockout model with complete removal of 11β-HSD1 activity in the

brain. This will further understanding on not only the mechanisms of action of 11β-HSD1 but also provide insight into the effect of 11β-HSD1 on other cognitive processes which may be altered with age.

As such, the aims of this thesis were as follows:

1) **To examine the longitudinal effects of lifelong removal of 11β-HSD1 on spatial learning and memory processes and working memory processes with age by examining a different 11β-HSD1$^{-/-}$ mouse model, with complete removal of 11β-HSD1 activity, and their wild-type counterparts in the water maze and radial arm water maze over the span of 24 months.**

2) **To investigate molecular, structural and metabolite mechanisms through which 11β-HSD1 may act by investigating changes in these three markers with age and their correlation cognitive performance in a subset of the longitudinal colony of wild-type and 11β-HSD1$^{-/-}$ mice.**

3) **To determine the role of 11β-HSD1 on both acute neuroinflammatory responses and neuroinflammation with age by investigating changes in inflammatory markers in response to LPS administration and with age and their correlation with cognitive performance in a subset of the longitudinal colony of wild-type and 11β-HSD1$^{-/-}$ mice.**

Chapter 2 : Materials and Methods

2.1 Materials

Materials were sourced from the following:

2.1.1 General Chemicals

10mM dNTP	Promega UK Ltd, Delta House, Enterprise Road, Chilworth Research Centre, Southampton, SO16 7NS
Agarose	Bio-Rad Laboratories Ltd, Bio-Rad House, Maxted Road, Hemel Hempstead, Hertfordshire, HP2 7DX, UK
Borate Buffer	Fisher Scientific, Fisher Scientific UK Ltd, Bishop Meadow Road, Loughborough, LE11 5RG
Ethanol	Fisher Scientific, Fisher Scientific UK Ltd, Bishop Meadow Road, Loughborough, LE11 5RG
Ethylene Glycol	Sigma-Aldrich, The Old Brickyard, New Road, Gillingham, Dorset, SP8 4XT
Fluoromount Aqueous Mounting Media	Sigma-Aldrich, The Old Brickyard, New Road, Gillingham, Dorset, SP8 4XT
Glycine	Sigma-Aldrich, The Old Brickyard, New

	Road, Gillingham, Dorset, SP8 4XT
Hydrochloric Acid	Sigma-Aldrich, The Old Brickyard, New Road, Gillingham, Dorset, SP8 4XT
Hydrogen Peroxide	VWR International Ltd, Hunter Boulevard, Magna Park, Lutterworth, Leicestershire, LE17 4XN
Lightcycler480 Master Mix	Roche, Hexagon Place, 6 Falcon Way, Shire Park, Welwyn Garden City, AL7 1TW
Lipopolysaccharide (LPS)	Sigma-Aldrich, The Old Brickyard, New Road, Gillingham, Dorset, SP8 4XT
Liquid Latex (SBR Polymer)	Bonnymans, Willowburn Road, Willowyard Industrial Estate, Beith, North Ayrshire
Methanol	Fisher Scientific, Fisher Scientific UK Ltd, Bishop Meadow Road, Loughborough, LE11 5RG
Paraformaldehyde	Sigma-Aldrich, The Old Brickyard, New Road, Gillingham, Dorset, SP8 4XT
Phosphate Buffered Saline (PBS; Tablets)	Sigma-Aldrich, The Old Brickyard, New Road, Gillingham, Dorset, SP8 4XT

Protein assay dye reagent concentrate	Bio-Rad Laboratories Ltd, Bio-Rad House, Maxted Road, Hemel Hempstead, Hertfordshire, HP2 7DX, UK
Protein Assay Reagent A	Bio-Rad Laboratories Ltd, Bio-Rad House, Maxted Road, Hemel Hempstead, Hertfordshire, HP2 7DX, UK
Protein Assay Reagent B	Bio-Rad Laboratories Ltd, Bio-Rad House, Maxted Road, Hemel Hempstead, Hertfordshire, HP2 7DX, UK
QIAgen RNAeasy Kit	Qiagen, Skelton House, Lloyd Street, North Manchester, M15 6SH
Sodium Chloride	Sigma-Aldrich, The Old Brickyard, New Road, Gillingham, Dorset, SP8 4XT
Sodium Citrate	Sigma-Aldrich, The Old Brickyard, New Road, Gillingham, Dorset, SP8 4XT
Sodium Hydroxide	Sigma-Aldrich, The Old Brickyard, New Road, Gillingham, Dorset, SP8 4XT
Sodium Phosphate	Fisher Scientific, Fisher Scientific UK Ltd, Bishop Meadow Road, Loughborough, LE11 5RG

Sucrose	Sigma-Aldrich, The Old Brickyard, New Road, Gillingham, Dorset, SP8 4XT
SuperScript III First Strand Synthesis System	Promega UK Ltd, Delta House, Enterprise Road, Chilworth Research Centre, Southampton SO16 7NS
SYBR Safe DNA Gel Stain	Life Technologies, 3 Fountain Drive, Inchinnan Business Park, Paisley PA4 9RF, UK
Tris	Fisher Scientific, Fisher Scientific UK Ltd, Bishop Meadow Road, Loughborough, LE11 5RG
Triton-X 100	Sigma-Aldrich, The Old Brickyard, New Road, Gillingham, Dorset, SP8 4XT

2.1.2 Antibodies

Rabbit GFAP	Sigma, G9269-2ML	1:500
Sheep 11β-HSD1	Scott Webster	1:1000
Rabbit Iba-1	Wako, 019-19741	1:500
Mouse NeuN	Millipore, MAB377	1:500
Donkey Anti-Sheep Alexa Fluor 488	Invitrogen, A110015	1:500
Donkey anti-Rabbit Alexa Fluor 555	Invitrogen, A31572	1:500
Donkey anti-Mouse Alexa Fluor 555	Invitrogen, A31570	1:500
Donkey anti-Rabbit Alexa Fluor 555	Invitrogen, A31572	1:500
Donkey Serum	Sigma-Aldrich, D9663-10ML	

2.1.3 Primers

Gene	Primer Sequence	Probe Number
11β-HSD1	For: GGAGCCCATGTGGTATTGAC Rev: TTCAAGGCAGCGAGACACTA	69
Arg1	For: GAATCTGCATGGGCAAC Rev: GAATCCTGGTACATCTGGGAAC	2
IL-1β	For: AGTTGACGGACCCCAAAA Rev:TTTGAAGCTGGATGCTCTCA	26
TNFα	For: CTGTAGCCCACGTCGTAG Rev: TTTGAGATCCATGCCGTT	25
YM1	For: AAGAACACTGAGCTAAAAACTCTCC Rev: GAGACCATGGCACTGAAC	88

2.2 Methods

2.2.1 AnimalsGeneration of 11β-HSD1 knockout mice

Global 11β-HSD1 knockout mice with complete removal of 11β-HSD1 knockout were generated in-house by crossing 11β-HSD1$^{flox/flox}$ mice with Hprt-Cre mice (unpublished). Hprt-Cre mice were bred to 11β-HSD1$^{flox/flox}$ mice. The 11β-HSD1$^{flox/flox}$ mice have exon 3 of the 11β-HSD gene flanked by loxP sites, allowing Cre-driven recombination. The resulting F1 progeny were bred to 11β-HSD1$^{flox/flox}$ to generate a global 11β-HSD1 knockout mouse.

Cre genotyping identified presence (or absence) of the Cre transgene and "Flox" genotyping was carried out to check the homozygous state of the "floxed" 11β-HSD1 gene.

2.2.1.2 Housing

Animals were housed in standard cages upon controlled lighting (12h:12h, lights on at 7.00), were fed a standard chow and given water ad libitum. All procedures were performed in strict accordance with the United Kingdom Animals (Scientific Procedures) Act (1986).

2.2.1.3 Ageing Colony

11β-HSD1$^{-/-}$ mice and their wild-type littermates were housed as above. At 6, 12, 18 and 24 months of age, mice underwent cognitive testing in the water maze and radial arm water maze as described below.

A subset of the colony underwent proton magnetic resonance spectroscopy (^{1}H-MRS) following cognitive testing.

Following the final testing at 24 months, mice were culled and tissues extracted according to the protocol below.

2.2.2 LPS Experiment

2.2.2.1 Optimisation of LPS Dose and Incubation

Mice were administered with either 5mg/kg of LPS (n=4) or saline (n=4) and returned to their home cage for 12, 24 hours or 48 hours. Mice then received an overdose of sodium pentobarbital (0.4ml) and were then perfused with 4% PFA through cardiac puncture. Dose was determined based on previous studies showing morphological transition of microglia at 5 mg/kg and peak inflammatory response between 8-24 hours (Buttini et al., 1996).

Immunohistochemistry was performed according to the protocol detailed below for free floating sections. Sections were stained for 11B-HSD1, microglia, neuron and glial expression.

2.2.2.2 LPS Experiment

C57BL/6J mice were housed in standard cages as above. Mice were administered with either 5mg/kg of LPS (n=4) or saline (n=4) and returned to their home cage for 24 hours. Following this, mice were culled and tissues extracted according to the protocol below.

2.2.2.3 Tissue Collection

Mice then received an overdose of sodium pentobarbital (0.4ml) and were then perfused with saline through cardiac puncture. Brains were then dissected out and half the brain placed in 4% Paraformaldehyde (4% PFA) before being processed for immunofluorescence as described below. The remaining half of the brain was taken for real-time PCR analysis and the hippocampus and cortex removed and placed on dry ice before being processed as described below.

2.2.3 Morris Water maze

2.2.3.1 Apparatus

A pool 2m in diameter and 60cm in height painted white was used. The pool was filled with water ($25^{o}C \pm 2$) and rendered opaque by the addition of liquid latex (SBR polymer). The pool was arbitrarily divided into 4 quadrants – North West, South West, North East and South East (Fig. 2.1).

Behaviour in the maze was analysed using Water maze image tracking software, which tracked the following dependent measures in the 4 quadrants: 1) Time in seconds; 2) Percentage time; and 3) Latency to platform.

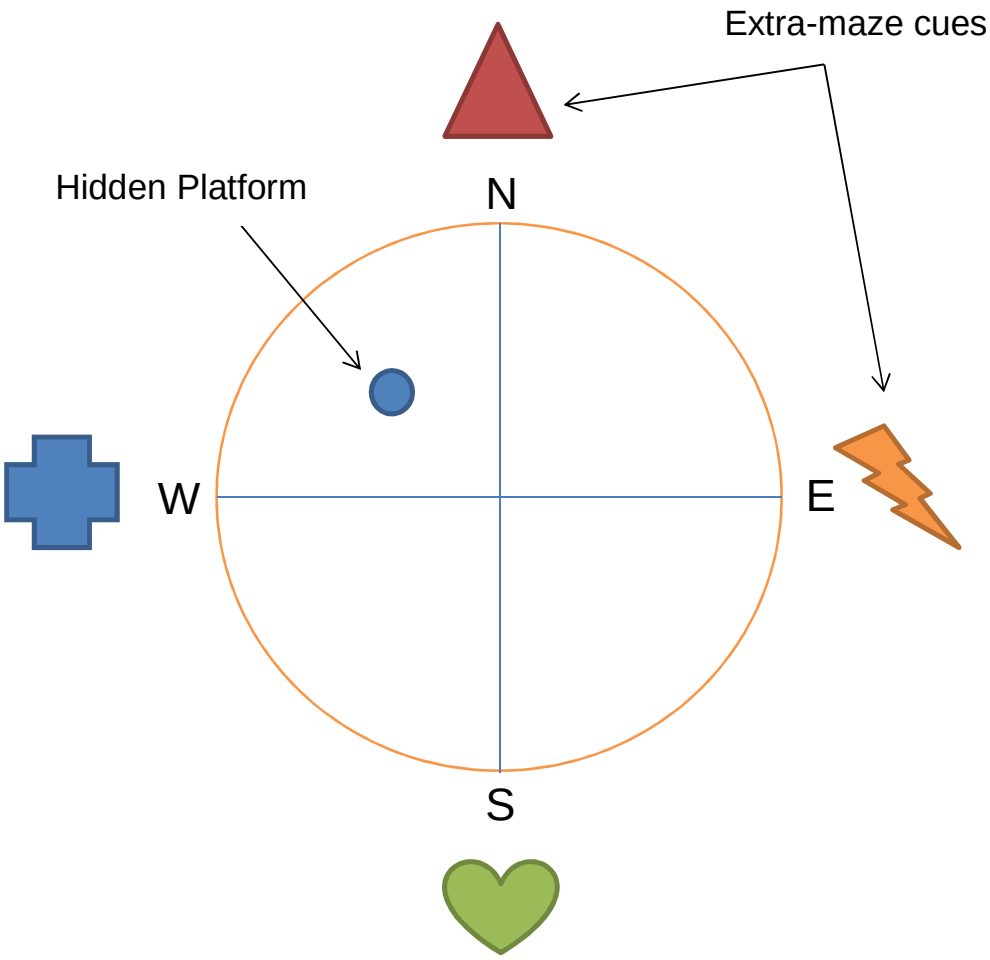

Figure 2.1 Illustration of Spatial Learning Water Maze Set-Up

A pool 2m in diameter and 60cm in height painted white was used. The pool was filled with water (25^{o}C ± 2) and rendered opaque by the addition of liquid latex (SBR polymer). The pool was arbitrarily divided into 4 quadrants – North West, South West, North East and South East. Extra-maze cues were placed around the pool during spatial learning.

2.2.3.2 Visual Training Procedure

Mice were required to locate a hidden submerged platform 10cm in diameter marked by a visual cue (a lego wall). Curtains were drawn around the pool to prevent the use of extra maze spatial cues during location of the platform. Four trials each day were performed over a period of 3 days. Starting position was varied between trials and days. Platform position was varied between days. Each trial was ended after 120s or when the platform was correctly located and mounted. If mice were not able to locate the platform after 120s they were guided to the platform. Once on the platform, mice were left there for 30s.

2.2.3.3 Spatial Learning Test Procedure

Following the 3 days of visual training, mice were tested for spatial reference memory. The test consisted of 5 days of training with 4 trials a day, followed by a probe test 24hours after the final training trial. Within each trial, mice were required to locate a hidden submerged platform 10cm in diameter. Curtains around the pool were pulled open so that extra maze spatial cues could be seen around the room. The position of the platform was not changed throughout the test. Starting positions were varied between trials and days to ensure the use of spatial cues to locate the platform. Each trial was ended after 120s or when the platform was correctly located and mounted. If mice were not able to locate the platform after 120s they were guided to the platform. Once on the platform, mice were left there for 30s.

A probe test was conducted 24 hours after the final spatial training trial. For the test, mice were placed in the pool for 60s in the absence of a platform. Water maze image

tracking software recorded the above measures for the 60s in addition to percentage zone time, where the zone was a 7.5cm radius around the platform.

2.2.3.4 Animals

At each age point, mice were included for testing in the water maze if they were physically able, regardless of performance. Mice with obvious visual impairments (such as the development of cataracts) and physical limitations as a result of age or sickness were not tested.

2.2.3.5 Morris Water maze Data

Following initial water maze testing at 6-9 months of age, a minimum criterion was established in order to exclude, from the longitudinal data analyses, mice failing to develop a spatial strategy after extended training. Performance incompetent mice were excluded by the following criteria: 1) outliers in the last block of visible platform training (visible training day 3) with escape latencies ≥ 2 SDs above the mean escape latency of wild-type mice; 2) consistently failing to follow the escape scoop upon failure to find the platform within the 2 minute trial; 3) failing to swim over the 5 acquisition training days (i.e. mice floating for the duration of the trial with no sign of goal directed swimming); and 4) failure to swim over the previous location of the platform (location of the platform over the 5 acquisition training days) during the 60 second probe trial. Over the course of the longitudinal study, mice exhibiting changes limiting their ability to perform competently in the water maze (e.g. development of cataracts) were also excluded from the group.

Accordingly, 4 wild-type mice and 5 11β-HSD1$^{-/-}$ mice were excluded from group analysis after failing to cross the previous platform location following 5 days (20

trials) of spatial acquisition training. The remaining 11β-HSD1$^{-/-}$ (n = 14) and wild-type (n = 14) met the inclusion criteria and were assessed when they were young (6-9 months), middle-aged (12-15 months) and aged (18-24 months).

Two principle measures of spatial performance were recorded on a given trial: 1) Time taken to find the platform (latency to escape); and 2) Distance travelled before escape onto hidden platform. Changes in spatial learning with age were assessed by examining the time taken for mice to escape onto a hidden platform and the distance travelled before escape over successive acquisition training trials when they were young (6-9 months), middle-aged (12-15 months) and aged (18-24 months).

Long-term spatial memory was then assessed utilising a probe trial 24hours following their final acquisition trial. A long interval between the last training trial and the probe trial is essential if long-term spatial memory is to be determined independent of the memory of the last acquisition training session. Mice were placed in the water maze with no platform and their swim paths monitored over 60 seconds to examine their retention and retrieval of the platform location over the 5 training days and their response to the absence of a platform in the expected location. For analysis the water maze was divided into four quadrants: 1) the target quadrant, the quadrant where the platform had been located during training; 2) quadrant 2, the quadrant next to the target quadrant in a clockwise direction; 3) quadrant 3, the quadrant opposite the target quadrant; and 4) quadrant 4, the quadrant next to the target quadrant in an anti-clockwise direction. The primary measures of long-term spatial memory are latency to the target zone (the circular region where the platform was) and time spent in the target quadrant with shorter latencies to the target zone

and a longer percentage of time spent in the target quadrant [greater than predicted by chance (25%)] indicating retention of spatial reference memory.

2.2.4 Radial Arm Water Maze

2.2.4.1 Apparatus

Following the spatial reference training, mice were tested for spatial reference working memory. The radial arm water maze was chosen over the typical radial arm maze to assess spatial reference working memory as mice were trained to swim in the pool following the Morris water maze. As such, the need for food deprivation and further training, as would have been required in other versions of the radial arm maze, were eliminated and the number of confounding factors reduced. Previous studies have established the radial arm water maze as a robust measure of spatial reference working memory.

For this test, white acrylic inserts were placed into the tank, as described above, to create eight arms coming out from the central region of the tank (Figure 2.2).

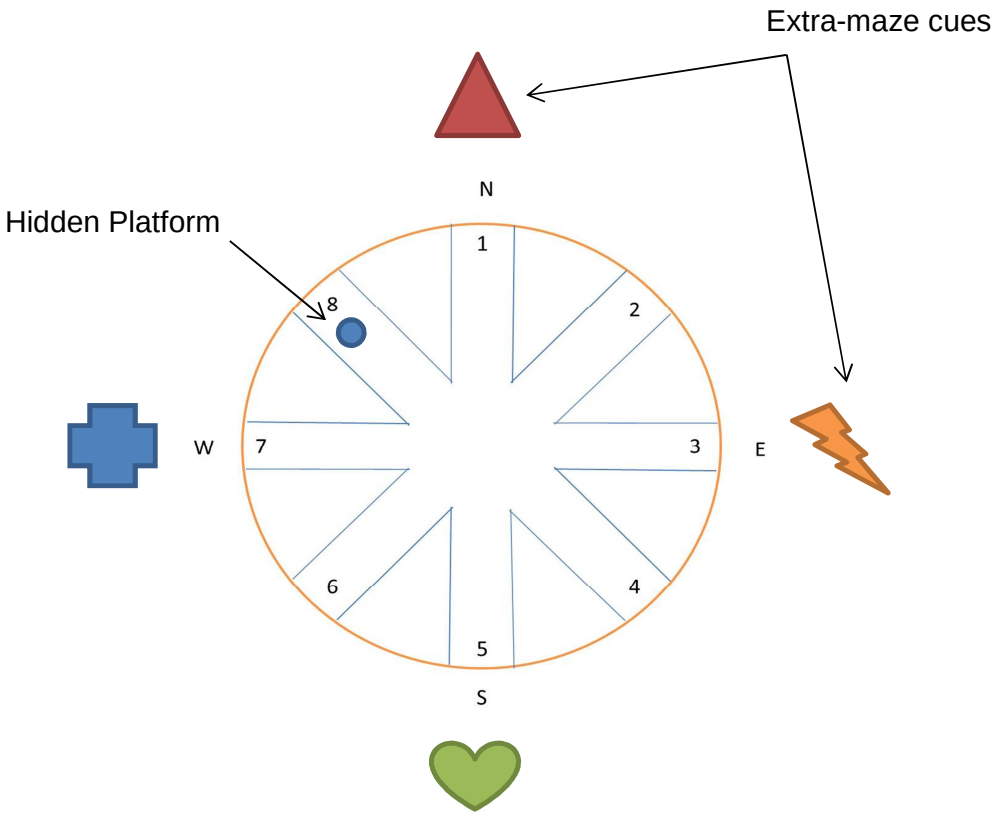

Figure 2.2 Illustration of Radial Arm Maze Set-Up

Acrylic inserts were used to divide the tank into 8 arms coming out from a central region of the tank. The arms were labelled as above, with the North arm labelled as Arm 1 and other arms labelled consecutively in a clockwise direction. For each day a platform was placed at the end of one of the arms, 8cm from the side of the wall.

2.2.4.2 Spatial Working Memory Test Procedure

The test consisted of 6 days of training with 5 trials a day. Within each trial, mice were required to locate a hidden submerged platform 10cm in diameter placed at the end of one of the eight arms and 8cm from the tank wall. Curtains around the pool were pulled open so that extra-maze spatial cues could be seen around the room. The position of the platform was changed between days but remained in the same position within the trials of the day. Starting positions were varied between trials and days to ensure the use of spatial cues to locate the platform.

Between the first and second trial each day there was a retention interval. The ITI between the remaining trials was 20mins. Each trial was ended after 120s or when the platform was correctly located and mounted. If mice were not able to locate the platform after 120s they were guided to the platform. Once on the platform, mice were left there for 30s.

At 6 months of age, a retention interval of 1 hour was used across all 6 days of training. However, at 12 and 18 months of age, a shorter and longer retention interval was included. Therefore, over the first 2 days of the task, a 15 minute retention interval was used between the first and second trial. This was followed by two days with a 1 hour retention interval and a final two days with a 2 hour retention interval.

Water maze image tracking software recorded the above measures for the 120s in addition to the following measures taken manually: 1) Number of Errors (where one error was taken as a full body entry into an incorrect arm or entry into the correct arm without locating the platform); and 2) Number of entries into previous day's target arm.

2.2.4.3 Animals

At each age point, mice were included for testing in the radial arm water maze if they were physically able, regardless of performance. Mice with obvious visual impairments (such as the development of cataracts) and physical limitations as a result of age or sickness were not tested.

2.2.4.4 Radial Arm Water maze Data

Spatial working memory was assessed by 4 measures: 1) Latency to escape onto platform; 2) Distance travelled before escape onto platform (swim path length); 3) Errors (incorrect arm entries before escape onto platform); and 4) Savings Data. Data for each trial was averaged over the days with the same retention trial length. Better performance is indicated by shorter escape latencies, shorter swim path lengths, fewer errors and larger savings.

Savings data was calculated by calculating the difference between performance during the acquisition trial and performance on the trial immediately following the retention interval, as assessed by time to platform, number of errors and distance travelled before escape. If performance was worse on the trial following the retention interval in comparison to the acquisition trial, the savings was zero.

2.2.5 Proton Magnetic Resonance Spectroscopy and Imaging (^{1}H-MRS)

2.2.5.1 MR Measurements

Scanning was performed on a 7T Varian/Agilent Technologies Preclinical System with a mouse coil. Scanning sessions started with anatomical scans employing a T2-

weighted fast spin-echo sequence (TR 2500ms; TE 36ms; Echo-train length 8) with contiguous 0.4mm sections (in-plane resolution, 0.15 x 0.15mm). Subsequently, four spectroscopic measurements were performed using the point-resolved spectroscopy (PRESS) technique at short echo time and long repetition time (TR 3000ms; TE 23; NEX 480).

The T1-weighted and T2-weighted images (19 axial slices and 19 coronal slices) were used to place the volume-of-interest (VOI) over a unilateral hippocampal area (Fig. 2.3). Subsequent repositioning of VOIs at different points in time was done by careful three-dimensional visual comparison with the VOI placement for the first session.

The VOI size in the hippocampus was 2.2 x 2.7 x 1.4 mm^3. Before the spectroscopic acquisitions, shimming of magnetic homogeneity and optimisation of water suppression were done. Usually, a linewidth of 14Hz (FWHM) was achieved on the water resonance of the VOI.

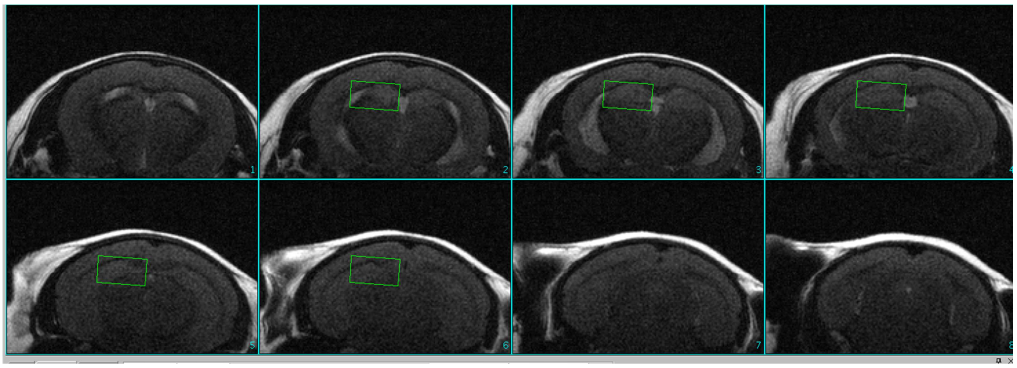

Figure 2.3 Representative coronal section images of the area and size of the voxel taken during MRS scan of the unilateral hippocampus of a wild-type mouse

[Voxel Size: 2.2µm x 2.7µm x 1.5µm, 8.91µl volume]

2.2.5.2 ^{1}H-MRS Analysis

The spectral raw data were analysed user-independently employing the linear combination method (LCModel, Version 6.01, Provencher) with water referencing.

2.2.5.3 Structural Analysis

Hippocampal volume was analysed user-independently using T2-weighted coronal images and software Analyze. Hippocampal, ventricle and total brain structures were manually traced using the software Analyze and volume calculated by multiplying the area of the traced structure by section thickness (0.4mm). Hippocampal volume was then calculated as a percentage of total brain volume.

2.2.6 11β-HSD1 Antibody

2.2.6.1 Sample Preparation

Sheep 11β-HSD1 antibody in serum (obtained from Scott Webster's Laboratory, University of Edinburgh) was prepared for purification by adjusting it to buffer composition by adding 1ml of sample to 5ml of Binding Buffer [20mM Sodium Phosphate, pH7.0: $Na_2HPO_4.2H^2O$, NaH_2PO_4].

2.2.6.2 Purification

Prior to loading sample into purification column (HiTrap Protein GHP, GE Healthcare), column was washed with 10ml of Binding Buffer. Following this, sample was then loaded into the column and subsequently the column was washed again with 10ml of Binding Buffer. Sample was then eluted with Elution Buffer [0.1M Glycine-HCl, pH 2.7] in 1ml fractions into tubes containing 200ul of Tris-HCl, pH 9.0, to preserve the activity of labile IgGs.

2.2.6.3 Characterisation

Protein was extracted from the livers of wild type, 11β-HSD1 liver overexpressor and 11β-HSD1/ApoE double knockout mice. Samples were prepared and run through the western blot protocol described below.

Primary antibodies used were unpurified sheep 11B-HSD1 antibody [1:1000; obtained from Scott Webster], purified sheep 11β-HSD1 antibody [1:1000; purified in Holmes Lab as above], mouse β-tubulin [1:10000]. Secondary antibodies used were anti-sheep AlexaFluor 680 [1:10000; Molecular Probes, A-21101] and anti-mouse IRDye 800 [1:10000; Rockland, USA].

11β-HSD1 was observed to be expressed in the liver of both wild type mice and mice overexpressing 11β-HSD1 in the liver, with higher expression observed in the livers of mice overexpressing 11β-HSD1. 11β-HSD1 was not expressed in the mice with an 11B-HSD1 /ApoE double knockout (Fig. 14).

Comparison of membrane blotted with unpurifed 11B-HSD1 antibody (Fig. 14A) and membrane blotted with purified 11β-HSD1 antibody (Fig. 14B) revealed differences in the specificity of the antibodies. It was observed that purification of the 11β-HSD1 antibody resulted in less bands being observed at sizes other than 34K. However, it was also observed that the purified 11β-HSD1 antibody resulted in lower intensity bands at 34K despite similar intensities in β-tubulin.

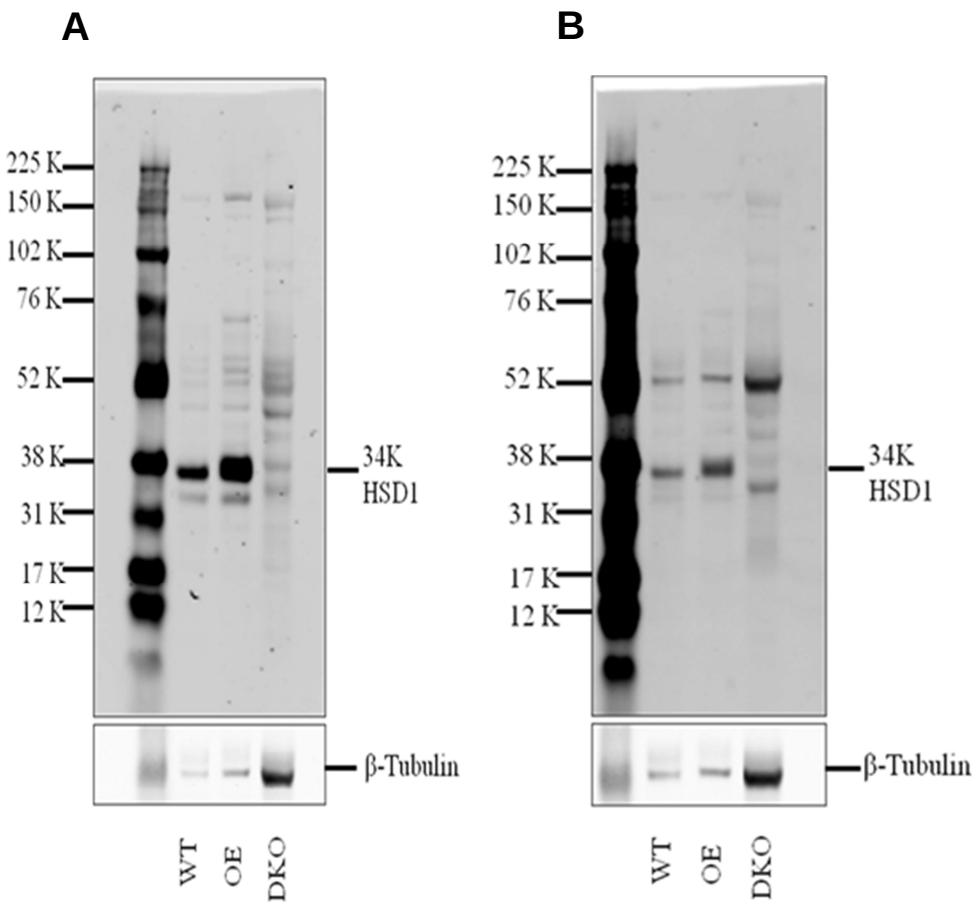

Figure 2.4. Western blot showing the specificity of both the original antibody in serum and purified antibody on liver protein extracts from wild type (WT), HSD1 liver overexpressors (OE) and 11β-HSD1 double knockout (DKO) mice

The antibodies used to assess levels of 11B-HSD1 were able to specifically recognise a 34K band, co-migrating with β-tubulin. **[A]** Representative immunoblot to visualise 11B-HSD1 expression in the livers of wild type mice (WT), mice overexpressing 11B-HSD1 in the liver (OE) and 11B-HSD1 /ApoE double knockout mice (DKO) using unpurified sheep 11B-HSD1 antibody [1:1000, Scott Webster]. **[B]** Representative immunoblot to visualise 11B-HSD1 expression in the livers of wild type mice (WT), mice overexpressing 11B-HSD1 in the liver (OE) and 11B-HSD1 /ApoE double knockout mice (DKO) using purified sheep 11B-HSD1 antibody [1:1000].

2.2.7 Western Blots

2.2.7.1 Protein Extraction

50-100mg of tissue was sliced on dry ice into 2ml eppendorf tubes. Samples were homogenised in 500µl of lysis buffer and placed on a rotator for 1 hour at 4^{o}C. Samples were then spun down at 13,000 rpm for 15mins at 4^{o}C. The supernatant was then pipetted off and placed in a new eppendorf tube and spun down at 13,000rpm for a further 10mins at 4^{o}C.

2.2.7.2 Bradford Protein Assay

Protein concentration of lysates was determined by Bradford Assay (Bio-Rad, USA) as per manufacturer instructions. A standard curve was prepared using BioRad Protein Assay Standard (Bio-Rad, USA)

2.2.7.3 Separation of Proteins by Electrophoresis

Protein extracts were resolved by SDS-PAGE at 120V on precast NuPage 4-12% Bis-Tris polyacrylamide gels (Invitrogen) for 3 hours according to manufacturer instructions.

2.2.7.4 Transfer of Proteins

Following electrophoresis, a transfer sandwich was made using 0.2um nitrocellulose membranes [2x sponge/ 1x blotting paper/ gel/ 1x nitrocellulose membrane/ 1x blotting paper/ 2x sponge]. Transfer sandwich was loaded into transfer tank (BioRad) and tank filled with Transfer Buffer [Trizma Base, Glycine, Methanol, dH_2O]. Transfer was performed at 30V for 1 hour at 4^{o}C. Following transfer, membrane was stained with Ponceau Stain to confirm successful transfer of proteins.

2.2.7.5 Immunoblotting

Membrane was blocked in 5% non-fat dry milk in TBSTw Buffer [27% Tris, 89% NaCl pH 7.6, 0.1% Tween-20] for 30mins at room temperature and subsequently washed incubated with primary antibody diluted in 5% semi-skimmed milk in TBSTw for 1 hour and then washed 3 times in TBSTw for 10 minutes each wash. Following this membrane was incubated with secondary antibody diluted in 5% semi-skimmed milk in TBSTw for 1hour at room temperature and then washed in TBSTw 2 times for 10 minutes each before a final 10 minute was in TBS [27% Tris, 89% NaCl pH 7.6]. The membrane was scanned and band intensities were quantified using the Odyssey infrared imaging system (Licor Biosciences; Lincoln, NE).

2.2.8 Immunohistochemistry

2.2.8.1 Optimisation of Immunohistochemistry

In order to determine the optimal conditions for immunohistochemistry on brain sections, a variety of conditions were tested. Three types of sections were tested: 1) Paraffin-Wax embedded; 2) Free-Floating; and 3) Fresh Frozen. Additionally, two types of slides were tested: 1) Silane coated; and 2) Superfrost slides. Finally, three protocols were tested: 1) Streptavidin-DAB; 2) Streptavidin-Fluorescent; and 3) Immunofluorescence.

Trials carried out on Paraffin-Wax embedded sections found no positive staining for 11B-HSD1 or Cd11B in either the Streptavidin-Fluorescent and Immunofluorescent protocol. In the Streptavidin-DAB protocol, brown staining did occur, however, this staining was also observed on both the primary and negative control.

Trials utilising Fresh Frozen sections were successful, when staining for 11B-HSD1 and Cd11B using the immunofluorescence protocol. Positive staining was observed in both the cerebellum and hippocampus of the brain. However, brain morphology was sometimes damaged and brain sections often had 'holes' in them following cryostating.

Trials carried out using Free-Floating sections were successful, when staining for 11B-HSD1 and Cd11B using the immunofluorescence protocol. Positive staining was observed in both the cerebellum and hippocampus of the brain. As brains had been fixed prior to cryostating, sections were more robust than fresh frozen sections with less damage to the sections observed in the immunohistochemistry process. As such, this method was chosen and is detailed below.

2.2.8.2 Tissue Preparation

Brain samples were left in 4% PFA for 2 days before being removed and placed in a 30% sucrose solution. After 4 days, samples were removed from the sucrose solution and frozen on dry ice before being stored at -80^{o}C.

Brains were subsequently sectioned at 30um thickness into cryoprotectant [Sucrose, 0.1M PBS, Ethylene Glycol] and stored at -20^{o}C.

2.2.8.3 Double Immunofluorescence for Free-Floating Sections

Sections were washed in PBS and then underwent antigen retrieval in sodium citrate buffer (0.01M, pH 8.5) for 30 minutes at 80^{o}C in a water bath. Sections were subsequently left to cool and then washed in PBS before undergoing permeabilization in 0.3% PBT (PBS plus 0.3% Triton-X 100) for 15 minutes and blocking in 10% normal serum in 0.3% PBT for 30 minutes. Sections were then

incubated with both primary antibodies diluted in the same blocking solution overnight at 4^{o}C. To ensure no cross-reactivity occurred, primary antibodies raised in different species were chosen. Following this, sections were washed in PBS and then incubated with both secondary antibodies diluted in 1% normal serum in 0.3% PBT for 1 hour at room temperature. From this point onwards, sections were kept in a foil covered container or dark box to block out the light and prevent photo bleaching. Samples were then washed in PBS and incubated with TOPRO for 10 minutes at room temperature and then washed in PBS again. Sections were then floated onto a slide and left to air dry in a dark box. Following drying, sections were mounted in aqueous mounting media and cover slipped.

Sections were stained for 11β-HSD1, microglia, neuron and glial expression using primary antibodies sheep purified 11β-HSD1 [1:1000; Obtained from Scott Webster and purified as above in Holmes Lab], Rabbit Iba-1 [1:500; Wako, 019-19741], Mouse NeuN [1:500, Millipore, MAB377] and Rabbit GFAP [1:500, Sigma, G9269-2ML] and secondary antibodies donkey anti-Sheep Alexa Fluor 488 [1:500; Invitrogen, A110015], donkey anti-Rabbit Alexa Fluor 555 [1:500; Invitrogen, A31572], donkey anti-Mouse Alexa Fluor 555 [1:500; Invitrogen, A31570] and donkey anti-Rabbit Alexa Fluor 555 [1:500; Invitrogen, A31572] respectively. Double immunofluorescent stains were conducted on the following combinations: 1) 11β-HSD1 and Iba-1; 2) 11β-HSD1 and NeuN; and 3) 11β-HSD1 and GFAP.

2.2.8.4 Immunofluorescent Quantification

Samples were analysed under an Axioskop microscope (Carl Zeiss Ltd, Welwyn Garden City) at x30 magnification. Three fields per hippocampal and cortex subregion were taken and analysed as below.

Images were then quantified using ImageJ software and area measurements. Images from a wild-type/control mouse were used to select a threshold for the fluorescence of the target protein being quantified. The area of fluorescence meeting settings was then calculated as a percentage of the total area of the image.

Where specified, images were also quantified through cell counting.

Data was averaged over the three fields per subregion.

2.2.9 Quantitative PCR (qPCR)

2.2.9.1 RNA Extraction

RNA was extracted from mice brains using the QIAgen RNAeasy Kit according to manufacturer instructions with the DNase step included.

2.2.9.2 Reverse Transcription-PCR

RNA samples were used for RT-PCR to produce cDNA. Samples underwent reverse transcription using SuperScript III First Strand Synthesis System according to manufacturer instructions.

2.2.9.3 Quantitative-PCR

RT-PCR products were then used for qPCR to quantify 11β-HSD1 and cytokine levels. A standard curve was prepared by mixing equal volumes of all cDNA

samples and serially diluting from 1:8 to 1:512. cDNA samples were diluted 1:20 before adding to reaction mix. The reaction mix was prepared as follows: 5µl Lightcycler480 Master-Mix (Roche; Burgess Hill, UK), 0.1µl For primer, 0.1µl Rev primer, 0.1µl primer-probe (Applied Biosystems; Warrington, UK) and 2.7µl of RNase-free H_2O per sample. The reaction mix was then added to the plate in triplicate, followed by 2µl of cDNA. Plates were then sealed and centrifuged at 2000g for 2 minutes. Negative controls were included in each plate to ensure no contamination had taken place. Internal controls included housekeeping genes HPRT and GAPDH.

2.2.9.4 Data Analysis

The LightCycler software provided relative quantification using the maximum second derivative method, where a fractional cycle (Cp) is determined from the amplification curve's second derivative max indicating the cycle at which exponential amplification can no longer be sustained and starts to decline towards linear growth. The standard curve was used as a reference for extrapolating quantitative information for mRNA targets of unknown concentrations.

2.2.10 Statistical Analysis

For statistical analysis, GraphPad Prism 5 was used.

Comparisons between 2 groups (e.g. 11β-HSD1$^{-/-}$ versus WT) were made by Student's t-test (unpaired).

For the analysis of performance over a period of time, a two-way repeated measures ANOVA with Tukey's post-hoc test was used.

Correlations were determined using Pearson's correlation.

Values are shown as means ± SEM. Significance was set as $p<0.05$. Full details of statistical analyses are contained within in each chapter.

Chapter 3 : Distinct Roles for 11B-HSD1 on Spatial Learning and Memory and Spatial Working Memory Impairment

3.1 Introduction

Cognitive impairment is often observed in ageing and mild cognitive impairment is associated with dementia. However, within the population there is a large variation in the occurrence and rate of progression of cognitive impairment with age.

Studies have shown that these variations can be attributed, in part, to glucocorticoids where elevated glucocorticoids in ageing with adverse effects on hippocampal structure and vulnerability (Landfield et al., 2007). 11β-HSD1 catalyses the reduction of 11-keto derivatives to active glucocorticoids, amplifying intracellular glucocorticoid levels. In particular and of importance to this project, 11β-HSD1 is expressed abundantly in the hippocampus and frontal cortex of the brain (Moisan et al., 1990) – key structures in cognition and executive function.

Investigations have suggested that inhibition of 11β-HSD1 may attenuate the deleterious effects of glucocorticoids on cognitive function and brain integrity in ageing. Yau et al. (2001) found that in 11β-HSD1 knockout mice, despite elevated basal corticosterone levels, aged mice showed significantly lower hippocampal corticosterone levels when compared to aged wild-type mice. In addition to this, it was observed that whilst aged wild-type mice experienced spatial learning deficits

associated with elevated glucocorticoid levels, an attenuated learning deficit was observed in aged knockout mice.

Further studies revealed better spatial memory is correlated with enhanced long-term potentiation in hippocampal slices of 11β-HSD1 knockout mice compared to age matched wild-type controls (Yau et al., 2007). Additionally, the inhibition of 11β-HSDs has been associated with improved memory and cognitive function in healthy elderly humans (Sandeep et al., 2004) and more recent studies have suggested a predictive link between 11β-HSD1 activity, progressive brain atrophy and cognitive decline (MacLullich et al., 2010). Sooy et al. (2010) have also demonstrated that specific inhibition of 11β-HSD1 in C57BL/6J mice results in the prevention of age-related spatial memory impairments.

Nevertheless, normal age-associated memory decline is not uniform. Studies have indicated differences in both the type of memory impaired with age and the age of onset of memory decline. Whilst older adults exhibit impairments in spatial and episodic memory - finding one's way around an environment and remembering the events that occur within it – a marked decline in working memory has also been observed in ageing.

Working memory is the capacity to temporarily keep in mind information from previous experiences in order to monitor and manipulate new information for a specific goal. Working memory is therefore essential to integrate different information for planning and for goal-directed, purposeful action such as everyday decision-making and problem-solving. Results from cross-sectional and longitudinal studies suggest that subtle memory changes can begin as early as the early or middle

twenties and continue to decline linearly with age. Hence, performance on tasks of episodic and working memory decline in the twenties and continue to decline linearly across the life span (Park et al., 1996, 2002).

Previous studies have established significant effects of glucocorticoids on working memory function, namely, working memory is impaired following both acute and chronic glucocorticoid administration (Diamond et al., 1996; Barsegyan et al., 2010). However, little work has been done on the effects of intracellular glucocorticoid levels on age-associated working memory processes. Although elevated intracellular glucocorticoid levels have been associated with age-associated hippocampal dependent learning and memory impairments, they may have distinct effects on working memory processes during ageing. Furthermore, the effect of 11β-HSD1 removal on cognitive processes has only ever been examined cross-sectionally preventing the effects of intracellular glucocorticoid levels on age-associated cognitive decline to be examined over the entire lifespan of an animal. Therefore, this chapter reports the longitudinal effects of lifelong removal of 11β-HSD1 on learning and memory processes and working memory processes with age by examining 11β-HSD1$^{-/-}$ and their wild-type counterparts in the water maze and radial arm water maze over the span of 24 months.

3.2 Methods

3.2.1 Animals

Male 11β-HSD1$^{-/-}$ mice and their wild-type littermates were maintained in standard cages upon controlled lighting (12h:12h, lights on at 7.00), were fed a standard chow and given water ad libitum as described in Chapter 2.

At 6, 12, 18 and 22 months of age, animals underwent behavioural testing and subsequently tail nicked for plasma samples.

Figure 3.1 illustrates the number of animals tested at each age in the water maze and radial arm water maze. At 6 months, no mice were excluded from testing. At 12 months, one mouse was excluded from testing following the development of cataracts. At 18 months, one wild-type mouse died. At 24 months, 3 wild-type mice and 7 11β-HSD1$^{-/-}$ mice died from age related factors or were terminated following the development of tumours. At 24 months, mice were considered too frail to undergo radial arm water maze testing following the initial water maze testing and as such, none were tested in the radial arm water maze.

Wild-type	**n=18**	**n=18**	**n=17**	**n=14**
11β-HSD1$^{-/-}$	**n=19**	**n=18**	**n=17**	**n=10**

Figure 3.1. Number of wild-type and 11β-HSD1$^{-/-}$ mice tested in the water maze and radial arm water maze at each time point

3.2.2 Morris Water maze

Spatial learning and memory was assessed at 6, 12, 18 and 22 months of age in the Morris Water maze (MWM) as outlined in Chapter 2.

Following water maze testing at 6 months of age, a minimum criterion was established to exclude from analysis those mice failing to develop a spatial strategy and demonstrate long-term retention of spatial memory.

Figure 3.2 below illustrates the number of mice included in analysis at each age in the water maze and radial arm water maze. At 6 months, 3 wild-type and 4 11β-HSD1$^{-/-}$ mice were permanently excluded from analysis after failing to meet the inclusion criteria stated in Chapter 2. The data from these same mice were analysed at 12, 18 and 24 months if available (some data was not available at later ages following death due to age related disease or sickness).

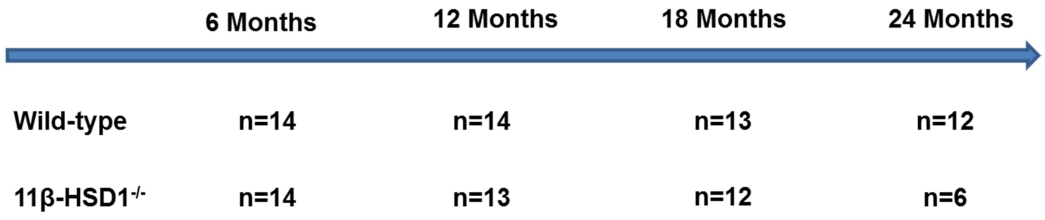

Figure 3.2. Number of wild-type and 11β-HSD1$^{-/-}$ mice analysed in the water maze and radial arm water maze at each time point.

3.2.3 Radial Arm Water Maze

Spatial working memory was assessed at 6, 12 and 18 months of age in the Morris Water maze (MWM) as outlined in Chapter 2.

3.2.4 Statistical Analysis

Two-way repeated measures ANOVA with Tukey's post-hoc test was used to analyse performance of wild-type and 11β-HSD1$^{-/-}$ mice over the testing period and longitudinally over the lifespan.

A two-way ANOVA with variables, quadrant and genotype, was used to analyse the time spent swimming in each quadrant of the water maze and an unpaired t-test used to analyse differences in latency to platform between genotypes.

3.3 Results

3.3.1 Water Maze Results

3.3.1.1 Young

Both wild-type and 11β-HSD1$^{-/-}$ animals learned to find the platform during visual training with a decrease in latency to platform [$F(2, 70) = 97.36$, $p < 0.0001$].

When young (6 months), wild-type and 11β-HSD1$^{-/-}$ mice showed a progressive reduction in the latency to escape onto a hidden platform over the 5 training days [$F(4, 104) = 28.07$, $p < 0.001$; Fig. 3.3A]. Swim path data recapitulated escape latency results with a progressive reduction in swim path length over the 5 training days in both genotypes [$F(4, 104) = 30.98$, $p < 0.001$; Fig. 3.3B]. No difference in escape latency [$F(1, 26) = 0.07269$, $p = 0.7896$; Fig. 3.3A] nor swim path length [$F(1, 26) = 0.16$, $p = 0.689$; Fig. 3.3B] was observed between genotypes. These results were observed independent of swim speed and indicate good spatial learning in both wild-type and 11β-HSD1$^{-/-}$ mice when young.

Analysis of all mice, including mice not meeting the inclusion criteria, revealed similar results showing a progressive reduction in the latency to escape onto a hidden platform over the 5 training days [$F(4, 140) = 39.21$, $p < 0.0001$] and distance travelled in both genotypes [$F(4, 140) = 44.13$, $p < 0.0001$]. No difference in escape latency [$F(1, 35) = 0.01887$, $p = 0.8915$] nor swim path length [$F(1, 35) = 0.3074$, $p = 0.5828$] was observed between genotypes.

There was no difference in latency savings between the first trial and second trial in wild-type and 11β-HSD1$^{-/-}$ mice [11β-HSD1$^{-/-}$: M = 21.01, SD = 5.158; wild-type: M = 23.22, SD = 5.877; t(26) = 0.2824, p = 0.7799].

3.3.1.2 Middle-Age

Both wild-type and 11β-HSD1$^{-/-}$ animals learned to find the platform during acquisition when middle-aged (12 months), as indicated by a decrease in latency over training days [F (3, 75) = 29.25, p < 0.0001; Fig. 3.4A] and a decrease in swim path length [F (3, 75) = 31.36, p < 0.0001; Fig. 3.4B] over training days. Escape latencies [F (1, 25) = 1.792, p = 0.8582; Fig. 3.4A] and swim path length [F (1, 25) = 0.1179, p = 0.7342; Fig. 3.4B] did not differ between the wild-type and 11β-HSD1$^{-/-}$ mice, indicating that spatial learning was not affected by genotype at this age.

Analysis of all mice, including mice not meeting the inclusion criteria, revealed similar results showing a progressive reduction in the latency to escape onto a hidden platform over the 5 training days [F (3, 102) = 38.40, p < 0.0001] and distance travelled in both genotypes [F (3, 102) = 38.84, p < 0.0001]. No difference in escape latency [F (1, 34) = 0.002263, p = 0.9623] nor swim path length [F (1, 34) = 0.1262, p = 0.7246] was observed between genotypes.

There was no difference in latency savings between the first trial and second trial in wild-type and 11β-HSD1$^{-/-}$ mice [11β-HSD1$^{-/-}$: M = 0.6339, SD = 0.2582; wild-type: M = 0.2963, SD = 0.1308; t(25) = 1.192, p = 0.2444].

Figure 3.3. Water Maze performance in Young Wild-type (WT) and 11β-HSD1$^{-/-}$ (KO) mice

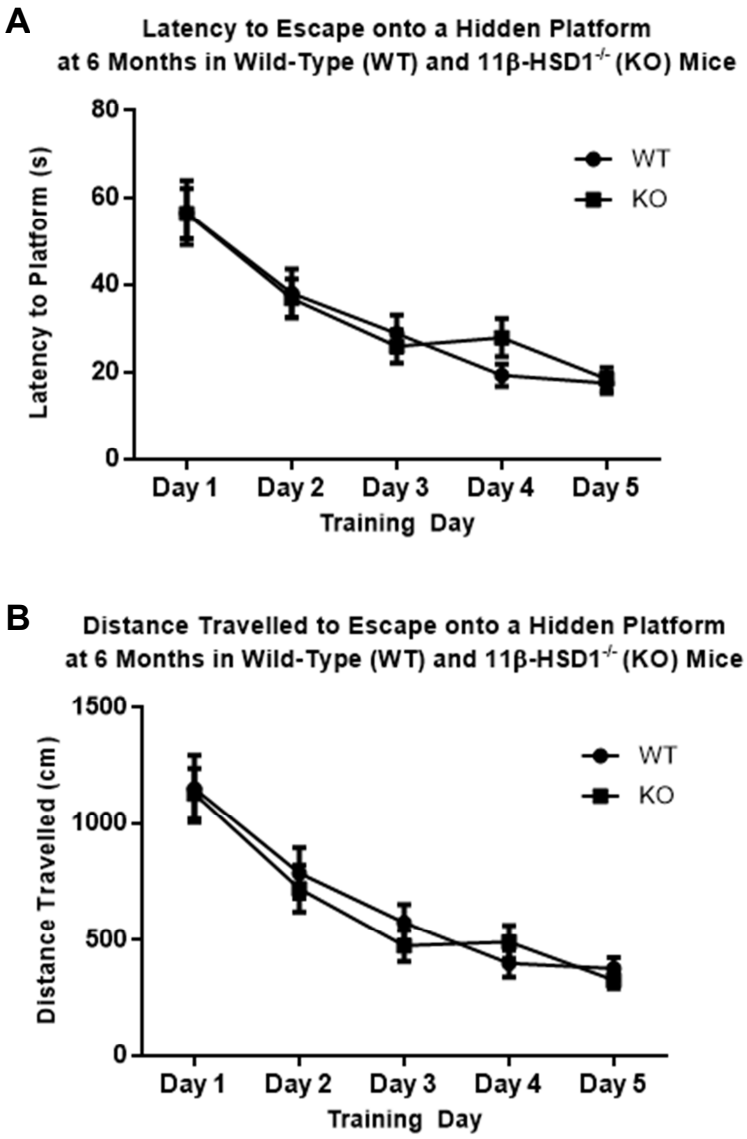

Fig. 3.3. Graphs showing unimpaired water maze performance in young wild-type mice (WT; n = 14) and 11β-HSD1$^{-/-}$ mice (KO; n = 14) as measured by **[A]** the latency to escape onto the hidden platform; and **[B]** the distance travelled before escape (swim path length). A significant effect of training day was observed. No effect of genotype was observed. Values represent average latency and swim path length taken over 4 trials each day +SEM.

Figure 3.4. Water Maze performance in Middle-Aged Wild-type (WT) and 11β-HSD1$^{-/-}$ (KO) mice

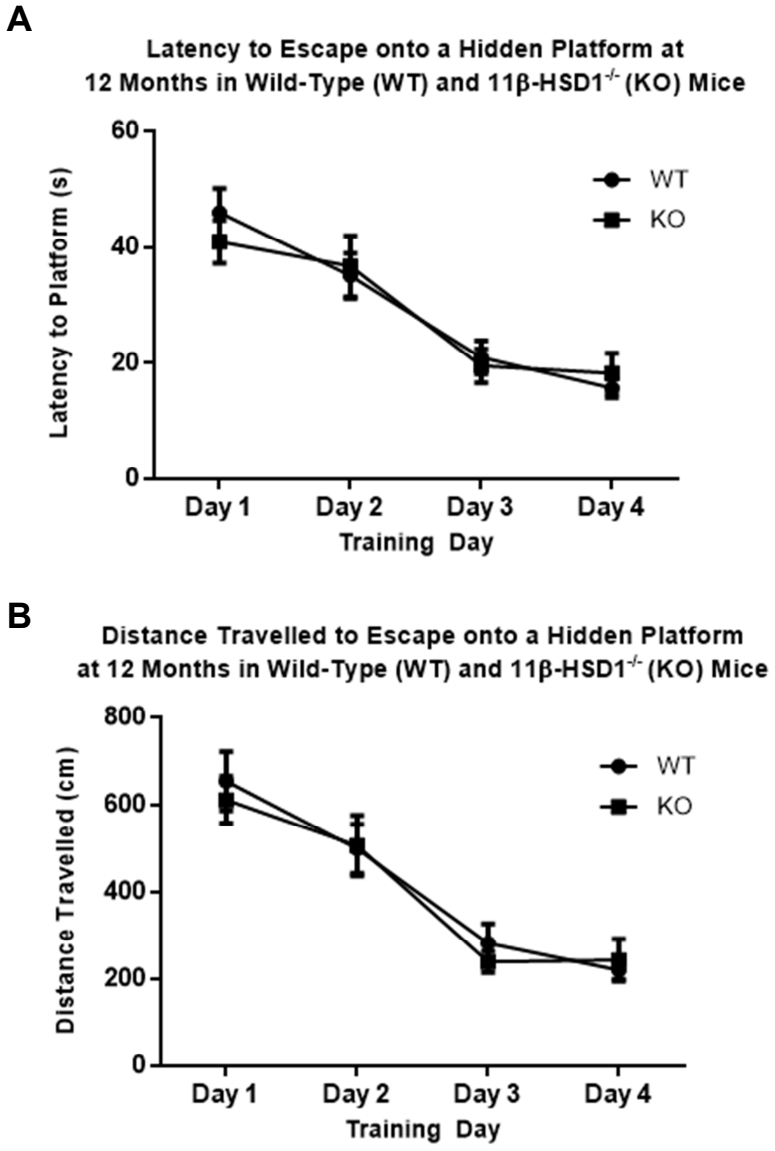

Fig. 3.4. Graphs showing unimpaired water maze performance in middle-aged wild-type mice (WT; n = 14) and 11β-HSD1$^{-/-}$ mice (KO; n = 13) as measured by **[A]** the latency to escape onto the hidden platform; and **[B]** the distance travelled before escape (swim path length). A significant effect of training day was observed. No effect of genotype was observed. Values represent average latency and swim path length taken over 4 trials each day +SEM.

3.3.1.3 Aged

At 18 months, both wild-type and 11β-HSD1$^{-/-}$ animals were able to find the platform following a visual cue. No decrease was observed over the visual training days as mice were able to locate the platform quickly from the first day [F (1, 33) = 0.8319, p=0.3684].

When aged (18 months), swim speed of the mice decreased across training days [F (4, 92) = 5.02, p = 0.0011; Fig. 3.5] with no effect of genotype on swim speed [F (1, 23) = 0.00096, p = 0.9755; Fig. 3.5]. As swim speed would have a significant effect on the latency to escape, the distance travelled before escape onto the hidden platform was analysed to provide a measure of spatial learning independent of swim speed at 18 months of age. As seen when young and middle-aged, an effect of training day on swim path length in the water maze [F (4, 92) = 8.73, p < 0.0001; Fig. 3.6] and no effect of genotype on swim path length [F (1, 23) = 0.30, p = 0.5885; Fig. 3.6] was observed indicating that spatial learning was not affected by genotype at this age.

Analysis of all mice, including mice not meeting the inclusion criteria, revealed similar results showing a progressive reduction in the latency to escape onto a hidden platform over the 5 training days [F (4, 128) = 19.61, p < 0.0001] and distance travelled in both genotypes [F (4, 128) = 15.29, p < 0.0001]. No difference in escape latency [F (1, 32) = 0.4619, p = 0.5016] nor swim path length [F (1, 32) = 0.1087, p = 0.7438] was observed between genotypes.

There was no difference in latency savings between the first trial and second trial in wild-type and 11β-HSD1$^{-/-}$ mice [11β-HSD1$^{-/-}$: M = 17.64, SD = 5.119; wild-type: M = 11.35, SD = 3.596; t(23) = 1.017, p = 0.3197].

At 24 months, both wild-type and 11β-HSD1$^{-/-}$ animals were able to find the platform following a visual cue. No decrease was observed over the visual training days as mice were able to locate the platform quickly from the first day [F (1, 25) = 2.038, p=0.1658].

At the final testing at 24 months of age, a general decrease in latency over the 5 training days [F (4, 64) = 12.15, p < 0.0001; Fig. 3.7A] and no effect of genotype on latency to escape [F (1, 64) = 0.47, p = 0.503; Fig. 3.7A] was observed, post hoc tests revealed that latency to escape in wild-type mice was only significantly reduced in the latter training days whilst 11β-HSD1$^{-/-}$ mice showed significantly shorter latencies on training day 2 onwards. Swim path length supported escape latency results with an overall decrease in swim path length over training days [F (4, 64) = 14.34, p < 0.0001; Fig. 3.7B] and no effect of genotype on swim path length [F (1, 64) = 2.94, p = 0.1057; Fig. 3.7B] indicating no effect of genotype on spatial learning at 24 months of age.

Analysis of all mice, including mice not meeting the inclusion criteria, revealed similar results showing a progressive reduction in the latency to escape onto a hidden platform over the 5 training days [F (4, 88) = 10.31, p < 0.0001] and distance travelled in both genotypes [F (4, 88) = 14.67, p < 0.0001]. No difference in escape latency [F (1, 22) = 0.07977, p = 0.7802] nor swim path length [F (1, 22) = 2.516, p = 0.1269] was observed between genotypes.

There was no difference in latency savings between the first trial and second trial in wild-type and 11β-HSD1$^{-/-}$ mice [11β-HSD1$^{-/-}$: M = 9.438, SD = 3.636; wild-type: M = 23.37, SD = 9.270; t(16) = 1.695, p = 0.1094].

Figure 3.5. Swim speed in 18 Month old Wild-type (WT) and 11β-HSD1$^{-/-}$ (KO) mice

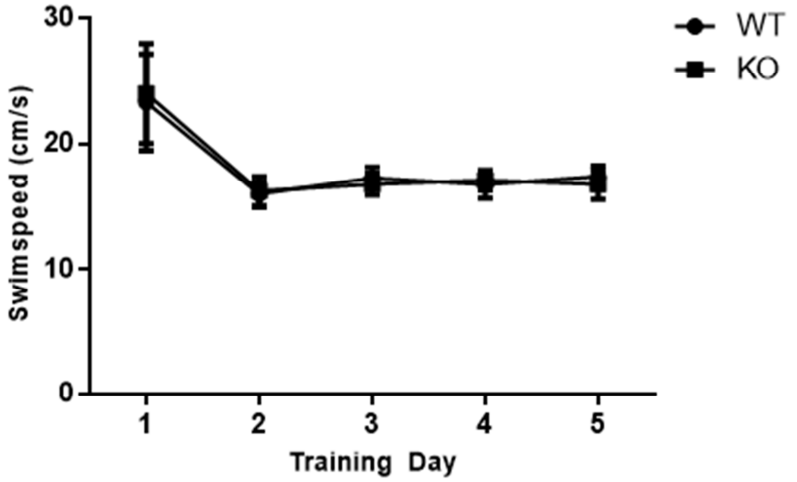

Fig. 3.5. Graph showing swim speed in the water maze over the 5 training days in18 month old wild-type (WT; n = 13) and 11β-HSD1$^{-/-}$ mice (KO; n = 12). A significant effect of training day was observed. No effect of genotype was observed. Values represent the average swim speed over 4 trials per day +SEM.

Figure 3.6. Water Maze performance in 18 Month Aged Wild-type (WT) and 11β-HSD1$^{-/-}$ (KO) mice

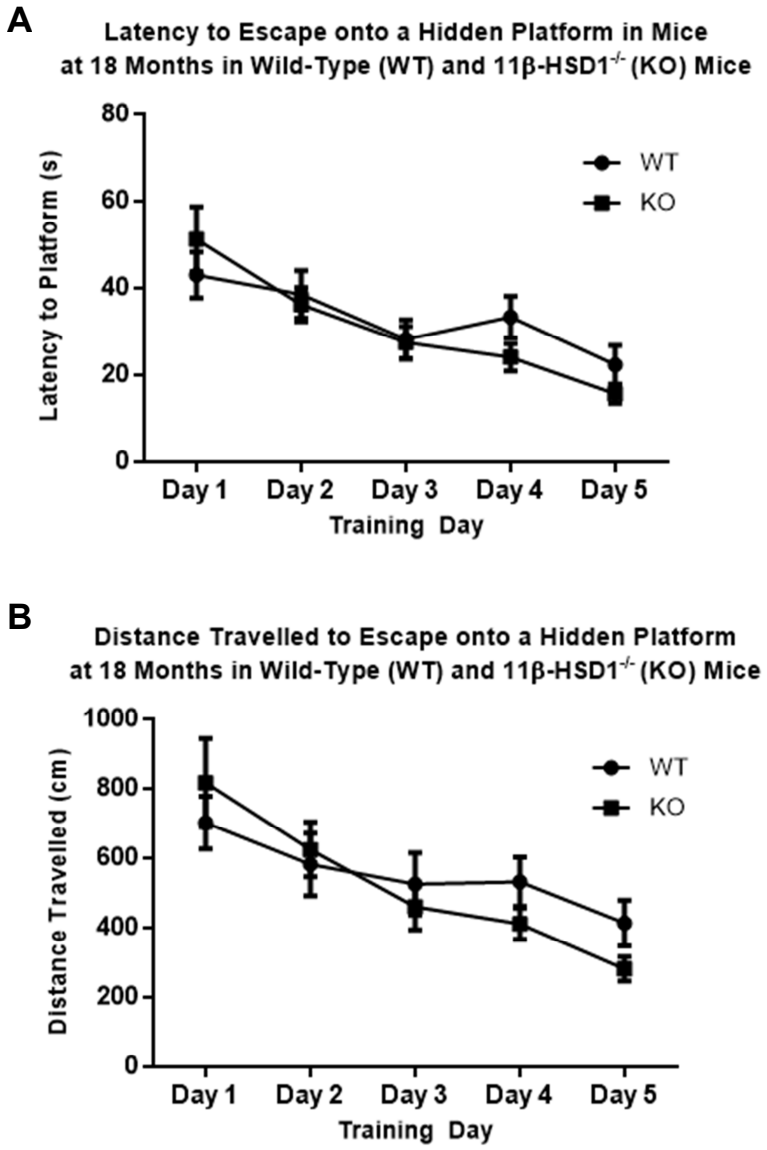

Fig. 3.6. Graphs showing water maze performance in aged wild-type (WT; n = 12) and 11β-HSD1$^{-/-}$ mice (KO; n = 6) as measured by **[A]** the latency to escape onto the hidden platform; and **[B]** the distance travelled before escape (swim path length). A significant effect of training day was observed. No effect of genotype was observed. Values represent average latency and swim path length taken over 4 trials each day +SEM.

Figure 3.7. Water Maze performance in 24 Month old Wild-type (WT) and 11β-HSD1$^{-/-}$ (KO) mice

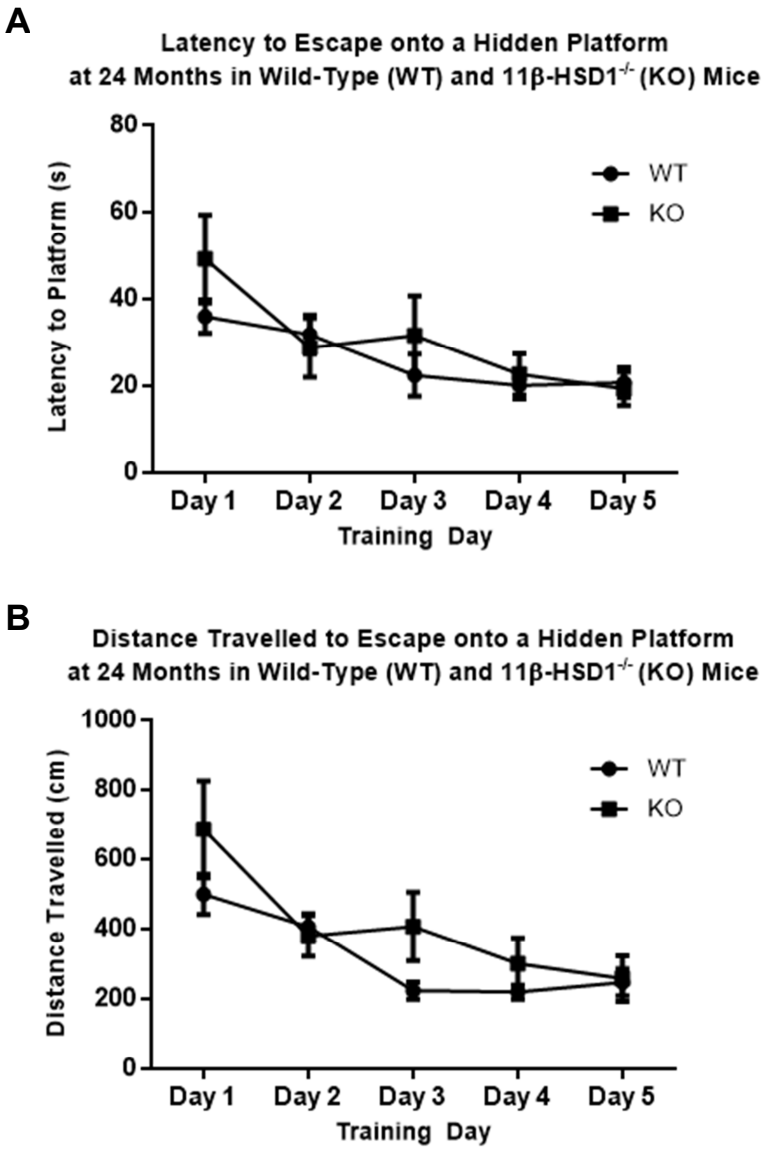

Fig. 3.7. Graphs showing water maze performance in aged wild-type (WT; n = 12) and 11β-HSD1$^{-/-}$ mice (KO; n = 6) as measured by **[A]** the latency to escape onto the hidden platform; and **[B]** the distance travelled before escape (swim path length). A significant effect of training day was observed. No effect of genotype was observed. Values represent average latency and swim path length taken over 4 trials each day +SEM.

3.3.1.4 Ageing Effects

Ageing effects in both wild-type and 11β-HSD1$^{-/-}$ mice were analysed using swim path data throughout the lifespan of the colony. Spatial learning capacities were represented by the total distance covered to locate the hidden platform. A two-way repeated measures ANOVA revealed total swim path length decreased with age in both wild-type and 11β-HSD1$^{-/-}$ mice [$F(3, 48) = 11.82$, $p < 0.0001$; Fig. 3.8] with no effect of genotype [$F(1, 16) = 3.130$, $p = 0.0959$; Fig. 3.8]. In wild-type mice, distance travelled was found to decrease between 6 and 12 months and then again between 18 and 24 months of age [6 vs 12 months, $p < 0.01$; 6 vs 18 months, NS; 12 vs 18 months, NS; 6 vs 24 months, $p < 0.0001$; 12 vs 24 months, NS; 18 vs 24 months, $p < 0.05$]. Interestingly, 11β-HSD1$^{-/-}$ mice showed decreased distance travelled only at 24 months of age [6 vs 24 months, $p < 0.05$; 6 vs 12 months, NS; 6 vs 18 months, NS; 12 vs 18 months, NS; 12 vs 24 months, NS; 18 vs 24 months, NS].

Thus, wild-type and 11β-HSD1$^{-/-}$ mice did not appear to differ in learning capacity throughout life. Moreover, animals appeared to improve their performance with age as revealed by a decrease in the distance covered in both wild-type [$F(3, 36) = 21.90$, $p < 0.0001$] and 11β-HSD1$^{-/-}$ mice [$F(3, 28) = 37.84$, $p < 0.0001$].

Figure 3.8. Longitudinal Water Maze performance in Wild-type (WT) and 11β-HSD1$^{-/-}$ (KO) mice at the ages of 6, 12, 18 and 24 months

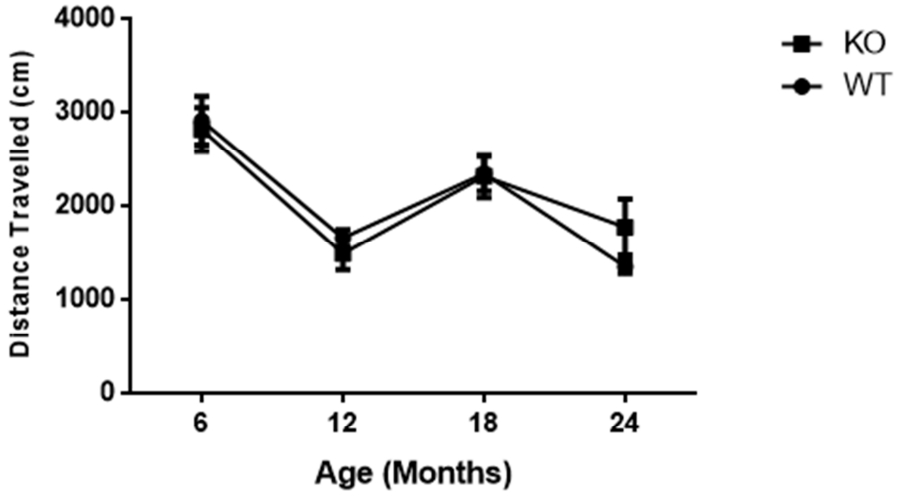

Fig. 3.8. Graph showing improved water maze performance with age in wild-type mice (n = 14) and 11β-HSD1$^{-/-}$ mice (n = 14) as measured by the distance travelled before escape (swim path length). A significant effect of age was observed. No effect of genotype was observed. Values represent average swim path length taken over 4 trials each day +SEM.

3.3.2 Probe Test Results

3.3.2.1 Young

When young, mice spent the greatest percentage time in the target quadrant (i.e. the quadrant where the platform was previously) regardless of genotype. A two-way ANOVA with variables, quadrant and genotype, revealed that young 11β-HSD1$^{-/-}$ and wild-type mice spent the greatest percentage time swimming in the target quadrant compared to the other quadrants [$F(3,104) = 5.789$, $p = 0.0011$; Fig. 3.9A] whilst no effect of genotype was observed [$F(1,104) = 4.6 \times 10^{-10}$, $p > 0.999$; Fig. 3.9A].

In wild-type mice, the percentage time spent swimming in the target quadrant (36.7%) was significantly higher than percentage time spent swimming in quadrant 2 (20%; $p < 0.001$), quadrant 3 (23.3%; $p < 0.01$) and quadrant 4 (20%; $p < 0.001$) [Fig. 3.9A]. However, in young 11β-HSD1$^{-/-}$ mice there was no significant difference in percentage time swimming in the target quadrant compared to quadrants 2, 3 and 4. However, the highest percentage of time swimming was in the target quadrant (28.4%) and greater than predicted by chance indicating memorisation of the platform quadrant.

There was no difference in time taken to swim to the previous platform location between wild-type and 11β-HSD1$^{-/-}$ mice [11β-HSD1$^{-/-}$: $M = 26.6$, $SD = 5.708$; wild-type: $M = 19.4$, $SD = 2.809$; $t(26) = 1.132$, $p = 0.2679$; Fig. 3.9B].

Analysis of all mice, including mice not meeting the inclusion criteria, showed an effect of quadrant [$F(3,140) = 4.035$, $p = 0.0087$] and no effect of genotype was

observed [F (1,140) = 7.367 x 10^{-10}, p > 0.999]. No difference in time taken to swim to the previous platform location between wild-type and 11β-HSD1$^{-/-}$ mice [11β-HSD1$^{-/-}$: M = 35.39, SD = 5.418; wild-type: M = 28.42, SD = 4.632; t(35) = 0.9727, p = 0.3374].

3.3.2.2 Middle-Age

At middle-age, a two-way ANOVA revealed that quadrant had a significant effect on the percentage of time spent swimming in each quadrant [F (3,100) = 10.61, p < 0.0001; Fig. 3.10A] but no effect of genotype on the percentage time spent swimming in the four quadrants [F (1,100) = 3e^{-12}, p > 0.999; Fig. 3.10A]. However, there was a significant interaction between genotype and quadrant [F (3,100) = 3.19, p = 0.0269] suggesting that there are varying effects of genotype on time spent in each quadrant.

Converse to what was observed when young, middle-aged wild-type mice spent less time in the target quadrant. Whilst the percentage time spent swimming in the target quadrant (29.8%) differed significantly from percentage time spent swimming in quadrant 2 (p < 0.01) it did not differ significantly from quadrant 3 (27%) and quadrant 4 (27%) [Fig. 3.10A]. However, middle-aged 11β-HSD1$^{-/-}$ mice swam longer in the target quadrant over the 60 second probe trial. Significant differences in percentage time swimming in the target quadrant (38%) compared to quadrants 2 (19.3%; p < 0.001), quadrant 3 (19.7%; p < 0.001) and quadrant 4 (23%; p < 0.01) [Fig. 3.10A].

Despite the above differences 11β-HSD1$^{-/-}$ mice $^{-/-}$ (M = 36.66, SD = 5.813) did not take longer to swim to the previous platform location or swim further from the

previous platform over the 60 second probe test than wild-type mice (M = 29.84, SD = 5.286) [t(25) = 0.8632, p = 0.6540; Fig. 3.10B].

Analysis of all mice, including mice not meeting the inclusion criteria, showed an effect of quadrant [F (3,136) = 15.06, $p < 0.0001$] and no effect of genotype was observed [F (1,136) = 9.663×10^{-10}, $p > 0.999$]. No difference in time taken to swim to the previous platform location between wild-type and 11β-HSD1$^{-/-}$ mice [11β-HSD1$^{-/-}$: M = 32.55, SD = 4.186; wild-type: M = 35.88, SD = 4.949; t(34) = 0.5144, p = 0.6101].

Figure 3.9. Probe Test Performance in Young Wild-type (WT) and 11β-HSD1$^{-/-}$ (KO) mice

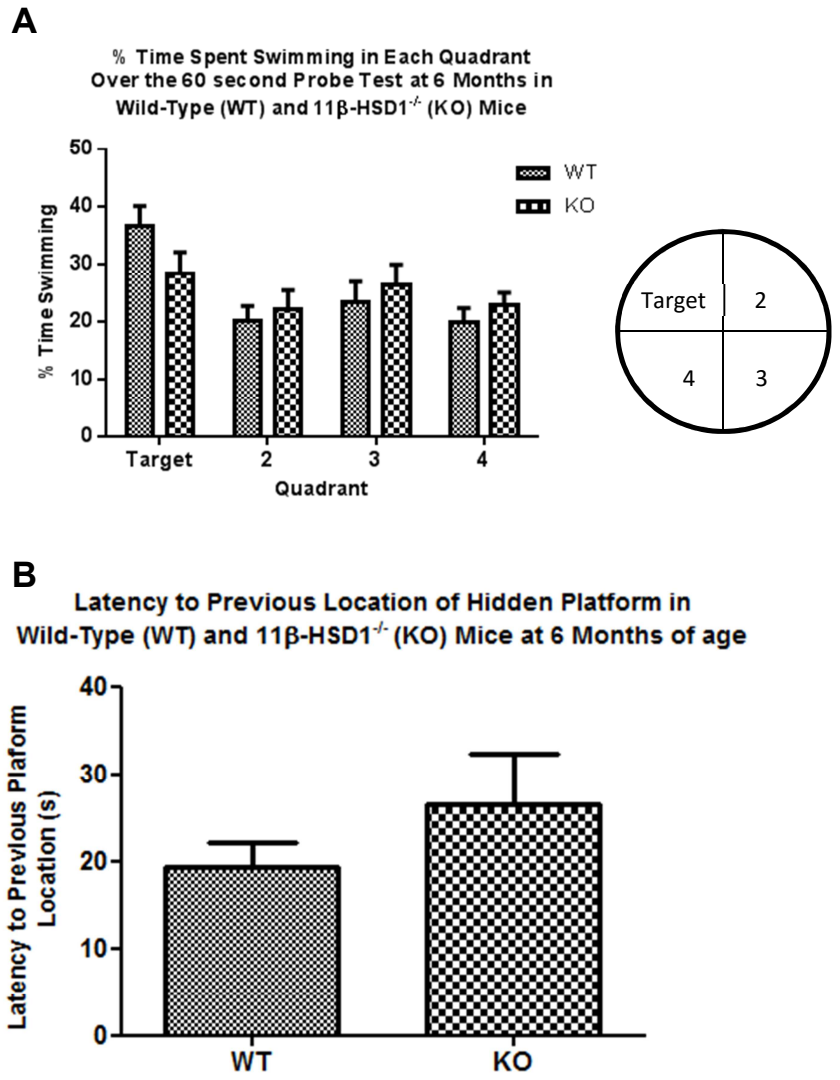

Fig. 3.9. Graph showing probe test acquisition in young wild-type mice (WT; n = 14) and 11β-HSD1$^{-/-}$ mice (KO; n = 14) as measured by **[A]** percentage time spent swimming in the target quadrant and the remaining 3 quadrants; and **[B]** latency taken for mice to swim to the previous platform location. A significant effect of quadrant was observed. No effect of genotype was observed. Values represent percentage time spent swimming during a 60 second probe test conducted 24 hours proceeding the final day of spatial learning +SEM.

Figure 3.10. Probe Test Performance in Middle-Aged Wild-type (WT) and 11β-HSD1$^{-/-}$ (KO) mice

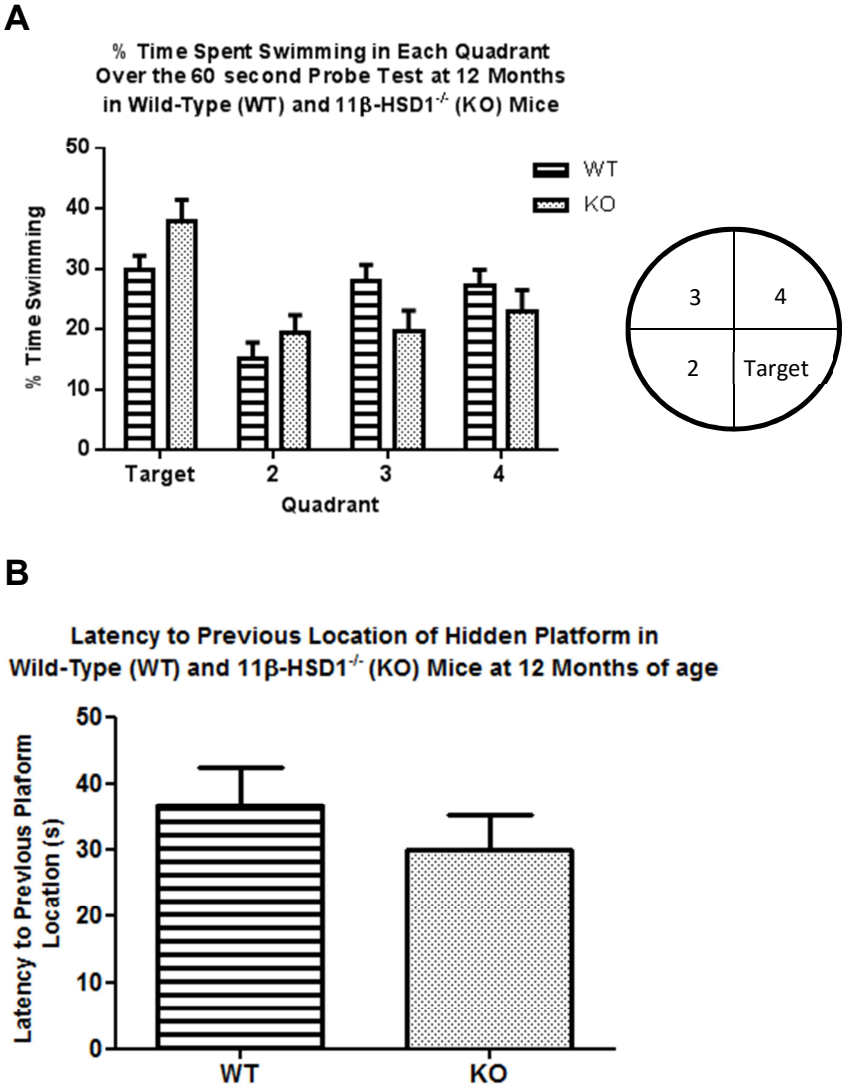

Fig. 3.10. Graph showing probe test acquisition in middle-aged 11β-HSD1$^{-/-}$ mice (KO; n = 13) but not wild-type mice (WT; n = 14) as measured by **[A]** percentage time spent swimming in the target quadrant and the remaining 3 quadrants; and **[B]** latency taken for mice to swim to the previous platform location. A significant effect of quadrant was observed. No effect of genotype was observed. Values represent percentage time spent swimming during a 60 second probe test conducted 24 hours proceeding the final day of spatial learning +SEM.

3.3.2.3 Aged

When aged at 18 months, no preference for the target quadrant was observed, with no significant effect of quadrant on the percentage time spent swimming in that quadrant was observed [F (3, 92) = 2.46, p < 0.0674; Fig. 3.11A] and no effect of genotype on the percentage time spent swimming in the four quadrants [F (1, 92) = $8.693e^{-11}$, p = 1.00; Fig. 3.11A].

An unpaired t-test of latency to the previous platform data in young 11β-HSD1$^{-/-}$ (M = 28.808, SD = 4.303) and wild-type (M = 39.99, SD = 5.945) mice revealed no difference in latency between the two groups [t(23) = 1.6, p = 0.1232; Fig. 3.11B].

Analysis of all mice, including mice not meeting the inclusion criteria, showed an effect of quadrant [F (3,128) = 3.590, p = 0.0156] and no effect of genotype was observed [F (1,128) = 9.219 x 10^{-11}, p > 0.999]. A significant difference in time taken to swim to the previous platform location between wild-type and 11β-HSD1$^{-/-}$ mice was observed [11β-HSD1$^{-/-}$: M = 27.93, SD = 3.860; wild-type: M = 42.37, SD = 5.074; t(32) = 2.265, p = 0.0304].

However, at 24 months, a two-way ANOVA showed that quadrant had a significant effect on the percentage of time spent swimming in that quadrant [F (3, 64) = 13.67, p < 0.0001; Fig. 3.12A] with no effect of genotype on the percentage time spent swimming in the four quadrants [F (1, 64) = 0.00, p = 1.00; Fig. 3.12A]. Converse to what was observed at 18 months of age, wild-type mice exhibited a preference for the target quadrant, swimming for the greatest percentage time in the target quadrant (38.2%) as compared to the other quadrants [Fig. 3.12A]. 11β-HSD1$^{-/-}$ mice also

showed unimpaired spatial memory, showing a preference for the quadrant where the platform was previously located (32.4%) [Fig. 3.12A].

An unpaired t-test of latency to the previous platform data in aged 11β-HSD1$^{-/-}$ mice (M = 30.01, SD = 9.83) and wild-type (M = 27.42, SD = 4.595) mice revealed no significant difference in latency between the two groups [t(16) = 0.2751, p = 0.7867; Fig. 3.12B].

Analysis of all mice, including mice not meeting the inclusion criteria, showed an effect of quadrant [F (3,88) = 12.48, p < 0.0001] and no effect of genotype was observed [F (1,88) = 9.255 x 10^{-10}, p > 0.999]. No difference in time taken to swim to the previous platform location between wild-type and 11β-HSD1$^{-/-}$ mice [11β-HSD1$^{-/-}$: M = 33.50, SD = 7.075; wild-type: M = 29.49, SD = 4.570; t(22) = 0.4991, p = 0.6226].

Figure 3.11. Probe Test Performance in 18 Month Aged Wild-type (WT) and 11β-HSD1$^{-/-}$ (KO) mice

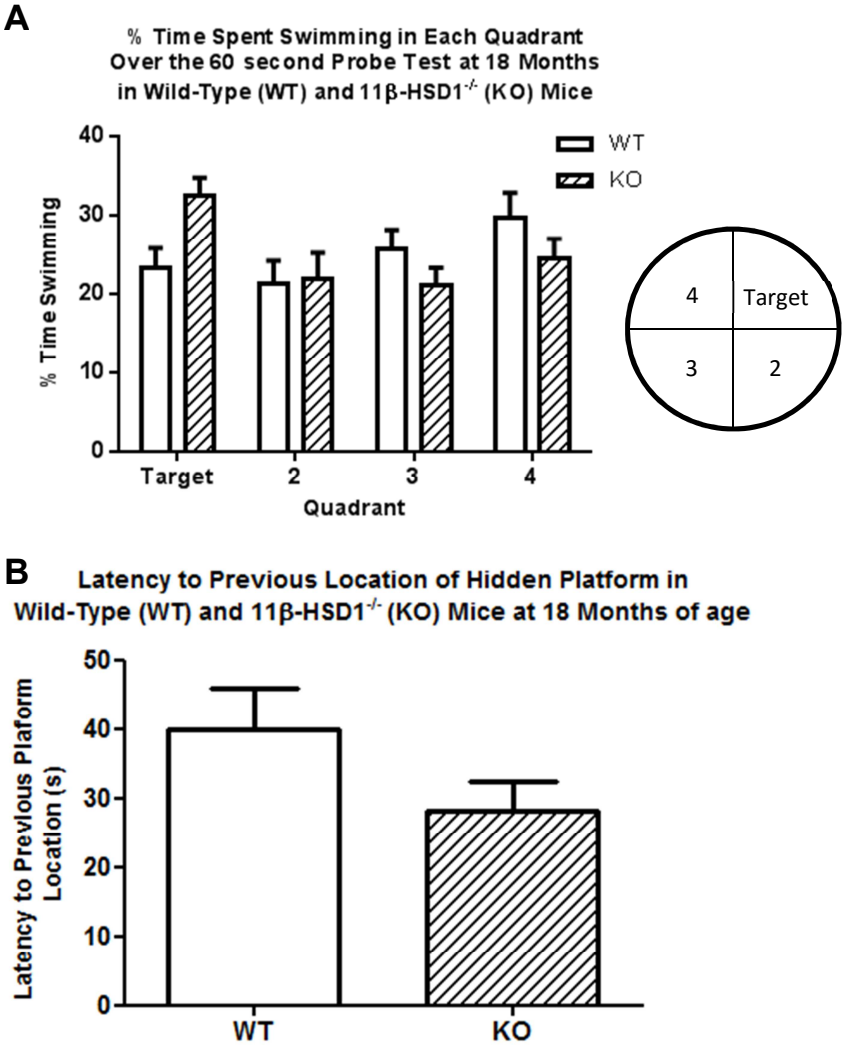

Fig. 3.11. Graph showing probe test acquisition in 11β-HSD1$^{-/-}$ mice (KO; n = 12) but not wild-type mice (WT; n = 13) as measured by **[A]** percentage time spent swimming in the target quadrant and the remaining 3 quadrants; and **[B]** latency taken for mice to swim to the previous platform location. No effect of quadrant was observed. No effect of genotype was observed. Values represent percentage time spent swimming during a 60 second probe test conducted 24 hours proceeding the final day of spatial learning +SEM.

Figure 3.12. Probe Test Performance in 24 Month old Wild-type (WT) and 11β-HSD1$^{-/-}$ (KO) mice

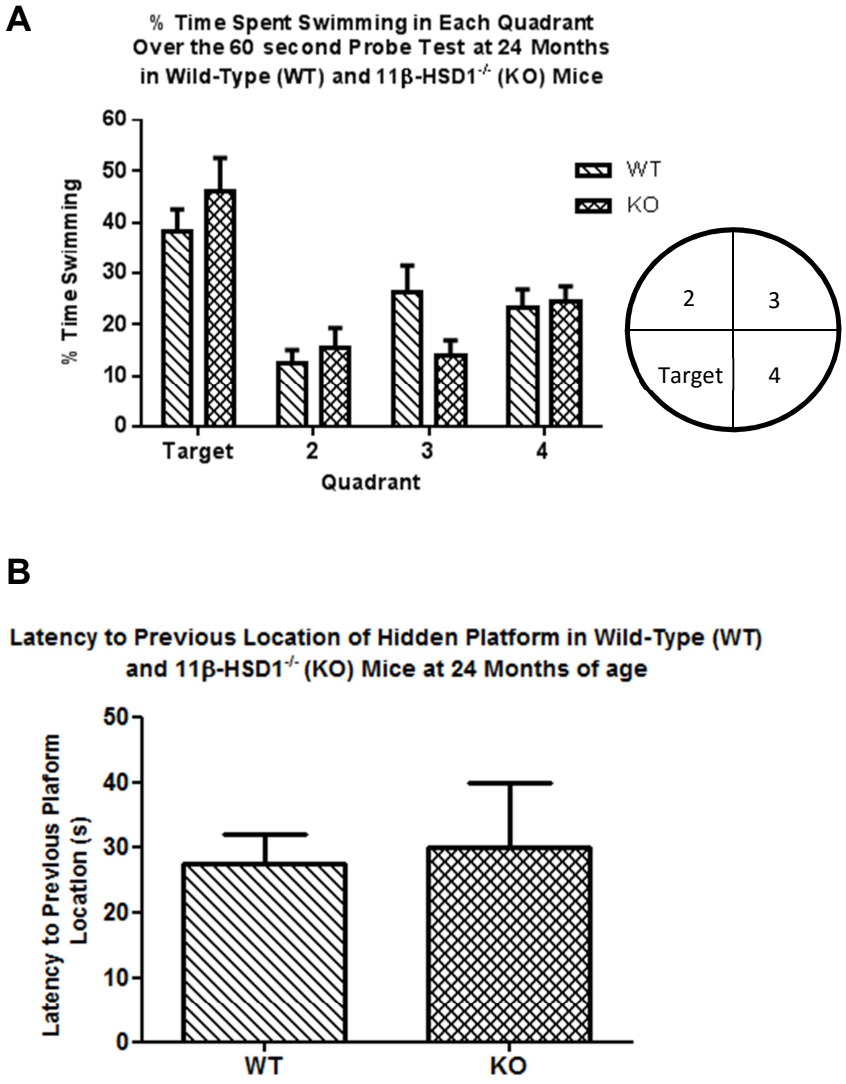

Fig. 3.12. Graph showing performance in aged wild-type (WT; n = 12) and 11β-HSD1$^{-/-}$ mice (KO; n = 6) as measured by **[A]** percentage time spent swimming in the target quadrant and the remaining 3 quadrants; and **[B]** latency taken for mice to swim to the previous platform location. A significant effect of quadrant was observed. No effect of genotype was observed. Values represent percentage time spent swimming during a 60 second probe test conducted 24 hours proceeding the final day of spatial learning +SEM.

3.3.2.4 Ageing Effects

The effect of ageing on probe test performance was analysed using data representing the percentage time spent swimming in the target quadrant and latency to the previous platform location.

The amount of time spent swimming in the target quadrant was affected by age [$F(3, 48) = 4.669$, $p = 0.0061$; Fig. 3.13] but not genotype [$F(1, 16) = 0.9601$, $p = 0.3417$; Fig. 3.13]. In both wild-type and 11β-HSD1$^{-/-}$ mice, time spent swimming in the target quadrant was noted to increase at 24 months further indicating habituation to the task through repeated testing.

Similarly, the latency to the previous platform location was noted to change with age [$F(3, 48) = 4.669$, $p = 0.0061$; Fig. 3.14] but not genotype [$F(3, 48) = 4.669$, $p = 0.0061$; Fig. 3.14]. In wild-type mice, latency to the platform location was noted to increase at 12 months compared to their performance at 6 months, however, when aged at 18 and 24 months, latency was not observed to be higher than when young [Fig. 3.14A]. In 11β-HSD1$^{-/-}$ mice, latency to the platform decreased significantly at 18 months when mice were aged [Fig. 3.14B].

Figure 3.13. Longitudinal Probe Test performance in Wild-Type and 11β-HSD1$^{-/-}$ (KO) mice at the ages of 6, 12, 18 and 24 months

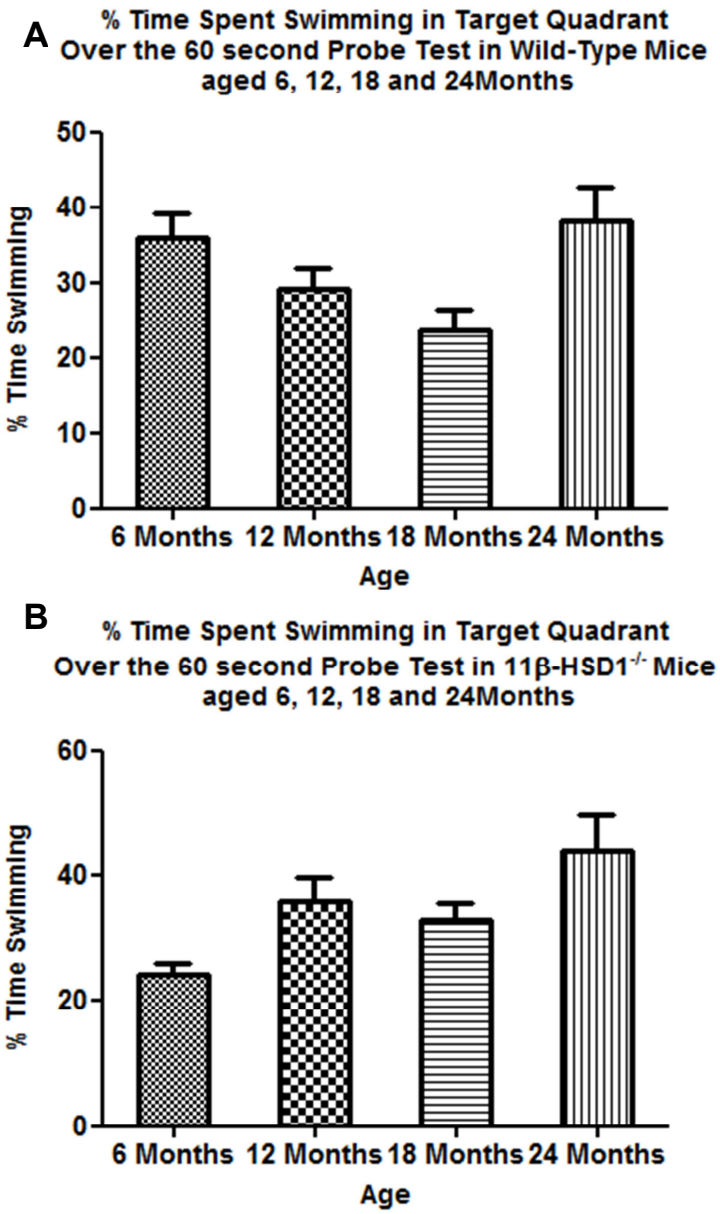

Fig. 3.13. Graph showing percentage time spent swimming in the target quadrant in **[A]** wild-type mice (n = 14) and **[B]** 11β-HSD1$^{-/-}$ mice (n = 14) as they age. A significant effect of age was observed. No effect of genotype was observed. Values represent percentage time spent swimming during a 60 second probe test conducted 24 hours proceeding the final day of spatial learning +SEM.

Figure 3.14. Longitudinal Probe Test performance in Wild-type (WT) and 11β-HSD1$^{-/-}$ (KO) mice at the ages of 6, 12, 18 and 24 months

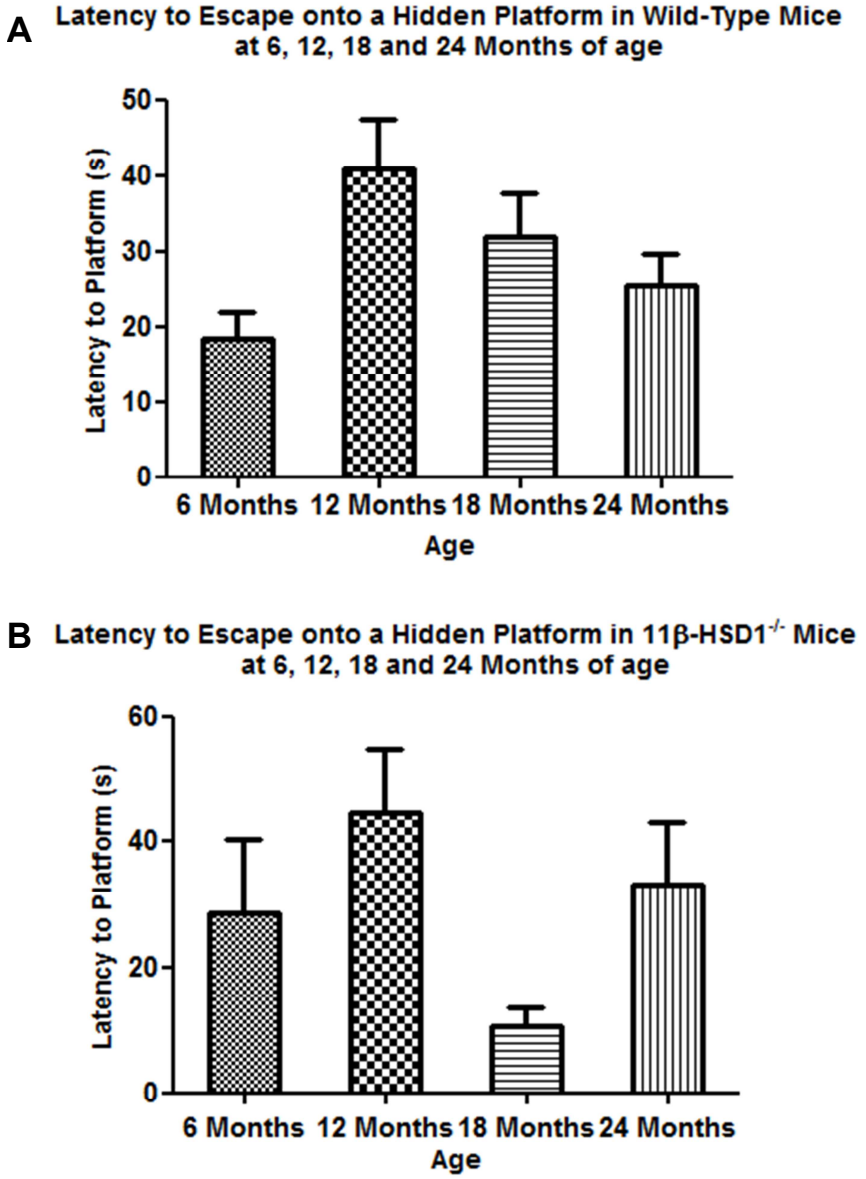

Fig. 3.14. Graph showing latency taken for mice to swim to the previous platform location in the probe test in **[A]** wild-type mice (WT; n = 14) and **[B]** 11β-HSD1$^{-/-}$ mice (KO; n = 14) as they age. A significant effect of age was observed. No effect of genotype was observed. Values represent latency in seconds 24 hours proceeding the final day of spatial learning +SEM.

3.3.3 Radial Arm Water Maze Results

3.3.3.1 Young

Young wild-type and 11β-HSD1$^{-/-}$ mice showed no difference in performance in the radial arm water maze and there was a progressive improvement in all measures of performance (latency, swim path length and errors) over the 5 trials. A two-way repeated measures ANOVA revealed that the latency to escape [$F(1,25) = 0.26$, $p = 0.6138$; Fig. 3.15A], swim path length [$F(1,25) = 0.12$, $p = 0.7283$; Fig. 3.15B] and number of errors [$F(1,25) = 0.83$, $p = 0.3717$; Fig. 3.15C] was not different between genotypes. However, there was a significant effect of trial on latency to escape [$F(4,100) = 23.80$, $p < 0.0001$; Fig. 3.15A], swim path length [$F(4,100) = 19.31$, $p < 0.0001$; Fig. 3.15B] and errors [$F(4,100) = 17.58$, $p < 0.0001$; Fig. 3.15C]. Post-hoc tests revealed significantly lower latencies to escape, swim path length and errors in the trials 1h following the acquisition trial in wild-type mice but not in 11β-HSD1$^{-/-}$ mice [Fig. 3.15].

However, no difference was observed in savings made in escape latency across the 1 hour retention interval between genotypes. An unpaired t-test revealed no significant difference in savings following the 1 hour retention interval [$t(25) = 1.268$, $p = 0.2164$; Fig. 3.16] in both young wild-type ($M = 36.05$, $SD = 5.182$) and young 11β-HSD1$^{-/-}$ mice ($M = 27.58$, $SD = 3.527$).

Figure 3.15. Radial Arm Water Maze Performance in Young Wild-type (WT) and 11β-HSD1$^{-/-}$ (KO) mice

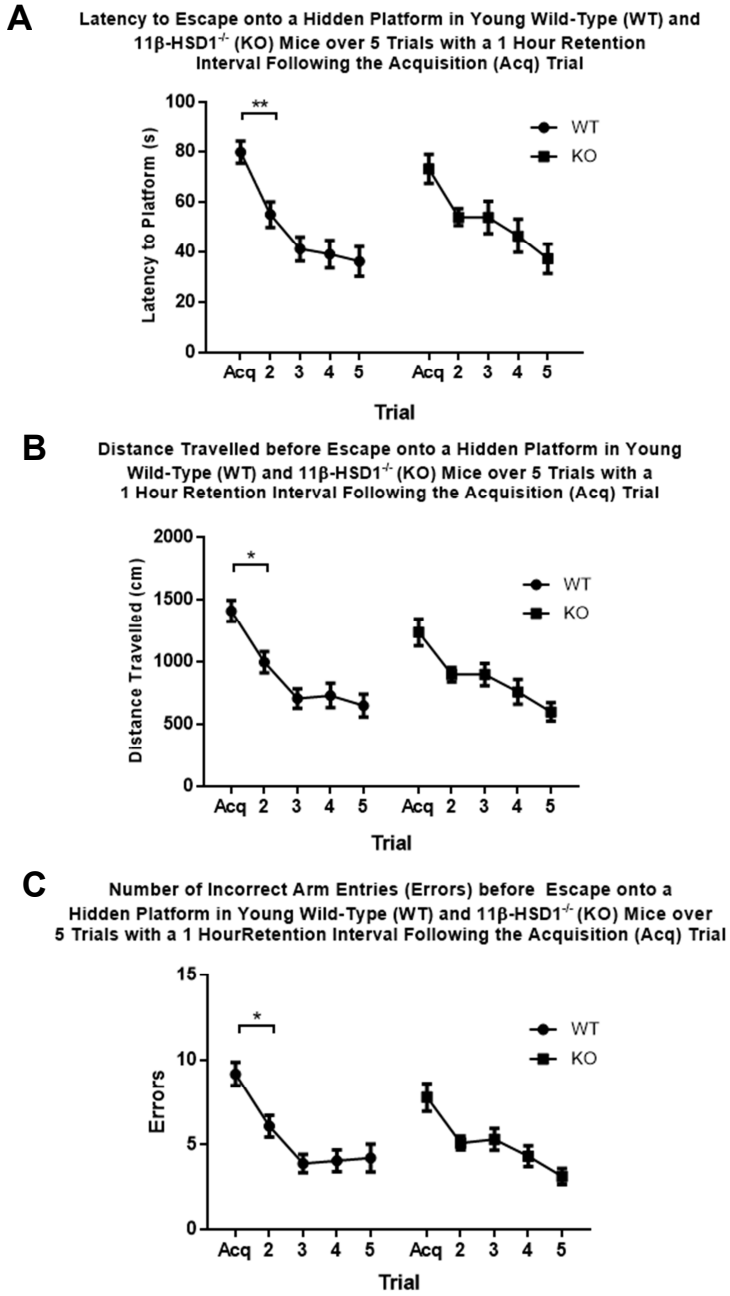

Fig. 3.15. Graphs showing radial arm water maze task acquisition in young wild-type mice (WT; n = 14) but not young 11β-HSD1$^{-/-}$ mice (KO; n = 14) as measured by **[A]** the latency to escape onto the hidden platform; **[B]** the distance travelled (swim path length) before escape onto the hidden platform; and **[C]** the number of incorrect arm entries before escape onto the hidden platform. A significant effect of trial was observed. No effect of genotype was observed. Values represent latency, swim path length and errors for each trial averaged over 5 days of testing +SEM.

Figure 3.16. Savings across a 1 Hour Retention Interval in Young Wild-type (WT) and 11β-HSD1$^{-/-}$ (KO) mice

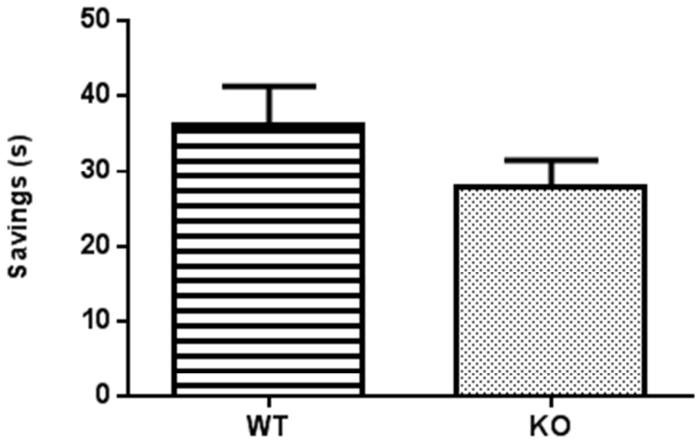

Fig. 3.16. Graph showing the savings across a 1 hour retention interval in the radial arm water maze in young wild-type (WT; n = 14) and 11β-HSD1$^{-/-}$ mice (KO; n = 14). Savings were not significantly different between genotypes. Values represent the difference in latency to escape between the acquisition trial and trial 2 +SEM.

3.3.3.2 Middle-Age

Spatial working memory was then assessed in middle-aged wild-type and 11β-HSD1$^{-/-}$ mice in the radial arm water maze. At 6 months of age a 1 hour retention interval was used to assess spatial working memory in wild-type and 11β-HSD1$^{-/-}$ mice. However, at 12 months of age, two new retention interval lengths were introduced to allow a comparison of spatial working memory at shorter and longer retention intervals of 15 minutes and 2 hours respectively.

3.3.3.2.1 15 Minute retention trial interval

A two-way repeated measures ANOVA revealed no significant effect of genotype on latency to escape [$F(1, 25) = 0.67$, $p = 0.4213$; Fig. 3.17A], swim path length [$F(1, 25) = 0.45$, $p = 0.5099$; Fig. 3.17B] and number of errors [$F(1, 25) = 0.00$, $p = 0.9643$; Fig. 3.17C]. However there was a significant effect of trial on latency to escape [$F(4, 100) = 18.53$, $p < 0.0001$; Fig. 3.17A], swim path length [$F(4, 100) = 20.68$, $p < 0.0001$; Fig. 3.17B] and errors [$F(4, 100) = 21.95$, $p < 0.0001$; Fig. 3.17C].

Post-hoc tests revealed significant reductions in escape latency over the trials proceeding the acquisition trial and retention interval in middle-aged 11β-HSD1$^{-/-}$ mice but not wild-type mice [Fig. 3.17].

An unpaired t-test of savings data, calculated from the savings following the 15 minute retention interval, showed no significant difference in latency savings after a 15 minute retention interval [$t(25) = 0.8664$, $p = 0.3945$; Fig. 3.18] between middle-aged wild-type mice ($M = 33.04$, $SD = 7.462$) and 11β-HSD1$^{-/-}$ ($M = 41.48$, $SD = 6.130$).

Figure 3.17. Radial Arm Water Maze Performance in Middle-Aged Wild-type (WT) and 11β-HSD1$^{-/-}$ (KO) mice following a 15 Minute Retention Trial Interval

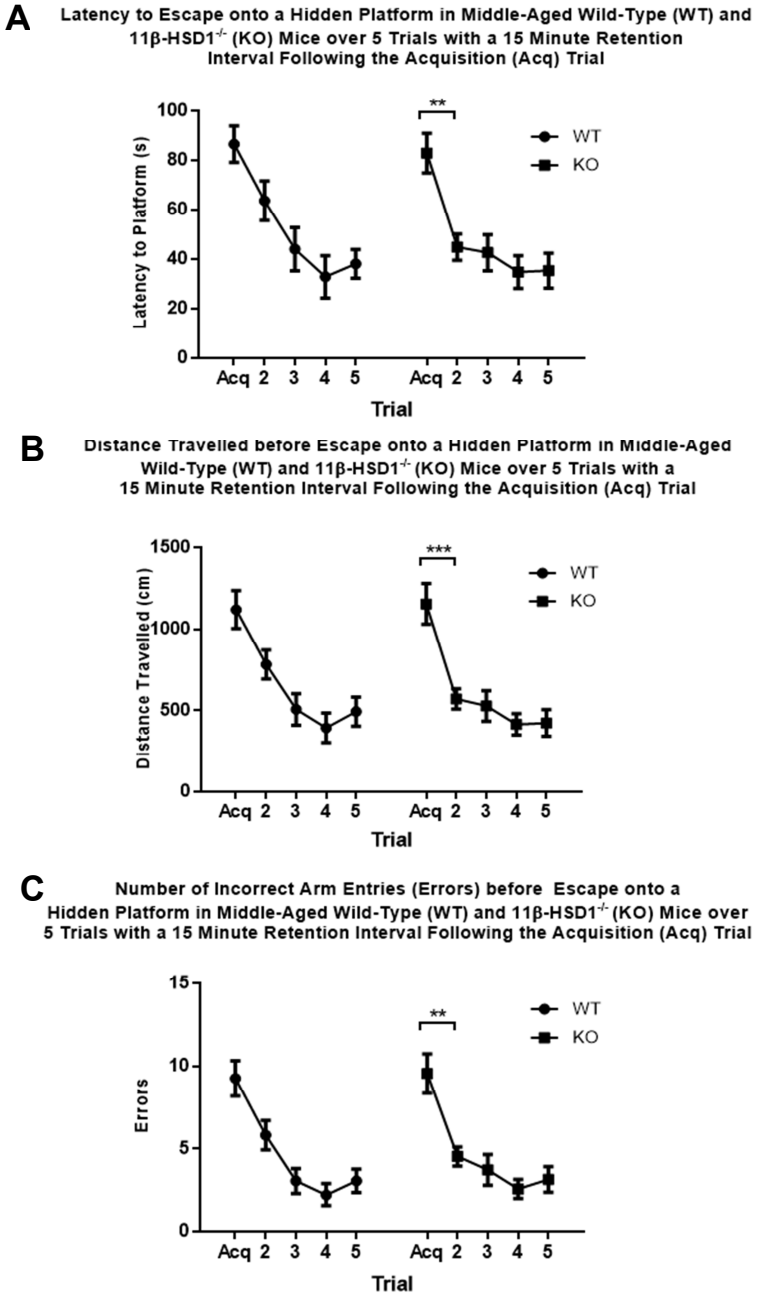

Fig. 3.17. Graphs showing radial arm water maze acquisition in middle-aged 11β-HSD1$^{-/-}$ mice (KO; n = 13) but not wild-type mice (WT; n = 14) following a 15 minute retention trial interval as measured by **[A]** the latency to escape onto the hidden platform; **[B]** the distance travelled (swim path length) before escape onto the hidden platform; and **[C]** the number of incorrect arm entries before escape onto the hidden platform. Retention interval was between the acquisition trial and Trial 2. A significant effect of trial was observed. No effect of genotype was observed. Values represent latency, swim path length and errors for each trial averaged over 5 days of testing +SEM.

Figure 3.18. Savings across a 15 Minute Retention Interval in Middle-Aged Wild-type (WT) and 11β-HSD1$^{-/-}$ (KO) mice

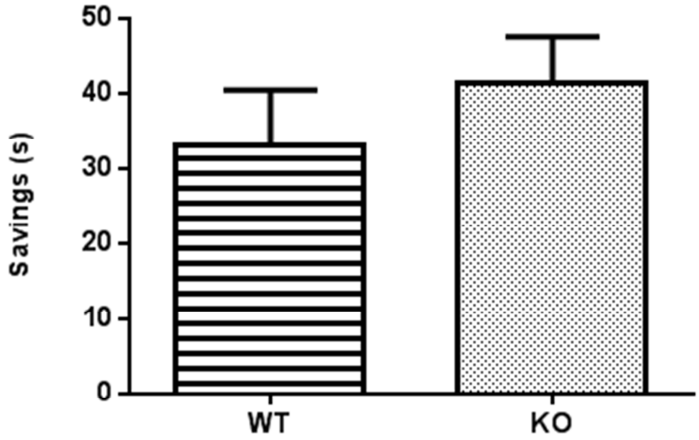

Fig. 3.18. Graph showing the savings across a 15 minute retention interval in the radial arm water maze in middle-aged wild-type (WT; n = 14) and 11β-HSD1$^{-/-}$ mice (KO; n = 13). Savings were not significantly different between genotypes. Values represent the difference in latency to escape between the acquisition trial and trial 2 +SEM.

3.3.3.2.2 1 hour retention trial interval

A two-way repeated measures ANOVA revealed no significant effect of genotype on latency to escape [F (1,25) = 0.00, p = 0.9558; Fig. 3.19A], swim path length [F (1,25) = 0.04, p = 0.8346; Fig. 3.19B] or incorrect arm entries before escape (errors) [F (1,25) = 0.04, p = 0.8516; Fig. 3.19C]. However there was a significant effect of trial on latency to escape [F (4,100) = 48.89, p < 0.0001; Fig. 3.19A], swim path length [F (4,100) = 53.48, p < 0.0001; Fig. 3.19B] and errors [F (4,100) = 53.45, p < 0.0001; Fig. 3.19C] following a 1 hour inter-trial interval between all the trials.

Post hoc tests revealed significant reductions in escape latency following the 1 hour retention interval in middle-aged 11β-HSD1$^{-/-}$ mice. Despite not showing a significant reduction in latency to escape in the trial following the 1 hour retention interval, wild-type mice showed reductions in swim path length and errors in trial 2.

An unpaired t-test revealed no difference in the savings between wild-type mice (M = 33.27, SD = 4.009) and 11β-HSD1$^{-/-}$ mice (M = 36.01, SD = 5.273) over the 1 hour retention interval [t(25) = 0.4180, p = 0.6795; Fig. 3.20].

3.3.3.2.3 2 hour retention trial interval

A two-way repeated measures ANOVAs revealed no significant effect of genotype on latency to escape [F (1,25) = 0.06, p = 0.8053; Fig. 3.21A], swim path length [F (1,25) = 0.02, p = 0.8982; Fig. 3.21B] or errors [F (1,25) = 0.13, p = 0.7231; Fig. 3.21C]. However there was a significant effect of trial on latency to escape [F (4,100) = 32.56, p < 0.0001; Fig. 3.19A], swim path length [F (4,100) = 25.77, p < 0.0001; Fig. 3.21B] and errors [F (4,100) = 17.86, p < 0.0001; Fig. 3.21C].

Post hoc tests revealed reductions in latency, swim path length and errors in the trial immediately following the retention interval in wild-type mice. 11β-HSD1$^{-/-}$ mice demonstrated lower latencies, swim path length and errors only in the trials proceeding the trial immediately after the retention interval.

Savings did not differ between genotype across the 2 hour retention interval. An unpaired t-test revealed no significant difference in savings [$t(25) = 0.9684$, $p = 0.3421$; Fig. 3.22B] following the 2 hour retention interval in wild-type ($M = 35.37$, $SD = 8.026$) and 11β-HSD1$^{-/-}$ mice ($M = 25.10$, $SD = 6.799$).

Figure 3.19. Radial Arm Water Maze Performance in Middle-Aged Wild-type (WT) and 11β-HSD1$^{-/-}$ (KO) mice following a 1 Hour Retention Trial Interval

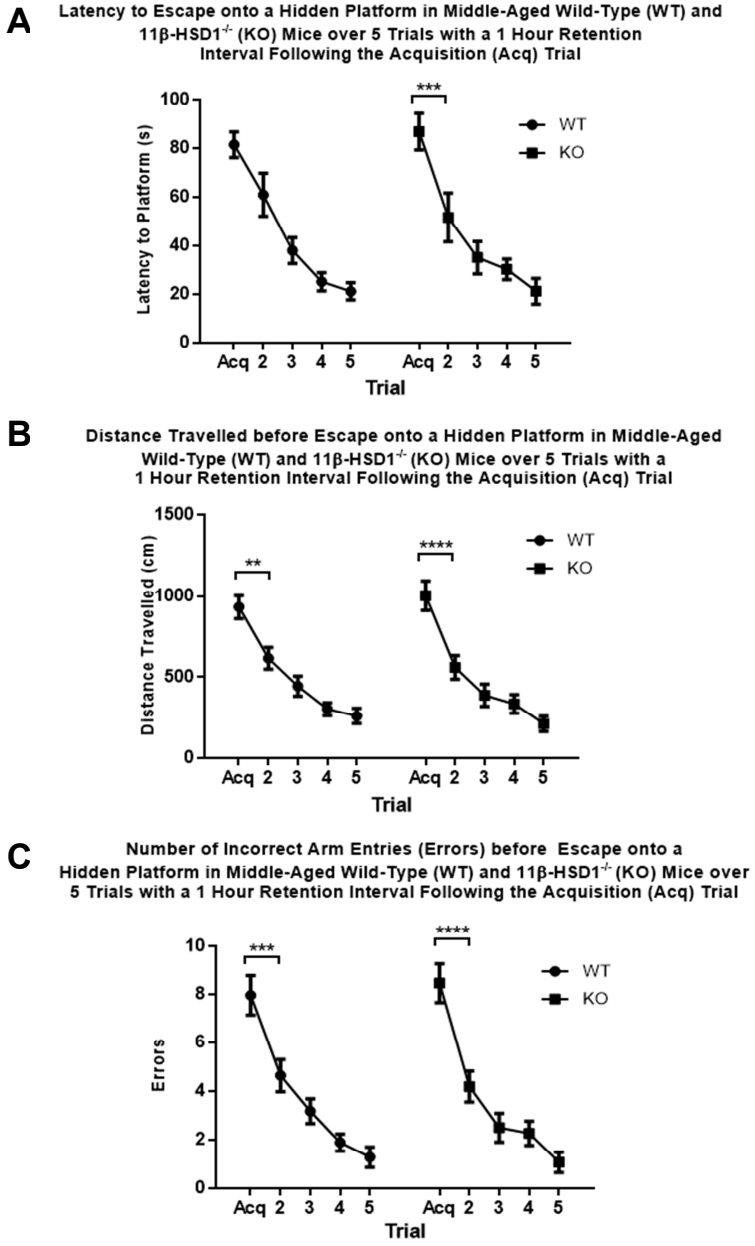

Fig. 3.19. Graphs showing radial arm water maze task acquisition in middle-aged wild-type mice (WT; n = 14) and 11β-HSD1$^{-/-}$ mice (KO; n = 13) following a 1 hour retention trial interval as measured by **[A]** the latency to escape onto the hidden platform; **[B]** the distance travelled (swim path length) before escape onto the hidden platform; and **[C]** the number of incorrect arm entries before escape onto the hidden platform. Retention interval was between the acquisition trial and Trial 2. A significant effect of trial was observed. No effect of genotype was observed. Values represent latency, swim path length and errors for each trial averaged over 5 days of testing +SEM.

Figure 3.20. Savings across a 1 Hour Retention Interval in Middle-Aged Wild-type (WT) and 11β-HSD1$^{-/-}$ (KO) mice

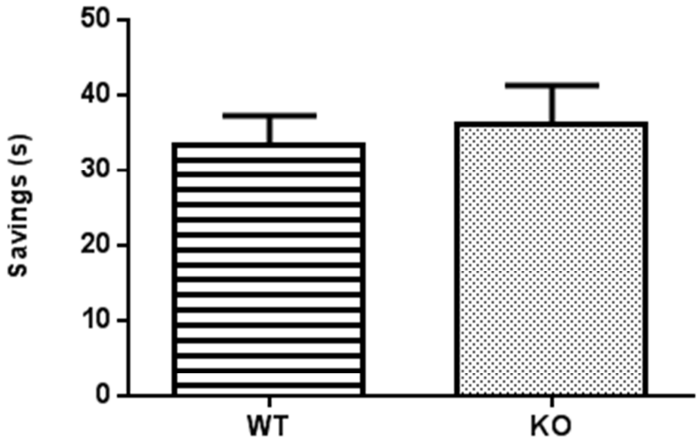

Fig. 3.20. Graph showing the savings across a 1 hour retention interval in the radial arm water maze in middle-aged wild-type (WT; n = 14) and 11β-HSD1$^{-/-}$ mice (KO; n = 13). Savings were not significantly different between genotypes. Values represent the difference in latency to escape between the acquisition trial and trial 2 +SEM.

Figure 3.21. Radial Arm Water Maze Performance in Middle-Aged Wild-type (WT) and 11β-HSD1$^{-/-}$ (KO) mice following a 2 Hour Retention Trial Interval

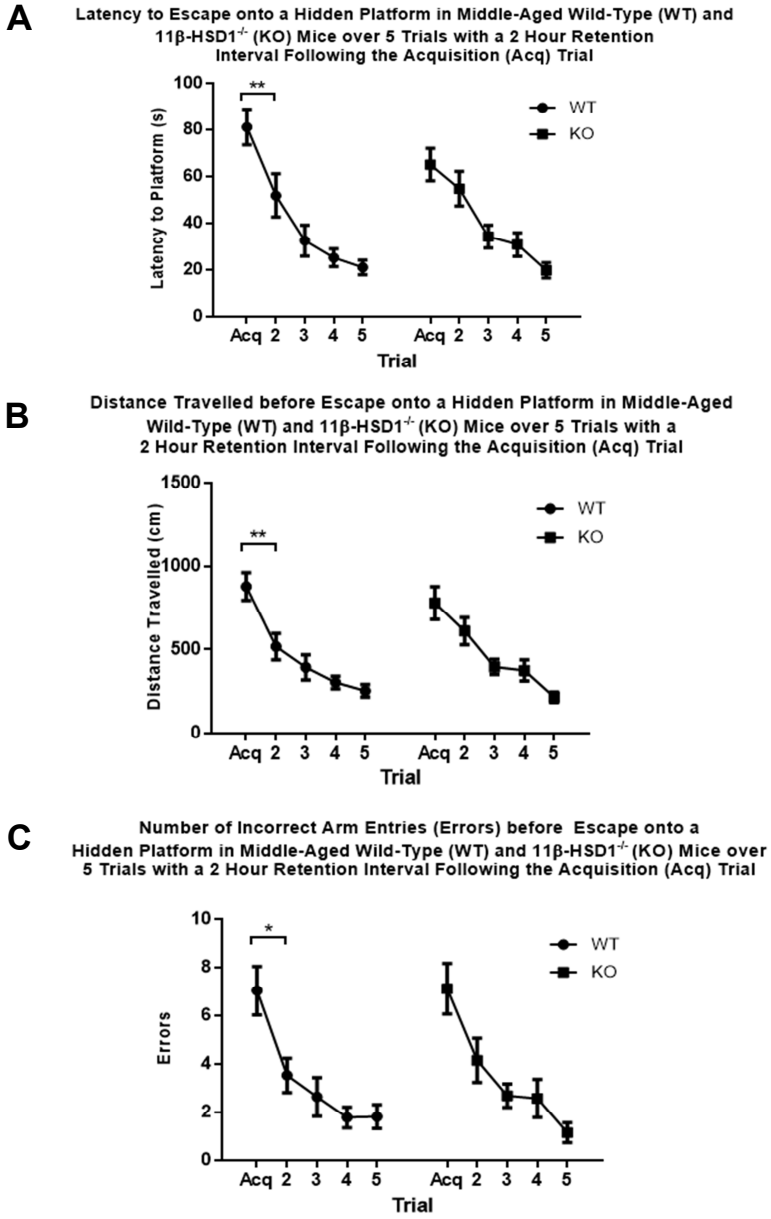

Fig. 3.21. Graphs showing radial arm water maze performance in middle-aged wild-type mice (WT; n = 14) and 11β-HSD1$^{-/-}$ mice (KO; n = 13) following a 2 hour retention interval as measured by **[A]** the latency to escape onto the hidden platform; **[B]** the distance travelled (swim path length) before escape onto the hidden platform; and **[C]** the number of incorrect arm entries before escape onto the hidden platform. Retention interval was between the acquisition trial and Trial 2. A significant effect of trial was observed. No effect of genotype was observed. Values represent latency, swim path length and errors for each trial averaged over 5 days of testing +SEM.

Figure 3.22. Savings across a 2 Hour Retention Interval in Young Wild-type (WT) and 11β-HSD1$^{-/-}$ (KO) mice

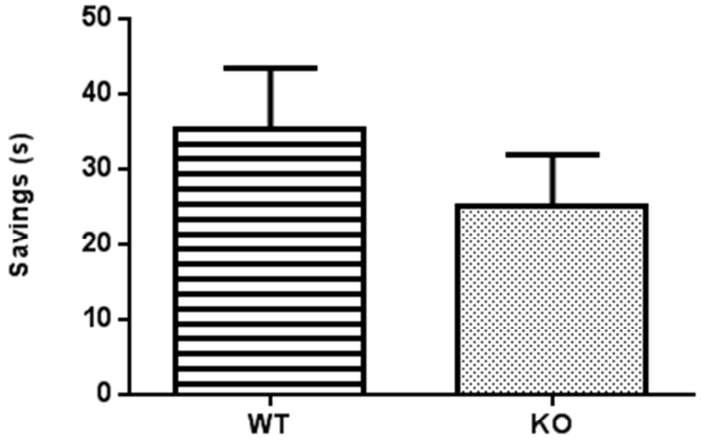

Fig. 3.22. Graph showing the savings across 2 hour retention interval in the radial arm water maze in middle-aged wild-type (WT; n = 14) and 11β-HSD1$^{-/-}$ mice (KO; n = 13). Savings were not significantly different between genotypes. Values represent the difference in latency to escape between the acquisition trial and trial 2 +SEM.

3.3.3.3 Aged

3.3.3.3.1 15 Minute retention trial interval

Following a 15 minute retention interval, aged wild-type mice showed good spatial working memory whilst data suggested impaired spatial working memory in 11β-HSD1$^{-/-}$ mice. A two-way repeated measures ANOVA revealed no significant effect of genotype on latency to escape [$F(1, 23) = 0.47$, $p = 0.4990$; Fig 3.23A], swim path length [$F(1, 23) = 0.83$, $p = 0.3719$; Fig 3.23B] or incorrect arm entries before escape (errors) [$F(1, 23) = 0.85$, $p = 0.3657$; Fig 3.23C]. However there was a significant effect of trial on latency to escape [$F(4, 92) = 11.60$, $p < 0.0001$; Fig 3.23A], swim path length [$F(4, 92) = 9.78$, $p < 0.0001$; Fig 3.23B] and errors [$F(4, 92) = 10.84$, $p < 0.0001$; Fig 3.23C] following a 15 minute inter-trial interval between all the trials.

Post-hoc tests revealed significant reductions in wild-type mice escape latency, swim path length and errors in the trial immediately following the retention interval. On the other hand, aged 11β-HSD1$^{-/-}$ mice demonstrated results similar to those observed when middle-aged following a 2 hour retention interval with no significant difference in latency, swim path length and errors compared to the acquisition trial on the trial immediately following the short 15 minute retention interval, trial 2.

Savings data also revealed a trend for lower savings over the 15 minute retention trial in 11β-HSD1$^{-/-}$ mice. An unpaired t-test showed no significant difference in savings after a 15 minute retention interval between aged wild-type ($M = 40.04$, $SD = 7.948$) and 11β-HSD1$^{-/-}$ ($M = 21.85$, $SD\ 6.387$) mice [$t(23) = 1.765$, $p = 0.0908$; Fig. 3.24].

This data indicates good spatial working memory across a short 15 minute inter-trial interval in aged wild-type mice which is demonstrated by significantly faster and shorter escape onto the hidden platform and fewer errors over the 15 minute retention interval. However, aged 11β-HSD1$^{-/-}$ mice do not perform as well with latencies, swim path lengths and errors in trial 2 which do not differ from acquisition trial suggesting they were unable to retain and retrieve the information across the short 15 minute retention interval.

Figure 3.23. Radial Arm Water Maze Performance in Aged Wild-type (WT) and 11β-HSD1$^{-/-}$ (KO) mice following a 15 Minute Retention Trial Interval

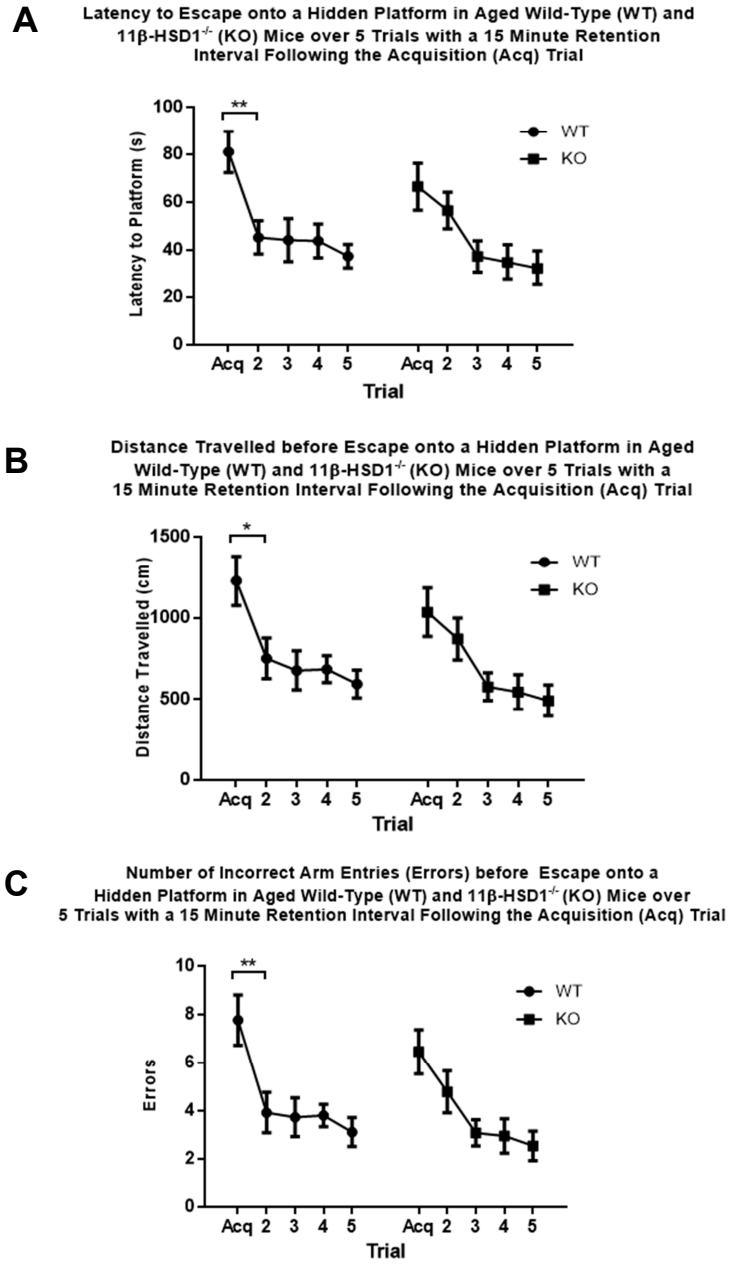

Fig. 3.23. Graphs showing radial arm water maze task acquisition in aged wild-type mice (WT; n = 13) but 11β-HSD1$^{-/-}$ mice (KO; n = 12) following a 15 minute retention interval as measured by **[A]** the latency to escape onto the hidden platform; **[B]** the distance travelled (swim path length) before escape onto the hidden platform; and **[C]** the number of incorrect arm entries before escape onto the hidden platform. Retention interval was between the acquisition trial and Trial 2. A significant effect of trial was observed. No effect of genotype was observed. Values represent latency, swim path length and errors for each trial averaged over 5 days of testing +SEM.

Figure 3.24. Savings across a 15 Minute Retention Interval in Aged Wild-type (WT) and 11β-HSD1$^{-/-}$ (KO) mice

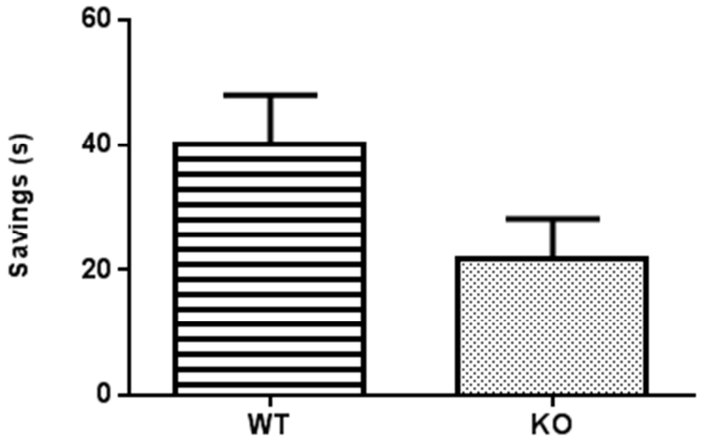

Fig. 3.24. Graph showing the savings across 15 minute retention interval in the radial arm water maze in aged wild-type (WT; n = 13) and 11β-HSD1$^{-/-}$ mice (KO; n = 12). Savings were not significantly different between genotypes. Values represent the difference in latency to escape between the acquisition trial and trial 2 +SEM.

3.3.3.3.2 1 hour retention trial interval

When a 1 hour retention trial interval was introduced, aged mice exhibited impaired spatial working memory regardless of genotype. A two-way repeated measures ANOVA revealed no significant effect of genotype on latency to escape [$F(1, 23) = 0.4637$, $p = 0.5027$; Fig 3.25A], swim path length [$F(1, 23) = 0.5298$, $p = 0.82$; Fig 3.25B] or incorrect arm entries before escape (errors) [$F(1, 23) = 0.1709$, $p = 0.6832$; Fig 3.25C]. However there was a significant effect of trial on latency to escape [$F(4, 92) = 17.34$, $p < 0.0001$; Fig 3.25A], swim path length [$F(4, 92) = 13.09$, $p < 0.0001$; Fig 3.25B] and errors [$F(4, 92) = 11.38$, $p < 0.0001$; Fig 3.25C].

However, whilst shorter latencies were observed immediately following the retention interval, swim path length and number of errors were not significantly reduced following the 1 hour retention interval in both wild-type and 11β-HSD1$^{-/-}$ mice.

Additionally, no difference in savings across the 1 hour retention interval was observed between genotypes. An unpaired t-test revealed no difference in the savings between aged wild-type ($M = 33.84$, $SD = 5.793$) and 11β-HSD1$^{-/-}$ ($M = 28.16$, SD 5.532) mice [$t(23) = 7067$, $p = 0.4868$; Fig. 3.26] over the 1 hour retention interval.

Taken together all of this demonstrates that at 24 months spatial working memory is impaired irrespective of genotype.

Figure 3.25. Radial Arm Water Maze Performance in Aged Wild-type (WT) and 11β-HSD1$^{-/-}$ (KO) mice following a 1 Hour Retention Trial Interval

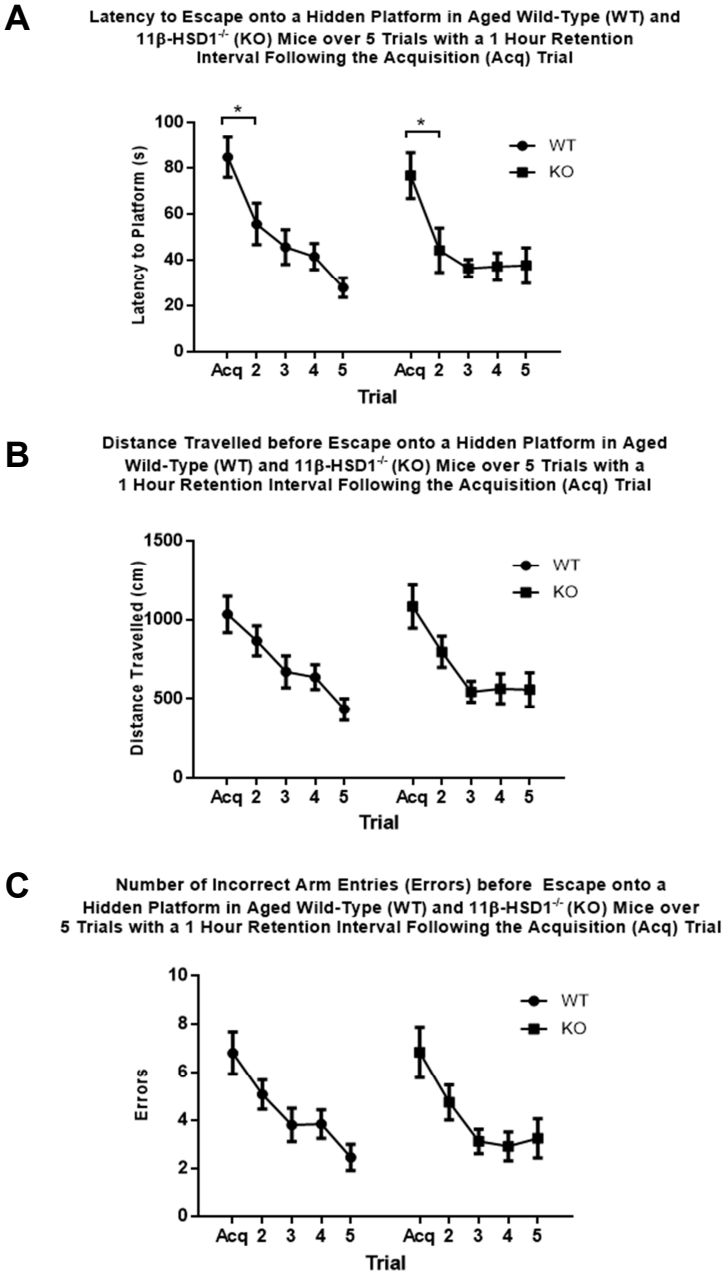

Fig. 3.25. Graphs showing radial arm water maze performance in aged wild-type mice (WT; n = 13) and 11β-HSD1$^{-/-}$ mice (KO; n = 12) following a 1 hour retention interval as measured by **[A]** the latency to escape onto the hidden platform; **[B]** the distance travelled (swim path length) before escape onto the hidden platform; and **[C]** the number of incorrect arm entries before escape onto the hidden platform. Retention interval was between the acquisition trial and Trial 2. A significant effect of trial was observed. No effect of genotype was observed. Values represent latency, swim path length and errors for each trial averaged over 5 days of testing +SEM.

Figure 3.26. Savings across a 1 Hour Retention Interval in Aged Wild-type (WT) and 11β-HSD1$^{-/-}$ (KO) mice

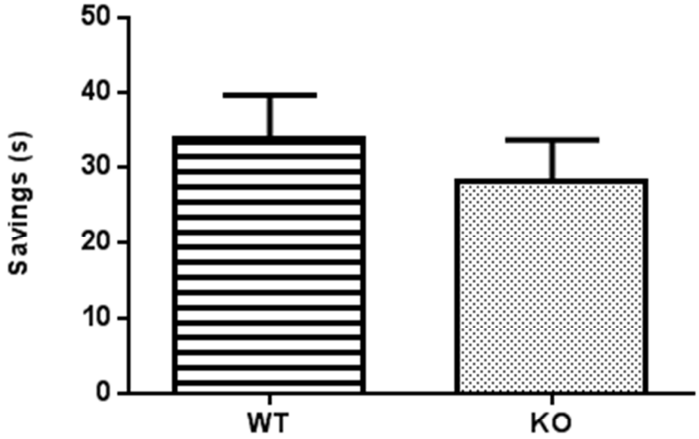

Fig. 3.26. Graph showing the savings across 1 hour retention interval in the radial arm water maze in aged wild-type (WT; n = 13) and 11β-HSD1$^{-/-}$ mice (KO; n = 12). Savings were not significantly different between genotypes. Values represent the difference in latency to escape between the acquisition trial and trial 2 +SEM.

3.3.3.3.3 2 hour retention trial interval

Following a 2 hour retention trial interval, aged wild-type and 11β-HSD1$^{-/-}$ mice exhibited impaired spatial working memory. No significant effect of genotype on latency to escape [F (1, 23) = 0.01525, p = 0.9028; Fig 3.27A], swim path length [F (1, 23) = 0.3086, p = 0.5839; Fig 3.27B] or incorrect arm entries before escape (errors) [F (1, 23) = 0.5449, p = 0.4679; Fig 3.27C]. However there was a significant effect of trial on latency to escape [F (4, 92) = 10.77, p < 0.0001; Fig 3.27A], swim path length [F (4, 92) = 6.741, p < 0.0001; Fig 3.27B] and errors [F (4, 92) = 5.540, p < 0.0005; Fig 3.27C].

Further analysis revealed that both wild-type and 11β-HSD1$^{-/-}$ mice did not show reductions in escape latency, swim path length and errors in the trial immediately following the 2 hour retention interval. This suggests that neither aged wild-type nor 11β-HSD1$^{-/-}$ mice were able to hold spatial information for the platform in mind across the 2 hour interval. Additionally, it was noted that whilst aged wild-type mice showed shorter latencies to escape, swim path lengths and fewer errors in trial 3, aged 11β-HSD1$^{-/-}$ mice did not show improvement in the task until the final 2 trials. This suggests that aged 11β-HSD1$^{-/-}$ mice may be exhibit more impaired spatial working memory than aged wild-type mice.

However, no difference in savings across the 2 hour retention interval was observed between genotype by an unpaired t-test [Wild-type: M = 32.67, SD = 8.477); 11β-HSD1$^{-/-}$ (M = 27.45, SD 6.45); t(23) = 0.4843, p = 0.6327; Fig. 3.28].

Figure 3.27. Radial Arm Water Maze Performance in Aged Wild-type (WT) and 11β-HSD1$^{-/-}$ (KO) mice

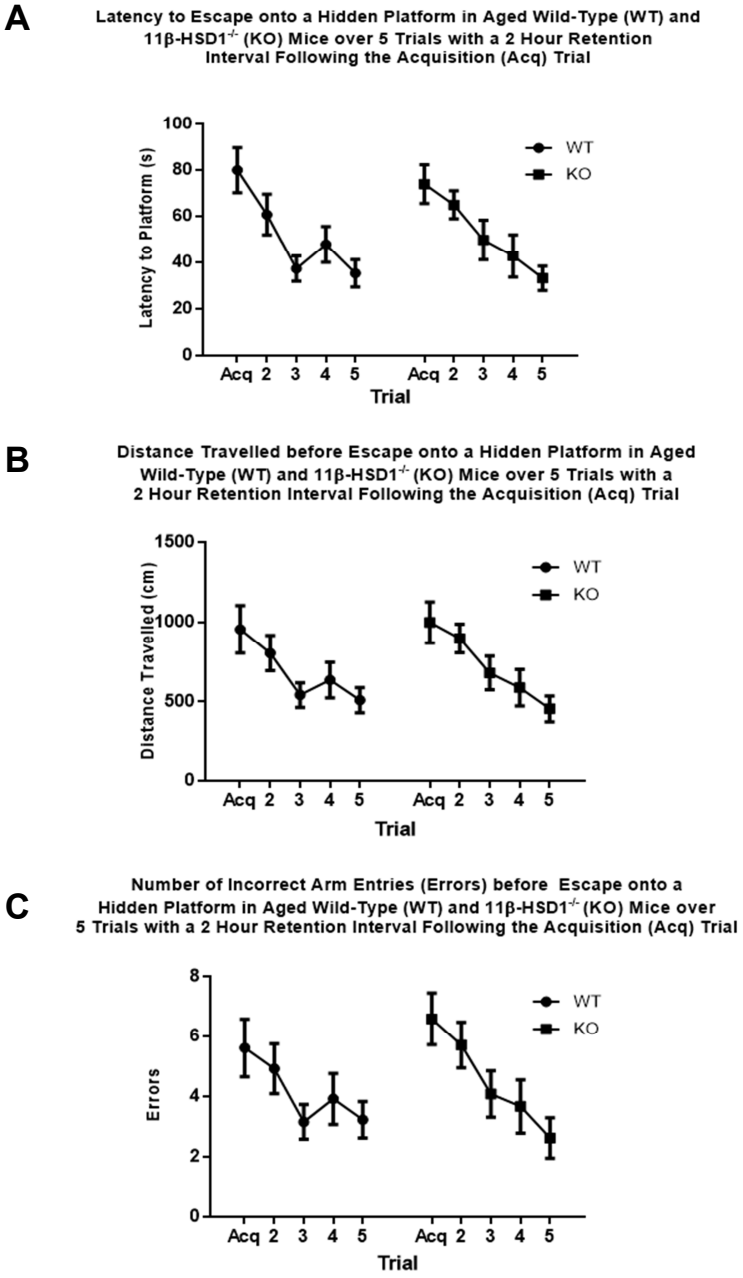

Fig. 3.27. Graphs showing impaired radial arm water maze performance in aged wild-type mice (WT; n = 13) and 11β-HSD1$^{-/-}$ mice (KO; n = 12) following a 2 hour retention trial interval as measured by **[A]** the latency to escape onto the hidden platform; **[B]** the distance travelled (swim path length) before escape onto the hidden platform; and **[C]** the number of incorrect arm entries before escape onto the hidden platform. Retention interval was between the acquisition trial and Trial 2. A significant effect of trial was observed. No effect of genotype was observed. Values represent latency, swim path length and errors for each trial averaged over 5 days of testing +SEM.

Figure 3.28. Savings across a 2 Hour Retention Interval in Aged Wild-type (WT) and 11β-HSD1$^{-/-}$ (KO) mice

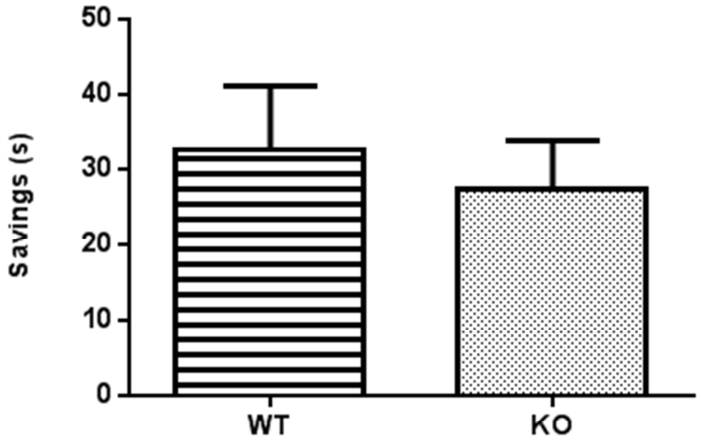

Fig. 3.28. Graph showing the savings across 2 hour retention interval in the radial arm water maze in aged wild-type (WT; n = 13) and 11β-HSD1$^{-/-}$ mice (KO; n = 12). Savings were not significantly different between genotypes. Values represent the difference in latency to escape between the acquisition trial and trial 2 +SEM.

3.3.3.3.4 Ageing Effects

The effects of ageing on spatial working memory across a 1 hour retention interval were analysed using latency and error savings across the 1 hour retention interval when mice were young, middle-aged and aged.

Latency savings data showed no effects of ageing with no change in savings observed with age [$F(2, 46) = 0.18$, $p = 0.8362$; Fig. 3.29A] and no effect of genotype [$F(1, 46) = 0.76$, $p = 0.3917$; Fig. 3.29A]. Errors savings data showed no effects of ageing with no change in savings observed with age [$F(2, 46) = 1.267$, $p = 0.2909$; Fig. 3.29B] and no effect of genotype [$F(1, 46) = 0.03554$, $p = 0.8520$; Fig. 3.29B].

Figure 3.29. Longitudinal Radial Arm Water maze performance in Wild-Type and 11β-HSD1$^{-/-}$ (KO) mice at the ages of 6, 12 and 18 months

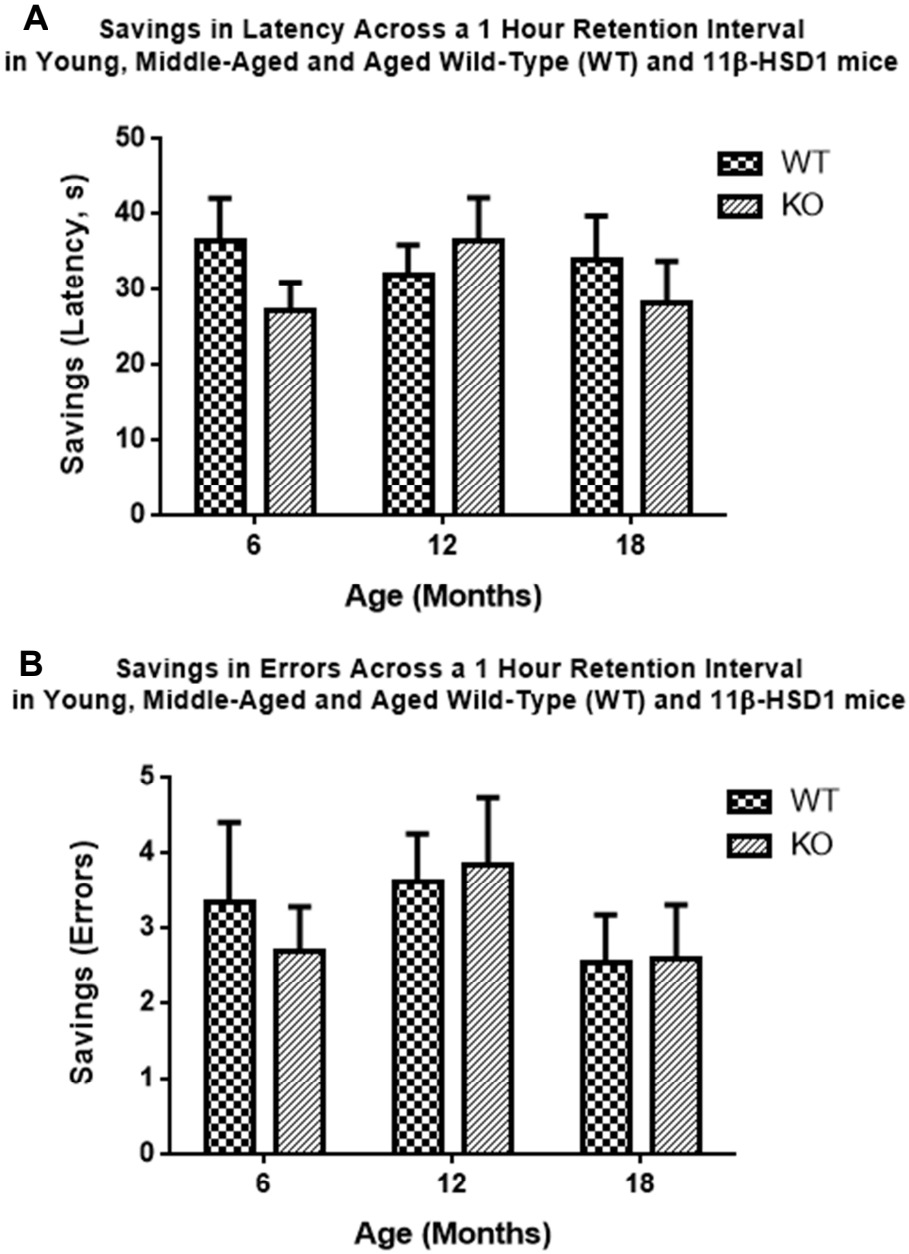

Fig. 3.29. Graphs showing radial arm water maze performance wild-type mice (n = 13) and 11β-HSD1$^{-/-}$ mice (n = 12) as they age, following a 1 hour retention interval as measured by savings in **[A]** the latency to escape and **[B]** number of errors before escape onto the hidden platform. No effect of age was observed. No effect of genotype was observed. Values represent latency or number of errors for each trial averaged over 2 days of testing +SEM.

3.4 Discussion

Our study examined the longitudinal effects of lifelong removal of 11β-HSD1 on learning and memory processes and working memory processes with age by examining 11β-HSD1$^{-/-}$ mice and their wild-type counterparts in the water maze and radial arm water maze over the span of 24 months. Both wild-type and 11β-HSD1$^{-/-}$ mice showed no impairment in spatial learning in the training portion of the water maze. Impairment in spatial memory was observed at middle-age and 18 months wild-type mice in the probe test portion of the water maze. Interestingly, spatial working memory was observed to be impaired with age in both wild-type and 11β-HSD1$^{-/-}$ mice.

In both wild-type and 11β-HSD1$^{-/-}$ mice, the latency to escape and distance travelled before escape onto the platform were observed to decrease over the 5 training days at all age time-points. These data indicate no impairment in spatial learning with age. These findings differ from those of previous experiments showing an attenuation of age-associated cognitive impairment when 11β-HSD1 is removed or inhibited. Yau et al. (2001) documented that aged 11β-HSD1 knockout mice had lower hippocampal intracellular corticosterone levels and no learning deficits associated with elevated glucocorticoid levels whilst aged wild-type mice had learning impairments associated with glucocorticoid levels. Meanwhile, the inhibition of 11β-HSDs has been associated with improved memory and cognitive function in healthy elderly humans (Sandeep et al., 2004) and a 11β-HSD1 activity, progressive brain atrophy and cognitive decline have been found to be linked (MacLullich et al., 2012).

Inhibition of 11β-HSD1 in C57BL/6J mice has also been noted to prevent age-related spatial memory impairments (Sooy et al., 2010).

Repeated testing over the 2 years may have resulted in over training of the mice resulting in a learning effect and masking age-associated impairments which may otherwise have been observed. Despite efforts to vary the testing arena at each time-point - by alternating testing arenas, extra-maze cues, platform location and entry position – the number of alterations which could be made were still limited. Consequently, with repeated testing mice may have become more familiar with the task requirements resulting in consistent learning curves across the ages. Indeed, Jansen et al. (2013) observed habituation of mice to the water maze task following repeated testing at a later age noting a similar decrease in latency and distance travelled when mice were tested again at a later age. Furthermore, some studies have suggested that repeated testing in the water maze may not be robust enough to effectively assess long-term deficits (Hodges, 1996). Therefore, age-associated impairments in spatial learning are possibly not evident in this study as a result of repeated testing resulting in over-training.

However, it is notable that in our study wild-type mice were found to have impaired performance in the probe test from middle-age and at 18 months of age whilst 11β-HSD1$^{-/-}$ mice had no impairment in spatial memory at all ages. As the probe test portion of the water maze represents spatial memory which is different from spatial learning, it suggests that whilst wild-type mice were able to perform well when continuously trained over 5 days, their ability to retain the information over longer periods of time was impaired with age. However, the lifelong removal of 11β-HSD1

was able to attenuate these age-associated spatial memory impairments. Interestingly, both wild-type and 11β-HSD1$^{-/-}$ mice did not show any impairment in spatial memory at 24 months. It is tenable that the difference in complexity of the cognitive processes required for spatial learning and spatial memory is also reflected in the extent of a learning or practice effect in a task, with wild-type mice only demonstrating habituation to the task following more 'sessions'. Altogether these data highlight the distinct memory processes of spatial learning and spatial memory suggesting that whilst age-associated impairments in spatial learning can be attenuated through repeated practice, the ability to hold information in mind over a long period of time is more susceptible to age-associated cognitive impairments and less susceptible, though not completely, to learning effects. Furthermore, it and suggests that the process of long-term memory formation is sensitive to changes in glucocorticoids and reductions in the levels of glucocorticoids through lifelong removal of 11β-HSD1 is beneficial for these processes.

Despite demonstrating no change in savings in both latency and number of errors with age, it was observed that with age the latency to platform and number of errors were not significantly decreased in the trial following the retention interval both wild-type and 11β-HSD1$^{-/-}$ mice suggesting an impairment in the ability to actively maintain spatial information in mind whilst another task is being performed. Most notably, impairments were observed in both wild-type and 11β-HSD1$^{-/-}$ mice, suggesting that whilst lifelong removal of 11β-HSD1 may attenuate age-associated spatial memory impairments, it does not attenuate age-associated impairments in spatial working memory. Previous studies have found that working memory reflects the use of measures that incorporate not only storage but also processing, making it

more cognitively demanding. Thus, the higher cognitive demands required for spatial working memory may mean that lifelong removal of 11β-HSD1 does not attenuate age-associated spatial working memory impairments in the same way it does spatial memory. Furthermore, spatial working memory also involves activation of brain areas in addition to the hippocampus, such as the prefrontal cortex, and removal of 11β-HSD1 in these brain areas may be detrimental to the cognitive processes occurring within these areas. Furthermore, it was noted that 11β-HSD1$^{-/-}$ mice started to exhibit impairments at middle-age following the 2 hour retention interval, supporting the suggestion that lifelong removal of 11β-HSD1 may actually be detrimental to processes involved in spatial working memory. These data are contrary to a previous study documenting no impairment in spatial working memory with age in both wild-type and 11β-HSD1$^{-/-}$ mice (Yau et al., 2007). However, it is notable that previous 11β-HSD1 mouse knockout models demonstrated some residual low level 11β-HSD1 activity whilst 11β-HSD1 activity was completely removed in the mouse model used in our study. As it is well established that glucocorticoids have an inverted-U shape relationship with cognition, it is possible that the residual activity in previous mouse models offered protection from age-associated spatial working memory impairments whilst the complete absence of 11β-HSD1 in our study accelerates impairments in spatial working memory. Taken all together our data suggest that whilst removal of 11β-HSD1 may be beneficial in age-associated changes in spatial memory, the presence of 11β-HSD1 may be essential for other cognitive processes such as spatial working memory.

The present study had a number of limitations. Firstly, longitudinal testing appeared to result in a learning effect and, as such, may mask age-associated impairments in

spatial learning processes. Secondly, external factors beyond experimental control may alter the performance of mice during the task. Particularly notable in our series of experiments was ongoing construction work which may have adversely affect cognitive performance in mice and an outbreak of pinworm in the research facility requiring the colony of mice to be administered medicine which may affect behaviour. Finally, testing constraints arising from the size of the colony and availability of equipment may have resulted in more variation, particularly in the radial arm maze, as data could not be averaged over as many days.

In conclusion, our results from this chapter suggest that repeated testing may help with performance in tasks requiring information to be held for a short period of time whilst being learnt when aged, however, the transfer of this information to long-term spatial memory may be impaired with age and attenuated with lifelong deletion of 11β-HSD1. Finally, our results show that 11β-HSD1 may have a distinct function in spatial memory and spatial working memory, as lifelong removal of 11β-HSD1 appeared to accelerate age-associated spatial working memory impairments. Further work investigating the mechanisms through which 11β-HSD1 levels affect spatial memory and spatial working memory performance with age will provide better insights and enable the development of specific therapeutic interventions for cognitive dysfunction.

Chapter 4 : Mechanisms of 11β-HSD1 Action on Age-Associated Spatial Learning and Memory Performance

4.1 Introduction

Data gathered in the previous chapter showed that lifelong removal of 11β-HSD1 attenuated age-associated spatial memory impairments but not spatial working memory impairments. However, the mechanisms through which 11β-HSD1 may alter cognitive function with age have yet to be fully established. In particular, the relationship between the expression of 11β-HSD1 and biomarkers linked to age-associated cognitive decline has not yet been investigated. Therefore, this chapter will focus on investigating the possible mechanisms through which 11β-HSD1 may act on spatial memory and spatial working memory by examining the relationship between 11β-HSD1, age-associated cellular, metabolite and structural changes, and spatial memory and spatial working memory.

Numerous studies have highlighted a variety of cellular, structural and metabolite changes in the brain with age, in particular in the hippocampus, a brain structure essential for spatial memory. Neurobiological research utilising models of age-related spatial learning impairment have found associations between changes in the size, number and structure of hippocampal neurons and spatial learning performance, whilst further studies have suggested that synaptic connectivity between neurons may also change with age and play a large role in age-related cognitive impairment.

Additionally, previous studies into structural markers of cognitive ageing have observed marked changes in brain morphology including a decline in total brain volume, cortical thinning and gyral atrophy (Uylings and de Brabander, 2002; Rodrigue and Raz, 2004). Numerous imaging studies have confirmed age-related changes in morphological characteristics of the brain (Pfefferbaum et al., 1994; Blatter et al., 1995; Raz et al., 1997; Resnick et al., 2003) and that these are found particularly in the prefrontal cortex (PFC) (Raz et al., 1997). White matter hyperintensities, reduced white-matter integrity and volume loss have also been observed (Ylikoski et al., 1995; Gunning-Dixon and Raz, 2000; Sullivan et al., 2001; Bartzokis et al., 2004; Head et al., 2004). Furthermore, the hippocampal formation, a structure important to declarative memory, experiences volume loss in advanced aging and this volume loss correlates with impaired memory performance with age and has been observed to be significantly accelerated in early stages of Alzheimer's disease (for reviews, see Raz et al. 2005). Finally, proton magnetic resonance spectroscopy (MRS) studies have identified metabolite changes linked with cognitive impairment with age including, but not limited to, changes in levels of the neuronal metabolic marker (N-acetylaspartate, NAA), glial metabolite marker (Inositol, Ins) and cellular membrane turnover/breakdown (Choline, Cho). In particular, higher levels of NAA were observed in younger adults who showed better spatial memory performance than their older counterparts (Driscoll et al., 2003) whilst increased levels of Ins have been observed in subjects with mild cognitive impairment.

Notably, 11β-HSD1 mRNA is highly expressed in the hippocampus of humans (Sandeep et al., 2002) and rodents (Moisan et al., 1990). In-situ hybridisation methods show a punctate expression in and around the cornu ammonis of the

hippocampus suggesting 11β-HSD1 plays a key role in mechanisms and processes occurring within the hippocampus. However, the expression of 11β-HSD1 in various cells within the hippocampus and associated metabolite levels and structural changes have yet to be investigated. Determining the association between 11β-HSD1 and cellular, metabolite and structural markers of ageing, and the association of these markers with cognitive decline, is key in underpinning the role 11β-HSD1 plays in age-associated cognitive impairment.

Thus, we hypothesised altered molecular physiology, structural integrity or metabolite levels in the hippocampus would be observed with age and these changes would be associated with the spatial memory and spatial working memory performance observed at 18 months in wild-type and 11β-HSD1$^{-/-}$ mice assessed in Chapter 3, respectively. Therefore, this chapter aims to explore the possible molecular, structural and metabolite mechanisms through which 11β-HSD1 may alter age-associated cognitive function by investigating: 1) The expression of 11β-HSD1 within the hippocampus; 2) Cellular, metabolite and structural changes with age; 3) The relationship between these markers and the cognitive performance of the respective wild-type and 11β-HSD1$^{-/-}$ mice tested in Chapter 3.

4.2 Methods

4.2.1 Animals

Male 11β-HSD1$^{-/-}$ mice and their Wild-type littermates were maintained in standard cages upon controlled lighting (12h:12h, lights on at 7.00), were fed a standard chow and given water ad libitum as described in Chapter 2.

A subgroup of mice underwent MRS and MRI in a 7Tesla Varian/Agilent Technologies MRI Scanner at 6, 18 and 24 months of age, as described in Chapter 2.

At 24 months of age, brains were removed and half the brain fixed for immunofluorescent analysis and the remaining half dissected for real time PCR analysis as outlined in Chapter 2. Figure 4.1 illustrates the number of animals undergoing MRS and MRI at each time point and the collection of brain tissue. Tissue was collected following the final testing at 24 months, unless mice were culled earlier due to age.

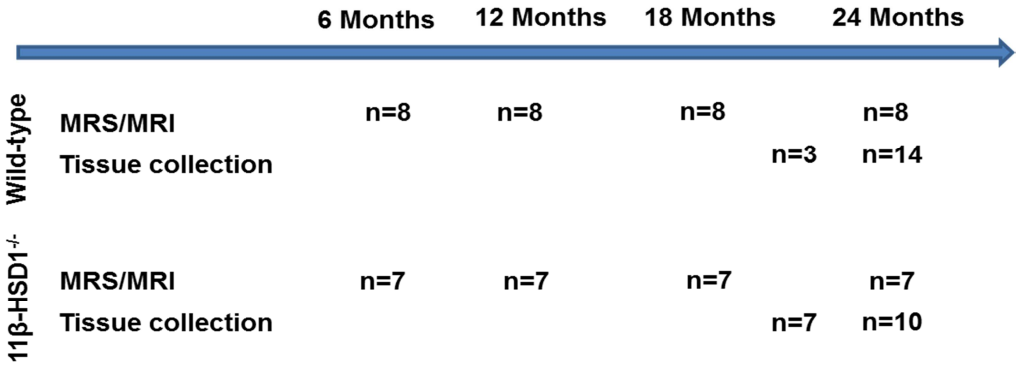

Figure 4.1. Number of wild-type and 11β-HSD1$^{-/-}$ mice undergoing MRS/MRI at each timepoint and timeline of tissue collected.

4.2.2 MRS Analysis

LC Model method was utilised to analyse the spectrum produced. This model analyses and quantitates an in vivo spectrum of brain metabolites as outlined in Chapter 2.

4.2.3 MRI Structural Analysis

The software ANALYZE was used to analyse hippocampal and whole brain volumes from T2 weighted structural scans obtained during the MRS scan as described in Chapter 2.

4.2.4 Immunofluorescence

Hippocampal brain sections were processed as outlined in Chapter 2 and stained for 11B-HSD1, microglia, neuron and glial expression using primary antibodies purified sheep 11β-HSD1, Mouse NeuN and Rabbit GFAP respectively and secondary antibodies anti-Sheep Alexa Fluor 488, anti-Mouse Alexa Fluor 555 and anti-Rabbit Alexa Fluor 555 respectively.

4.2.5 Statistics

Statistical analysis was conducted using PRISM and significant differences determined by unpaired t-test where appropriate with a P value < 0.05 signifying a significant difference.

Differences between young and aged mice were calculated using a two-way ANOVA or unpaired T-Test with a P value < 0.05 signifying a significant effect or difference of means difference.

The relationship between variables (11β-HSD1, Probe test data, Radial arm water maze savings data, NeuN, GFAP, metabolites, structural data) was analysed using Pearson's correlation with a P value < 0.05 signifying a significant difference.

4.3 Results

4.3.1 11β-HSD1 expressed in glial cells

Previous in-situ hybridisation studies have identified the possible expression of 11β-HSD1 mRNA in hippocampal neurons. Therefore, to investigate if neuronal 11β-HSD1 expression and neuronal physiology was altered with age in wild-type mice and determine if lifelong deletion of 11β-HSD1 attenuated these changes, a qualitative and quantitative analysis of cellular markers was performed on brain sections of the longitudinally aged colony of wild-type and 11β-HSD1$^{-/-}$ mice at 24 months.

Interestingly, qualitative results from double immunofluorescent stains for 11β-HSD1 expression and a neuronal marker, Neuronal Nuclei (NeuN), in hippocampal brain sections of aged wild-type mice revealed limited expression of 11β-HSD1 in hippocampal neurons (Fig. 4.2). No expression of 11β-HSD1 was observed in 11β-HSD1$^{-/-}$ mice, confirming deletion of 11β-HSD1 in the 11β-HSD1$^{-/-}$ mouse colony (Fig. 4.3).

Similarly, in the cortex, no colocalisation of 11β-HSD1 and NeuN was observed in aged wild-type mice (Fig. 4.2).

Figure 4.2. 11β-HSD1 and NeuN expression in aged wild-type mice

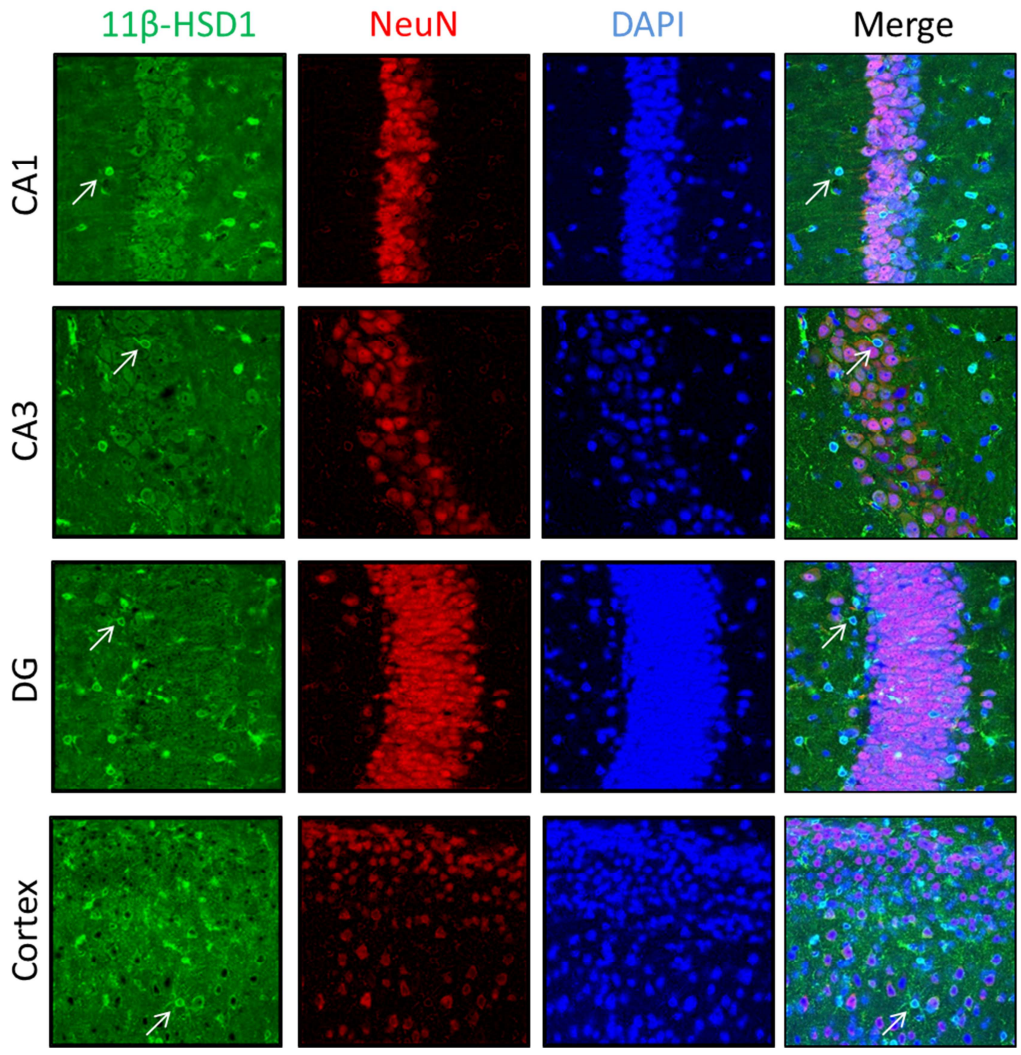

Fig. 4.2. Representative images of patterns of 11β-HSD1(Green) and NeuN (Red) expression in the CA1, CA3, Dentate Gyrus (DG) and Cortex of aged wild-type mice. Images of hippocampal subregions CA1, CA3 and DG captured at 30x magnification using a Zeiss Axioskop confocal laser microscope. Blue represents DAPI stained nuclei. White arrows indicate example of positive expression of 11β-HSD1.

Figure 4.3. 11β-HSD1 and NeuN expression in aged 11β-HSD1$^{-/-}$ mice

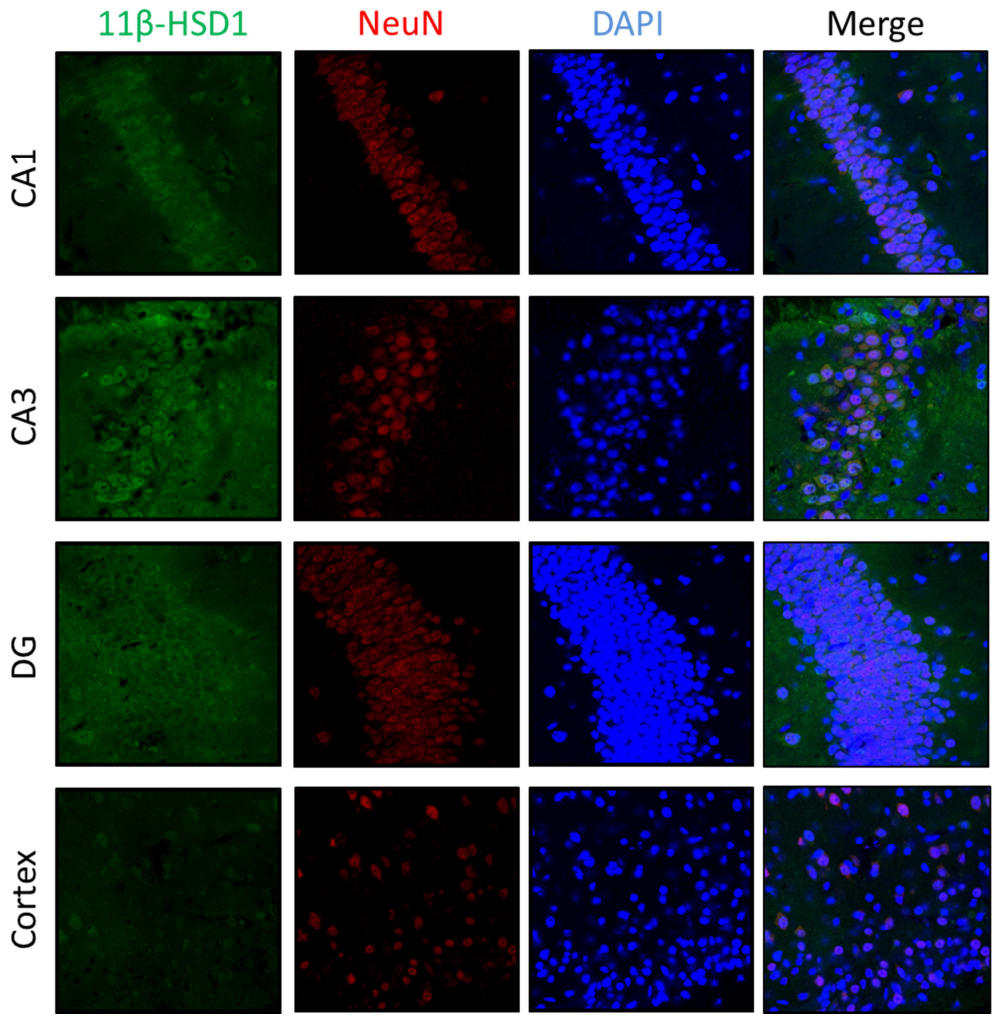

Fig. 4.3. Representative images of patterns of 11β-HSD1(Green) and NeuN (Red) expression in the CA1, CA3, Dentate Gyrus (DG) and Cortex of aged 11β-HSD1$^{-/-}$ mice. Images of CA1, CA3 and DG captured at 30x magnification using a Zeiss Axioskop confocal laser microscope. Blue represents DAPI stained nuclei.

However, 11β-HSD1 appears to be expressed in another group of cells thought to be glial cells due to their processes. Double staining for the glial cell marker, glial fibrillary acidic protein (GFAP), and 11β-HSD1 confirmed the expression of 11β-HSD1 in glial cells (Fig. 4.4). In particular, 11β-HSD1 was observed to be expressed largely in the cell membrane and dendritic processes of the glial cells.

These results show that 11β-HSD1 protein is rarely expressed in neurons contrary to what was previously thought.

Figure 4.4. 11β-HSD1 and GFAP colocalisation in aged wild-type mice

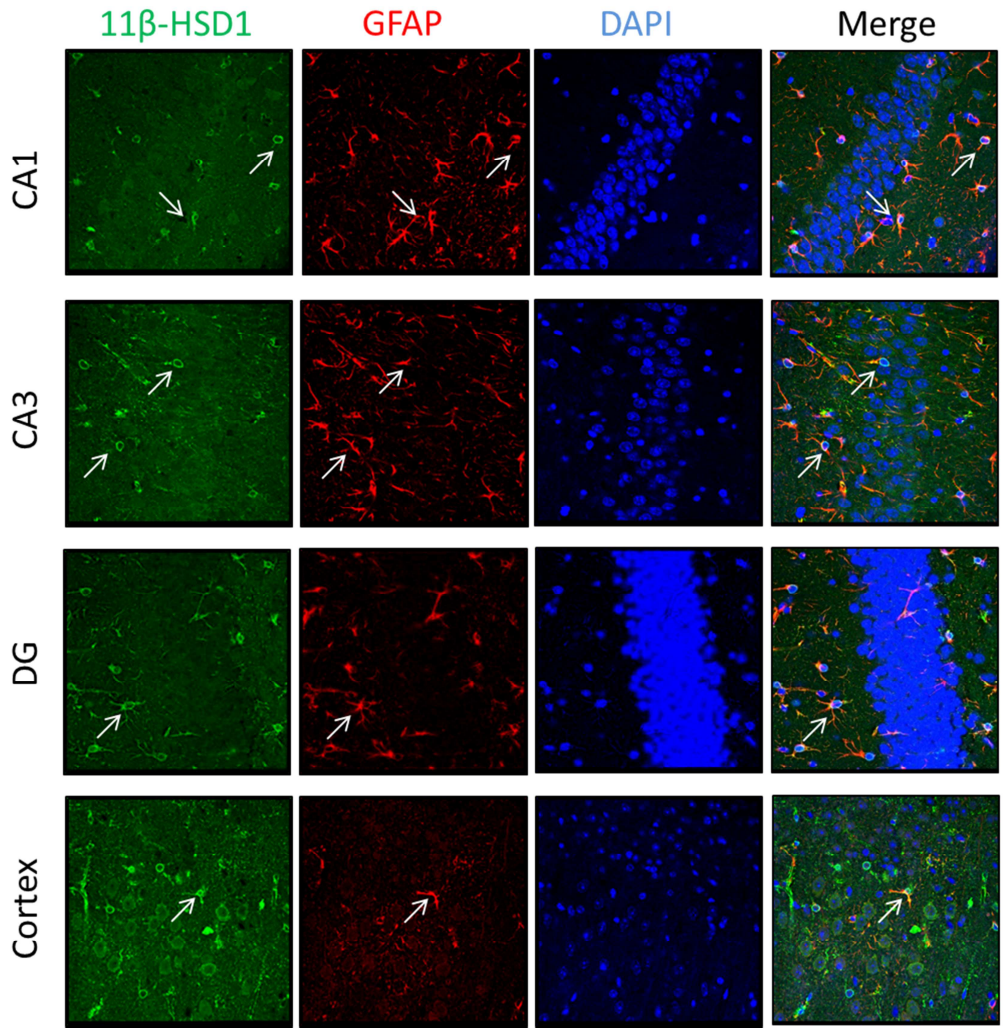

Fig. 4.4. Representative images of patterns of 11β-HSD1(Green) and GFAP (Red) expression in the CA1, CA3, Dentate Gyrus (DG) and Cortex of aged 11β-HSD1$^{-/-}$ mice. Images of CA1, CA3 and DG captured at 30x magnification using a Zeiss Axioskop confocal laser microscope. Blue represents DAPI stained nuclei. White arrows indicate example of positive expression of 11β-HSD1, GFAP and colocalisation.

4.3.2 Hippocampal 11β-HSD1 protein expression and ageing

Previous studies have established that levels of 11β-HSD1increase with age and are associated with spatial impairments observed with age (Holmes et al., 2010).

A quantitative analysis of the immunofluorescence was performed utilising two measures: 1) the area of fluorescence for the specified stain meeting a predefined intensity as a percentage of the total area; and 2) the number of cells expressing the protein.

Therefore, we wished to determine if the expression of 11β-HSD1 in the hippocampus and cortex is altered with age. As the colony of wild-type and 11β-HSD1$^{-/-}$ mice were culled at 24 months following longitudinal assessment, a cross sectional experimental design was utilised to examine age-related changes. Young (6 months) wild-type and 11β-HSD1$^{-/-}$ mice were culled and their brain sections processed alongside the brain sections of the aged wild-type and 11β-HSD1$^{-/-}$ mice colony.

As expected, both young and aged 11β-HSD1$^{-/-}$ mice showed no expression of 11β-HSD1 (data not shown for young brains but for aged brains see Fig. 4.1)

A significantly lower percentage fluorescence of 11β-HSD1 was observed in the CA1 of aged wild-type mice [Young: M = 1.436, SD = 0.5126; Aged: M = 0.3720, SD = 0.09967; t(16) = 3.369, p = 0.0071; Fig. 4.5A] compared to young mice (unpaired T-Test). Significantly lower expression of 11β-HSD1 in aged wild-type mice was also observed in the CA3 [Young: M = 4.391, SD = 1.679; Aged: M = 0.8164, SD = 0.2210; t(17) = 3.501, p < 0.0001; Fig. 4.5B] and dentate gyrus of the

hippocampus [Young: M = 4.473, SD = 1.893; Aged: M = 0.9684, SD = 0.2348; $t(17) = 3.069$, $p < 0.0001$; Fig. 4.5C]. However, there was no significant difference in the expression of 11β-HSD1 in the cortex of young and aged wild-type mice [Young: M = 2.744, SD = 0.6810; Aged: M = 1.343, SD = 0.4173; $t(16) = 1.620$, $p = 0.9285$; Fig. 4.5D].

The number of cells expressing 11β-HSD1 did not differ between groups in any region studied. The number of cells expressing 11β-HSD1 between young and aged wild-type mice in the CA1 [Young: M = 6.667, SD = 0.9428; Aged: M = 5.286, SD = 0.7718; $t(7) = 1.33$, $p = 0.5251$; Fig. 4.6A], CA3[Young: M = 5.567, SD = 0.5364; Aged: M = 5.167, SD = 0.5834; $t(13) = 0.5047$, $p = 0.2571$; Fig. 4.6B], DG [Young: M = 7.4, SD = 1.404; Aged: M = 6.857, SD = 0.6836; $t(6) = 0.3476$, $p = 0.5146$; Fig. 4.6C] and cortex [Young: M = 12.42, SD = 1.96; Aged: M = 9.893, SD = 1.289; $t(5) = 1.076$, $p = 0.8181$; Fig. 4.6D].

Figure 4.5. Percentage Fluorescence of 11β-HSD1 expression in young and aged wild-type mice

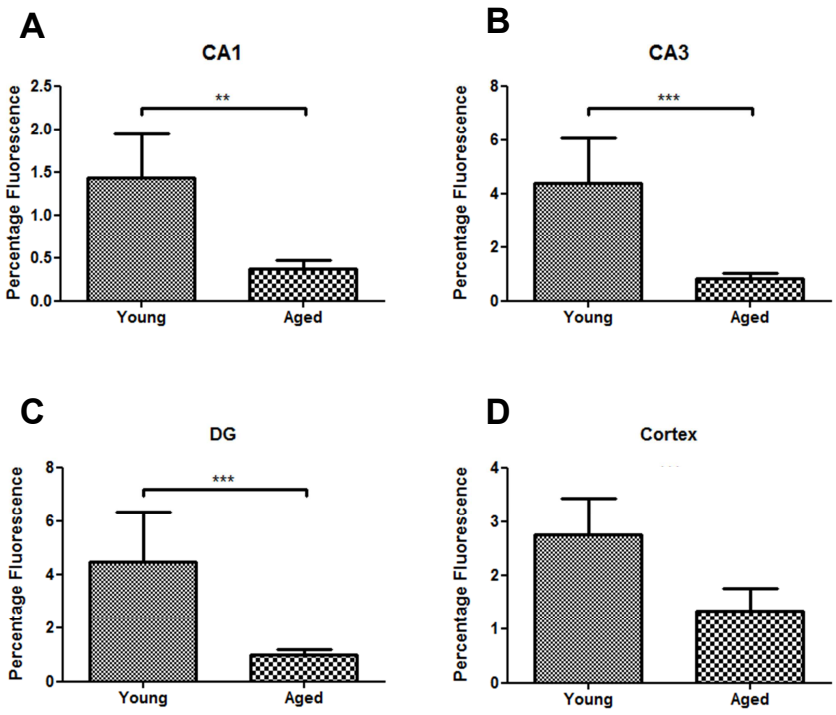

Fig. 4.5. Graphs showing the percentage area of fluorescence of 11β-HSD1 in **[A]** CA1 of young (n=4) and aged (n=14) wild-type mice; **[B]** CA3 of young (n=5) and aged (n=14) wild-type mice; **[C]** dentate gyrus (DG) of young (n=5) and aged (n=14) wild-type mice; and **[D]** cortex of young (n=4) and aged (n=15) wild-type mice. Values represent mean percentage area of fluorescence (across three fields per animal) +SEM. *$p < 0.05$; ** $p < 0.01$; *** $p < 0.001$.

Figure 4.6. Number of cells co-expressing 11β-HSD1 and GFAP in young and aged wild-type mice

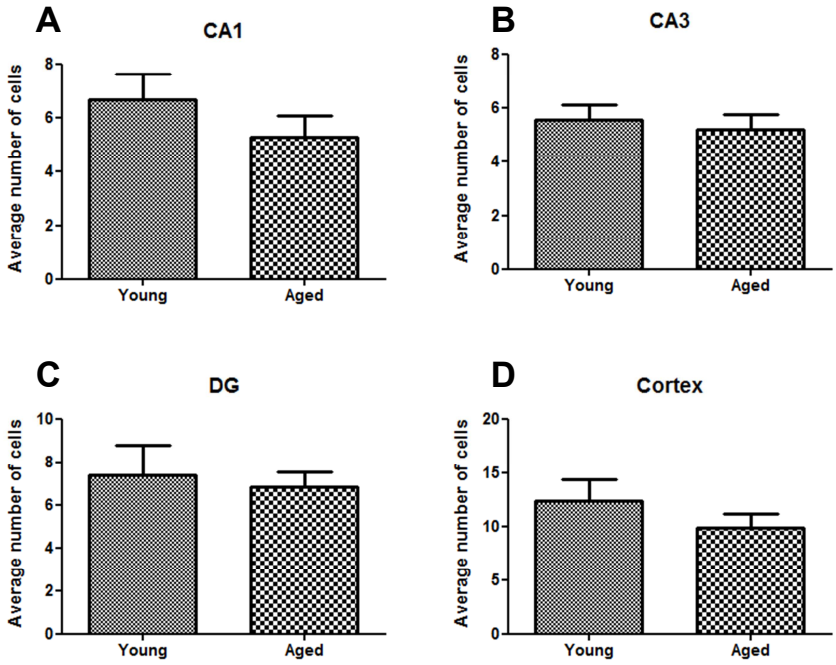

Fig. 4.6. Graphs showing the number of cells expressing 11β-HSD1 in **A]** CA1 of young (n=4) and aged (n=14) wild-type mice; **[B]** CA3 of young (n=5) and aged (n=14) wild-type mice; **[C]** dentate gyrus (DG) of young (n=5) and aged (n=14) wild-type mice; and **[D]** cortex of young (n=4) and aged (n=15) wild-type mice. Values represent mean number of cells (across three fields per animal) +SEM.

4.3.3 11β-HSD1 protein expression and spatial memory and spatial working memory

4.3.3.1 Probe test performance

No correlation was observed between the percentage time spent swimming in the target quadrant and percentage area of fluorescence in the CA1 [r = -0.4042, p = 0.2467], CA3 [r = -0.3641, p = 0.3010], DG [r = -0.06404, p = 0.8605] and cortex [r = -0.2246, p = 0.5328] of the brain.

Similarly, no correlation was observed between the latency to previous platform location and percentage area of fluorescence in the CA1 [r = 0.5468, p = 0.1019], CA3 [r = 0.3778, p = 0.2817], DG [r = 0.5594, p = 0.0927] and cortex [r = 0.3781, p = 0.2814].

4.3.3.2 Radial Arm Water Maze

In wild-type mice, there was no correlation between 11β-HSD1 expression and latency savings over the 1 hour retention interval in the CA1 [r = 0.008253, p = 0.9821], CA3 [r = 0.01376, p = 0.9676], DG [r = -0.04952, p = 0.8753] and cortex [r = 0.2146, p = 0.4780]. There was no correlation between 11β-HSD1 expression and error savings over the 1 hour retention interval in the CA1 [r = 0.07652, p = 0.8039], CA3 [r = 0.1049, p = 0.7311], DG [r = 0.1049, p = 0.7311] and cortex [r = 0.1899, p = 0.5299].

In 11β-HSD1$^{-/-}$ mice, there was no correlation between 11β-HSD1 expression and latency savings over the 1 hour retention interval in the CA1 [r = 0.01667, p = 0.9816], CA3 [r = -0.5000, p = 0.1777], DG [r = -0.02510, p = 0.9574] and cortex [r

= -0.6276, p = 0.0773]. There was no correlation between 11β-HSD1 expression and error savings over the 1 hour retention interval in the CA1 [r = -0.1167, p = 0.7756], CA3 [r = -0.5500, p = 0.1328], DG [r = 0.2008, p = 0.6024] and cortex [r = -0.6360, p = 0.0716].

4.3.4 Number of neurons and hippocampal 11β-HSD1 expression

Hippocampal neurons have been found to be a principal site of glucocorticoid action and glucocorticoid sensitive. Subsequently, glucocorticoids have been observed to be neurotoxic in some cases with prolonged glucocorticoid exposure resulting in hippocampal neuron loss. Thus, 11β-HSD1 protein levels were tested to see if they affected the number of neurons in the hippocampus and cortex of aged mice to determine if the number of neurons was altered by 11β-HSD1 protein levels.

Indeed, higher levels of 11β-HSD1 were associated with more neurons in the hippocampus of wild-type mice. Percentage area fluorescence of NeuN was positively correlated with the percentage area of 11β-HSD1 in the CA1 [r = 0.5549, p = 0.049], CA3 [r = 0.6648, p = 0.0132] and DG [r = 0.5989, p = 0.0306] of the hippocampus, but not in the cortex [r = 0.5330, p = 0.0607].

4.3.5 Number of neurons and spatial memory and spatial working memory

Spatial learning and memory is a hippocampal dependent task. As such, the association between the number of neurons and latency to escape on the final day of spatial learning and performance measures in the probe test was tested to assess the

relationship between the number of neurons and spatial learning in aged wild-type and 11β-HSD1$^{-/-}$ mice.

4.3.5.1 Probe test performance

No correlation was observed between the percentage time spent swimming in the target quadrant the number of neurons in the CA1 [r = -0.03178, p = 0.9305], CA3 [r = -0.0003894, p = 0.9991], DG [r = 0.06712, p = 0.8538]. Similarly, no correlation was observed between the latency to previous platform location and neuronal number CA1 [r = 0.5027, p = 0.1386], CA3 [r = 0.4880, p = 0.1525] and DG [r = 0.5112, p = 0.1310] in wild-type mice.

However, in the cortex of wild-type mice, higher neuronal number was associated with longer latencies to the previous platform location in the probe test [r = 0.7105, p = 0.0213] but not the time spent swimming in the target quadrant [r = -0.2936, p = 0.4102].

In 11β-HSD1$^{-/-}$ mice, probe test performance was not associated with the number of neurons in hippocampal subregions CA1 and CA3 and the cortex. No correlation was observed between the percentage time swimming in the target quadrant and number of neurons in the CA1 [r = -0.4476, p = 0.4498], CA3 [r = -0.5483, p = 0.3387] and cortex [r = -0.7248, p = 0.1160] of the brain. Similarly, no correlation was observed between the latency to previous platform location and number of neurons in the CA1 [r = 0.2126, p = 0.7314], CA3 [r = 0.2343, p = 0.7045], DG [r = 0.4851, p = 0.5149] and cortex [r = 0.3524, p = 0.5608] of the brain.

However, a significant correlation was observed between percentage time spent swimming in the target quadrant and number of neurons in the DG [r = -0.9914, p =

0.0086] suggesting that the number of neurons in the dentate gyrus are associated with spatial memory.

4.3.5.2 Radial Arm Water Maze

In wild-type mice, there was no correlation between NeuN expression and latency savings over the 1 hour retention interval in the CA1 [r = -0.005502, p = 0.9889], CA3 [r = 0.1403, p = 0.6457], DG [r = 0.1051, p = 0.7443] and cortex [r = 0.2767, p = 0.3811]. There was no correlation between NeuN expression and error savings over the 1 hour retention interval in the CA1 [r = 0.1417, p = 0.6412], CA3 [r = 0.2863, p = 0.3389], DG [r = 0.2547, p = 0.4196] and cortex [r = 0.4476, p = 0.1452]. Similarly, no correlation was observed between the number of neurons and latency savings over the 1 hour retention interval in the CA1 [r = 0.1623, p = 0.5939], CA3 [r = 0.01926, p = 0.9532], DG [r = 0.1576, p = 0.6227] and cortex [r = 0.2242, p = 0.4801] and no correlation was observed between the number of neurons and error savings over the 1 hour retention interval in the CA1 [r = 0.3599, p = 0.2248], CA3 [r = 0.1757, p = 0.5618], DG [r = 0.3639, p = 0.2426] and cortex [r = 0.3312, p = 0.2896].

In 11β-HSD1$^{-/-}$ mice, there was no correlation between NeuN expression and latency savings over the 1 hour retention interval in the CA1 [r = -0.1865, p = 0.6384], CA3 [r = -0.4746, p = 0.2003], DG [r = -0.06093, p = 0.8792] and cortex [r = -0.4532, p = 0.3143]. There was no correlation between NeuN expression and error savings over the 1 hour retention interval in the CA1 [r = -0.2712, p = 0.4811], CA3 [r = -0.5085, p = 0.1688], DG [r = 0.06093, p = 0.8792] and cortex [r = -0.7684, p = 0.0667]. Similarly, no correlation was observed between the number of neurons and latency

savings over the 1 hour retention interval in the CA1 [r = -0.06723, p = 0.8685], CA3 [r = -0.1017, p = 0.8011], DG [r = -0.1423, p = 0.7174] and cortex [r = 0.04372, p = 0.9161] and no correlation was observed between the number of neurons and error savings over the 1 hour retention interval in the CA1 [r = -0.1167, p = 0.7756], CA3 [r = -0.2767, p = 0.5809], DG [r = 0.06667, p = 0.8801] and cortex [r = 0.5000, p = 0.2667].

4.3.6 Glial reactivity, density and hippocampal 11β-HSD1 expression

As our study noted 11β-HSD1 to be expressed in glial cells, expression of 11β-HSD1 was tested to see if it would alter glial cell reactivity or the number of glial cells.

GFAP fluorescence was associated with 11β-HSD1 expression in all hippocampal regions. Positive correlations were noted in the CA1 [r = 0.7319, p = 0.0029], CA3 [r = 0.7143, p = 0.0041] and DG [r = 0.6, p = 0.0233], however, GFAP fluorescence was not correlated with 11β-HSD1 expression in the cortex [r = 0.3407, p = 0.233].

The number of glial cell bodies was positively correlated with the number of 11β-HSD1 expressing cells in the CA1[r = 0.7682, p = 0.0013] and DG [r = 0.6236, p = 0.0172] but not the CA3[r = 0.5270, p = 0.0528] and cortex[r = 0.2228, p = 0.444].

This suggests that an increase in glial cell number gives a parallel increase in 11β-HSD1, as 11β-HSD1 is expressed in glial cells. However, it also suggests that 11β-HSD1 expression and glial reactivity are related although it cannot be determined whether increased11β-HSD1 leads to increased GFAP or vice versa.

4.3.7 Glial reactivity, density and spatial memory and spatial working memory

Traditionally, neurons were considered the basic functional units of the brain with glial cells supporting neuronal function. However, more recent evidence has suggested that a neuronal-microglia-glia triad is essential for functional organisation of the brain (Barres, 2008; Allen and Barres, 2009). Therefore we tested to see if the percentage fluorescence of GFAP and the number of glial cells in aged wild-type and 11β-HSD1$^{-/-}$ mice would alter distance travelled on the final day of spatial learning and measures of probe test performance.

4.3.7.1 Probe test performance

In wild-type mice, there was no correlation between GFAP expression and the percentage time spent in the target quadrant in the CA1 [r = -0.4608, p = 0.2119], CA3 [r = -0.3801, p = 0.3129], DG [r = -0.3729, p = 0.3230] and cortex [r = -0.3348, p = 0.3784]. Similarly, no correlation was observed between the number of glial cells and percentage time spent in the target quadrant in the CA1 [r = -0.4874, p = 0.1778], CA3 [r = -0.2941, p = 0.4257], DG [r = -0.35, p = 0.3586] and cortex [r = -0.1461, p = 0.5470].

However, increased expression of GFAP was associated with longer latencies to the previous platform location in the hippocampal regions CA1 [r = 0.7532, p = 0.0191; Fig. 4.7A], CA3 [r = 0.6840, p = 0.0422; Fig. 4.7B] and DG [r = 0.6704, p = 0.0481; Fig. 4.7B] but not the cortex [r = 0.5355, p = 0.1373]. But number of glial cells in the CA1 [r = 0.3614, p = 0.3384], CA3 [r = 0.2521, p = 0.5108], DG [r = 0.5333, p =

0.1475] and cortex [r = 0.6390, p = 0.0747] was not related to latency to previous platform

In 11β-HSD1$^{-/-}$ mice, neither GFAP expression nor number of glial cells number was associated with either measure of probe test performance. There was no correlation between the two measures and the percentage time spent in the target quadrant in the CA1 [GFAP: r = 0.2304, p = 0.7696; Density: r = 0.8, p = 0.333], CA3 [GFAP: r = 0.2304, p = 0.7696; Density: r = 0.6325, p = 0.5], DG [GFAP: r = 0.2304, p = 0.7696; Density: r = 0.8, p = 0.333] and cortex [GFAP: r = 0.2304, p = 0.7696; Density: r = -0.6325, p = 0.333]. Similarly, no correlation was observed between expression of GFAP and the latency to previous platform location in the CA1 [GFAP: r = 0.2304, p = 0.7696; Density: r = -0.4, p = 0.75], CA3 [GFAP: r = 0.2304, p = 0.7696; Density: r = -0.3162, p = 0.5], DG [GFAP: r = 0.2304, p = 0.7696; Density: r = 0.6, p = 0.4167] and cortex [GFAP: r = 0.2304, p = 0.7696; Density: r = -0.7379, p = 0.1667].

4.3.7.2 Radial Arm Water Maze

In wild-type mice, there was no correlation between GFAP expression and latency savings over the 1 hour retention interval in the CA1 [r = -0.1045, p = 0.7328], CA3 [r = -0.2806, p = 0.3499], DG [r = -0.05502, p = 0.8592] and cortex [r = -0.2201, p = 0.4665]. There was no correlation between GFAP expression and error savings over the 1 hour retention interval in the CA1 [r = -0.1275, p = 0.6760], CA3 [r = -0.4280, p = 0.1447], DG [r = -0.2069, p = 0.4929] and cortex [r = -0.2324, p = 0.4401]. Similarly, no correlation was observed between the number of glial cells and latency savings over the 1 hour retention interval in the CA1 [r = -0.1506, p = 0.6197], CA3

[r = -0.08183, p = 0.7887], DG [r = 0.2837, p = 0.3438] and cortex [r = -0.2525, p = 0.4004] and no correlation was observed between the number of glial cells and error savings over the 1 hour retention interval in the CA1 [r = -0.2078, p = 0.4896], CA3 [r = 0.03572, p = 0.9078], DG [r = -0.01987, p = 0.9490] and cortex [r = -0.1034, p = 0.7350].

In 11β-HSD1$^{-/-}$ mice, there was no correlation between GFAP expression and latency savings over the 1 hour retention interval in the CA1 [r = -0.0500, p = 0.9116], CA3 [r = -0.4500, p = 0.2298], DG [r = -0.5167, p = 0.1618] and cortex [r = 0.1167, p = 0.7756]. There was no correlation between GFAP expression and error savings over the 1 hour retention interval in the CA1 [r = -0.2667, p = 0.4933], CA3 [r = -0.5000, p = 0.1777], DG [r = -0.6833, p = 0.0503] and cortex [r = -0.0500, p = 0.9116]. Similarly, no correlation was observed between the number of glial cells and latency savings over the 1 hour retention interval in the CA1 [r = -0.06723, p = 0.8685], CA3 [r = -0.1017, p = 0.8011], DG [r = -0.1423, p = 0.7174] and cortex [r = 0.04372, p = 0.9161] and no correlation was observed between the number of glial cells and error savings over the 1 hour retention interval in the CA1 [r = -0.2941, p = 0.4392], CA3 [r = -0.2712, p = 0.4803], DG [r = -0.5439, p = 0.1352] and cortex [r = -0.04372, p = 0.9161].

4.3.8 Hippocampal volume and ageing

As glucocorticoids are known to alter hippocampal volume, we investigated changes in hippocampal and ventricle volume with age. Structural scans were used to determine the hippocampal and ventricle volume in the same wild-type and 11β-

HSD1$^{-/-}$ mice at 6, 18 and 24 months of age. Hippocampal volume was measured as a percentage of total brain volume.

Hippocampal volume decreased with age in wild-type mice but not 11β-HSD1$^{-/-}$ mice. A two-way ANOVA revealed a significant effect of age on hippocampal volume [$F(2,39) = 5.821$, $p = 0.0061$; Fig. 4.8], however, there was no significant effect of genotype on hippocampal volume [$F(1,39) = 2.353$, $p = 0.603$; Fig. 4.8]. Post hoc tests revealed smaller hippocampal volumes compared to when they were young in aged wild-type mice but not aged 11β-HSD1$^{-/-}$ mice.

A two-way ANOVA revealed no effect of age on whole brain volume [$F(2,42) = 3.081$, $p = 0.0564$], and no significant effect of genotype on hippocampal volume [$F(1,42) = 0.9065$, $p = 0.3465$].

Figure 4.8. Hippocampal Volume (as a % of Total Brain Volume) in Young and Aged Wild-Type (WT) and 11β-HSD1$^{-/-}$ (KO) mice

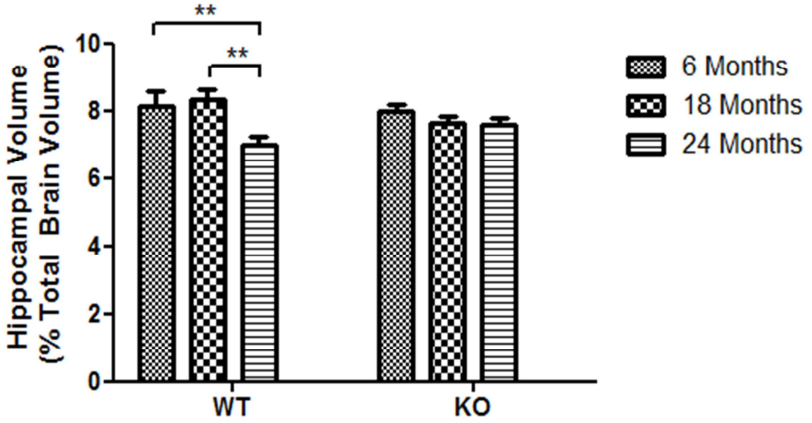

Fig. 4.8. Graph showing hippocampal volume (as a percentage of total brain volume) in young (n=7) and aged (n=7) wild-type mice (WT) and young (n=8) and aged (n=8) 11β-HSD1$^{-/-}$ mice (KO). Values represent mean volume +SEM. *$p < 0.05$; ** $p < 0.01$; *** $p < 0.001$.

4.3.9 Hippocampal volume and spatial memory and spatial working memory

4.3.9.1 Probe test performance

Hippocampal volumes were correlated with spatial memory measures from the probe test to examine if hippocampal volume was related to spatial memory.

Hippocampal volume was not associated with probe test performance in either genotype.

There was no correlation between hippocampal volume and percentage time spent in the target quadrant [r = -0.1369, p = 0.8263] and latency to the previous platform location [r = -0.1446, p = 0.8165] during the probe test in wild-type mice.

No correlation between hippocampal volume and percentage time spent in the target quadrant [r = -0.6967, p = 0.1911] and latency to the previous platform location [r = -0.7728, p = 0.1255] during the probe test in 11β-HSD1$^{-/-}$ mice.

4.3.9.2 Radial Arm Water Maze

In wild-type mice, there was no correlation between hippocampal volume and latency savings over the 1 hour retention interval [r = 0.2319, p = 0.6500]. There was no correlation between hippocampal volume and error savings over the 1 hour retention interval [r = 0.3043, p = 0.6000].

In 11β-HSD1$^{-/-}$ mice, there was no correlation between hippocampal volume and latency savings over the 1 hour retention interval [r = -0.09524, p = 0.8401]. There was no correlation between hippocampal volume and error savings over the 1 hour retention interval [r = 0.3976, p = 0.3250].

4.3.10 Age-associated changes in hippocampal metabolite levels

Changes in neuronal viability, membrane turnover/breakdown, glial cells, excitatory neurotransmission and energy metabolism with age and following lifelong removal of 11β-HSD1 were investigated. Proton magnetic resonance spectroscopy (^{1}H-MRS) was carried out on wild-type and 11β-HSD1$^{-/-}$ mice when they were 6, 18 and 24 months of age. Specifically, changes in metabolites N-acetylaspartate (NAA), Choline (Cho), Inositol (Ins), Glucose (Glc), Glutamate (Glu), Glutamine (Gln) and Glutamate/Glutamine complex (Glx) which are associated with neuronal viability, membrane turnover/breakdown, glial cells, energy metabolism and excitatory neurotransmission respectively were investigated (Fig. 4.9).

There was a significant effect of age on hippocampal Cho levels [$F(2,28) = 4.645$, $p = 0.00181$; Fig. 4.10] but no effect of genotype [$F(1,28) = 2.37$, $p = 0.1349$; Fig. 4.10]. No interaction was found, but post hoc tests revealed significantly higher Cho levels in 11β-HSD1$^{-/-}$ mice at 18 months and 24 months of age compared to 6 months of age. However, no significant differences in Cho levels were observed between 6, 18 and 24 month aged wild-type mice. This suggests that there is an increase in membrane turnover/breakdown with age in mice where 11β-HSD1 is absent.

A two-way ANOVA of age and genotype on hippocampal NAA levels revealed a significant effect of age on hippocampal NAA levels [$F(2,35) = 3.542$, $p = 0.0397$; Fig. 4.11] but no significant effect of genotype on hippocampal NAA levels [$F(1,35) = 0.2004$, $p = 0.6572$; Fig. 4.11]. However, post hoc tests revealed no significant

differences between young and aged wild-type mice hippocampal NAA levels and young and aged 11β-HSD1$^{-/-}$ mice hippocampal NAA levels.

Similarly, a two-way ANOVA of age and genotype on hippocampal Ins levels revealed a significant effect of age on hippocampal Ins levels [$F(2,35) = 4.069$, $p = 0.0258$; Fig. 4.12] but no significant effect of genotype on hippocampal Ins levels [$F(1,35) = 0.3855$, $p = 0.5387$; Fig. 4.12]. No interaction was observed, however, post hoc tests revealed no significant differences between young and aged wild-type mice hippocampal Ins levels and young and aged 11β-HSD1$^{-/-}$ mice hippocampal Ins levels. This suggests that there is an effect of age on gliosis within the hippocampus.

No effect of age or genotype was observed for hippocampal levels of glucose, glutamate, glutamine and glutamate/glutamine complex.

Figure 4.9. Hippocampal ^{1}H-MRS spectra of a wild-type mouse

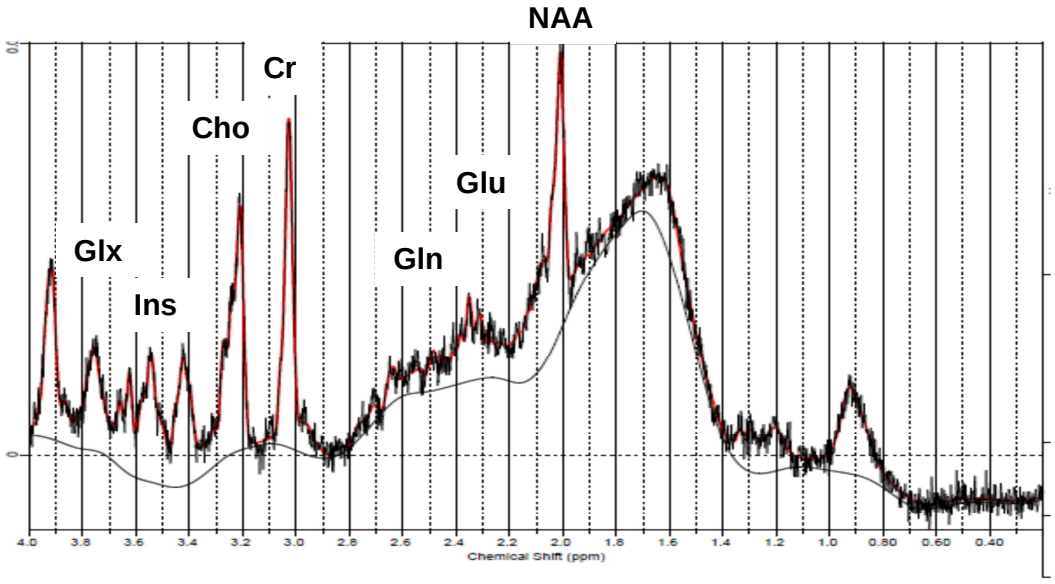

Fig. 4.9. Representative unilateral hippocampus ^{1}H-MRS spectra of a wild-type mouse. The chemical shift for each peak is shown in parts per million (ppm), and the area under the curve of the peak indicates the relative amount of a particular metabolite. The major peaks represent choline (Cho) [3.2 ppm], creatine (Cr) [3.05 ppm], N-acetyl aspartate (NAA) [2.0 ppm] the glutamate –glutamine complex (Glx) [3.75ppm], glutamate [3.34ppm] and glutamine [2.42ppm]. These metabolites can be identified by their chemical shift on the spectrum.

Figure 4.10. Choline (Cho) Levels in Young and Aged Wild-Type (WT) and 11β-HSD1$^{-/-}$ (KO) mice

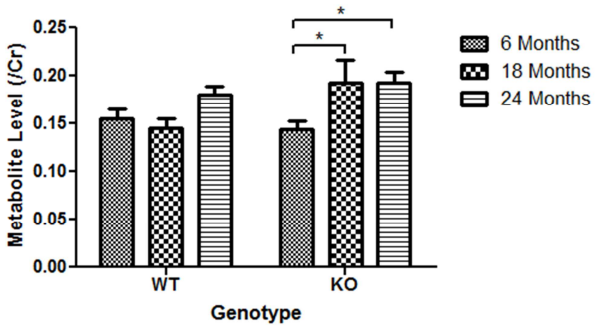

Fig. 4.10. Graph showing Choline (Cho) levels (as a ratio of Creatine, Cr) in young (n=7) and aged (n=7) wild-type mice (WT) and young (n=8) and aged (n=8) 11β-HSD1$^{-/-}$ mice (KO). Values represent mean metabolite level (/Cr) +SEM. *$p < 0.05$;

Figure 4.11. NAA Levels in Young and Aged Wild-Type (WT) and 11β-HSD1$^{-/-}$ (KO) mice

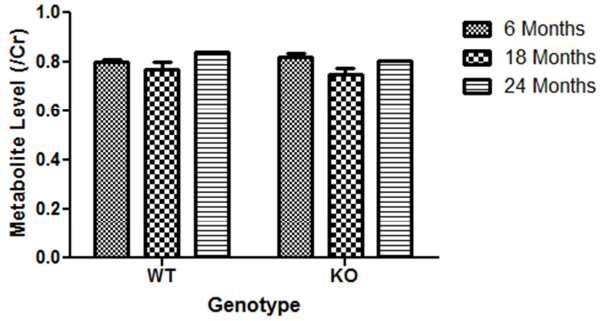

Fig. 4.11. Graph showing N-acetylaspartate (NAA) levels (as a ratio of Creatine, Cr) in young (n=7) and aged (n=7) wild-type mice (WT) and young (n=8) and aged (n=8) 11β-HSD1$^{-/-}$ mice (KO). Values represent mean metabolite level (/Cr) +SEM.

Figure 4.12. Ins Levels in Young and Aged Wild-Type (WT) and 11β-HSD1$^{-/-}$ (KO) mice

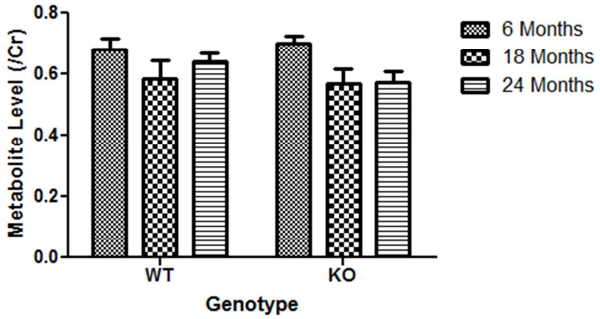

Fig. 4.12. Graph showing Inositol (Ins) levels (as a ratio of Creatine, Cr) in young (n=7) and aged (n=7) wild-type mice (WT) and young (n=8) and aged (n=8) 11β-HSD1$^{-/-}$ mice (KO). Values represent mean metabolite level (/Cr) +SEM.

4.3.11 Hippocampal metabolite levels and spatial memory and spatial working memory

4.3.11.1 Probe test performance

Metabolite levels at 18 months were correlated with their performance in the probe test at 18 months of age to investigate if age-associated spatial learning impairment was related to metabolite levels.

In the probe test, no relationship was observed between any of the metabolites and the measures of probe test performance in wild-type mice.

However, in the probe test, N-acetylaspartate (NAA) [r = 0.9662, p = 0.0074; Fig. 4.13] and Glutamate (Glu) [r = 0.9752, p = 0.0047; Fig. 4.14] were observed to be correlated with percentage time spent in the target quadrant in 11β-HSD1$^{-/-}$ mice.

No correlation was observed between probe test performance and any other

4.3.11.2 Radial Arm Water Maze

No relationship was observed between any of the metabolites and the measures of spatial working memory in wild-type and 11β-HSD1$^{-/-}$ mice

.

Figure 4.13. 18 Months: Correlations between hippocampal NAA levels and probe test performance in aged 11β-HSD1$^{-/-}$ mice

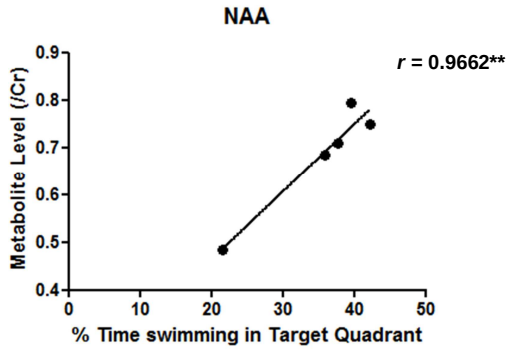

Fig. 4.13. Correlation coefficient (*r*) of the correlation calculated between N-acetylaspartate (NAA) and percentage time swimming in the target quadrant in the probe test in 18 month aged 11β-HSD1$^{-/-}$ mice (n=5). ** $p < 0.01$.

Figure 4.14. 18 Months: Correlations between hippocampal Glu levels and probe test performance in aged 11β-HSD1$^{-/-}$ mice

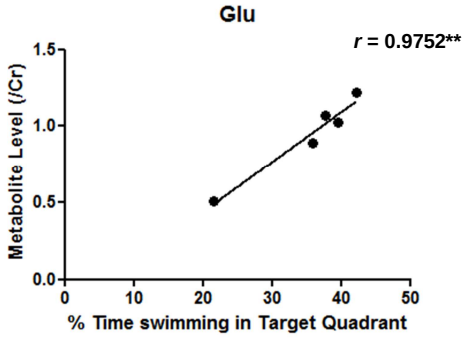

Fig. 4.14. Correlation coefficient (*r*) of the correlation calculated between Glutamate (Glu) and percentage time swimming in the target quadrant in the probe test in 18 month aged 11β-HSD1$^{-/-}$ mice (n=5). ** $p < 0.01$

4.4 Discussion

This chapter aimed to explore the possible molecular, structural and metabolite mechanisms through which 11β-HSD1 expression may alter cognitive function. Age-associated changes in 11β-HSD1, hippocampal volume and metabolites choline, inositol and NAA were observed. However, these markers were not associated with spatial memory performance at 18 months. 11β-HSD1 was observed to be expressed in glial cells in the brain and associated with glial reactivity and neuronal expression, and both glial reactivity and neuronal expression were associated with spatial memory ability in wild-type mice. Levels of glutamine and the glutamate-glutamine complex were correlated with spatial memory performance in the water maze in aged wild-type mice but not aged 11β-HSD1$^{-/-}$ mice, suggesting that age-associated impairments in spatial memory in wild-type mice are associated with altered glial cell activity and altered levels of glutamate and the glutamate-glutamine complex. Spatial working memory measures in aged mice were not associated with any cellular, metabolite or structural markers.

Previous research has demonstrated a large role for glucocorticoids and glial cell regulation (Jauregui-Huerta et al., 2010), with immunohistochemical studies also noting increased GFAP reactivity in response to chronic glucocorticoid exposure (Bridges et al., 2008). Furthermore, in more recent years, animal models of stress have observed elevated GFAP-immunoreactive astrocytes in the hippocampus (Lambert et al., 2000). Thus, our results add to previous data, suggesting that intracellular glucocorticoid levels regulated through 11β-HSD1 may alter glial cell reactivity. In turn, glial cell activity was found to be correlated with spatial memory

performance in aged mice pointing to a possible mechanism through which the increase of intracellular glucocorticoids through 11β-HSD1 may impact cognitive function with age.

Notably, in our study higher levels of glutamine and the glutamate-glutamine complex were correlated with poorer performance in the water maze in wild-type mice. Previous studies have shown that glial cells play a large role in the glutamate-glutamine cycle playing an essential role in producing glutamate for neurons (Hertz and Zielke, 2004). Furthermore, glutamate dysfunction has been implicated in cognitive impairment in a variety of diseases (Merritt et al., 2013). In particular, elevated levels of glutamate-glutamine have been associated with age-related diseases such as mild cognitive impairment (Olson et al., 2008) and further studies have implicated chronically elevated levels of glucocorticoids with poor glutamate uptake subsequently impairing damaging glutamate from being removed from synapses resulting in neuronal damage (Virgin et al., 1991).

Taken all together our data suggest that altered glutamatergic neurotransmission may play a key role in age-related cognitive impairment and that this role may be mediated by 11β-HSD1 activity on glial cell reactivity.

The previous chapter showed age-associated impairments in spatial working memory were observed to be accelerated in both wild-type and 11β-HSD1$^{-/-}$ mice, with 11β-HSD1$^{-/-}$ mice showing impairments earlier than wild-type mice. However, performance in the radial arm water maze, as assessed by savings across the 1 hour retention interval, was not associated with any changes in neurons, glial cells, hippocampal metabolite levels or hippocampal structure. This suggests that

impairments in spatial working memory may be mediated by other mechanisms. Notably, measures of these metabolite and structural changes were taken in the hippocampus and previous studies have established key structures in addition to the hippocampus to also be involved in working memory. Spatial working memory requires both short-term storage and online manipulation of information which are processes sub-served by distinct cortical structures (Cohen et al., 1997). In particular numerous studies have shown the prefrontal cortex to be vital for the manipulation and retrieval of information with more posterior regions of the brain responsible for active maintenance of information (Cohen et al., 1997; van Asselen et al., 2006). Furthermore, some studies have suggested that the hippocampus plays a limited role in spatial working memory (Cave and Squire, 1992). Therefore, our data suggest that age-associated spatial working memory impairments are not mediated by age-associated cellular, metabolite or structural changes within the hippocampus. As such, further work examining changes in metabolites and structure in 11β-HSD1$^{-/-}$ mice in other key brain regions involved in working memory will help identify the mechanisms through which 11β-HSD1 mediates working memory processes.

This study had a number of limitations. Firstly, as mentioned previously, the longitudinal aspect of this study resulted in overtraining of mice on the water maze task, which may itself impact cellular, structural and metabolite changes with age. Additionally, as tissue could not be obtained on the longitudinal colony of mice till they were aged, it was not possible to include cell and protein data from when they were young and middle-aged. Consequently, the range of data available to test whether protein levels were related to cognitive performance was small, limiting correlational analysis to individual differences when aged. Furthermore, this meant

that data sets were used for multiple comparisons increasing the chance of false positive errors. Sample size for longitudinal H-MRS analysis was small which may have resulted in changes in metabolites being missed. Furthermore, metabolite levels in this study may have been at the level of detectability which may mask differences between genotypes and throughout ageing. Finally, analysis of protein expression through percentage fluorescence required a background fluorescence level to be set for determination of changes in fluorescence. Although background fluorescence was determined using negative control sections, analysis of changes in fluorescence may have been limited by comparing fluorescent changes to a predetermined background level as opposed to background for each individual sample.

However, it is notable that repeated testing in such a longitudinal manner may itself be advantageous in replicating the ongoing use of cognitive faculties required throughout an individual's lifespan and as such may provide clues as to the mechanisms through which age and glucocorticoids may affect performance in tasks and situations encountered throughout a lifespan as opposed to novel cognitively demanding situations.

In conclusion, it was noted that elevated levels of intracellular glucocorticoids may alter cognitive function through altered glial reactivity profiles and altered glutamatergic neurotransmission. Indeed, in recent years, glial cells have been found to play key roles in modulation of neurotransmission (Auld and Robitaille, 2003) and have been noted to increase reactivity in inflammatory and neurodegenerative states. Examining how glucocorticoids might regulate neuroinflammation will provide a better insight into the processes affecting cognitive function with age.

Chapter 5 : Mechanisms of 11β-HSD1 Action on Acute and Age-Related Neuroinflammation

5.1 Introduction

In the previous chapter, an altered glial reactivity profile was observed in wild-type (but not 11β-HSD1$^{-/-}$ mice) and associated with cognitive function when aged, suggesting neuroinflammation may play a role in age-associated cognitive deficits. Therefore, in this chapter we will be focusing on the role of 11β-HSD1 on acute and age-related inflammatory changes and the effect of this on cognitive ageing.

The immune system is essential in protecting organisms from disease by preventing and responding to the entry of pathogens into an organism. Within the CNS, the immune response is regulated by microglia (brain macrophages) comprising 10-15% of the cells in the brain and are concentrated in the hippocampus, hypothalamus, basal ganglia and substantia nigra (Lawson et al., 1990).

Recent evidence has suggested that the aged brain is characterised by a chronic low level inflammation and 'primed' microglia – microglia demonstrating heightened reactivity in response to activation of the immune system (Sparkman and Johnson, 2009; Frank et al., 2010). Additionally, it has been observed that genes involved in oxidative stress, inflammation and glial activation are increased during ageing whilst genes associated with synaptic function and growth factors decrease (Lee et al., 2000; Blalock et al., 2003; Bishop et al., 2010). Despite a large number of studies demonstrating the anti-inflammatory properties of glucocorticoids, recent studies

have suggested there is also a pro-inflammatory role for glucocorticoids with potentiation of the inflammatory response with elevated acute and chronic glucocorticoid levels. In particular, this potentiation was observed to result in altered cognitive function and behaviour (Munhoz et al., 2010) and increased microglial activation, reactivity and proliferation (Johnson et al., 2002; Munhoz et al., 2006). Furthermore, studies have shown that prolonged activation of microglia can result in autoregulatory negative feedback with microglia consequently shifting phenotype from a classically activated state (M1) to and alternatively activated state (M2) which inactivates the initial immune response and activates genetic pathways associated with tissue repair (For review see Mantovani et al., 2004). However, whether intracellular regulation of glucocorticoids by 11β-HSD1 contributes to neuroinflammation and cognitive impairment with age has not yet been investigated.

Thus, we hypothesised that 11β-HSD1 may contribute to cognitive decline by altering neuroinflammatory processes in the hippocampus. Therefore, this chapter aims to explore the role of 11β-HSD1 on both acute neuroinflammatory responses and neuroinflammation with age by investigating changes in inflammatory markers in response to LPS administration and with age and their correlation with cognitive performance in a subset of the longitudinal colony of wild-type and 11β-HSD1$^{-/-}$ mice tested in Chapter 3.

5.2 Methods

5.2.1 Animals

Male 11β-HSD1$^{-/-}$ mice and their wild-type littermates were maintained in standard cages upon controlled lighting (12h:12h, lights on at 7.00), were fed a standard chow and given water ad libitum as described in Chapter 2.

5.2.1.1 LPS Experiment

A pilot study was conducted to determine the optimal time and dose. Mice were administered with either 5mg/kg or 10mg/kg of LPS or saline and returned to their home cage for 12, 24 or 48 hours. Mice then received an overdose of sodium pentobarbital (0.4ml) and were then perfused with saline through cardiac puncture. Brains were then removed and half the brain fixed for immunofluorescent analysis and the remaining half dissected out for real time PCR analysis as outlined in Chapter 2. Levels of pro-inflammatory and anti-inflammatory cytokines were assessed and the dose and time-point producing the highest inflammatory response were chosen.

Mice were administered with either 5mg/kg of LPS or saline and returned to their home cage for 24 hours. Mice then received an overdose of sodium pentobarbital (0.4ml) and were then perfused with saline through cardiac puncture. Brains were then removed and half the brain fixed for immunofluorescent analysis and the remaining half dissected out for real time PCR analysis as outlined in Chapter 2. Figure 5.1 illustrates the number of wild-type and 11β-HSD1$^{-/-}$ mice administered LPS or saline and the number from which tissue was obtained 24 hours post-treatment administration. Over the 24 hour post-treatment period, one wild-type mice

died and four 11β-HSD1$^{-/-}$ mice died following poor recovery from LPS administration or treatment injection.

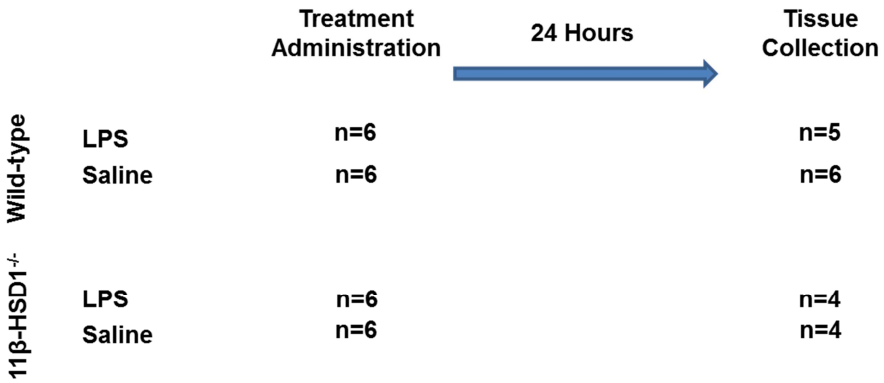

Figure 5.1. Number of wild-type and 11β-HSD1$^{-/-}$ mice administered LPS or saline and the number from which tissue was obtained 24 hours post-treatment administration.

5.2.1.2 Ageing Experiment

Mice utilised were the same colony of mice examined Chapters 1 and 2.

Following the final scan at 24 months of age, mice were perfused with saline through cardiac puncture and brains were removed. Half the brain was fixed for immunofluorescent analysis and the remaining half dissected out for real time PCR analysis as outline in Chapter 2.

5.2.2 Immunofluorescence

Sections were processed as outlined in Chapter 2 and stained for 11B-HSD1, microglia, neuron and glial expression using primary antibodies sheep purified, Rat Cd11B, Mouse NeuN and Rabbit GFAP and secondary antibodies anti-Sheep Alexa

Fluor 488, anti-Rat Alexa Fluor 555 , anti-Mouse Alexa Fluor 555 and anti-Rabbit Alexa Fluor 555 respectively.

A quantitative analysis of the immunofluorescence was performed utilising ImageJ to calculate the area of fluorescence for the specified stain meeting a predefined intensity as a percentage of the total area with higher fluorescent percentages indicate a greater expression of 11β-HSD1 protein. The average area of fluorescence was taken over three fields from each brain region per mouse.

5.2.3 Quantitative PCR

Tissue was processed as outlined in Chapter 2 and RT-PCR products were then used for qPCR to quantify mRNA levels of: a) 11B-HSD1; b) Pro-inflammatory cytokines – TNFα and IL-1β; and c) Alternative activated microglia markers – YM1 and Arg 1. Negative controls were included in each plate to ensure no contamination had taken place. Internal controls included housekeeping genes HPRT and GAPDH. The LightCycler software provided relative quantification using the maximum second derivative method.

5.2.4 Statistical Analysis

Statistical analysis was conducted using PRISM with a P value < 0.05 signifying significance.

Differences in neuroinflammatory markers in LPS and saline treated 11β-HSD1$^{-/-}$ and wild-type mice were calculated using a two-way ANOVA. Differences in neuroinflammatory markers in aged mice were calculated using an unpaired T-Test.

The relationship between variables (Probe test data, Radial arm water maze savings data, pro-inflammatory cytokine levels, anti-inflammatory cytokine levels) was analysed using Pearson's correlation with a P value < 0.05 signifying a significant difference.

5.3 Results

5.3.1 11β-HSD1 in acute inflammation

To determine if 11β-HSD1 mediates increased neuroinflammation in ageing and subsequently age-associated cognitive decline we investigated if 11β-HSD1 was expressed in microglia in-vivo and if the expression of 11β-HSD1 was altered in activated microglia following acute LPS administration.

In wild-type mice, 11β-HSD1 was not expressed in the microglia in either saline treated or LPS treated mice (Figure 5.2). As expected, no 11β-HSD1 staining was observed in both saline and LPS treated 11β-HSD1$^{-/-}$ mice.

A quantitative analysis of the immunofluorescence was performed utilising ImageJ as described in the methods section.

There was no difference in levels of 11β-HSD1 protein in wild-type mice in any hippocampal subregion in response to LPS as measured by fluorescent immunohistochemistry. This was observed 24 hours following LPS administration suggesting that, contradictory to previous studies, 11β-HSD1 is not highly expressed in microglia in a basal state nor when activated by LPS. An unpaired t-test of 11β-HSD1 fluorescence in saline and LPS treated wild-type mice revealed no significant difference in 11β-HSD1 fluorescence between saline and LPS treated wild-type mice in the CA1 [Saline: M = 1.436, SD = 0.5126, n = 4; LPS treated: M = 1.301, SD = 0.2566, n = 6; t(4) = 0.2353, p = 0.3187; Fig. 5.3A], CA3 [Saline: M = 4.391, SD = 1.679, n = 5; LPS treated: M = 3.916, SD = 1.493, n = 6; t(8) = 0.2112, p = 0.92951; Fig. 5.3B], DG [Saline: M = 4.473, SD = 1.893, n = 4; LPS treated: M = 4.129, SD =

0.8022, n = 5; t(5) = 0.167, p = 0.1250; Fig. 5.3C] and cortex [Saline: M = 2.744, SD = 0.6810, n = 5; LPS treated: M = 5.181, SD = 1.345, n = 5; t(5) = 1.616, p = 0.2238; Fig. 5.3D]

The expression of 11β-HSD1 mRNA in wild-type and 11β-HSD1$^{-/-}$ mice was also analysed by qPCR to investigate if 11β-HSD1 mRNA expression was altered following LPS administration.

Hippocampal 11β-HSD1 mRNA was not altered by LPS compared to saline administration in wild-type mice [Saline: M = 1.019, SD = 0.2397, n = 4; LPS treated: M = 0.9435, SD = 0.3533, n = 5; t(5) = 0.1772, p = 0.5943; Fig. 5.4]. As expected, and in support of previous immunofluorescent data, 11β-HSD1 mRNA was not present in both saline and LPS treated 11β-HSD1$^{-/-}$ mice.

These results suggest that 11β-HSD1 expression is not altered following activation of the immune system by LPS administration.

Figure 5.2. 11β-HSD1 and Iba-1 expression in wild-type mice

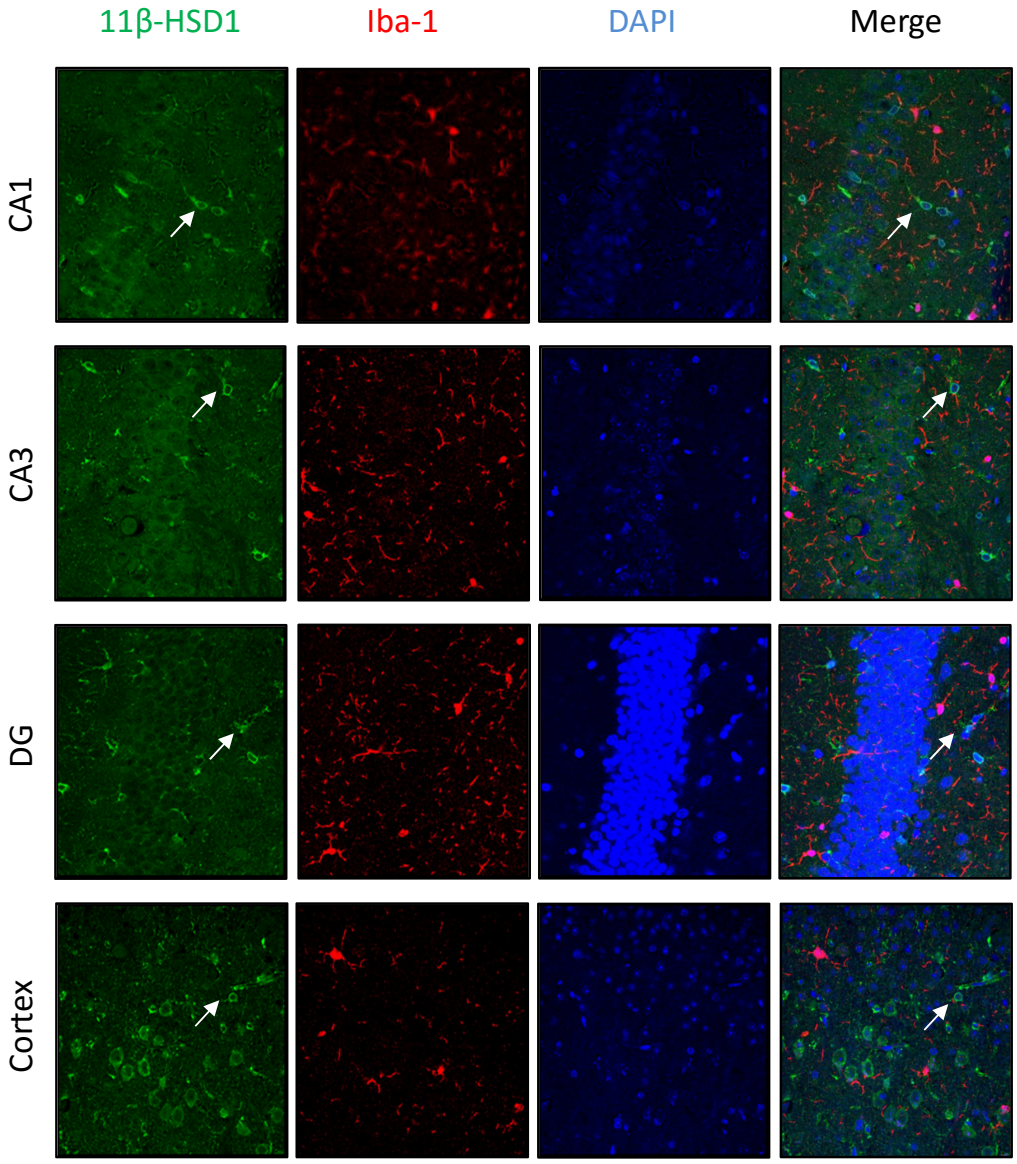

Fig. 5.2. Representative images of patterns of 11β-HSD1(Green) and Iba-1 (Red) expression in the CA1, CA3, Dentate Gyrus (DG) and Cortex of aged wild-type mice. Images of CA1, CA3 and DG captured at 30x magnification using a Zeiss Axioskop confocal laser microscope. Blue represents DAPI stained nuclei. White arrows indicate an example of positive expression of 11β-HSD1.

Figure 5.3. Percentage Fluorescence of 11β-HSD1 expression in saline and LPS treated wild-type mice

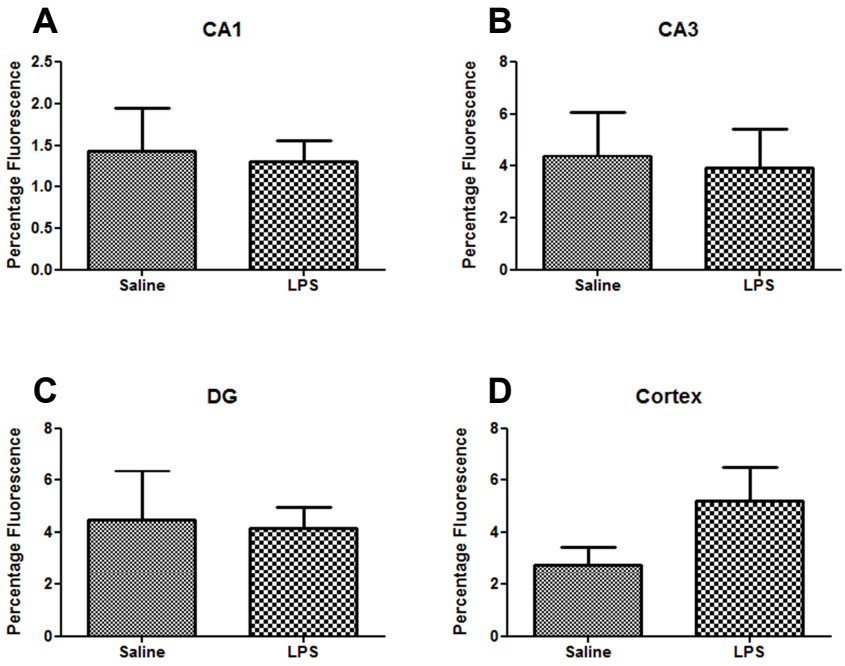

Fig. 5.3. Graphs showing the percentage area of fluorescence of 11β-HSD1 in the **[A]** CA1 in young saline treated (n=4) and young wild-type mice treated with lipopolysaccharide over 24 hours (LPS; n=5); **[B]** CA3 in young saline treated (n=5) and young LPS treated (n=6) wild-type mice; **[C]** dentate gyrus (DG) in young saline treated (n=5) and young LPS treated (n=5) wild-type mice; and **[D]** cortex in young saline treated (n=4) and young LPS treated (n=5) wild-type mice. Values represent mean percentage area of fluorescence (across three fields per animal) +SEM.

Figure 5.4. 11β-HSD1 mRNA expression in saline and LPS treated wild-type mice

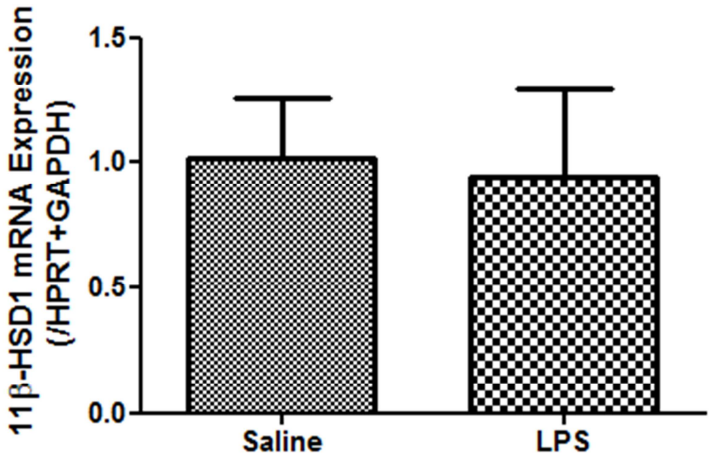

Fig. 5.4. Graphs showing 11β-HSD1 mRNA expression in the whole hippocampus of saline treated wild-type mice (n=5) and wild-type mice treated with lipopolysaccharide over 24 hours (LPS; n=4). Values represent mean relative mRNA expression as a ratio of housekeeping genes HPRT and GAPDH +SEM.

5.3.2 Microglia activation in acute LPS administration

Microglial activation during an inflammatory response has been noted to result in the up-regulation of Iba-1, allowing activated and resting microglia to be differentiated (Ito et al., 1998). To investigate if microglia activation, following an acute inflammatory response, was altered by the lifelong deletion of 11β-HSD1, brain sections from young mice treated with LPS and saline were stained for microglia marker Iba-1 and immunofluorescence quantified.

Interestingly, LPS treatment did not appear to stimulate microglia activation in either control or 11β-HSD1$^{-/-}$ mice. A two-way ANOVA analysis of percentage fluorescence of Iba-1 revealed no significant effect of treatment on the percentage fluorescence of Iba-1 in the CA1[$F(1,13) = 4.143$, $p = 0.0627$; Fig. 5.5A], CA3[$F(1,13) = 1.258$, $p = 0.2838$; Fig. 5.5B], DG [$F(1,13) = 1.703$, $p = 0.2145$; Fig. 5.5C] and cortex [$F(1,13) = 2.698$, $p = 0.1244$; Fig. 5.5D] and no effect of genotype on the percentage fluorescence of Iba-1 in the CA1 [$F(1,13) = 0.05132$, $p = 0.8243$; Fig. 5.5A], CA3 [$F(1,13) = 0.3955$, $p = 0.5403$; Fig. 5.5B], DG [$F(1,13) = 0.3560$, $p = 0.5610$; Fig. 5.5C] and cortex [$F(1,13) = 2.609$, $p = 0.1303$; Fig. 5.5D].

This suggests that 24 hours following LPS treatment, there is no change in microglial activation and that removal of 11β-HSD1 has no effect on microglial activation.

Figure 5.5. Percentage Fluorescence of Iba-1 expression in saline and LPS treated Wild-Type (WT) and 11β-HSD1$^{-/-}$ (KO) mice

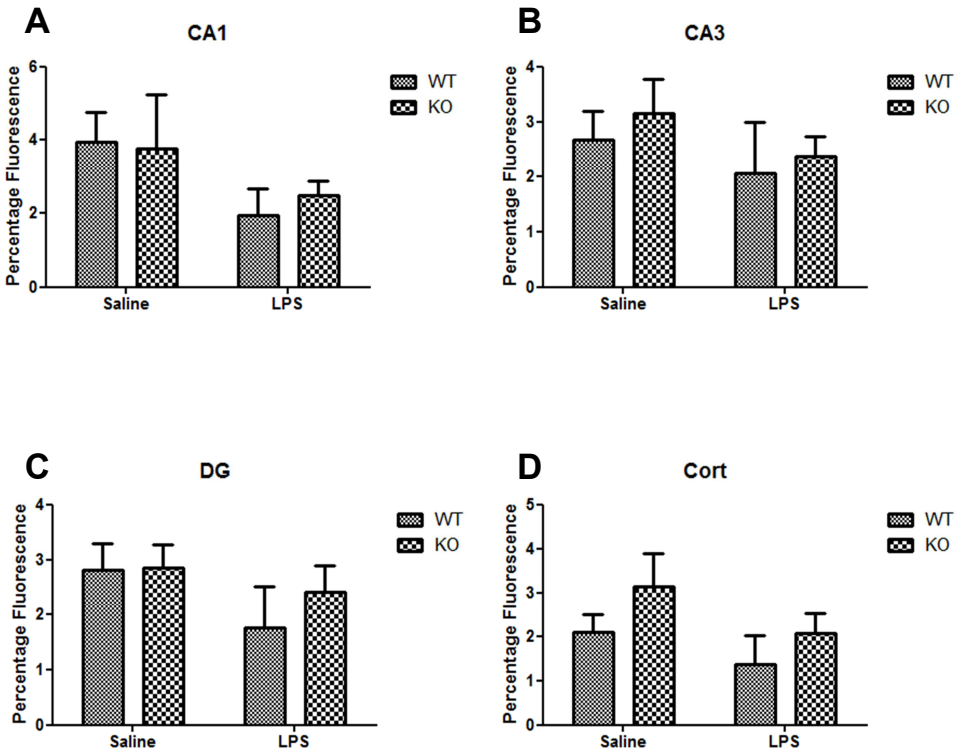

Fig. 5.5. Graphs showing the percentage area of fluorescence of 11β-HSD1 in **[A]** CA1 in young saline treated wild-type mice (Saline; WT; n=5), young wild-type mice treated with lipopolysaccharide over 24 hours (LPS; WT; n=3), young saline treated 11β-HSD1$^{-/-}$ mice (Saline; KO; n=4) and young 11β-HSD1$^{-/-}$ mice treated with lipopolysaccharide over 24 hours (LPS; KO; n=5); **[B]** CA3 in young saline treated wild-type mice (Saline; WT; n=5), young wild-type mice treated with lipopolysaccharide over 24 hours (LPS; WT; n=3), young saline treated 11β-HSD1$^{-/-}$ mice (Saline; KO; n=4) and young 11β-HSD1$^{-/-}$ mice treated with lipopolysaccharide over 24 hours (LPS; KO; n=5); **[C]** dentate gyrus (DG) in young saline treated wild-type mice (Saline; WT; n=5), young wild-type mice treated with lipopolysaccharide over 24 hours (LPS; WT; n=3), young saline treated 11β-HSD1$^{-/-}$ mice (Saline; KO; n=4) and young 11β-HSD1$^{-/-}$ mice treated with lipopolysaccharide over 24 hours (LPS; KO; n=5); and **[D]** cortex in young saline treated wild-type mice (Saline; WT; n=5), young wild-type mice treated with lipopolysaccharide over 24 hours (LPS; WT; n=3), young saline treated 11β-HSD1$^{-/-}$ mice (Saline; KO; n=4) and young 11β-HSD1$^{-/-}$ mice treated with lipopolysaccharide over 24 hours (LPS; KO; n=5). Values represent mean percentage area of fluorescence (across three fields per animal) +SEM.

5.3.3 Expression of pro-inflammatory cytokine mRNAs following acute LPS administration

An attack on the immune system results in an inflammatory response which is typically accompanied by an increase in pro-inflammatory cytokines, in particular tumour necrosis factor (TNF), interleukin (IL)-1, IL-6, IL-12 and IL-18. These cytokines then signal the activation of the adaptive immune system to aid in the defence of the organism.

Therefore, to investigate if there was an increase in pro-inflammatory cytokines following acute LPS administration, brains were dissected out according to the protocol listed above and the expression of pro-inflammatory cytokine mRNA in the hippocampus and cortex was assessed using quantitative PCR.

LPS significantly increased expression of TNFα mRNA in the hippocampus of 11β-HSD1$^{-/-}$ mice independent of genotype. A two-way ANOVA revealed a significant effect of treatment on mRNA expression of pro-inflammatory cytokine TNFα in the hippocampus following LPS administration [$F(1,15) = 10.5$, $p = 0.055$; Fig. 5.6A] but no effect of genotype on mRNA expression of pro-inflammatory cytokine TNFα in the hippocampus [$F(1,15) = 0.1088$, $p = 0.7460$; Fig. 5.6A]. Post hoc tests revealed significantly increased levels of TNFα mRNA in LPS treated 11β-HSD1$^{-/-}$ mice ($p < 0.05$) compared to their saline controls, however, wild-type TNFα mRNA levels were not significantly altered by LPS treatment.

However, there was no significant effect of LPS treatment on mRNA expression of pro-inflammatory cytokine TNFα in the cortex [$F(1,13) = 4.407$, $p = 0.0559$; Fig.

5.6B] and no effect of genotype on mRNA expression of pro-inflammatory cytokine TNFα in the cortex [F (1,13) = 0.00007313, p = 0.9933; Fig. 5.6B].

LPS had no effect on IL-1β in the hippocampus or cortex irrespective of genotype. A two-way ANOVA revealed no significant effect of treatment on mRNA expression of pro-inflammatory cytokine IL-1β in the hippocampus [F (1,15) = 1.420, p = 0.2519; Fig. 5.7A] and cortex [F (1,13) = 0.6413, p = 0.4376; Fig. 5.7B] following LPS administration and no effect of genotype on mRNA expression of pro-inflammatory cytokine IL-1β in the hippocampus [F (1,15) = 0.1049, p = 0.7505; Fig. 5.7A] and cortex [F (1,13) = 0.01075, p = 0.919; Fig. 5.7B] following LPS administration.

These results indicate that an inflammatory response was induced by acute LPS administration in 11β-HSD1$^{-/-}$ mice but not wild-type mice. The lack of increase in pro-inflammatory cytokine IL-1β suggests that each cytokine has its own time-course of expression in response to LPS and IL-1β may not be induced at this time point. Indeed, in our pilot study, we observed not only a much larger expression of TNFα following an acute inflammatory response but also a differing time-course of expression (Fig. 5.8)

Figure 5.6. TNFα mRNA expression in saline and LPS treated Wild-Type (WT) and 11β-HSD1$^{-/-}$ (KO) mice

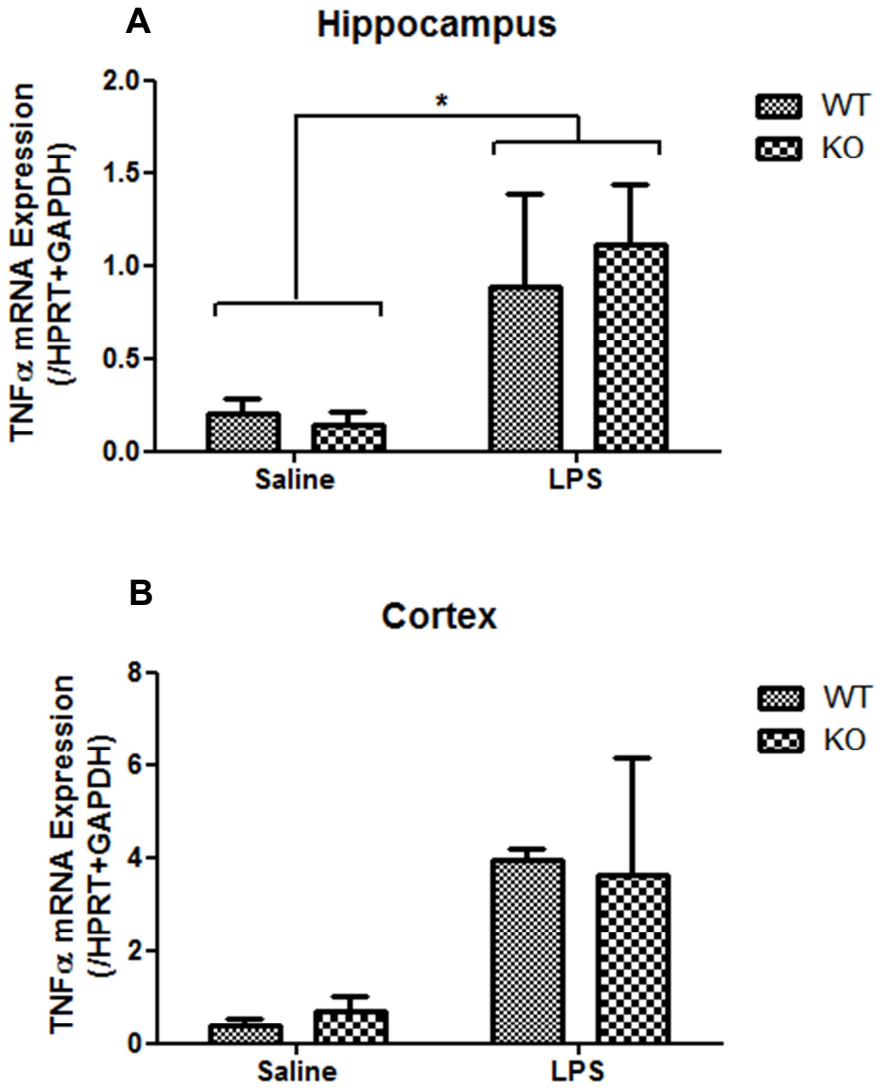

Fig. 5.6. Graphs showing TNFα mRNA expression in **[A]** the hippocampus of young saline treated wild-type mice (Saline; WT; n=5), young wild-type mice treated with lipopolysaccharide over 24 hours (LPS; WT; n=6), young saline treated 11β-HSD1$^{-/-}$ mice (Saline; KO; n=4) and young 11β-HSD1$^{-/-}$ mice treated with lipopolysaccharide over 24 hours (LPS; KO; n=4); and **[B]** cortex of saline treated wild-type mice (Saline; WT; n=4), young wild-type mice treated with lipopolysaccharide over 24 hours (LPS; WT; n=5), young saline treated 11β-HSD1$^{-/-}$ mice (Saline; KO; n=3) and young 11β-HSD1$^{-/-}$ mice treated with lipopolysaccharide over 24 hours (LPS; KO; n=5). Values represent mean relative mRNA expression as a ratio of housekeeping genes HPRT and GAPDH +SEM. *$p < 0.05$ compared to respective saline control.

Figure 5.7. IL-1β mRNA expression in saline and LPS treated Wild-Type (WT) and 11β-HSD1$^{-/-}$ (KO) mice

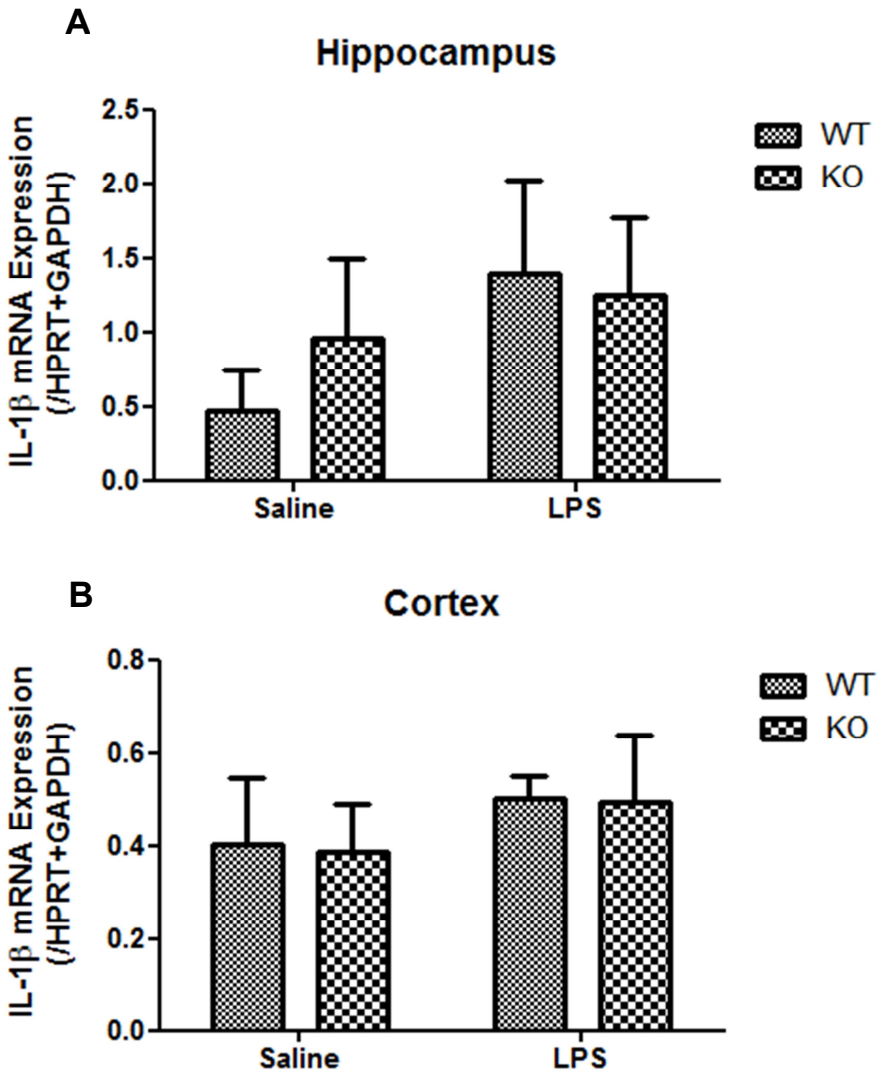

Fig. 5.7. Graphs showing IL-1β mRNA expression in **[A]** the hippocampus of young saline treated wild-type mice (Saline; WT; n=5), young wild-type mice treated with lipopolysaccharide over 24 hours (LPS; WT; n=6), young saline treated 11β-HSD1$^{-/-}$ mice (Saline; KO; n=4) and young 11β-HSD1$^{-/-}$ mice treated with lipopolysaccharide over 24 hours (LPS; KO; n=4); and **[B]** cortex of saline treated wild-type mice (Saline; WT; n=4), young wild-type mice treated with lipopolysaccharide over 24 hours (LPS; WT; n=5), young saline treated 11β-HSD1$^{-/-}$ mice (Saline; KO; n=3) and young 11β-HSD1$^{-/-}$ mice treated with lipopolysaccharide over 24 hours (LPS; KO; n=5). Values represent mean relative mRNA expression as a ratio of housekeeping genes HPRT and GAPDH +SEM. *$p < 0.05$; ** $p < 0.01$; *** $p < 0.001$.

Figure 5.8. Time-course of pro-inflammatory mRNA expression in LPS treated wild-type mice

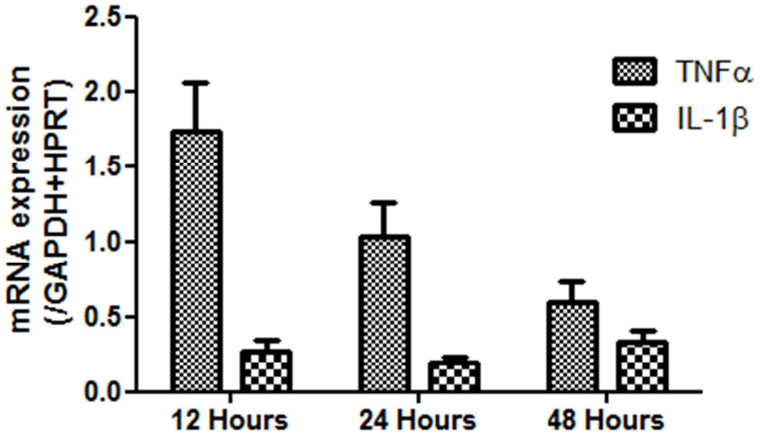

Fig. 5.8. Graph showing TNFα and IL-1β mRNA expression in the hippocampus of young wild-type mice treated with lipopolysaccharide at 12, 24 and 48 hours post LPS administration (n=5).

5.3.4 Expression of alternative activated microglia (M2) markers following acute LPS administration

Previous research has indicated that in addition to the classical response of microglia (M1) and the release of pro-inflammatory cytokines to defend the body, microglia are also alternatively activated (M2). Although the classical activation of microglia is effective and essential in responding to pathogens, the response can often result in damage to the surrounding tissue and is typically associated with disease states that are partially driven by low grade inflammation and in particular is associated with Alzheimer's disease. However, microglia also exhibit a response which inactivates the initial immune response and activates genetic pathways associated with tissue repair, M2-type activation. This activity is associated with the production of anti-inflammatory cytokines by glia and neurons, such as IL-4 and IL-10, and is characterised by suppression of pro-inflammatory cytokines, TNFα and IL-1β.

Therefore, to investigate if the lack of increase in pro-inflammatory cytokine IL-1β was the result of M2-type microglia activation and subsequently the suppression of pro-inflammatory factors, the expression of markers M2-type activated microglia were examined following acute LPS administration in wild-type and 11β-HSD1$^{-/-}$ mice. The expression of mRNA for YM1 and Arg1, markers for activated microglia, in the hippocampus and cortex were assessed using quantitative PCR.

LPS increased YM1 above saline controls irrespective of genotype. A two-way ANOVA revealed a significant effect of treatment on mRNA expression of activated microglia marker YM1 in the hippocampus [$F(1,15) = 8.715$, $p = 0.0099$; Fig. 5.9A] but not the cortex [$F(1,13) = 3.796$, $p = 0.0733$; Fig. 5.9B] following LPS

administration and no effect of genotype on mRNA expression of YM1 in the hippocampus [F (1,15) = 0.9522, p = 0.3446; Fig. 5.9A] and cortex [F (1,13) = 0.5207, p = 0.4833; Fig. 5.9B] following LPS administration.

However, there was no effect of treatment [F (1,15) = 0.007006, p = 0.9344; Fig. 5.10] or genotype [F (1,15) = 1.036, p = 0.3249; Fig. 5.10] on mRNA expression of activated microglia marker Arg1 in the hippocampus whilst Arg1 mRNA levels in the cortex were undetectable.

This suggests that removal of 11β-HSD1 had no effect on the alternative activation of microglia 24 hours following LPS administration.

Figure 5.9. YM1 mRNA expression in saline and LPS treated Wild-Type (WT) and 11β-HSD1$^{-/-}$ (KO) mice

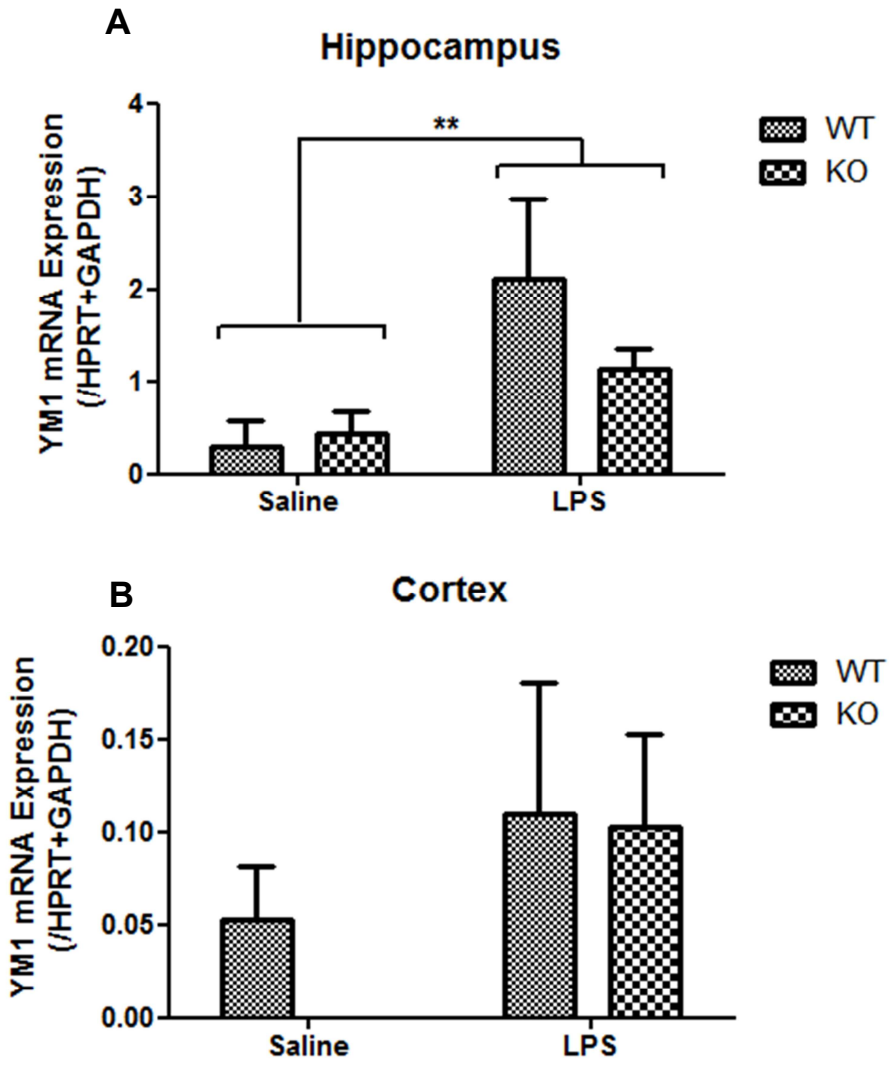

Fig. 5.9. Graphs showing YM1 mRNA expression in **[A]** the hippocampus of young saline treated wild-type mice (Saline; WT; n=5), young wild-type mice treated with lipopolysaccharide over 24 hours (LPS; WT; n=6), young saline treated 11β-HSD1$^{-/-}$ mice (Saline; KO; n=4) and young 11β-HSD1$^{-/-}$ mice treated with lipopolysaccharide over 24 hours (LPS; KO; n=4); and **[B]** cortex of saline treated wild-type mice (Saline; WT; n=4), young wild-type mice treated with lipopolysaccharide over 24 hours (LPS; WT; n=5), young saline treated 11β-HSD1$^{-/-}$ mice (Saline; KO; n=3) and young 11β-HSD1$^{-/-}$ mice treated with lipopolysaccharide over 24 hours (LPS; KO; n=5). Values represent mean relative mRNA expression as a ratio of housekeeping genes HPRT and GAPDH +SEM. ** $p < 0.01$.

Figure 5.10. Arg1 mRNA expression in saline and LPS treated Wild-Type (WT) and 11β-HSD1$^{-/-}$ (KO) mice

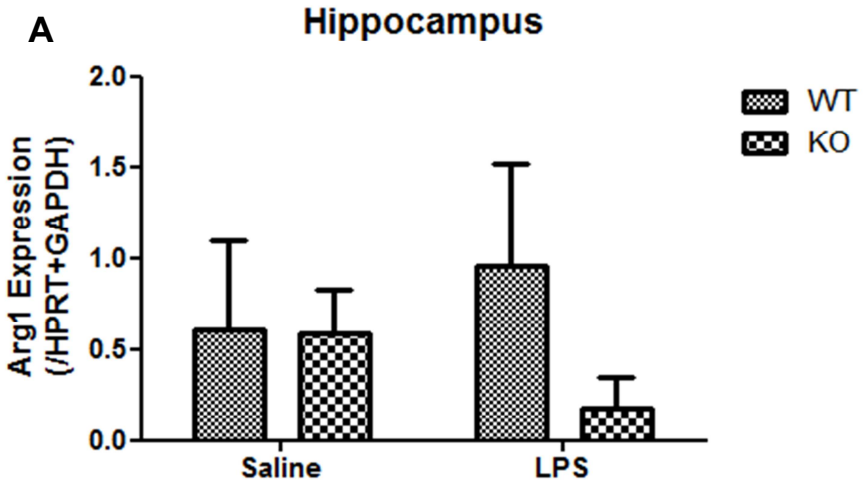

Fig. 5.9. Graph showing Arg1 mRNA expression in the hippocampus of young saline treated wild-type mice (Saline; WT; n=5), young wild-type mice treated with lipopolysaccharide over 24 hours (LPS; WT; n=6), young saline treated 11β-HSD1$^{-/-}$ mice (Saline; KO; n=4) and young 11β-HSD1$^{-/-}$ mice treated with lipopolysaccharide over 24 hours (LPS; KO; n=4). Values represent mean relative mRNA expression as a ratio of housekeeping genes HPRT and GAPDH +SEM.

5.3.5 GFAP expression following acute LPS administration

In the previous chapter, 11β-HSD1 was found to be expressed in glial cells. Previous research has suggested that glia and neurons may play an interactive role in the production of anti-inflammatory cytokines and suppression of the inflammatory response. In particular, glia cells have been noted to exhibit altered morphology and an upregulated expression of cell specific markers such as glial fibrillary acidic protein (GFAP) in response to inflammation. This enhanced GFAP expression has been associated with astrogliosis which can be both beneficial for neuronal growth and survival but also detrimental to the brain (Eng and Ghirnikar, 1994). Therefore, we aimed to investigate if GFAP expression would be altered during an inflammatory response and if lifelong removal of 11β-HSD1 would alter this expression.

Therefore, hippocampal sections of wild-type and 11β-HSD1$^{-/-}$ mice treated with saline or LPS were stained with the GFAP marker and immunofluorescent staining quantified to assess glial reactivity.

LPS did not alter percentage fluorescence of GFAP in control or 11β-HSD1 knockout hippocampus (any subregion) or cortex. A two-way ANOVA revealed no significant effect of genotype on percentage fluorescence of GFAP in the CA1 [$F(1,14) = 0.09013$, $p = 0.7684$; Fig. 5.11A], CA3 [$F(1,14) = 0.9947$, $p = 0.3355$; Fig. 5.11B] and DG [$F(1,13) = 0.5992$, $p = 0.1818$; Fig. 5.11C] of the hippocampus and no effect of treatment on percentage fluorescence of GFAP in the CA1 [$F(1,14) = 0.4311$, $p = 0.5221$; Fig. 5.11A], CA3 [$F(1,14) = 0.7333$, $p = 0.4062$; Fig. 5.11B] and DG [$F(1,13) = 1.990$, $p = 0.1818$; Fig. 5.11C] of the hippocampus.

A two-way ANOVA revealed a significant effect of treatment on percentage fluorescence of GFAP in the cortex [$F(1,11) = 6.696$, $p = 0.0252$; Fig. 5.11D] but no significant effect of genotype on percentage fluorescence of GFAP in the cortex [$F(1,11) = 0.2157$, $p = 0.6514$; Fig. 5.11D]. However, post hoc tests revealed a significant increase in percentage fluorescence of GFAP in LPS treated 11β-HSD1$^{-/-}$ mice compared to saline treated 11β-HSD1$^{-/-}$ mice ($p < 0.05$) while no effect was seen in wild-type mice.

Figure 5.11. Percentage Fluorescence of GFAP expression in saline and LPS treated Wild-Type (WT) and 11β-HSD1$^{-/-}$ (KO) mice

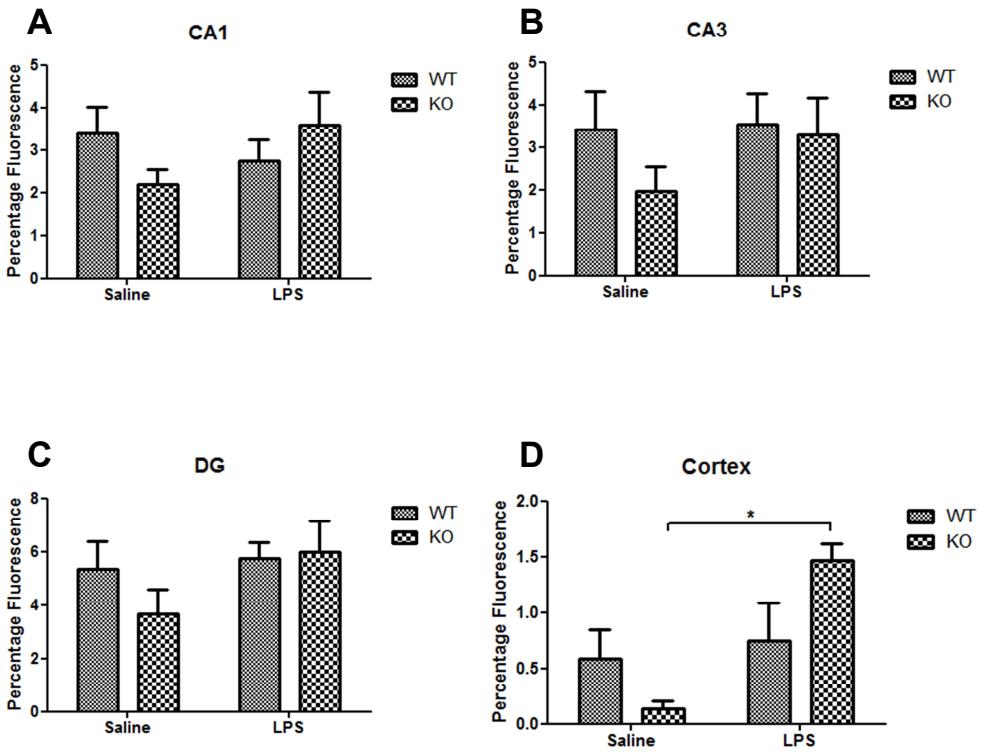

Fig. 5.11. Graphs showing percentage fluorescence of GFAP expression in **[A]** the CA1 of young saline treated wild-type mice (Saline; WT; n=5), young wild-type mice treated with lipopolysaccharide over 24 hours (LPS; WT; n=6), young saline treated 11β-HSD1$^{-/-}$ mice (Saline; KO; n=4) and young 11β-HSD1$^{-/-}$ mice treated with lipopolysaccharide over 24 hours (LPS; KO; n=4); and **[B]** CA3 of saline treated wild-type mice (Saline; WT; n=4), young wild-type mice treated with lipopolysaccharide over 24 hours (LPS; WT; n=5), young saline treated 11β-HSD1$^{-/-}$ mice (Saline; KO; n=3) and young 11β-HSD1$^{-/-}$ mice treated with lipopolysaccharide over 24 hours (LPS; KO; n=5); **[C]** CA3 of saline treated wild-type mice (Saline; WT; n=4), young wild-type mice treated with lipopolysaccharide over 24 hours (LPS; WT; n=5), young saline treated 11β-HSD1$^{-/-}$ mice (Saline; KO; n=3) and young 11β-HSD1$^{-/-}$ mice treated with lipopolysaccharide over 24 hours (LPS; KO; n=5); and **[D]** CA3 of saline treated wild-type mice (Saline; WT; n=4), young wild-type mice treated with lipopolysaccharide over 24 hours (LPS; WT; n=5), young saline treated 11β-HSD1$^{-/-}$ mice (Saline; KO; n=3) and young 11β-HSD1$^{-/-}$ mice treated with lipopolysaccharide over 24 hours (LPS; KO; n=5). Values represent mean percentage area of fluorescence (across three fields per animal) +SEM. *$p < 0.05$.

5.3.6 NeuN expression following acute LPS administration

Whilst neurons have been thought to play a role in the production of anti-inflammatory cytokines, neurodegenerative diseases are typically characterised by neuronal loss and evidence has also pointed to neuronal death as a consequence of neuroinflammation and elevated levels of pro-inflammatory cytokines (Qin et al., 2007). Therefore, we aimed to investigate if neuronal death would be observed during an inflammatory response and if lifelong removal of 11β-HSD1 would alter this expression.

Therefore, hippocampal sections of wild-type and 11β-HSD1$^{-/-}$ mice treated with saline or LPS were stained for neuronal expression with the NeuN marker and immunofluorescent staining quantified. NeuN is a widely used marker which binds to an antigen expressed solely in neuronal nuclei, therefore, giving an indication of neuronal loss.

Both wild-type and 11β-HSD1$^{-/-}$ mice exhibited significant neuronal loss in all hippocampal subregions and the cortex in response to LPS treatment, with a significant effect of treatment on percentage fluorescence of NeuN in the CA1 [$F(1,13) = 84.45$, $p < 0.0001$; Fig. 5.12A], CA3 [$F(1,13) = 97.86$, $p < 0.0001$; Fig. 5.12B], DG [$F(1,13) = 25.63$, $p = 0.0003$; Fig. 5.12C] and cortex [$F(1,13) = 95.28$, $p < 0.0001$; Fig. 5.12D]. Post hoc tests indicated a decrease in percentage fluorescence of NeuN in LPS treated wild-type and 11β-HSD1$^{-/-}$ mice compared to saline treated wild-type and 11β-HSD1$^{-/-}$ mice ($p < 0.05$).

No effect of genotype in any hippocampal subregions CA1 [$F(1,13) = 0.8261$, $p = 0.7783$; Fig. 5.12A], CA3 [$F(1,13) = 2.825$, $p = 0.1167$; Fig. 5.12B], DG [$F(1,13) =$

0.4195, p = 0.5294; Fig. 5.12C] and the cortex [F (1,13) = 0.009432, p = 0.9244; Fig. 5.12D] was observed.

Figure 5.12. Percentage Fluorescence of NeuN expression in saline and LPS treated Wild-Type (WT) and 11β-HSD1$^{-/-}$ (KO) mice

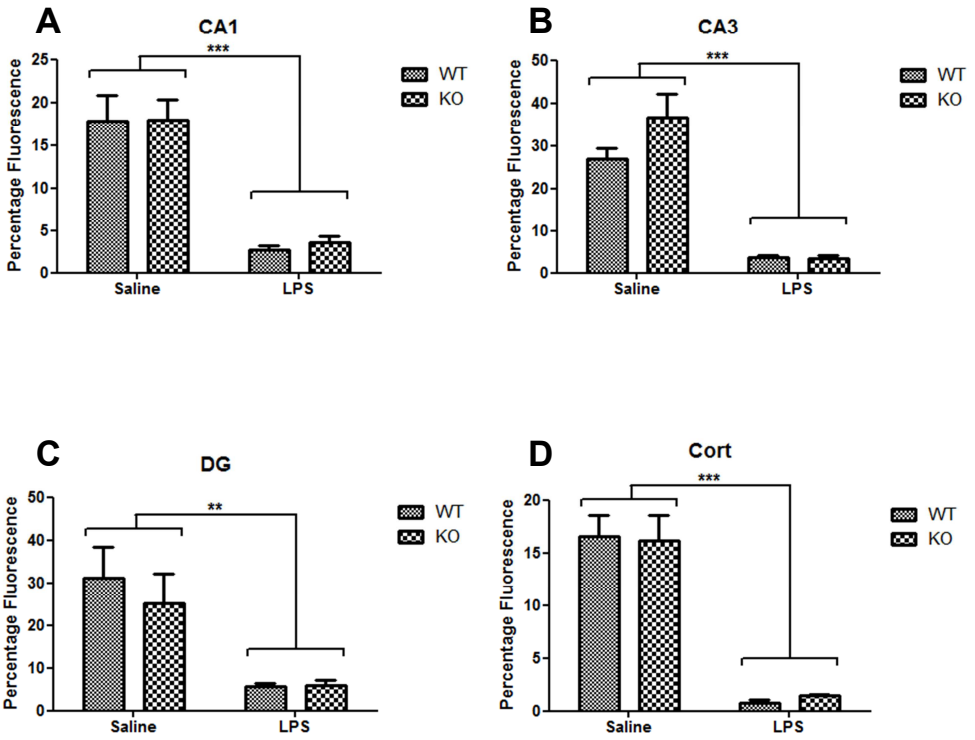

Fig. 5.12. Graphs showing percentage fluorescence of NeuN expression in **[A]** the CA1 of young saline treated wild-type mice (Saline; WT; n=5), young wild-type mice treated with lipopolysaccharide over 24 hours (LPS; WT; n=6), young saline treated 11β-HSD1$^{-/-}$ mice (Saline; KO; n=4) and young 11β-HSD1$^{-/-}$ mice treated with lipopolysaccharide over 24 hours (LPS; KO; n=4); and **[B]** CA3 of saline treated wild-type mice (Saline; WT; n=4), young wild-type mice treated with lipopolysaccharide over 24 hours (LPS; WT; n=5), young saline treated 11β-HSD1$^{-/-}$ mice (Saline; KO; n=3) and young 11β-HSD1$^{-/-}$ mice treated with lipopolysaccharide over 24 hours (LPS; KO; n=5); **[C]** CA3 of saline treated wild-type mice (Saline; WT; n=4), young wild-type mice treated with lipopolysaccharide over 24 hours (LPS; WT; n=5), young saline treated 11β-HSD1$^{-/-}$ mice (Saline; KO; n=3) and young 11β-HSD1$^{-/-}$ mice treated with lipopolysaccharide over 24 hours (LPS; KO; n=5); and **[D]** CA3 of saline treated wild-type mice (Saline; WT; n=4), young wild-type mice treated with lipopolysaccharide over 24 hours (LPS; WT; n=5), young saline treated 11β-HSD1$^{-/-}$ mice (Saline; KO; n=3) and young 11β-HSD1$^{-/-}$ mice treated with lipopolysaccharide over 24 hours (LPS; KO; n=5). Values represent mean percentage area of fluorescence (across three fields per animal) +SEM. ** $p < 0.01$; *** $p < 0.001$.

5.3.7 Microglia expression in aged mice

Our study revealed no alteration in expression of microglia marker Iba-1 following LPS administration in both wild-type and 11β-HSD1$^{-/-}$ mice. However, previous research has suggested that ageing is associated with chronic low level inflammation and primed microglia.

Therefore, to investigate if microglia expression was altered by age and lifelong removal of 11β-HSD1, sections were stained for the microglia marker Iba-1 and immunofluorescence quantified.

There was no change in Iba-1 expression with age in the hippocampus or cortex suggesting there is a not significant activation of microglia in either genotype with age. A two-way ANOVA analysis of percentage fluorescence of Iba-1 revealed no significant effect of age on the percentage fluorescence of Iba-1 in the CA1 [$F(1,24) = 4.883$, $p = 0.4914$; Fig. 5.13A], CA3 [$F(1,23) = 1.554$, $p = 0.2251$; Fig. 5.13B] and DG [$F(1,24) = 0.07533$, $p = 0.7858$; Fig. 5.13C] of the hippocampus and no effect of genotype on the percentage fluorescence of Iba-1 in the CA1 [$F(1,24) = 0.001155$, $p = 0.9732$; Fig. 5.13A], CA3 [$F(1,23) = 0.3426$, $p = 0.5640$; Fig. 5.13B] and DG [$F(1,24) = 0.1620$, $p = 0.6909$; Fig. 5.13C] of the hippocampus.

A two-way ANOVA revealed a significant effect of treatment on the percentage fluorescence of Iba-1 in the cortex [$F(1,24) = 6.413$, $p = 0.0183$; Fig. 5.13D] and an effect of genotype on percentage fluorescence of Iba-1 in the cortex [$F(1,24) = 4.353$, $p = 0.0477$; Fig. 5.13D].

Figure 5.13. Percentage Fluorescence of Iba-1 expression in young and aged wild-type mice

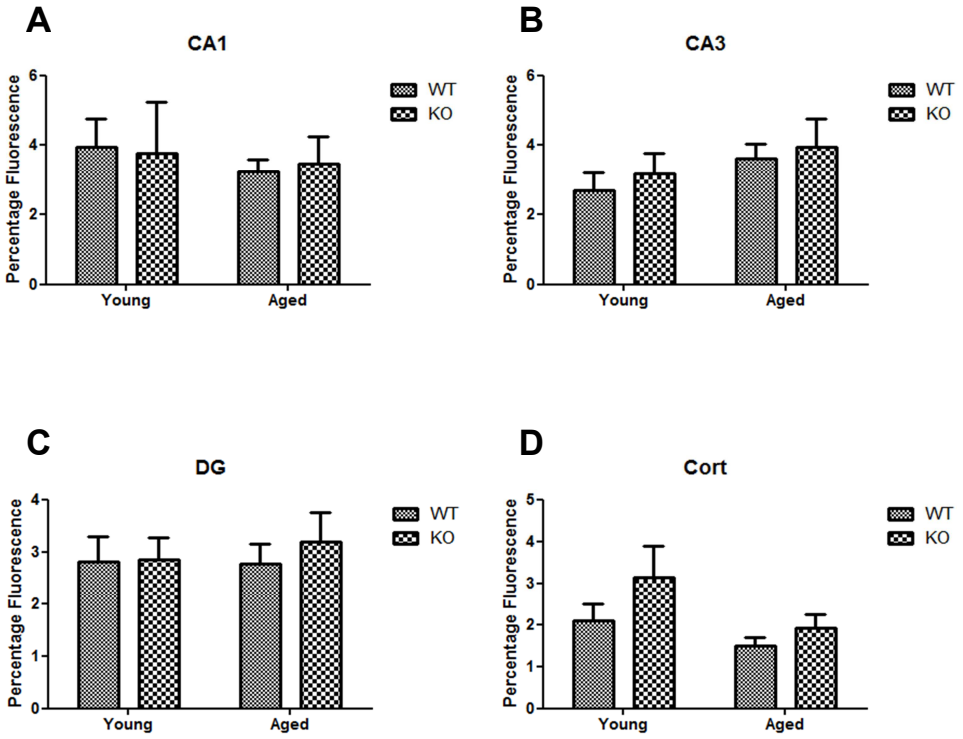

Fig. 5.13. Graphs showing the percentage area of fluorescence of Iba-1 in young (n=4) and aged (n=13) wild-type mice (WT) and young (n=3) and aged (n=5) 11β-HSD1$^{-/-}$ mice (KO) in the **[A]** CA1; **[B]** CA3; **[C]** dentate gyrus (DG); and **[D]** cortex. Values represent mean percentage area of fluorescence (across three fields per animal) +SEM.

5.3.8 Pro-inflammatory mRNA expression in aged mice

Altered levels of pro-inflammatory cytokine TNFα were observed following acute LPS administration in 11β-HSD1$^{-/-}$ mice. These results suggest that whilst wild-type mice did not have a large immune response to acute LPS administration, 11β-HSD1$^{-/-}$ mice have a large response to LPS induced inflammation suggesting that lifelong deletion of 11β-HSD1 alters the immune response to acute inflammation.

Previous research has also suggested that chronic low level inflammation is associated with ageing. Therefore, to investigate if inflammation was present during ageing and the effect of lifelong deletion of 11β-HSD1 on age-related inflammatory changes, levels of pro-inflammatory cytokine mRNA was examined in our aged mice colony.

As was observed following acute LPS administration, an unpaired t-test revealed significantly higher levels of TNFα mRNA in aged 11β-HSD1$^{-/-}$ mice compared to aged wild-type mice [11β-HSD1$^{-/-}$: M = 0.9026, SD = 0.1083; Wild-type: M = 0.3667, SD = 0.07763; $t(18) = 4.021$, $p = 0.0008$; Fig. 5.14A].

However, an unpaired t-test revealed no difference in levels of pro-inflammatory cytokine IL-1β between aged 11β-HSD1$^{-/-}$ mice and aged wild-type mice [11β-HSD1$^{-/-}$: M = 1.844, SD = 0.5369; Wild-type: M = 1.372, SD = 0.3783; $t(18) = 0.7193$, $p = 0.4812$; Fig. 5.14B].

These results show elevated levels of pro-inflammatory cytokine TNFα in 11β-HSD1$^{-/-}$ mice compared to wild-type mice and that this is observed with ageing as well as following acute inflammatory responses.

However, it is worthy to note that only elevated levels of TNFα were observed in 11β-HSD1$^{-/-}$ mice whilst mRNA levels of pro-inflammatory cytokine IL-1β were found to remain unaltered both with age and following an acute inflammatory response.

These results suggest that lifelong deletion of 11β-HSD1 has an impact on the levels of pro-inflammatory cytokine TNFα both following an acute inflammatory response and with ageing where low level chronic inflammation may occur.

Figure 5.14. TNFα and IL-1β mRNA expression in aged Wild-Type (WT) and 11β-HSD1$^{-/-}$ (KO) mice

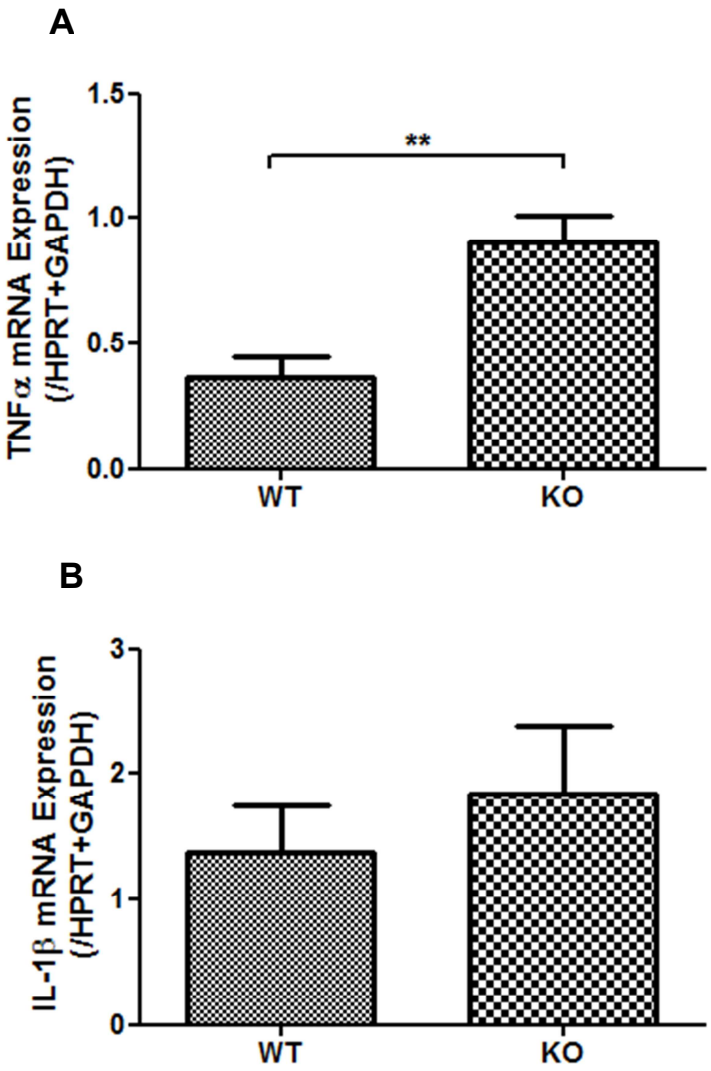

Fig. 5.14. Graphs showing hippocampal mRNA expression of **[A]** TNFα and **[B]** IL-1β in aged wild-type (WT; n=12) and 11β-HSD1$^{-/-}$ mice (KO; n=11). Values represent mean relative mRNA expression as a ratio of housekeeping genes HPRT and GAPDH +SEM.

5.3.9 Expression of alternative activated microglia (M2) markers with age

Previous research has suggested that during inflammation microglia also exhibit a response which suppresses the expression of pro-inflammatory cytokines and inactivates the initial immune response and activates signalling pathways associated with tissue repair.

We investigated if the elevated levels of TNFα in 11β-HSD1$^{-/-}$ mice with age would alter the expression of alternative activated microglia and in turn aid in the attenuation of age-related spatial learning and memory impairments.

YM1 mRNA expression was not altered in aged 11β-HSD1$^{-/-}$ mice compared to aged wild-type mice. An unpaired t-test no difference in levels of YM1 mRNA in aged 11β-HSD1$^{-/-}$ mice compared to aged wild-type mice [11β-HSD1$^{-/-}$: M = 1.643, SD = 0.3431; Wild-type: M = 1.155, SD = 0.3613; t(20) = 0.9792, p = 0.3392; Fig. 5.15A].

Similarly, another alternative activated microglia marker Arg1 between aged 11β-HSD1$^{-/-}$ mice and aged wild-type mice was unchanged [11β-HSD1$^{-/-}$: M = 0.7059, SD = 0.2135; Wild-type: M = 0.7457, SD = 0.2517; t(20) = 1.207, p = 0.9051; Fig. 5.15B].

These results suggest that the expression of alternative activated microglial markers with age are not altered by lifelong deletion of 11β-HSD1.

Figure 5.15. YM1 and Arg1 mRNA expression in aged Wild-Type (WT) and 11β-HSD1$^{-/-}$ (KO) mice

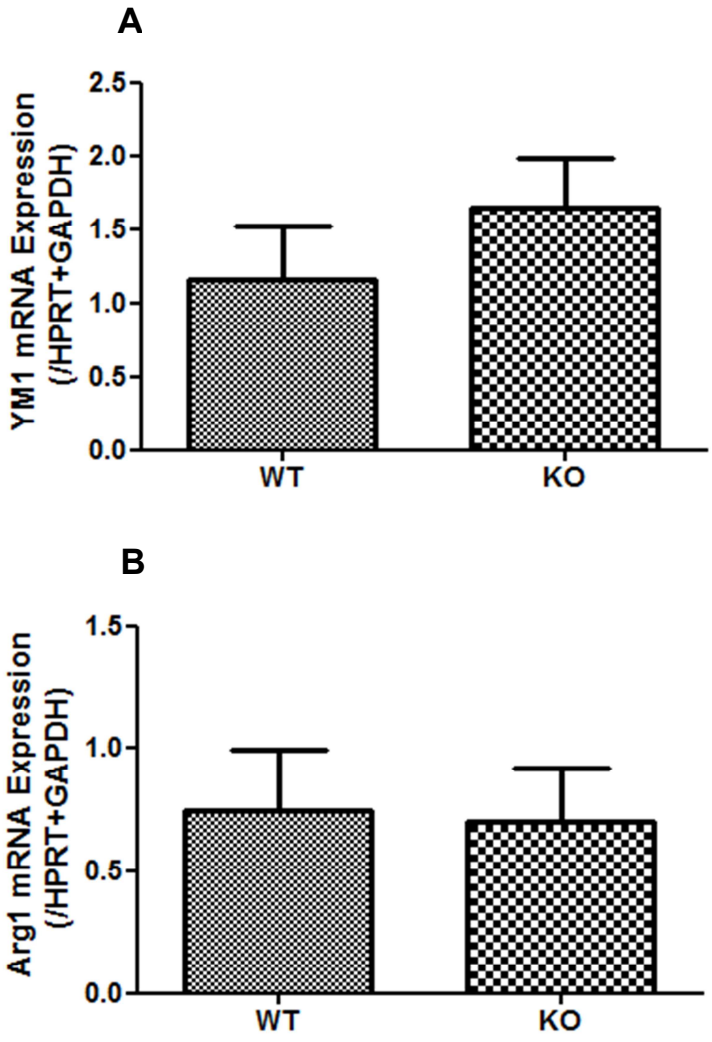

Fig. 5.15. Graphs showing hippocampal mRNA expression of **[A]** YM1 and **[B]** Arg1 in aged wild-type (WT; n=12) and 11β-HSD1$^{-/-}$ mice (KO; n=11). Values represent mean relative mRNA expression as a ratio of housekeeping genes HPRT and GAPDH +SEM.

5.3.10 Pro-inflammatory cytokine mRNA expression and spatial memory and spatial working memory

5.3.10.1 Probe Test

We tested if expression of pro-inflammatory cytokines would alter spatial memory in aged wild-type and 11β-HSD1$^{-/-}$ mice.

mRNA levels of pro-inflammatory cytokines TNFα and IL-1β were tested to see if they would alter probe test performance at 24 months of age. Specifically, the latency to previous platform location and percentage time spent swimming in the target quadrant were used to assess probe test performance.

In the probe test, TNFα and IL-1β mRNA expression was not observed to be correlated with probe test performance in aged wild-type mice [TNFα x Latency to previous platform location: r = 0.1769, p = 0.6250; TNFα x Percentage time spent swimming in target quadrant: r = -0.5731, p = 0.0833; IL-1β x Latency to previous platform location: r = -0.1241, p = 0.7326; IL-1β x Percentage time spent swimming in target quadrant: r = -0.1557, p = 0.6675; Fig. 5.16].

However, aged 11β-HSD1$^{-/-}$ mice with higher expression of TNFα mRNA exhibited lower latencies to previous platform location in the probe test [r = -0.8137, p = 0.0489; Fig 5.16C]. However, no correlation was observed between the time spent swimming in the target quadrant and TNFα mRNA expression in aged 11β-HSD1$^{-/-}$ mice [r = 0.1888, p = 0.7202; Fig. 5.16D].

No correlation was observed between the latency to previous platform location and IL-1β mRNA expression in aged 11β-HSD1$^{-/-}$ mice [r = 0.6637, p = 0.1506] and

time spent swimming in the target quadrant and IL-1β mRNA expression in aged 11β-HSD1$^{-/-}$ mice [r = -0.2, p = 0.7041].

Figure 5.16. Correlation of TNFα mRNA expression and probe test performance in aged Wild-Type (WT) and 11β-HSD1$^{-/-}$ (KO) mice

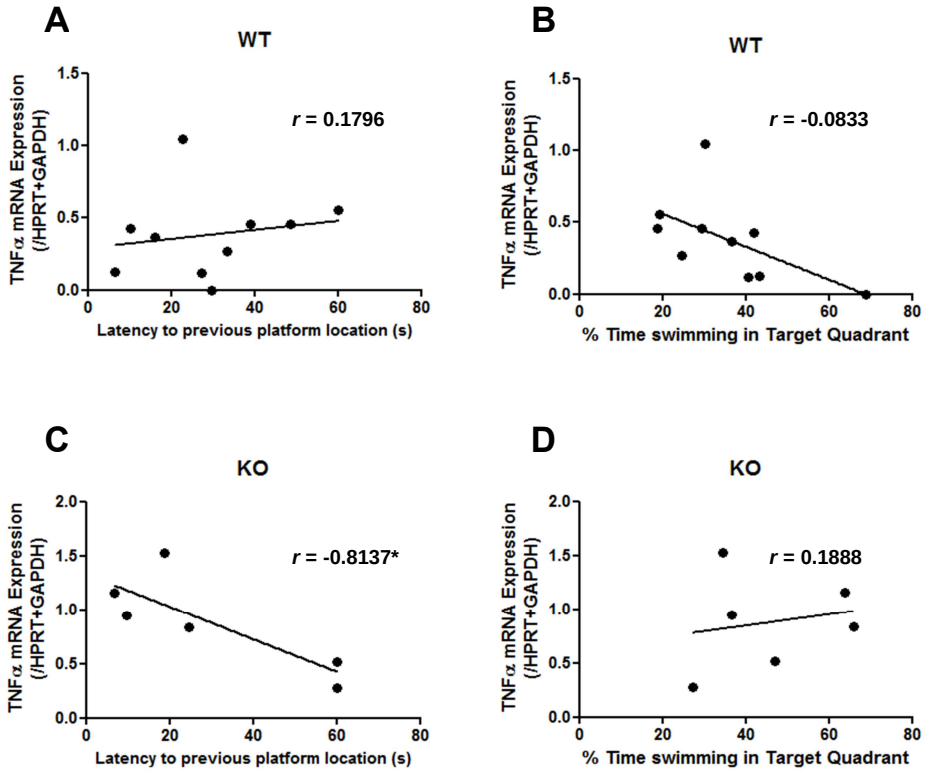

Fig. 5.16. Correlation coefficients (*r*) of the correlations calculated between hippocampal TNFα mRNA expression and **[A]** latency to previous platform location in the probe test in wild-type mice (WT; n=10); **[B]** percentage time spent swimming in the target quadrant in the probe test in wild-type mice (WT; n=10); **[C]** latency to previous platform location in the probe test in 11β-HSD1$^{-/-}$ mice (KO; n=6); and **[D]** percentage time spent swimming in the target quadrant in the probe test in 11β-HSD1$^{-/-}$ mice (KO; n=6). *$p < 0.05$; ** $p < 0.01$; *** $p < 0.001$.

5.3.10.2 Radial Arm Water Maze

No correlation was observed between the latency savings over the 1 hour retention interval and TNFα mRNA expression in aged wild-type [r = 0.3190, p = 0.2460] and 11β-HSD1$^{-/-}$ mice [r = -0.3168, p = 0.2678] and error savings over the 1 hour retention interval and TNFα mRNA expression in aged wild-type [r = 0.1681, p = 0.5454] and 11β-HSD1$^{-/-}$ mice [r = -0.2055, p = 0.4794].

No correlation was observed between the latency savings over the 1 hour retention interval and IL-1β mRNA expression in aged wild-type [r = 0.2135, p = 0.4416] and 11β-HSD1$^{-/-}$ mice [r = 0.1520, p = 0.6006] and error savings over the 1 hour retention interval and IL-1β mRNA expression in aged wild-type [r = 0.2219, p = 0.4215] and 11β-HSD1$^{-/-}$ mice [r = 0.2396, p = 0.4053].

5.3.11 Expression of alternative activated microglia markers and spatial memory and spatial working memory

5.3.11.1 Probe Test

mRNA levels of alternative activated microglia markers YM1 and Arg1 were tested to see if they would alter spatial learning performance and probe test performance at 24 months of age.

Performance in the probe test section of the water maze was not associated with mRNA expression of alternative microglia activation markers YM1 and Arg1 in aged wild-type mice and aged 11β-HSD1$^{-/-}$ mice. No significant correlation between YM1 mRNA expression and latency to previous platform location [r = -0.4852, p = 0.1552] and time spent swimming in the target quadrant [r = -0.03068, p = 0.9329]

was observed in wild-type mice and no correlation was observed between YM1 mRNA expression and latency to previous platform location [r = 0.6118, p = 0.1968] and time spent swimming in the target quadrant and YM1 mRNA expression [r = -0.2169, p = 0.6797] in aged 11β-HSD1$^{-/-}$ mice.

No correlation was observed between the latency to previous platform location and Arg1 mRNA expression in aged wild-type mice [r = -0.3419, p = 0.3755; Fig 5.17A] and time spent swimming in the target quadrant and Arg1 mRNA expression in aged wild-type mice [r = 0.1770, p = 0.6248; Fig. 5.17B].

However, 11β-HSD1$^{-/-}$ mice with higher levels of Arg1 mRNA were noted to swim to the previous platform location faster with a significant correlation between the latency to previous platform location and Arg1 mRNA expression in aged 11β-HSD1$^{-/-}$ mice [r = -0.9740, p = 0.001; Fig. 5.17C]. No correlation was observed between the time spent swimming in the target quadrant and Arg1 mRNA expression in aged 11β-HSD1$^{-/-}$ mice [r = 0.2325, p = 0.6575; Fig. 5.17D].

Figure 5.17. Correlation of Arg1 mRNA expression and water maze performance in aged Wild-Type (WT) and 11β-HSD1$^{-/-}$ (KO) mice

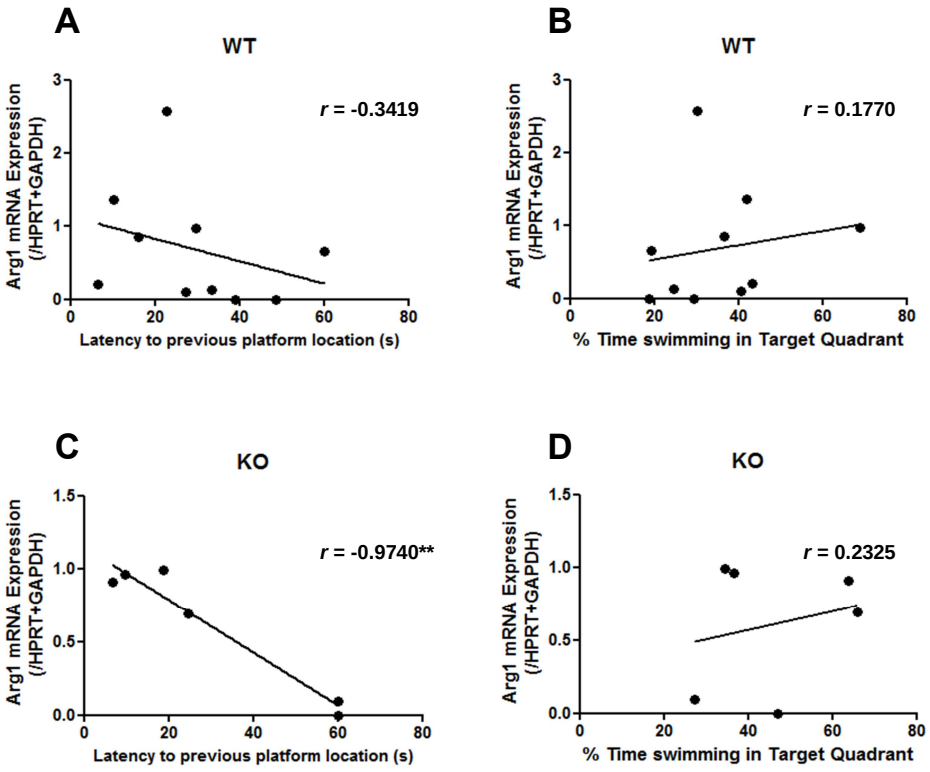

Fig. 5.17. Correlation coefficients (*r*) of the correlations calculated between hippocampal Arg1 mRNA expression and **[A]** latency to previous platform location in the probe test in wild-type mice (WT; n=10); **[B]** percentage time spent swimming in the target quadrant in the probe test in wild-type mice (WT; n=10); **[C]** latency to previous platform location in the probe test in 11β-HSD1$^{-/-}$ mice (KO; n=6); and **[D]** percentage time spent swimming in the target quadrant in the probe test in 11β-HSD1$^{-/-}$ mice (KO; n=6). **p* < 0.05; ** *p* < 0.01; *** *p* < 0.001.

5.3.11.2 Radial Arm Water Maze

No correlation was observed between the latency savings over the 1 hour retention interval and YM1 mRNA expression in aged wild-type [r = 0.05475, p = 0.8487] and 11β-HSD1$^{-/-}$ mice [r = 0.1414, p = 0.6269] and error savings over the 1 hour retention interval and YM1 mRNA expression in aged wild-type [r = 0.1518, p = 0.5691] and 11β-HSD1$^{-/-}$ mice [r = 0.3062, p = 0.2855].

No correlation was observed between the latency savings over the 1 hour retention interval and Arg1 mRNA expression in aged wild-type [r = 0.2170, p = 0.4338] and 11β-HSD1$^{-/-}$ mice [r = 0.1967, p = 0.4968] and error savings over the 1 hour retention interval and Arg1 mRNA expression in aged wild-type [r = 0.827, p = 0.3039] and 11β-HSD1$^{-/-}$ mice [r = 0.3425, p = 0.2300].

5.4 Discussion

The first part of this chapter aimed to examine the effect of acute inflammation on 11β-HSD1 expression and the effect of lifelong removal of 11β-HSD1 on an acute inflammatory response. 11β-HSD1 was not expressed in microglia and levels did not change following LPS induced inflammation. However, lifelong removal of 11β-HSD1 was found to potentiate the inflammatory response.

Previous studies have found 11β-HSD1 to be expressed in cultured in-vitro microglia and upregulated following LPS administration (Gottfried-Blackmore et al., 2010). However, Initial investigations into the expression of 11β-HSD1 in microglia showed that 11β-HSD1 is not expressed in microglia. One possible reason for the difference in expression is the difference in experimental methodology with Gottfried-Blackmore et al. (2010), where cultured microglia were used possibly altering cell conditions and expression.

LPS did not induce changes in either 11β-HSD1 protein or mRNA levels as observed by Gottfried-Blackmore et al. (2010) and studies demonstrating increased 11β-HSD1 expression by pro-inflammatory cytokines IL-1 and TNFα (Chapman et al., 2006a, 2006b; Cooper and Stewart, 2009), suggesting that in the brain 11β-HSD1 expression may be driven by other additional factors. Notably, pro-inflammatory cytokine expression also showed limited change in this study, both wild-type and 11β-HSD1$^{-/-}$ mice exhibited unaltered expression of the microglia marker, Iba-1, and pro-inflammatory cytokine IL-1β mRNA levels. These data indicate that the inflammatory response may not have been strong which may account for the absence of changes in 11β-HSD1 expression.

Interestingly, elevated levels of TNFα were observed following LPS administration in 11β-HSD1$^{-/-}$ mice. Previous research has suggested that whilst glucocorticoids inhibit both TNFα and IL-1β, there is a grading of sensitivity, with TNF having the greatest sensitivity and suppression occurring at physiological levels (O'Connor et al., 2000). Thus, our data suggest that 11β-HSD1$^{-/-}$ mice may be more sensitive to LPS administration. This is consistent with the classical view of glucocorticoids demonstrating anti-inflammatory effects through the inhibition of synthesis of cytokines and inflammatory mediators and resulting in a negative feedback loop. of glucocorticoids. Taken together our results suggest that 11β-HSD1$^{-/-}$ mice demonstrate a heightened inflammatory response following LPS administration, and that this response is likely mediated by the absence of anti-inflammatory actions of glucocorticoids.

The second part of this study aimed to examine if age and lifelong removal of 11β-HSD1 altered the inflammatory status of the brain and if this inflammatory status was associated with cognitive performance with age. Secondly, it aimed to examine if the improved cognitive performance associated with 11β-HSD1 deletion is associated with decreased inflammation in the aged brain.

Significantly higher mRNA levels of pro-inflammatory cytokine TNFα in aged 11β-HSD1$^{-/-}$ mice compared to aged wild-type mice although no difference in pro-inflammatory cytokine IL-1β was observed. Similarly, no difference in anti-inflammatory cytokines YM1 and Arg 1 were observed. These results are consistent with previous studies indicating higher levels of inflammation in 11β-HSD1$^{-/-}$ mice (Zhang and Daynes, 2007) and suggest that, when aged, 11β-HSD1$^{-/-}$ mice show

higher levels of age-related neuroinflammation. However, one key point to be taken into consideration when analysing these results is the unusual occurrence of tumours in a number of the aged 11β-HSD1$^{-/-}$ mice which may alter the inflammatory status observed.

Markers of neuroinflammation were not associated with measures of spatial memory and spatial working memory in wild-type mice. Previous investigations have established that pro-inflammatory cytokines can act directly on neurons in the hippocampus resulting in impaired synaptic plasticity as well as alter neuronal function, neurogenesis and impair long-term potentiation. Whilst more recently, Bonow et al. (2009) revealed during a microarray analysis of cortical tissue from mice injected with LPS that as well as in increase in inflammatory genes, neuroinflammation also leads to a decrease in genes related to learning and memory. However, TNFα mRNA levels were not related to spatial memory and spatial working memory in aged wild-type mice, suggesting that markers of neuroinflammation may not be directly related to cognitive performance.

Interestingly, in 11β-HSD1$^{-/-}$ mice, higher levels of TNFα were associated with better spatial memory performance in the probe test. Notably, in 11β-HSD1$^{-/-}$ mice, higher expression of alternative activated microglia markers was associated with better spatial memory performance in the probe test. Previous studies have observed two main activation states of microglia - classical (M1) and alternative (M2) – with alternative activation characterised by the inactivation of the initial immune response and activation of genetic pathways associated with tissue repair. This activity is associated with the production of anti-inflammatory cytokines by glia and neurons.

(For review see Mantovani et al., 2004). As such, our data suggest that the increased neuroinflammatory status of 11β-HSD1$^{-/-}$ mice may result in a shift of microglia states from classically activated microglial to alternatively activated microglia. This shift in activation may result in an attenuation of age-associated changes in the brain which may subsequently aid in the attenuation of processes contributing to age-associated cognitive decline.

However, some considerations to be made when examining the results of this chapter are the small group sizes. Although our study aimed to have group sizes as large as possible, experimental restraints and unforeseen tissue damage may have limited the group sizes.

In conclusion, our data show that lifelong removal of 11β-HSD1 results in higher levels of neuroinflammatory markers. However, this increase in pro-inflammatory markers may lead to alternative activation of microglia which may subsequently have beneficial effects on age-associated spatial memory impairments. Therefore, future work examining the relationship between alternative activated microglia and age-associated brain changes will help in determining mechanisms underlying age-associated impairments in cognitive processes.

Chapter 6 : General Discussion

The primary goal of the research described in this thesis was to determine the effect of reduced intracellular glucocorticoids through lifelong 11β-HSD1 removal on spatial memory and working memory over a lifespan and to investigate the possible mechanisms through which 11β-HSD1 removal may exert its effects. To this end, I used a longitudinal paradigm to examine how spatial memory and working memory were altered across the lifespan in wild-type mice and 11β-HSD1$^{-/-}$ mice. I tested spatial memory and working memory using a Morris water maze and the radial arm water maze respectively. I attempted to also examine longitudinally, structural and metabolite changes across the lifespan of the same wild-type and 11β-HSD1$^{-/-}$ mice by proton magnetic resonance spectroscopy (^{1}H-MRS). A subset of the wild-type and 11β-HSD1$^{-/-}$ mice undergoing longitudinal cognitive testing underwent ^{1}H-MRS scanning following cognitive testing and their structural and metabolite data tested for associations with their cognitive performance prior to scanning. Tissue samples were collected proceeding final cognitive testing when aged and used to examine neuronal and glial profiles in wild-type and 11β-HSD1$^{-/-}$ mice and to assess if they altered cognitive function when aged. Finally, I examined the possible role of neuroinflammation as a mechanism through which glucocorticoids may alter cognitive function with age. I investigated the effect of an acute LPS-induced inflammatory response on the neuroinflammatory profile of wild-type and 11β-HSD1$^{-/-}$ mice and examined the neuroinflammatory profile of the same wild-type and 11β-HSD1$^{-/-}$ mice undergoing longitudinal cognitive testing. I then investigated the relationship between their spatial memory when aged and their neuroinflammatory

profile. In the following discussion I will summarise my main findings, discuss their wider implications and highlight some suggestions for future work.

6.1 Spatial learning and memory with age

Wild-type mice showed no impairment in spatial learning with age and 11β-HSD1$^{-/-}$ mice were not found to perform better than wild-type mice when aged as observed in previous studies (Yau et al., 2007, 2015; Wheelan et al., 2014). Spatial memory was observed to be impaired in wild-type but not 11β-HSD1$^{-/-}$ mice at 18 months. However, at 24 months both wild-type and 11β-HSD1$^{-/-}$ mice performed equally as well. These results are most likely attributed to repeat testing over the lifespan of wild-type and 11β-HSD1$^{-/-}$ mice and highlight the difference in processes behind spatial learning and spatial memory. Practice effects are characteristic of serial neurocognitive assessments. They refer to changes in test performance as a result of increasing familiarity and exposure to test paradigms. Practice effects can be divided into two components - task familiarity and practice-related effects. These can result in the development of strategies over time that aid in the completion of the cognitive task, resulting in improvements that are unrelated to genotype. As spatial learning was assessed not only repeatedly with age, but also continuously over 5 days at each assessment, it is likely that mice became familiar with not only the task requirements but also with the testing arena. This may have resulted in the development of different strategies to find the hidden platform with age which could explain why no impairment was observed in their spatial learning with age. One possibility is that over time, mice were more able to identify the platform location through other cues such as shadows beneath the water.

The effect of repeated testing on cognitive function could also explain the impairment and then improvement in spatial memory with age in wild-type mice. In particular, it is notable that spatial memory is a different process from spatial learning, requiring the transfer of information from short to long term memory. This may account for the different effect of longitudinal testing on the mice with spatial memory being more susceptible to age-associated impairments as a result of the additional cognitive processes required for spatial information to be moved to long-term memory. As such, repeated testing may not attenuate spatial memory impairments as easily as for spatial learning impairments which may account for the u-shaped performance of wild-type mice in the probe test. Additionally, as the probe test was only conducted once at each time point, the practice effect may not have been as strong as seen in the spatial learning portion of the water maze.

Taken altogether, these data suggest that longitudinal testing may result in a practice effect in cognitive tests which may prevent changes with age being observed. Secondly, these results highlight the difference in cognitive processes, demonstrating that spatial memory is more susceptible to age-associated impairments than spatial learning processes. These results parallel what is seen in age-associated cognitive decline in human, with long-term memories of events showing the largest impairment with age and short-term memory and procedural memories showing little decline with age. Notably, cognitive function throughout an individual's lifespan, rarely consists of completely novel situations and task requirements. As such, whilst longitudinal testing may result in a practice effect and prevent changes in cognition from being observed, the effects occurring from longitudinal and repeated testing may accurately replicate cognitive ageing in humans.

Therefore these results highlight the role of practice and repeated use of cognitive faculties in cognitive ageing. Assessing age-associated cognitive decline with a more robust cognitive test which is less susceptible to the practice effect would help to determine not only the role of 11β-HSD1 in age-associated cognitive decline but also the extent to which practice and task repetition may be beneficial in maintaining cognitive function with age.

6.2 Spatial working memory with age

It was hypothesised that spatial working memory would be impaired with age (Park et al., 1996, 2002) and, as working memory is more cognitively demanding, it was expected that impairments would be observed earlier in life and that these impairments would be attenuated by 11β-HSD1 removal in similar manner to the attenuation of spatial learning and memory deficits. Spatial working memory did not appear to be affected by repeated testing in the same manner, with wild-type mice showing impaired spatial working memory with age. Most surprisingly, this impairment was not attenuated by 11β-HSD1 removal, rather, lifelong removal of 11β-HSD1 was found to result in spatial working memory impairments earlier in life. This finding is novel and previously unreported, and suggests that 11β-HSD1 may be essential for maintaining spatial working memory throughout ageing. In particular, these results imply a distinct role for 11β-HSD1 in spatial learning and memory and in spatial working memory. Whilst both spatial memory and spatial working memory share some neural components, studies have concluded that these memory processes are independently regulated by different neuroanatomical circuits. As such, these results suggest a similar distinction for the role of 11β-HSD1 in memory processes

involved in spatial working memory. Previous studies have found that spatial working memory involves activation of brain areas in addition to the hippocampus, such as the prefrontal cortex, and removal of 11β-HSD1 in these brain areas may be detrimental to the cognitive processes occurring within these areas (Cohen et al., 1997; van Asselen et al., 2006). In particular, studies have found that glucocorticoids are essential for the maintenance of prefrontal cortex cognitive function, with reduced glucocorticoid action resulting in impaired working memory through altered dopaminergic function (Mizoguchi et al., 2004). Furthermore Barsegyan et al. (2010) glucocorticoid action could both enhance and impair different cognitive process at the same time. Therefore, the removal of 11β-HSD1, whilst beneficial in the hippocampal dependent cognition, 11β-HSD1 may be essential for cognitive processes in other brain regions. In particular, our data show that removal of 11β-HSD1 does not attenuate age-associated working memory impairments and suggest that the absence of 11β-HSD1 may be detrimental to some aspects of cognition. Examining whether this is also the case when 11β-HSD1 is inhibited and whether inhibition completely removes 11β-HSD1 activity may be key in determining the extent to which 11β-HSD1 affects spatial working memory.

6.3 Glial cell activity and cognitive function

Interestingly, immunohistochemical data revealed 11β-HSD1 to be expressed in glial cells as opposed to neurons. This too was a novel finding and unreported by previous studies. Previous data had suggested that 11β-HSD1 may be expressed in neurons (Rajan et al., 1996; Wan et al., 2002), however, this study suggests that this is not the case and that 11β-HSD1 is in fact expressed in glial cells. This study went on to

show that higher levels of 11β-HSD1 were found to be correlated with greater glial reactivity in wild-type mice and, in turn, increased glial reactivity was associated with poorer spatial memory in the water maze. These results suggest that increased glial reactivity may be a mechanism through which elevated intracellular glucocorticoids exert negative effects on memory with age. Indeed, glial reactivity has been observed to increase with age in the hippocampus and reductions in glial reactivity have been associated with better neuronal survival and long-term potentiation (McCall et al., 1996; Menet et al., 2000, 2001). Therefore, elevated 11β-HSD1 and glucocorticoids with age may contribute to increased glial reactivity and subsequently alter cognitive function.

Furthermore, higher levels of the glutamate/glutamine complex were found to alter spatial memory in aged wild-type mice but not 11β-HSD1$^{-/-}$ mice. These results suggest that glutamate/glutamine levels may also be a mechanism through which glucocorticoids may act to alter cognitive function. Taken together with glial cell data discussed in the paragraph above, the data perhaps points to a process where intracellular glucocorticoids alter glial reactivity which in turn alters glutamate/glutamine expression and subsequently neuronal and cognitive function.

As such, the implications of this data are that age-associated memory impairments may be mediated by glial cells in the hippocampus and that these glial cells may alter neuronal function and cognitive performance through altered glutamate/glutamine cycling. Thus, it may be beneficial to further explore the role of 11β-HSD1 in glutamate/glutamine cycling in the hippocampus and how this may alter cognitive function.

6.4 Neuroinflammation and cognitive function

In our aged colony of mice, elevated levels of pro-inflammatory cytokines were observed in 11β-HSD1$^{-/-}$ mice compared to their wild-type counterparts. However, at the same time, increased expression of alternative activated microglia markers was found to be associated with better spatial memory.

These results suggest that elevated pro-inflammatory cytokine levels throughout the lifespan of 11β-HSD1$^{-/-}$ mice results in a shift in microglial activation from classically activated microglia to alternative activated microglia with a neuroprotective and neuron supporting phenotype (Mantovani et al., 2004). Thus, this study suggests that lifelong removal of 11β-HSD1 may alter the neuroinflammatory profile of the brain and this chronic or heightened neuroinflammatory profile may induce a microglial shift to a more protective state. This shift in microglial activation may then be beneficial during ageing when the neuroinflammatory profile of the brain is heightened and aid in attenuating any negative effects of neuroinflammation on cognition. Furthermore, taken together with

6.5 Proposed future work

This study was limited in a number of key ways, particularly for robustness of the water maze task to repeated testing and sample size. These limitations were due to a number of factors, including costs and limited resources and space to sufficiently vary the water maze arena when testing. Protein data was also unavailable at early ages due to the longitudinal nature of the experiment. This data will have proven useful in analysing relationships between cognitive function and various factors.

Ideally, the first step in creating follow up studies would be to combine groups of animals to be tested cognitively then culled and tissue collected for analysis at each age-point throughout the lifespan, this would provide a complete picture of alterations with age and their relationship to cognitive function and 11β-HSD1.

Additionally, further work investigating the extent to which 11β-HSD1 activity regulates prefrontal cortex cognitive function will be key in determining the overall functional benefits of 11β-HSD1 inhibition on age-associated cognitive impairments. Finally, examining the role of 11β-HSD1 in glial cell signalling and function and glutamate/glutamine cycling, and 11β-HSD1 in the activation of alternative activated microglia would enable a deeper understanding into how regeneration of intracellular glucocorticoids might alter cognitive function with age. This may help in identifying more specific therapeutic targets for age-associated cognitive impairments.

6.6 Final Conclusions

In conclusion, longitudinal testing resulted in a practice effect resulting in minimal impairments in spatial learning. Spatial memory showed some impairment with age, which were attenuated by 11β-HSD1 removal, highlighting the increased susceptibility of memory to age-associated long-term memory impairments and benefit of 11β-HSD1 removal on hippocampal dependent memory. These impairments in spatial memory were found to be associated with increased glial reactivity and increased glial reactivity. Notably, increased levels of the glutamate/glutamine complex, which is highly regulated by glial cells and plays an essential role in cognitive function, were also associated with poorer spatial memory,

suggesting an overall effect of glucocorticoids on cognitive function through increased glial cell reactivity and consequently altered glutamate/glutamine cycling.

Importantly, this study also highlighted the role of enzyme 11β-HSD1 in reducing, although not completely suppressing, neuroinflammation with age. However, it also indicated a role for 11β-HSD1 in altering the polarisation of classically activated microglia to alternative activated microglia, suggesting overall that memory impairments with age may also be mediated by the effect of glucocorticoids on microglial activation.

Finally, our study found that complete removal of 11β-HSD1 may not be beneficial for all cognitive processes, in particular working memory processes. This suggests that 11β-HSD1 may alter cognition through different mechanisms in different brain regions and highlights the need to further examine the impact of 11β-HSD1 on different cognitive processes to determine the overall benefit of 11β-HSD1 inhibition on age-associated cognitive impairments.

Chapter 7 : Bibliography

Adams MM, Donohue HS, Linville MC, Iversen EA, Newton IG, Brunso-Bechtold JK (2010) Age-related synapse loss in hippocampal CA3 is not reversed by caloric restriction. Neuroscience 171:373–382.

Angelie E, Bonmartin A, Boudraa A, Gonnaud P-M, Mallet J-J, Sappey-Marinier D (2001) Regional Differences and Metabolic Changes in Normal Aging of the Human Brain: Proton MR Spectroscopic Imaging Study. AJNR Am J Neuroradiol 22:119–127 Available at: http://www.ajnr.org/cgi/content/abstract/22/1/119.

Auld DS, Robitaille R (2003) Glial cells and neurotransmission: an inclusive view of synaptic function. Neuron 40:389–400.

Barsegyan A, Mackenzie SM, Kurose BD, McGaugh JL, Roozendaal B (2010) Glucocorticoids in the prefrontal cortex enhance memory consolidation and impair working memory by a common neural mechanism. Proc Natl Acad Sci U S A 107:16655–16660.

Bartnik Olson BL, Holshouser BA, Britt WIII, Mueller C, Baqai W, Patra S, Petersen F, Kirsch WM (2008) Longitudinal Metabolic and Cognitive Changes in Mild Cognitive Impairment Patients. Alzheimer Dis Assoc Disord 22 Available at: http://journals.lww.com/alzheimerjournal/Fulltext/2008/07000/Longitudinal_Metabolic_and_Cognitive_Changes_in.12.aspx.

Bartzokis G, Sultzer D, Lu PH, Nuechterlein KH, Mintz J, Cummings JL (2004) Heterogeneous age-related breakdown of white matter structural integrity: implications for cortical “disconnection” in aging and Alzheimer’s disease. Neurobiol Aging 25:843–851.

Becker JT, Walker JA, Olton DS (1980) Neuroanatomical bases of spatial memory. Brain Res 200:307–320 Available at: http://www.sciencedirect.com/science/article/pii/0006899380909221.

Bezzi P, Volterra A (2001) A neuron–glia signalling network in the active brain. Curr Opin Neurobiol 11:387–394.

Biber K, Vinet J, Boddeke HWGM (2008) Neuron-microglia signaling: chemokines as versatile messengers. J Neuroimmunol 198:69–74 Available at: http://www.ncbi.nlm.nih.gov/pubmed/18538419 [Accessed July 20, 2012].

Bilbo SD (2010) Early-life Infection is a Vulnerability Factor for Aging-Related Glial Alterations and Cognitive Decline. 94:57–64.

Bishop N a, Lu T, Yankner B a (2010) Neural mechanisms of ageing and cognitive decline. Nature 464:529–535 Available at: http://www.pubmedcentral.nih.gov/articlerender.fcgi?artid=2927852&tool=pmcentrez&rendertype=abstract [Accessed July 13, 2012].

Bizon JL, LaSarge CL, Montgomery KS, McDermott AN, Setlow B, Griffith WH (2009) Spatial reference and working memory across the lifespan of male Fischer 344 rats. Neurobiol Aging 30:646–655 Available at: http://www.sciencedirect.com/science/article/pii/S0197458007003351.

Blalock EM, Chen K-C, Sharrow K, Herman JP, Porter NM, Foster TC, Landfield PW (2003) Gene microarrays in hippocampal aging: statistical profiling identifies novel processes correlated with cognitive impairment. J Neurosci 23:3807–3819 Available at: http://www.ncbi.nlm.nih.gov/pubmed/12736351.

Blatter DD, Bigler ED, Gale SD, Johnson SC, Anderson C V, Burnett BM, Parker N, Kurth S, Horn SD (1995) Quantitative volumetric analysis of brain MR: normative database spanning 5 decades of life. AJNR Am J Neuroradiol 16:241–251.

Bonow RH, Aïd S, Zhang Y, Becker KG (2009) The brain expression of genes involved in inflammatory response, the ribosome, and learning and memory is altered by centrally injected lipopolysaccharide in mice. Pharmacogenomics J 9:116–126.

Bridges N, Slais K, Sykova E (2008) The effects of chronic corticosterone on hippocampal astrocyte numbers: a comparison of male and female Wistar rats. Acta Neurobiol Exp (Wars) 68:131–138.

Brody H (1955) Organization of the cerebral cortex. III. A study of aging in the human cerebral cortex. J Comp Neurol 102:511–556 Available at: http://dx.doi.org/10.1002/cne.901020206.

Brooks JCW, Roberts N, Kemp GJ, Gosney MA, Lye M, Whitehouse GH (2001) A proton magnetic resonance spectroscopy study of age-related changes in frontal lobe metabolite concentrations. Cereb Cortex 11:598–605.

Buckingham JC (2006) Glucocorticoids: exemplars of multi-tasking. Br J Pharmacol 147:S258–S268 Available at: http://dx.doi.org/10.1038/sj.bjp.0706456.

Burke SN, Barnes CA (2006) Neural plasticity in the ageing brain. Nat Rev Neurosci 7:30–40.

Buttini M, Limonta S, Boddekke HWG. (1996) PERIPHERAL ADMINISTRATION OF LIPOPOLYSACCHARIDE INDUCES ACTIVATION OF MICROGLIAL CELLS IN RAT BRAIN*. Neurochem Int 29:25–35 Available at: http://www.sciencedirect.com/science/article/pii/0197018695001417.

Carstensen L, Fung H, Charles S (2003) Socioemotional Selectivity Theory and the Regulation of Emotion in the Second Half of Life. Motiv Emot 27:103–123 Available at: http://dx.doi.org/10.1023/A:1024569803230.

Cave CB, Squire LR (1992) Intact verbal and nonverbal short-term memory following damage to the human hippocampus. Hippocampus 2:151–163 Available at: http://dx.doi.org/10.1002/hipo.450020207.

Chang L, Ernst T, Poland RE, Jenden DJ (1996) < i> In vivo</i> proton magnetic resonance spectroscopy of the normal aging human brain. Life Sci 58:2049–2056.

Chapman KE, Coutinho A, Gray M, Gilmour JS, Savill JS, Seckl JR (2006a) Local amplification of glucocorticoids by 11beta-hydroxysteroid dehydrogenase type 1 and its role in the inflammatory response. Ann N Y Acad Sci 1088:265–273 Available at: http://www.ncbi.nlm.nih.gov/pubmed/17192572 [Accessed July 25, 2012].

Chapman KE, Gilmour JS, Coutinho AE, Savill JS, Seckl JR (2006b) 11Beta-hydroxysteroid dehydrogenase type 1--a role in inflammation? Mol Cell Endocrinol 248:3–8.

Charles HC, Lazeyras F, Krishnan K, Boyko OB, Patterson LJ, Doraiswamy PM, Mcdonald WM (1994) Proton spectroscopy of human brain: effects of age and sex. Prog Neuro-Psychopharmacology Biol Psychiatry 18:995–1004.

Cohen JD, Perlstein WM, Braver TS, Nystrom LE, Noll DC, Jonides J, Smith EE (1997) Temporal dynamics of brain activation during a working memory task. Nature 386:604–608 Available at: http://dx.doi.org/10.1038/386604a0.

Cohen RM, Small C, Lalonde F, Friz J, Sunderland T (2001) Effect of apolipoprotein E genotype on hippocampal volume loss in aging healthy women. Neurology 57:2223–2228.

Convit A, Wolf OT, Tarshish C, de Leon MJ (2003) Reduced glucose tolerance is associated with poor memory performance and hippocampal atrophy among normal elderly. Proc Natl Acad Sci U S A 100:2019–2022 Available at: http://www.pnas.org/content/100/4/2019.abstract.

Cook IA, Leuchter AF, Morgan ML, Dunkin JJ, Witte E, David S, Mickes L, O'Hara R, Simon S, Lufkin R (2004) Longitudinal progression of subclinical structural brain disease in normal aging. Am J Geriatr psychiatry 12:190–200.

Cooper MS, Stewart PM (2009) 11Beta-hydroxysteroid dehydrogenase type 1 and its role in the hypothalamus-pituitary-adrenal axis, metabolic syndrome, and inflammation. J Clin Endocrinol Metab 94:4645–4654.

Cruz-Sánchez FF, Cardozo A, Tolosa E (1995) Neuronal changes in the substantia nigra with aging: a Golgi study. J Neuropathol Exp Neurol 54:74–81.

Czéh B, Michaelis T, Watanabe T, Frahm J, de Biurrun G, van Kampen M, Bartolomucci A, Fuchs E (2001) Stress-induced changes in cerebral metabolites, hippocampal volume, and cell proliferation are prevented by antidepressant treatment with tianeptine. Proc Natl Acad Sci U S A 98:12796–12801 Available at: http://www.ncbi.nlm.nih.gov/pmc/articles/PMC60133/.

Daffner KR (2010) Promoting Successful Cognitive Aging: A Comprehensive Review. J Alzheimers Dis 19:1101–1122 Available at: http://www.ncbi.nlm.nih.gov/pmc/articles/PMC3047597/.

Davis EJ, Foster TD, Thomas WE (1994) Cellular forms and functions of brain microglia. Brain Res Bull 34:73–78 Available at: http://www.ncbi.nlm.nih.gov/pubmed/8193937.

Dean RL, Scozzafava J, Goas JA, Regan B, Beer B, Bartus RT (1981) Age-related differences in behavior across the life span of the C57BL/6J mouse. Exp Aging Res 7:427–451 Available at: http://dx.doi.org/10.1080/03610738108259823.

Diamond DM, Fleshner M, Ingersoll N, Rose G (1996) Psychological stress impairs spatial working memory: relevance to electrophysiological studies of hippocampal function. Behav Neurosci 110:661.

Dickerson BC, Eichenbaum H (2009) The Episodic Memory System: Neurocircuitry and Disorders. Neuropsychopharmacology 35:86–104 Available at: http://dx.doi.org/10.1038/npp.2009.126.

Dixon R, Wahlin Å, Maitland S, Hultsch D, Hertzog C, Bäckman L (2004) Episodic memory change in late adulthood: Generalizability across samples and performance indices. Mem Cognit 32:768–778 Available at: http://dx.doi.org/10.3758/BF03195867.

Driscoll I, Hamilton DA, Petropoulos H, Yeo RA, Brooks WM, Baumgartner RN, Sutherland RJ (2003) The aging hippocampus: cognitive, biochemical and structural findings. Cereb cortex 13:1344–1351.

Duan H, Wearne SL, Rocher AB, Macedo A, Morrison JH, Hof PR (2003) Age-related dendritic and spine changes in corticocortically projecting neurons in macaque monkeys. Cereb Cortex 13:950–961.

Dumitriu D, Hao J, Hara Y, Kaufmann J, Janssen WGM, Lou W, Rapp PR, Morrison JH (2010) Selective changes in thin spine density and morphology in monkey prefrontal cortex correlate with aging-related cognitive impairment. J Neurosci 30:7507–7515.

Earnest MP, Heaton RK, Wilkinson WE, Manke WF (1979) Cortical atrophy, ventricular enlargement and intellectual impairment in the aged. Neurology 29:1138–1143.

Fjell AM, Walhovd KB, Reinvang I, Lundervold A, Salat D, Quinn BT, Fischl B, Dale AM (2006) Selective increase of cortical thickness in high-performing elderly—structural indices of optimal cognitive aging. Neuroimage 29:984–994.

Frank MG, Baratta M V, Sprunger DB, Watkins LR, Maier SF (2007) Microglia serve as a neuroimmune substrate for stress-induced potentiation of CNS pro-inflammatory cytokine responses. Brain Behav Immun 21:47–59 Available at: http://www.ncbi.nlm.nih.gov/pubmed/16647243 [Accessed July 17, 2012].

Frank MG, Barrientos RM, Biedenkapp JC, Rudy JW, Watkins LR, Maier SF (2006) mRNA up-regulation of MHC II and pivotal pro-inflammatory genes in normal brain aging. Neurobiol Aging 27:717–722 Available at: http://www.ncbi.nlm.nih.gov/pubmed/15890435 [Accessed July 25, 2012].

Frank MG, Barrientos RM, Watkins LR, Maier SF (2010) Aging sensitizes rapidly isolated hippocampal microglia to LPS ex vivo. J Neuroimmunol 226:181–184 Available at: http://www.pubmedcentral.nih.gov/articlerender.fcgi?artid=2937085&tool=pmcentrez&rendertype=abstract [Accessed July 25, 2012].

Frick KM, Baxter MG, Markowska AL, Olton DS, Price DL (n.d.) Age-related spatial reference and working memory deficits assessed in the water maze. Neurobiol Aging 16:149–160 Available at: http://www.sciencedirect.com/science/article/pii/0197458094001553.

Fromholt P, Mortensen D, Torpdahl P, Bender L, Larsen P, Rubin D (2003) Life-narrative and word-cued autobiographical memories in centenarians: Comparisons with 80-year-old control, depressed, and dementia groups. Memory 11:81–88 Available at: http://dx.doi.org/10.1080/741938171.

Fuller PJ, Young MJ (2005) Mechanisms of mineralocorticoid action. Hypertension 46:1227–1235.

Gallagher M, Burwell RD (1989) Relationship of age-related decline across several behavioral domains. Neurobiol Aging 10:691–708 Available at: http://www.neurobiologyofaging.org/article/0197-4580(89)90006-7/abstract.

Geinisman Y, de Toledo-Morrell L, Morrell F (1986) Aged rats need a preserved complement of perforated axospinous synapses per hippocampal neuron to maintain good spatial memory. Brain Res 398:266–275.

Godbout JP, Chen J, Abraham J, Richwine AF, Berg BM, Kelley KW, Johnson RW (2005) Exaggerated neuroinflammation and sickness behavior in aged mice

following activation of the peripheral innate immune system. FASEB J 19:1329–1331.

Golomb J, de Leon MJ, Kluger A, George AE, Tarshish C, Ferris SH (1993) Hippocampal atrophy in normal aging: an association with recent memory impairment. Arch Neurol 50:967–973.

Golomb J, Kluger A, de Leon MJ, Ferris SH, Convit A, Mittelman MS, Cohen J, Rusinek H, De Santi S, George AE (1994) Hippocampal formation size in normal human aging: a correlate of delayed secondary memory performance. Learn Mem 1 :45–54 Available at: http://learnmem.cshlp.org/content/1/1/45.abstract.

Goss JR, Finch CE, Morgan DG (1991) Age-related changes in glial fibrillary acidic protein mRNA in the mouse brain. Neurobiol Aging 12:165–170.

Gottfried-Blackmore A, Sierra A, McEwen BS, Ge R, Bulloch K (2010) Microglia express functional 11 beta-hydroxysteroid dehydrogenase type 1. Glia 58:1257–1266 Available at: http://www.ncbi.nlm.nih.gov/pubmed/20544861 [Accessed April 9, 2012].

GrÉGoire J, Van Der Linden M (1997) Effect of age on forward and backward digit spans. Aging, Neuropsychol Cogn 4:140–149 Available at: http://dx.doi.org/10.1080/13825589708256642.

Griffin R, Nally R, Nolan Y, McCartney Y, Linden J, Lynch M a (2006) The age-related attenuation in long-term potentiation is associated with microglial activation. J Neurochem 99:1263–1272 Available at: http://www.ncbi.nlm.nih.gov/pubmed/16981890 [Accessed July 25, 2012].

Gunning-Dixon FM, Raz N (2000) The cognitive correlates of white matter abnormalities in normal aging: a quantitative review. Neuropsychology 14:224.

Hackert VH, Den Heijer T, Oudkerk M, Koudstaal PJ, Hofman A, Breteler MMB (2002) Hippocampal head size associated with verbal memory performance in nondemented elderly. Neuroimage 17:1365–1372.

Han X, Chen M, Wang F, Windrem M, Wang S, Shanz S, Xu Q, Oberheim NA, Bekar L, Betstadt S (2013) Forebrain engraftment by human glial progenitor cells enhances synaptic plasticity and learning in adult mice. Cell Stem Cell 12:342–353.

Happe FG, Winner E, Brownell H (1998) The getting of wisdom: theory of mind in old age. Dev Psychol 34:358–362.

Hara Y, Rapp PR, Morrison JH (2012) Neuronal and morphological bases of cognitive decline in aged rhesus monkeys. Age (Omaha) 34:1051–1073.

Head D, Buckner RL, Shimony JS, Williams LE, Akbudak E, Conturo TE, McAvoy M, Morris JC, Snyder AZ (2004) Differential vulnerability of anterior white matter in nondemented aging with minimal acceleration in dementia of the Alzheimer type: evidence from diffusion tensor imaging. Cereb Cortex 14:410–423.

Hedden T, Gabrieli JDE (2004) Insights into the ageing mind: a view from cognitive neuroscience. Nat Rev Neurosci 5:87–96.

Hertz L, Zielke HR (2004) Astrocytic control of glutamatergic activity: astrocytes as stars of the show. Trends Neurosci 27:735–743.

Hodges H (1996) Maze procedures: the radial-arm and water maze compared. Brain Res Cogn Brain Res 3:167–181 Available at: http://www.ncbi.nlm.nih.gov/pubmed/8806020.

Holmes MC, Carter RN, Noble J, Chitnis S, Dutia A, Paterson JM, Mullins JJ, Seckl JR, Yau JLW (2010) 11{beta}-Hydroxysteroid Dehydrogenase Type 1 Expression Is Increased in the Aged Mouse Hippocampus and Parietal Cortex and Causes Memory Impairments. J Neurosci 30:6916–6920 Available at: http://www.jneurosci.org/cgi/content/abstract/30/20/6916.

Itzev D, Lolov S, Usunoff KG (2003) Comparative investigation of age-related changes in the synapses of rat's somatosensory cortex, neostriatum and paraventricular hypothalamic nucleus. Comptes Rendus l'Academie Bulg des Sci 56:109.

Itzev D, Lolova I, Lolov S, Usunoff KG (2001) Age-Related Changes in the Synapses of the Rat'Neostriatum. Arch Physiol Biochem 109:80–89.

Jansen D, Zerbi V, Janssen CIF, Dederen PJWC, Mutsaers MPC, Hafkemeijer A, Janssen A-L, Nobelen CLM, Veltien A, Asten JJ, Heerschap A, Kiliaan AJ (2013) A Longitudinal Study of Cognition, Proton MR Spectroscopy and Synaptic and Neuronal Pathology in Aging Wild-type and AβPPswe-PS1dE9 Mice. PLoS One 8:e63643 Available at: http://dx.doi.org/10.1371/journal.pone.0063643.

Jauregui-Huerta F, Ruvalcaba-Delgadillo Y, Gonzalez-Castañeda R, Garcia-Estrada J, Gonzalez-Perez O, Luquin S (2010) Responses of glial cells to stress and glucocorticoids. Curr Immunol Rev 6:195–204 Available at: http://www.ncbi.nlm.nih.gov/pmc/articles/PMC2924577/.

Jiang HK, Owyang V V, Hong JS, Gallagher M (1989) Elevated dynorphin in the hippocampal formation of aged rats: relation to cognitive impairment on a spatial learning task. Proc Natl Acad Sci 86 :2948–2951 Available at: http://www.pnas.org/content/86/8/2948.abstract.

Johnson JD, O'Connor K a., Deak T, Stark M, Watkins LR, Maier SF (2002) Prior Stressor Exposure Sensitizes LPS-Induced Cytokine Production. Brain Behav Immun 16:461–476 Available at: http://linkinghub.elsevier.com/retrieve/pii/S0889159101906385 [Accessed July 24, 2012].

Kettenmann H, Hanisch U, Noda M, Verkhratsky A (2011) Physiology of Microglia. :461–553.

Kino T (2010) The Glucocorticoid Receptor. Brain Immune Available at: http://brainimmune.com/the-glucocorticoid-receptor/.

Kohama SG, Goss JR, McNeill TH, Finch CE (1995) Glial fibrillary acidic protein mRNA increases at proestrus in the arcuate nucleus of mice. Neurosci Lett 183:164–166.

Kumar R, Thompson EB (2005) Gene regulation by the glucocorticoid receptor: structure:function relationship. J Steroid Biochem Mol Biol 94:383–394.

La Voie D, Light LL (1994) Adult age differences in repetition priming: a meta-analysis. Psychol Aging 9:539–553.

Lambert KG, Gerecke KM, Quadros PS, Doudera E, Jasnow AM, Kinsley CH (2000) Activity-stress increases density of GFAP-immunoreactive astrocytes in the rat hippocampus. Stress 3:275–284.

Lawson LJ, Perry VH, Dri P, Gordon S (1990) Heterogeneity in the distribution and morphology of microglia in the normal adult mouse brain. Neuroscience 39:151–170 Available at: http://www.ncbi.nlm.nih.gov/pubmed/2089275.

Lee CK, Weindruch R, Prolla T a (2000) Gene-expression profile of the ageing brain in mice. Nat Genet 25:294–297 Available at: http://www.ncbi.nlm.nih.gov/pubmed/10888876.

Lee I, Hunsaker MR, Kesner RP (2005) The Role of Hippocampal Subregions in Detecting Spatial Novelty. Behav Neurosci 119:145–153.

Lindsey JD, Landfield PW, Lynch G (1979) Early onset and topographical distribution of hypertrophied astrocytes in hippocampus of aging rats: a quantitative study. J Gerontol 34:661–671.

Lupien SJ, McEwen BS, Gunnar MR, Heim C (2009) Effects of stress throughout the lifespan on the brain, behaviour and cognition. Nat Rev Neurosci 10:434–445 Available at: http://dx.doi.org/10.1038/nrn2639.

MacLullich AMJ, Deary IJ, Starr JM, Ferguson KJ, Wardlaw JM, Seckl JR (2005) Plasma cortisol levels, brain volumes and cognition in healthy elderly men. Psychoneuroendocrinology 30:505–515 Available at:

http://www.sciencedirect.com/science/article/B6TBX-4FB9GXW-3/2/b5b6328baf1bb7fd10fa3372204985f0.

MacLullich AMJ, Ferguson KJ, Deary IJ, Seckl JR, Starr JM, Wardlaw JM (2002) Intracranial capacity and brain volumes are associated with cognition in healthy elderly men. Neurology 59:169–174 Available at: http://www.neurology.org/cgi/content/abstract/59/2/169.

MacLullich AMJ, Ferguson KJ, Reid LM, Deary IJ, Starr JM, Wardlaw JM, Walker BR, Andrew R, Seckl JR (2012) 11[beta]-hydroxysteroid dehydrogenase type 1, brain atrophy and cognitive decline. Neurobiol Aging 33:207 Available at: http://www.sciencedirect.com/science/article/B6T09-518F06G-8/2/5dc294859a719fe1b5096c762ab41fc4.

Madrigal JLM, Moro M a, Lizasoain I, Lorenzo P, Fernández a P, Rodrigo J, Boscá L, Leza JC (2003) Induction of cyclooxygenase-2 accounts for restraint stress-induced oxidative status in rat brain. Neuropsychopharmacology 28:1579–1588 Available at: http://www.ncbi.nlm.nih.gov/pubmed/12784118 [Accessed July 25, 2012].

Mantovani A, Sica A, Sozzani S, Allavena P, Vecchi A, Locati M (2004) The chemokine system in diverse forms of macrophage activation and polarization. Trends Immunol 25:677–686 Available at: http://www.ncbi.nlm.nih.gov/pubmed/15530839 [Accessed July 14, 2012].

Markham JA, McKian KP, Stroup TS, Juraska JM (2005) Sexually dimorphic aging of dendritic morphology in CA1 of hippocampus. Hippocampus 15:97–103.

Marquis S, Moore MM, Howieson DB, Sexton G, Payami H, Kaye JA, Camicioli R (2002) Independent predictors of cognitive decline in healthy elderly persons. Arch Neurol 59:601–606.

McArdle JJ, Hamgami F, Jones K, Jolesz F, Kikinis R, Spiro A, Albert MS (2004) Structural modeling of dynamic changes in memory and brain structure using longitudinal data from the normative aging study. Journals Gerontol Ser B Psychol Sci Soc Sci 59:P294–P304.

McCall MA, Gregg RG, Behringer RR, Brenner M, Delaney CL, Galbreath EJ, Zhang CL, Pearce RA, Chiu SY, Messing A (1996) Targeted deletion in astrocyte intermediate filament (Gfap) alters neuronal physiology. Proc Natl Acad Sci 93:6361–6366.

McNamara MC, Bepjignus G, Benignus VA, Miller Jr AT (1977) Active and passive avoidance in rats as a function of age. Exp Aging Res 3:3–16.

Menet V, Gimenez y Ribotta M, Chauvet N, Drian MJ, Lannoy J, Colucci-Guyon E, Privat A (2001) Inactivation of the glial fibrillary acidic protein gene, but not

that of vimentin, improves neuronal survival and neurite growth by modifying adhesion molecule expression. J Neurosci 21:6147–6158.

Menet V, Gimenez Y Ribotta M, Sandillon F, Privat A (2000) GFAP null astrocytes are a favorable substrate for neuronal survival and neurite growth. Glia 31:267–272.

Merritt K, McGuire P, Egerton A (2013) Relationship between Glutamate Dysfunction and Symptoms and Cognitive Function in Psychosis. Front psychiatry 4:151.

Mizoguchi K, Ishige A, Takeda S, Aburada M, Tabira T (2004) Endogenous Glucocorticoids Are Essential for Maintaining Prefrontal Cortical Cognitive Function. J Neurosci 24 :5492–5499 Available at: http://www.jneurosci.org/content/24/24/5492.abstract.

Moisan MP, Seckl JR, Edwards CR (1990) 11 beta-hydroxysteroid dehydrogenase bioactivity and messenger RNA expression in rat forebrain: localization in hypothalamus, hippocampus, and cortex. Endocrinology 127:1450–1455.

Moore a H, Wu M, Shaftel SS, Graham K a, O'Banion MK (2009) Sustained expression of interleukin-1beta in mouse hippocampus impairs spatial memory. Neuroscience 164:1484–1495 Available at: http://www.pubmedcentral.nih.gov/articlerender.fcgi?artid=2783232&tool=pmcentrez&rendertype=abstract [Accessed July 22, 2012].

Morgan TE, Rozovsky I, Goldsmith SK, Stone DJ, Yoshida T, Finch CE (1997) Increased transcription of the astrocyte gene GFAP during middle-age is attenuated by food restriction: implications for the role of oxidative stress. Free Radic Biol Med 23:524–528.

Morrison JH, Hof PR (1997) Life and death of neurons in the aging brain. Science 278:412–419.

Munhoz CD, Lepsch LB, Kawamoto EM, Malta MB, Lima LDS, Avellar MCW, Sapolsky RM, Scavone C (2006) Chronic unpredictable stress exacerbates lipopolysaccharide-induced activation of nuclear factor-kappaB in the frontal cortex and hippocampus via glucocorticoid secretion. J Neurosci 26:3813–3820 Available at: http://www.ncbi.nlm.nih.gov/pubmed/16597735 [Accessed July 25, 2012].

Munhoz CD, Sorrells SF, Caso JR, Scavone C, Sapolsky RM (2010) Glucocorticoids exacerbate lipopolysaccharide-induced signaling in the frontal cortex and hippocampus in a dose-dependent manner. J Neurosci 30:13690–13698 Available at: http://www.ncbi.nlm.nih.gov/pubmed/20943909 [Accessed July 16, 2012].

Nichols NR, Day JR, Laping NJ, Johnson SA, Finch CE (1993) GFAP mRNA increases with age in rat and human brain. Neurobiol Aging 14:421–429.

Nimmerjahn A, Kirchhoff F, Helmchen F (2005) Resting microglial cells are highly dynamic surveillants of brain parenchyma in vivo. Science (80-) 308:1314–1318.

O'Brien JT, Desmond P, Ames D, Schweitzer I, Chiu E, Tress B (1997) Temporal lobe magnetic resonance imaging can differentiate Alzheimer's disease from normal ageing, depression, vascular dementia and other causes of cognitive impairment. Psychol Med 27:1267–1275.

O'Connor TM, O'Halloran DJ, Shanahan F (2000) The stress response and the hypothalamic-pituitary-adrenal axis: from molecule to melancholia. QJM 93:323–333 Available at: http://qjmed.oxfordjournals.org/content/93/6/323.abstract.

Oitzl MS, Reichardt HM, Joëls M, de Kloet ER (2001) Point mutation in the mouse glucocorticoid receptor preventing DNA binding impairs spatial memory. Proc Natl Acad Sci 98:12790–12795.

Park DC, Lautenschlager G, Hedden T, Davidson NS, Smith AD, Smith PK (2002) Models of visuospatial and verbal memory across the adult life span. Psychol Aging 17:299–320.

Park DC, Smith AD, Lautenschlager G, Earles JL, Frieske D, Zwahr M, Gaines CL (1996) Mediators of long-term memory performance across the life span. Psychol Aging 11:621–637.

Perry VH, Matyszak MK, Fearn S (1993) Altered antigen expression of microglia in the aged rodent CNS. Glia 7:60–67 Available at: http://www.ncbi.nlm.nih.gov/pubmed/8423063.

Pfefferbaum A, Mathalon DH, Sullivan E V, Rawles JM, Zipursky RB, Lim KO (1994) A quantitative magnetic resonance imaging study of changes in brain morphology from infancy to late adulthood. Arch Neurol 51:874–887.

Pocock JM, Kettenmann H (2007) Neurotransmitter receptors on microglia. Trends Neurosci 30:527–535 Available at: http://www.ncbi.nlm.nih.gov/pubmed/17904651 [Accessed July 25, 2012].

Rajan V, Edwards CR, Seckl JR (1996) 11 beta-Hydroxysteroid dehydrogenase in cultured hippocampal cells reactivates inert 11-dehydrocorticosterone, potentiating neurotoxicity. J Neurosci 16:65–70.

Rapp PR, Gallagher M (1996) Preserved neuron number in the hippocampus of aged rats with spatial learning deficits. Proc Natl Acad Sci 93:9926–9930.

Rasmussen T, Schliemann T, Sørensen JC, Zimmer J, West MJ (1996) Memory impaired aged rats: no loss of principal hippocampal and subicular neurons. Neurobiol Aging 17:143–147.

Raz N, Gunning FM, Head D, Dupuis JH, McQuain J, Briggs SD, Loken WJ, Thornton AE, Acker JD (1997) Selective aging of the human cerebral cortex observed in vivo: differential vulnerability of the prefrontal gray matter. Cereb Cortex 7:268–282.

Raz N, Gunning-Dixon FM, Head D, Dupuis JH, Acker JD (1998) Neuroanatomical correlates of cognitive aging: evidence from structural magnetic resonance imaging. Neuropsychology 12:95.

Raz N, Lindenberger U, Rodrigue KM, Kennedy KM, Head D, Williamson A, Dahle C, Gerstorf D, Acker JD (2005) Regional brain changes in aging healthy adults: general trends, individual differences and modifiers. Cereb cortex 15:1676–1689.

Raz N, Williamson A, Gunning-Dixon F, Head D, Acker JD (2000) Neuroanatomical and cognitive correlates of adult age differences in acquisition of a perceptual-motor skill. Microsc Res Tech 51:85–93.

Resnick SM, Pham DL, Kraut MA, Zonderman AB, Davatzikos C (2003) Longitudinal magnetic resonance imaging studies of older adults: a shrinking brain. J Neurosci 23:3295–3301.

Rodrigue KM, Raz N (2004) Shrinkage of the entorhinal cortex over five years predicts memory performance in healthy adults. J Neurosci 24:956–963.

Rosi S, Vazdarjanova a, Ramirez-Amaya V, Worley PF, Barnes C a, Wenk GL (2006) Memantine protects against LPS-induced neuroinflammation, restores behaviorally-induced gene expression and spatial learning in the rat. Neuroscience 142:1303–1315 Available at: http://www.ncbi.nlm.nih.gov/pubmed/16989956 [Accessed July 25, 2012].

Saab BJ, Georgiou J, Nath A, Lee FJS, Wang M, Michalon A, Liu F, Mansuy IM, Roder JC (2016) NCS-1 in the Dentate Gyrus Promotes Exploration, Synaptic Plasticity, and Rapid Acquisition of Spatial Memory. Neuron 63:643–656 Available at: http://dx.doi.org/10.1016/j.neuron.2009.08.014.

Sandeep T, MacLullich A, Yau J, Noble J, Walker B, Seckl J (2002) 11beta-hydroxysteroid dehydrogenase type 1 (11beta HSD1) is expressed in human brain: inhibition with carbenoxolone improves cognitive function in healthy elderly men.

Sandeep TC, Yau JLW, Maclullich AMJ, Noble J, Deary IJ, Walker BR, Seckl JR (2004) 11β-Hydroxysteroid dehydrogenase inhibition improves cognitive function in healthy elderly men and type 2 diabetics. Proc Natl Acad Sci U S A

101:6734–6739 Available at: http://www.pnas.org/content/101/17/6734.abstract.

Sapolsky RM, Romero LM, Munck AU (2000) How do glucocorticoids influence stress responses? Integrating permissive, suppressive, stimulatory, and preparative actions 1. Endocr Rev 21:55–89.

Schaie KW, Willis SL, Caskie GIL (2004) The Seattle Longitudinal Study: Relationship Between Personality and Cognition. Neuropsychol Dev Cogn B Aging Neuropsychol Cogn 11:304–324 Available at: http://www.ncbi.nlm.nih.gov/pmc/articles/PMC1474018/.

Schuff N, Amend DL, Knowlton R, Norman D, Fein G, Weiner MW (1999) Age-related metabolite changes and volume loss in the hippocampus by magnetic resonance spectroscopy and imaging. Neurobiol Aging 20:279–285 Available at: http://www.ncbi.nlm.nih.gov/pmc/articles/PMC2733348/.

Shimada A, Tsuzuki M, Keino H, Satoh M, Chiba Y, Saitoh Y, Hosokawa M (2006) Apical vulnerability to dendritic retraction in prefrontal neurones of ageing SAMP10 mouse: a model of cerebral degeneration. Neuropathol Appl Neurobiol 32:1–14.

Shimamura AP, Berry JM, Mangels JA, Rusting CL, Jurica PJ (1995) Memory and cognitive abilities in university professors: Evidence for successful aging. Psychol Sci:271–277.

Shukitt-Hale B, McEwen JJ, Szprengiel A, Joseph JA (2004) Effect of age on the radial arm water maze—a test of spatial learning and memory. Neurobiol Aging 25:223–229.

Sierra A, Gottfried-blackmore AC, Mcewen BS (2007) Microglia Derived from Aging Mice Exhibit an Altered Inflammatory Profile. Glia 424:412–424.

Skullerud K (1985) Variations in the size of the human brain. Influence of age, sex, body length, body mass index, alcoholism, Alzheimer changes, and cerebral atherosclerosis. Acta Neurol Scand Suppl 102:1–94.

Soher BJ, van Zijl P, Duyn JH, Barker PB (1996) Quantitative proton MR spectroscopic imaging of the human brain. Magn Reson Med 35:356–363.

Sooy K, Webster SP, Noble J, Binnie M, Walker BR, Seckl JR, Yau JLW (2010) Partial Deficiency or Short-Term Inhibition of 11{beta}-Hydroxysteroid Dehydrogenase Type 1 Improves Cognitive Function in Aging Mice. J Neurosci 30:13867–13872 Available at: http://www.jneurosci.org/cgi/content/abstract/30/41/13867.

Sorrells SF, Sapolsky RM (2007) An inflammatory review of glucocorticoid actions in the CNS. Brain Behav Immun 21:259–272 Available at:

http://www.sciencedirect.com/science/article/B6WC1-4MNRN0H-2/2/70907897b004843cb3bee3c4d419f566.

Sparkman NL, Johnson RW (2008) Neuroinflammation Associated with Aging Sensitizes the Brain to the Effects of Infection or Stress. Neuroimmunomodulation 15:323–330 Available at: http://www.karger.com/DOI/10.1159/000156474.

Sparkman NL, Johnson RW (2009) Neuroinflammation Associated with Aging Sensitizes the Brain to the Effects of Infection or Stress. Neuroimmunomodulation 15:323–330.

Spencer WD, Raz N (1995) Differential effects of aging on memory for content and context: A meta-analysis. Psychol Aging 10:527–539.

Sugaya K, Chouinard M, Greene R, Robbins M, Personett D, Kent C, Gallagher M, McKinney M (1996) Molecular indices of neuronal and glial plasticity in the hippocampal formation in a rodent model of age-induced spatial learning impairment. J Neurosci 16:3427–3443.

Sullivan E V, Adalsteinsson E, Hedehus M, Ju C, Moseley M, Lim KO, Pfefferbaum A (2001) Equivalent disruption of regional white matter microstructure in ageing healthy men and women. Neuroreport 12:99–104.

Terry RD, Katzman R (2001) Life span and synapses: will there be a primary senile dementia? Neurobiol Aging 22:347–348.

Tisserand DJ, Visser PJ, Van Boxtel MPJ, Jolles J (2000) The relation between global and limbic brain volumes on MRI and cognitive performance in healthy individuals across the age range. Neurobiol Aging 21:569–576.

Urrila AS, Hakkarainen A, Heikkinen S, Vuori K, Stenberg D, Häkkinen A-M, Lundbom N, Porkka-Heiskanen T (2004) Stimulus-induced brain lactate: effects of aging and prolonged wakefulness. J Sleep Res 13:111–119 Available at: http://dx.doi.org/10.1111/j.1365-2869.2004.00401.x.

Uylings HBM, de Brabander JM (2002) Neuronal Changes in Normal Human Aging and Alzheimer's Disease. Brain Cogn 49:268–276 Available at: http://www.sciencedirect.com/science/article/pii/S0278262601915003.

Van Asselen M, Kessels RPC, Neggers SFW, Kappelle LJ, Frijns CJM, Postma A (2006) Brain areas involved in spatial working memory. Neuropsychologia 44:1185–1194 Available at: http://www.sciencedirect.com/science/article/pii/S0028393205003180.

Van Petten C (2004) Relationship between hippocampal volume and memory ability in healthy individuals across the lifespan: review and meta-analysis. Neuropsychologia 42:1394–1413.

Verzár-Mcdougall EJ (1957) Studies in Learning and Memory in Ageing Rats. Gerontology 1:65–85 Available at: http://www.karger.com/DOI/10.1159/000210684.

Virgin CE, Ha TP, Packan DR, Tombaugh GC, Yang SH, Homer HC, Sapolsky RM (1991) Glucocorticoids inhibit glucose transport and glutamate uptake in hippocampal astrocytes: implications for glucocorticoid neurotoxicity. J Neurochem 57:1422–1428.

Visser PJ, Scheltens P, Verhey FRJ, Schmand B, Launer LJ, Jolles J, Jonker C (1999) Medial temporal lobe atrophy and memory dysfunction as predictors for dementia in subjects with mild cognitive impairment. J Neurol 246:477–485.

Walhovd KB, Fjell AM, Reinvang I, Lundervold A, Fischl B, Quinn BT, Dale AM (2004) Size does matter in the long run Hippocampal and cortical volume predict recall across weeks. Neurology 63:1193–1197.

Wan SL, Liao MY, Sun K (2002) Postnatal development of 11β-hydroxysteroid dehydrogenase type 1 in the rat hippocampus. J Neurosci Res 69:681–686 Available at: http://dx.doi.org/10.1002/jnr.10325.

West MJ (1993) Regionally specific loss of neurons in the aging human hippocampus. Neurobiol Aging 14:287–293.

Wheelan N, Webster SP, Kenyon CJ, Caughey S, Walker BR, Holmes MC, Seckl JR, Yau JLW (2014) Short-term inhibition of 11beta-hydroxysteroid dehydrogenase type 1 reversibly improves spatial memory but persistently impairs contextual fear memory in aged mice. Neuropharmacology 91C:71–76.

White PC, Mune T, Agarwal AK (1997) 11β-Hydroxysteroid Dehydrogenase and the Syndrome of Apparent Mineralocorticoid Excess 1. Endocr Rev 18:135–156.

Wickelgren I (1996) The aging brain: for the cortex, neuron loss may be less than thought. Science (80-) 273:48.

Wyss JM, Chambless BD, Kadish I, van Groen T (2000) Age-related decline in water maze learning and memory in rats: strain differences. Neurobiol Aging 21:671–681.

Yau JLW, McNair KM, Noble J, Brownstein D, Hibberd C, Morton N, Mullins JJ, Morris RGM, Cobb S, Seckl JR (2007) Enhanced Hippocampal Long-Term Potentiation and Spatial Learning in Aged 11{beta}-Hydroxysteroid Dehydrogenase Type 1 Knock-Out Mice. J Neurosci 27:10487–10496 Available at: http://www.jneurosci.org/cgi/content/abstract/27/39/10487.

Yau JLW, Noble J, Kenyon CJ, Hibberd C, Kotelevtsev Y, Mullins JJ, Seckl JR (2001) Lack of tissue glucocorticoid reactivation in 11β-hydroxysteroid dehydrogenase type 1 knockout mice ameliorates age-related learning

impairments. Proc Natl Acad Sci U S A 98:4716–4721 Available at: http://www.pnas.org/content/98/8/4716.abstract.

Yau JLW, Wheelan N, Noble J, Walker BR, Webster SP, Kenyon CJ, Ludwig M, Seckl JR (2015) Intrahippocampal glucocorticoids generated by 11beta-HSD1 affect memory in aged mice. Neurobiol Aging 36:334–343.

Ylikoski A, Erkinjuntti T, Raininko R, Sarna S, Sulkava R, Tilvis R (1995) White matter hyperintensities on MRI in the neurologically nondiseased elderly Analysis of cohorts of consecutive subjects aged 55 to 85 years living at home. Stroke 26:1171–1177.

Zelinski EM, Burnight KP (1997) Sixteen-year longitudinal and time lag changes in memory and cognition in older adults. Psychol Aging 12:503–513.

Zhang TY, Daynes RA (2007) Macrophages from 11β-Hydroxysteroid Dehydrogenase Type 1-Deficient Mice Exhibit an Increased Sensitivity to Lipopolysaccharide Stimulation Due to TGF-β-Mediated Up-Regulation of SHIP1 Expression. J Immunol 179 :6325–6335 Available at: http://www.jimmunol.org/content/179/9/6325.abstract.

Zimmerman ME, Brickman AM, Paul RH, Grieve SM, Tate DF, Gunstad J, Cohen RA, Aloia MS, Williams LM, Clark CR (2006) The relationship between frontal gray matter volume and cognition varies across the healthy adult lifespan. Am J Geriatr psychiatry 14:823–833.